Inhibition of a conserved DNA repair complex promotes susceptibility of *Staphylococcus aureus* to host defences

Kam Pou Ha

Thesis submitted for the degree of Doctor of Philosophy

November 2019

Department of Infectious Disease
Imperial College London

Declaration of Originality

I can confirm that the work in this thesis is my own and that any work performed by anyone other than myself, has been appropriately credited. All resources and ideas from the work of others have been appropriately referenced.

Copyright Declaration

Acknowledgements

Thank you to my supervisor Andy, whose support and guidance were invaluable. Thank you for your patience, positivity and cracking sense of humour. You are, truly, a fantastic supervisor. I will forever be grateful and happy to have had the opportunity to be your student.

To Tom and Despoina – thank you for your support and advice. Thank you to Despoina for guiding me though the protein purification process and for providing the tools so I could get it done successfully. It was a long year, but it worked!

To members of the Edwards group and CMBI 5, past and present – I have enjoyed working with you all and the great conversations we've had along the way. Special thanks to Vera and Nisha, without whom I wouldn't have been able to dance (badly) around the lab without feeling embarrassed. To Aisha, who had the answer to every cloning question (the true Cloning Queen) and a remarkably well-organised freezer, which was very helpful. To Lizzie, whose daily lunch choice of a cheese toastie is still entertaining despite always staying the same. And to Akshay, who had the misfortune of being around during many of my stressful lab days, and got to experience first-hand exciting events such as the PBS incident, where my agar plates were behaving badly and I didn't know why.

A big thank you to the students I have supervised or part-supervised over the years: Anja, Dale, Carine, Adam and Declan, whose imitation of a bunsen burner I shall always remember with confusion. Thank you to CMBI 3 and 4 for being so friendly and generous whenever I had to borrow items or use equipment. There always seemed to be a petri dish shortage on the fifth floor and it was probably partly my fault.

Finally, the biggest thank you to my friends and family for their long-standing support. Thank you to Shahida and Sana, who are (most likely) still confused about what my PhD is about, but are always willing to listen. Thank you to Peggy, Nan, Saranja, and Cher for our food and travel adventures. And thank you to Mama, Papa and Auntie, who have made me the person I am today. Thank you to you all.

Abstract

Staphylococcus aureus is a leading cause of serious infections in humans, but treatment can be ineffective due to the emergence of antibiotic-resistant strains. During infection, the most important host defence mechanism against *Staphylococcus aureus* is the oxidative burst of neutrophils, which involves the rapid generation and release of reactive oxygen species. However, whilst it has been hypothesised that DNA is an important target of the oxidative burst, this had not been tested.

Work described in this thesis revealed that the neutrophil oxidative burst triggers the SOS DNA repair pathway in phagocytosed *S. aureus,* indicating that staphylococcal DNA is a target of the host immune response. A screen of a panel of mutants defective in various DNA repair processes revealed that the RexAB complex was essential for maximal staphylococcal survival in whole human blood, during incubation with purified human neutrophils and during invasive murine infection. This repair complex also conferred a survival benefit to *Streptococcus gordonnii* and *Enterococcus faecalis* in human blood, indicating that DNA is a conserved target of neutrophil-mediated killing.

Using recombinant *S. aureus* RexAB, it was demonstrated that this complex is a functional member of the AddAB family of helicase-nuclease enzymes, required for the repair of DNA double-strand breaks. In an effort to develop inhibitors of RexAB for use as potential therapeutics, subsequent work identified a compound that potentiated the activity of DNA-damaging antibiotics. However, it was not possible to demonstrate inhibition of RexAB.

In summary, these data demonstrate that RexAB is required for staphylococcal survival during infection by repairing DNA damage caused by the neutrophil oxidative burst. Future work will focus on the discovery and development of small-molecule inhibitors of RexAB that could be used therapeutically to sensitise *S. aureus* to host immune defences.

Contents

List of Figures

List of Tables

List of Abbreviations

A	
AddAB	ATP-dependent helicase/nuclease A and B
A-EJ	Alternative end-joining
agr	Accessory gene regulator operon
AhpC	Alkyl hydroperoxide reductase
AHT	Anhydrotetracycline
Amp	Ampicillin
AMP	Antimicrobial peptide
APC	Antigen-presenting cell
APS	Ammonium persulphate
B	
BCA	Bicinchoninic acid
BD	Becton Dickinson
BER	Base excision repair
bp	Base pair
BSA	Bovine serum albumin
C	
C1	Compound 1, also known as CID 1517823
C4	Compound 4
C13	Compound 13, the inactive control compound
Cam	Chloramphenicol
CA-MRSA	Community-associated methicillin-resistant *Staphylococcus aureus*
CBA	Columbia blood agar
CFU	Colony forming unit
CGD	Chonic granulomatous disease
Chi	Crossover hotspot instigator
CID	Compound identification number
CHIPS	Chemotaxis inhibitory protein of *Staphylococcus*
Clf	Clumping factor
Coa	Coagulase
CpG	Cytosine-phosphate-guanosine
CXCL	C-X-C motif chemokine ligand
CXCR	C-X-C motif chemokine receptor
D	
D-Ala D-Ala	D-alanyl-D-alanine
D-Ala D-Lac	D-alanyl-D-lactose
dlt	D-alanyl-lipoteichoic acid operon
DMSO	Dimethyl sulfoxide
DPI	Diphenyleneiodonium
DSB	Double-strand break
dsDNA	Double-stranded DNA

DTT	Dithiotheitol
E	
Eap	Extracellular adherence protein
ECL	Enhanced chemiluminenscence
EDTA	Ethylenediaminetetraacetic acid
Ecb	Extracellular complement-binding protein
Efb	Extracellular fibrinogen-binding protein
Erm	Erythomycin
EUCAST	European Committee on Antimicrobial Susceptibility Testing
F	
FpB	Fibrinopeptide B
Fc	Fragment crystallisable
FcR	Fragment crystallisable receptors
FI	Fluorescence intensity
FLIPr	FPR-like 1 inhibitory protein
FnBP	Fibronectin-binding protein
FPR	Formyl peptide receptor
FSC	Forward scatter
Fur	Ferric uptake regulator
G	
g	Gravitational acceleration
GFP	Green fluorescent protein
GraSR	Glycopeptide resistance associated SR two-component system
H	
HA-MRSA	Hospital associated methicillin-resistant *Staphylococcus aureus*
HBSS	Hanks' Balanced Salt Solution
His	Histidine
HMM	Hidden Markov model
Hmp	Flavohaemoglobin
H_2O_2	Hydrogen peroxide
HOCl	Hypochlorous acid
Hla	α-haemolysin
HP	Horseradish peroxidase
HSA	Human serum albumin
HtsABC	Haem-transport system ABC
hVISA	Heterogenous vancomycin-intermediate *Staphylococcus aureus*
I	
IE	Infective endocarditis
iE-DAP	γ-D-glutamyl-meso-diaminopimelic acid
IFN-γ	Interferon-γ
IPTG	Isopropyl β-D-1-thiogalactopyranoside
iNOS	Inducible nitric oxide synthase
IscS	Iron-sulphur cluster S
Isd	Iron-regulated surface determinant

I-TASSER	Iterative theading assembly refinement
K	
Kan	Kanamycin
KatA	Catalase
kb	Kilobase
kDa	Kilodalton
L	
LAC	Los Angeles County
LB	Lysogeny broth
LexA	Locus for X-ray sensitivity A
L-LDH	L-lactate dehydrogenase
L-NIO	L-N5-(1-iminoethyl)ornithine
L-NMMA	NG-monomethyl-L-arginine
LPS	Lipopolysaccharide
LTA	Lipoteichoic acid
LukGH	Leukotoxin GH
M	
M	Molar
MBL	Mannose-binding lectin
MSA	Mannitol salt agar
MBC	Minimum bactericidal concentration
MDP	Muramyl dipeptide
MGE	Mobile genetic element
MgrA	Multiple gene regulator A
MHC	Major histocompatibility complex
MIC	Minimum inhibitory concentration
MMR	Mismatch repair
MOI	Multiplicity of infection
MPO	Myeloperoxidase
MprF	Multiple peptide resistance factor
MrgA	Metallo-regulated gene A
MRSA	Methicillin-resistant *Staphylococcus aureus*
Msr	Methionine sulphoxide reductase
MSSA	Methicillin-sensitive *Staphylococcus aureus*
MurNAc	N-acetylmuramic acid
N	
NADPH	Nicotinamide adenine dinucleotide phosphate
NEB	New England Biolabs
NER	Nucleotide excision repair
NET	Neutrophil extracellular trap
NHEJ	Non-homologous end joining
NLR	Nucleotide oligomerisation domain (NOD)-like receptor
$NO^{\bullet}$	Nitric oxide
NO_2	Nitrogen dioxide

NTML	Nebraska Transposon Mutant Library
O	
$^1O_2$	Singlet oxygen
$O_2^{\bullet-}$	Superoxide
OatA	O-acetyltransferase A
OD	Optical density
$^{\bullet}OH$	Hydroxyl radical
ONOO−	Peroxynitrite
P	
PAGE	Polyacrylamide gel electrophoresis
PAMP	Pathogen-associated molecular pattern
PBS	Phosphate-buffered saline
PCR	Polymerase chain reaction
PDB	Protein Data Bank
PerR	Peroxide-responsive repressor
PF4	Platelet factor 4
PFA	Paraformaldahyde
P_i	Inorganic phosphate
PMBC	Peripheral blood mononuclear cell
PMN	Polymophonuclear leukocyte
PMP	Platelet microbicidal protein
P*recA*	*recA* promoter
PRR	Pattern recognition receptor
PSM	Phenol soluble modulin
PVL	Panton–Valentine leukocidin
R	
RecA	Recombinase A
RecBCD	Recombinase B, C and D
RexAB	Recombination exonuclease A and B
RNAP	RNA polymerase
RNS	Reactive nitrogen species
ROS	Reactive oxygen species
rpm	Revolutions per minute
S	
SAB	*Staphylococcus aureus* bacteraemia
SaeRS	*Staphylococcus aureus* exoprotein expression RS two-component system
Sbi	Staphylococcal binding immunoglobulin
SCC*mec*	Staphylococcal cassette chomosome *mec*
SCIN	Staphylococcal complement inhibitor
ScpA	Staphopain A
SCV	Small colony variant
SDM	Site-directed mutagenesis
SDS	Sodium dodecyl sulphate
SEB	Staphylococcal enterotoxin B

SEC	Staphylococcal enterotoxin C
SOK	Surface factor promoting resistance to oxidative killing
SpA	Staphylococcal protein A
SSB	Single-stranded DNA binding protein
SSC	Side scatter
ssDNA	Single-stranded DNA
SSL10	Staphylococcal superantigen-like 10
SSTI	Skin and soft tissue infection
STEB	Sucrose-Tris-ethylenediaminetetraacetic acid-bromophenol blue
Strep	Streptavidin
T	
TB	Terrific broth
TBE	Tris-borate-ethylenediaminetetraacetic acid
TBST	Tris-buffered saline with Tween 20
TCR	Transcription-coupled repair
TEMED	Tetramethylethylenediamine
THB	Todd Hewitt broth
TLR	Toll-like receptor
Tm	Melting temperature
TNF-α	Tumour necrosis factor-α
tPMP	Thombin-inducible PMPs
TrxA	Thioredoxin
TSA	Tryptic soy agar
TSB	Tryptic soy broth
TSST-1	Toxic shock syndrome toxin 1
V	
VISA	Vancomycin-intermediate *Staphylococcus aureus*
vra	Vancomycin-resistance associated operon
VRE	Vancomycin-resistant *Enterococcus faecalis*
VRSA	Vancomycin-resistant *Staphylococcus aureus*
VSSA	Vancomycin-sensitive *Staphylococcus aureus*
v/v	Volume per volume
W	
w/v	Weight per volume

1 Introduction

1.1 *Staphylococcus aureus*

1.1.1 General characteristics of *S. aureus*

Staphylococcus aureus is a Gram-positive bacterium that belongs to the phylum Firmicutes and is a member of the *Staphylococcaceae* family[1]. The bacterium was first discovered in 1880 by Sir Alexander Ogston, who examined the pus from an infected surgical wound under a microscope to reveal grape-like clusters of cocci, which he referred to as staphylococci[2]. Using the recovered bacteria, Ogston was able to recreate the infection in guinea pigs and mice, confirming that staphylococci were the causative agent of infection. In 1884, Friedrich Julius Rosenbach isolated and characterised a pure culture of the bacterium[3]. The species was named *S. aureus* after its characteristic golden colonies, the colour of which result from production of the carotenoid pigment staphyloxanthin[4].

The *S. aureus* genome was first sequenced in 2001 by Kuroda *et al.*[5]. This revealed a single, circular chomosome of ~2.8 Mb with a GC content of 36%, encoding approximately 2,800 proteins[5,6]. An estimated 78% of the genome is shared between different *S. aureus* strains, with up to 20% consisting of mobile genetic elements (MGEs) acquired by horizontal gene transfer[6,7]. These MGEs include pathogenicity islands, transposons, plasmids and prophages, many of which contribute towards virulence, host adaptation or antibiotic resistance. For example, the *mecA* gene found on the staphylococcal cassette chomosome *mec* (SCC*mec*) encodes resistance to methicillin[5,7].

S. aureus is a facultative anaerobe and a producer of both catalase and coagulase[8]. It can be distinguished from non-pathogenic species by plating onto mannitol salt agar (MSA), which contains a high concentration of salt that is selective for members of the *Staphylococcus* genus, but is inhibitory for most other bacteria. MSA also contains mannitol, which can be fermented by *S. aureus*, and a pH indicator (phenol red). Fermentation of mannitol lowers the pH, leading to a colour change in the agar from red to yellow[9].

1.1.2 Carriage of *S. aureus*

S. aureus primarily exists as a commensal organism, colonising the skin and mucosal surfaces such as the thoat and gastrointestinal tract[10,11]. The most common site of colonisation is the nasal cavity, on the squamous epithelial surface of the anterior nares[11,12]. Approximately 20% of the population are persistent nasal carriers, where *S. aureus* is present for longer than 154 days. Another 30% of the population are intermittent carriers and are transiently colonised for 4-14 days. The remaining 50% are non-carriers, where *S. aureus* nasal colonisation is present for less than four consecutive days[10,12,13].

Colonisation by *S. aureus* typically occurs early in life, with 50% of newborns testing positive for *S. aureus* nasal carriage at six weeks after birth[14]. This rate of carriage decreases within the first year, only to peak in individuals from 10 to 19 years of age, and then declines during adulthood. Although early colonisation is most likely due to transmission from the mother, the main route of transmission is from the environment to the hands and finally to the nasal cavity[14–16]. The carriage rate depends on multiple host factors, including gender, ethnicity, history of hospitalisation and underlying health conditions. For example, patients with HIV or diabetes tend to have higher rates of carriage of *S. aureus*[10,13,14,17]. Several bacterial factors also increase the rate of carriage and the presence of specific cell surface-associated proteins[11,18,19]. For example, staphylococcal clumping factor B (ClfB) binds to cytokeratin 10 and loricin found on the surface of the nasal epithelium[20,21]. Whilst carriage is asymptomatic, persistent carriers are more likely to suffer from *S. aureus* infections, usually caused by the colonising strain[10,11,13,15,22].

1.1.3 Infections caused by *S. aureus*

Whilst *S. aureus* is primarily a commensal organism, it is also an opportunistic pathogen that can cause a wide range of infections in humans (Figure 1.1). These infections can be mild and superficial, such as skin and soft tissue infections (SSTIs), or life-theatening and invasive, such as infective endocarditis (IE), meningitis and septic arthitis[8,17].

The first line of defence against bacterial infection is the skin, which acts as a physical barrier. When this barrier is disrupted, bacteria can invade the different layers of the skin architecture and cause SSTIs, which are the most common form of *S. aureus* infection[23,24]. Uncomplicated SSTIs involve the pores or superficial layers of skin, and are often resolved without treatment by an effective immune response mediated by neutrophils. These mild infections include furuncles (boils), impetigo and folliculitis[23–25]. Complicated SSTIs involve deeper layers of skin and underlying soft tissues, and include cellulitis, abscesses and necrotising fasciitis, which is a life-theatening condition that requires urgent surgery[23,25,26].

In addition to broken skin, *S. aureus* is able to colonise the surfaces of indwelling medical devices, such as prosthetic joints, prosthetic heart valves and intravenous catheters[27,28]. Colonisation typically leads to the formation of biofilms, which protect *S. aureus* from host immune defences and antibiotics. However, these devices also provide the pathogen with an entry point into the bloodstream, which facilitates metastatic spread of *S. aureus* and the development of secondary infections. This can lead to more serious, life-theatening conditions, such as meningitis, IE or sepsis[8,17].

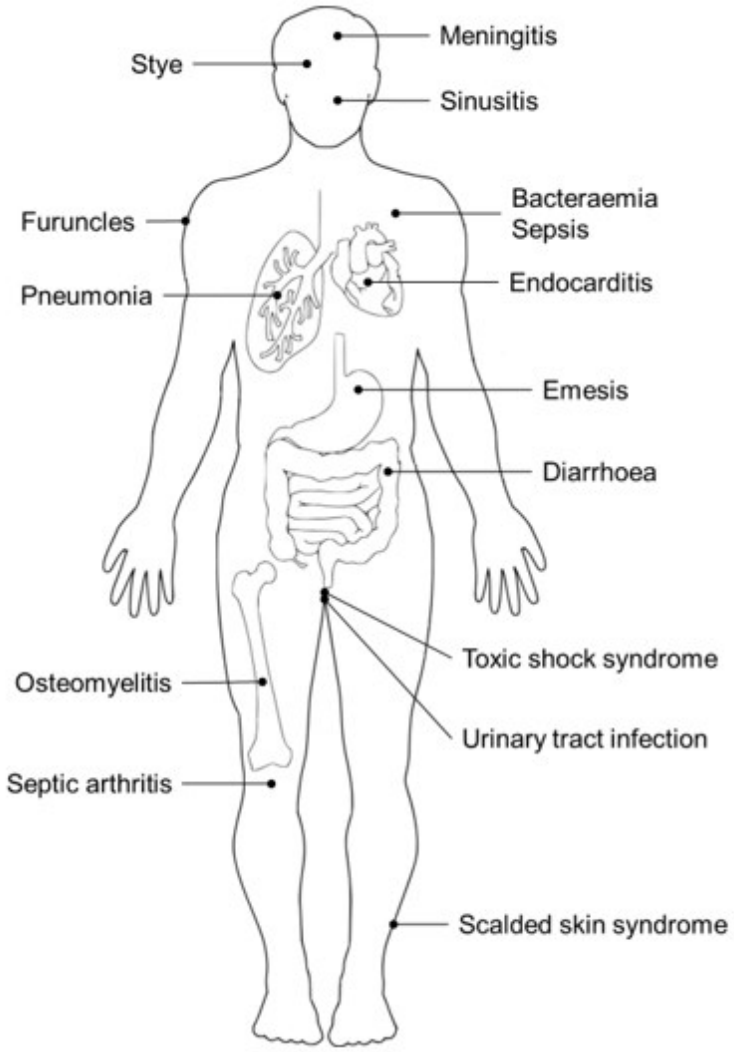

Figure 1.1. *S. aureus* infections in humans.

S. aureus can cause a wide range of infections at different sites in the human body, including skin and soft tissue infections (SSTIs), septic arthitis and bacteraemia. Adapted from Wertheim *et al.* (2005)[10].

1.1.3.1 Bloodstream infections

Bacteraemia, or bloodstream infection, is defined by the presence of viable bacteria in the circulating blood and is one of the most serious types of staphylococcal infection[29]. After *Escherichia coli*, *S. aureus* is the most common cause of bacteraemia[30]. In the UK, over 12,000 cases of *S. aureus* bacteraemia (SAB) are reported each year, with mortality rates of around 30%[29,31]. Groups most at risk of acquiring SAB include the elderly, those with indwelling medical devices (intravenous catheters, prosthetic joints or surgically-implanted materials), and patients with underlying medical comorbidities, such as diabetes, alcoholism or immunosuppression[32,33]. In most cases, SAB is caused by bacteria that are transferred from the nasal cavity to a body site where the strain can enter the bloodstream, for example, via a wound or an indwelling medical device[22,29]. Although *S. aureus* carriers are more susceptible to developing bacteraemia, they have lower SAB mortality rates than non-carriers, possibly due to the presence of protective antibodies against *S. aureus*[33,34].

The high mortality rate of SAB is due in part to the frequent dissemination of *S. aureus* to other sites of the body, where it can establish serious infections such as septic arthitis, osteomyelitis, IE and tissue abscesses[8,17]. Cases of SAB are classified as either complicated or uncomplicated[17]. Complicated infection occurs in approximately 40% of SAB cases and is defined by attributable mortality, involvement of the central nervous system, metastatic sites of infection, an embolic stroke or recurrent infection within 12 weeks[35]. Higher mortality rates are associated with complicated SAB, particularly when there is no clear focus of bacteraemia, or when the primary focus is from IE or pulmonary infections[33,36]. Therefore, timely treatment with appropriate antibiotics is essential for preventing or reducing metastatic spread in order to improve patient outcomes[33,37–39].

1.1.4 Treatment of *S. aureus* infections

Treatment of *S. aureus* infections is guided by the type of infection and antibiotic susceptibility of the infecting strain[8,40]. However, other factors that are taken into consideration include drug efficacy, toxicity, penetration of the antibiotic into certain tissues and dosing convenience[41].

For infections caused by methicillin-sensitive *S. aureus* (MSSA), semi-synthetic β-lactamase-resistant penicillins such as flucloxacillin remain the preferred choice for treating strains that produce β-lactamase, while benzylpenicillin is effective for the minority of *S. aureus* strains that do not produce β-lactamase[8,41]. For serious MSSA infections such as IE or osteomyelitis, the most effective antibiotics are flucloxacillin and dicloxacillin, which have greater bactericidal activity than cephalosporins[41]. However, due to their lower toxicity, cephalosporins are preferred over flucloxacillin or dicloxacillin for SSTIs. Non-β-lactam antibiotics used in MSSA treatment include clindamycin, used to treat osteomyelitis and septic arthitis, and co-trimoxazole (trimethoprim and sulphamethoxazole) for minor *S. aureus* infections[41–43].

The glycopeptide vancomycin is generally not used for treating MSSA infections because it is less effective than β-lactam antibiotics[44]. However, vancomycin is the preferred choice for treating methicillin-resistant *S. aureus* (MRSA) infections[8,41]. For severe SSTIs, vancomycin is given intravenously for two weeks to prevent bacterial dissemination into the bloodstream[45]. A combination of vancomycin and fusidic acid/rifampicin is used to treat SSTIs that do not respond to the glycopeptide antibiotic alone, and if vancomycin is unsuitable, linezolid or daptomycin are used[40]. Uncomplicated SSTIs are treated with tetracycline, clindamycin, co-trimoxazole or a combination of rifampicin and fusidic acid, which is given orally for five to ten days[40,45]. Urinary-tract infections (UTIs) caused by MRSA are treated with tetracycline or vancomycin depending on the severity of infection[40].

For SAB caused by MSSA or MRSA, treatment is given intravenously to directly sterilise the bloodstream[17,29]. This is continued for a minimum of two weeks for those with uncomplicated SAB, and for up to six weeks when the infection is complicated or has a deep focus. Cases of MSSA SAB are typically treated with semi-synthetic penicillins such as

flucloxacillin, or the lipopeptide antibiotic daptomycin if the patient has a penicillin allergy, whereas for MRSA SAB, patients are generally treated with vancomycin or daptomycin[17,29,46]. However, since daptomycin is more frequently associated with persistent and relapsing *S. aureus* infection, vancomycin is the preferred choice[46,47].

1.1.5 Antibiotic resistance of *S. aureus*

1.1.5.1 Penicillin resistance

Penicillin is a β-lactam antibiotic that is produced by members of the *Penicillium* genus of fungi[48]. The β-lactam ring of penicillin is structurally similar to the terminal D-alanyl-D-alanine (D-Ala D-Ala) moieties of peptidoglycan precursors, which are cross-linked by transpeptidases during cell wall synthesis[49,50]. Binding of pencillin by the transpeptidase, instead of its usual substrate, irreversibly blocks cross-linking of the peptidoglycan chains, leading to inhibition of cell wall synthesis and eventually to bacterial lysis[51,52].

Penicillin G was introduced in the 1940s and was considered a miracle drug as it drastically improved infection outcomes[52,53]. However, penicillin-resistant *S. aureus* strains appeared in hospitals after only two years, and by the 1960s, 80% of human isolates were resistant to the antibiotic[54–56]. Resistance to penicillin was mediated by the acquisition of a plasmid carrying the *blaZ* gene. This gene encodes for the β-lactamase enzyme that hydrolyses the β-lactam ring of penicillin, which inactivates the antibiotic[51,52,56,57].

1.1.5.2 Methicillin resistance

Resistance to penicillin led to the development of the semi-synthetic β-lactam methicillin, which was introduced in 1959. This antibiotic was derived from Penicillin G and possessed a large side group on its β-lactam ring that sterically hindered β-lactamase activity, making it effective against β-lactamase-producing *S. aureus* strains[51,52]. However, methicillin-resistant *S. aureus* (MRSA) isolates were reported within a year[58]. Since then, MRSA has become prevalent worldwide with up to 53 million people colonised with the organism globally, which

is associated with an increased risk of infection[59]. The morbidity and mortality associated with MRSA infections lead to significant and greater societal and economic costs than MSSA[52].

The mechanism of methicillin resistance took two decades to identify, and was found to result from horizontal gene transfer of a mobile genetic element termed the Staphylococcal Chomosome Cassette *mec* element (SCC*mec*)[60]. The SCC*mec* element contains the *mecA* gene, which encodes pencillin-binding protein 2a (PBP2a) that functions as a transpeptidase during cell wall synthesis. PBP2a has a very low affinity for β-lactams, which enables the bacterium to cross-link peptidoglycan even when other PBPs have been inactivated[52,56,61]. Eleven types of SCC*mec* element (I to XI) have been described to date, each with different combinations of *mec* gene and cassette chomosome recombinase (*crr*) gene complexes[52]. Detection of SCC*mec* by polymerase chain reaction (PCR) is often used in clinical diagnostic laboratories to determine whether an isolate is methicillin resistant[62]. Although methicillin is no longer used clinically, the term methicillin resistance applies to acquisition of the SCC*mec* element, which renders MRSA resistant to all β-lactam antibiotics, with the exception of the most recent generation of cephalosporin β-lactams[52].

The earliest strains of MRSA were identified in hospitals, and termed hospital-associated MRSA (HA-MRSA)[52]. HA-MRSA typically infects immunocompromised individuals with frequent or prolonged hospital stays, such as those with diabetes or human immunodeficiency virus (HIV)[63]. HA-MRSA strains usually carry SCC*mec* types I-III and are often multi-drug resistant, accounting for over 40% of hospital-acquired antibiotic-resistant infections per year[64,65]. In the UK, the most prevalent HA-MRSA strains are EMRSA-15 and EMRSA-16[66,67].

Since the 1990s, community-associated MRSA (CA-MRSA) strains have emerged in several parts of the world and are typically more virulent compared to HA-MRSA such that they are capable of infecting healthy individuals[68,69]. CA-MRSA strains have the capacity to colonise multiple sites within the body and to survive on environmental surfaces, making them more easily transmitted from person to person[63,70,71], and usually carry SCC*mec* types IV or V, which are believed to contribute towards a lower fitness cost due to their smaller size[64,72,73].

A particularly successful CA-MRSA strain is USA300, which has become the most common cause of CA-MRSA infections in the USA[74]. Although HA- and CA-MRSA were initially separate populations, this distinction has become blurred due to horizontal gene transfer between the two groups, and CA-MRSA strains are the leading cause of hospital-onset infections in the USA[67,75].

In addition to infecting humans, a third epidemiological form of MRSA has emerged in farm and domesticated animals, termed livestock-associated MRSA (LA-MRSA)[6]. Methicillin-resistance in LA-MRSA is conferred by the *mecC* gene, which is contained on SCC*mec* XI and has a 69% nucleotide identity to *mecA*[76]. The dominant LA-MRSA strain in Europe and the USA is ST398, which is primarily associated with pigs but has since been reported in other animal species, including cattle, chickens and horses[77,78]. A study by Price *et al.* (2012) found that ST398 originated as MSSA in humans, and that the β-lactam resistance in ST398 has evolved multiple times independently since its host jump from humans, implicating that antibiotic use in food animal production is a major driving force for the emergence of resistance[78]. Furthermore, host-switch events between humans and animals have led to the emergence of epidemic strains in new host populations. For example, CC97 is a major cause of bovine mastitis, but there have been increased reports of this lineage being associated with human infections[6,79]. This highlights the ability of *S. aureus* strains to spread and adapt to different host populations, as well as the impact of livestock production methods on the development of antibiotic resistance.

1.1.5.3 Vancomycin resistance

The widespread prevalence of MRSA has led to the increased use of the glycopeptide antibiotic vancomycin, and with it, selection for isolates with reduced vancomycin susceptibility[80]. Vancomycin inhibits peptidoglycan synthesis, but instead of acting as a structural mimic like the β-lactams, inhibition is achieved by binding to the terminal D-Ala D-Ala group of peptidoglycan precursors, which prevents cross-linking by PBPs[81,82].

Resistance to vancomycin has emerged in two forms, resulting in vancomycin-intermediate *S. aureus* (VISA) and vancomycin-resistant *S. aureus* (VRSA)[80,83]. VISA strains display reduced susceptibility to vancomycin and were first reported in 1997[80,84]. The minimum inhibitory concentration (MIC) of vancomycin in VISA strains is 4 to 8 μg/ml, though these strains can also exist as a sub-population within a vancomycin-sensitive *S. aureus* (VSSA) strain (vancomycin MIC of < 2 μg/ml), known as heterogenous VISA (hVISA)[81,85–87]. VISA strains have acquired adaptive mutations in response to vancomycin exposure, leading to increased peptidoglycan synthesis and thickened cell walls. The excess D-Ala D-Ala residues are thought to sequester vancomycin, while also reducing diffusion to sites of peptidoglycan synthesis[56,81]. Mutations have been reported in the accessory gene regulator (*agr*) operon, which is involved in virulence[88–90]; the vancomycin-resistance associated (*vra*) operon, involved in cell wall homeostasis[91,92]; and in subunits of RNA polymerase (RNAP)[93,94]. The sequential acquisition of these mutations leads to a gradual increase in the MIC[81].

VRSA strains were first identified in 2002 and are defined as having an MIC of > 16 μg/ml, although strains with vancomycin MICs of > 32 μg/ml have been reported[85,87,95]. Resistance is mediated by the *vanA* operon, acquired via horizontal gene transfer from vancomycin-resistant *Enterococcus faecalis* (VRE)[81,95]. The *vanA* operon encodes the alternative terminal peptide D-alanyl-D-lactose (D-Ala D-Lac), which is not recognised by vancomycin and enables *S. aureus* to continue with peptidoglycan synthesis in the presence of the antibiotic[56,96]. Although vancomycin resistance is not common, the emergence of VISA and VRSA strains is a concern due to the antibiotic being one of the first-line therapies for MRSA infections[17,81,95].

1.1.5.4 Daptomycin resistance

Daptomycin is a lipopeptide antibiotic that is used as a last resort for treating serious MRSA infections[97]. While the exact mechanism of action is still unclear, daptomycin has been shown to insert into and form oligomeric complexes withinin the membrane of Gram-positive bacteria. These oligomeric complexes disrupt the membrane integrity, leading to cell death[98–100].

Although resistance to daptomycin is rare, several mechanisms have been reported in *S. aureus* clinical isolates, including changes to membrane composition, cell wall homeostasis and cell membrane charge[98,101]. For example, gain-of-function mutations in the multiple peptide resistance factor (*mprF*) gene increases lysyl-phosphatidylglycerol content in the cell membrane, which is proposed to stabilise the membrane and/or repel the antibiotic[98,102]. Another mechanism is enhanced expression of the D-alanyl-lipoteichoic acid (*dlt*) operon. This increases D-alanine incorporation into teichoic acid, which has been suggested to repel daptomycin from the bacterial membrane[98]. Daptomycin resistance has also been associated with disruption of the *agr* operon, disruption of the cell wall stress stimulon and mutations in RNAP subunits[93,100,101,103].

Due to the emergence of VISA and VRSA strains, the clinical use of daptomycin is increasing and reports of resistance are becoming more common[101]. Since daptomycin is an antibiotic of last resort, treatment failure leads to poor patient outcomes. Therefore, it is necessary to develop new therapeutic strategies for the treatment of serious MRSA infections.

1.2 Immune response to *S. aureus* bloodstream infection

1.2.1 Recognition of *S. aureus* in the bloodstream

1.2.1.1 Pattern recognition receptors (PRRs)

The bloodstream contains many circulating immune cells, including dendritic cells, neutrophils and monocytes, which are precursors to tissue macrophages[104]. These immune cells express specialised cell-surface receptors, known as pattern recognition receptors (PRRs), that are capable of recognising pathogens such as *S. aureus*[105]. PRRs bind directly to surface-bound or secreted bacterial products, known as pathogen-associated molecular patterns (PAMPs) (Figure 1.2A). PAMPs are conserved microbial components that are not produced by mammals and include peptidoglycan, lipopolysaccharide and unmethylated cytosine-phosphate-guanosine (CpG) motifs on DNA[105,106].

Binding of PAMPs to PRRs primes immune cells to undertake phagocytosis, stimulates bactericidal activity in neutrophils, and induces the release of cytokines and chemokines, which promote the recruitment and activation of other immune cells[104,107]. PRR binding also enables the function of antigen-presenting cells (APCs), such as dendritic cells, that process and display foreign antigens to T cells for the adaptive immune response[105,108]. The importance of PRRs in host defence is demonstrated by the enhanced susceptibility of TLR2 deficient mice to *S. aureus* infection when compared to wild-type mice[109].

There are several different types of PRRs, including Toll-like receptors (TLRs) and nucleotide oligomerisation domain (NOD)-like receptors (NLRs)[105]. The TLR family consists of ten membrane-bound receptors that each recognise different PAMPs[110]. These receptors may be found on the cell membrane or the endosomal membrane, which enables the recognition of both extracellular and engulfed pathogens[104]. *S. aureus* PAMPs that are recognised by TLRs include peptidoglycan (TLR2), leukocidins (TLR4), CpG-rich DNA (TLR9) and diacylated lipoproteins (TLR2/6 heterodimers)[111–113]. Another family of PRRs are the NLRs, which are located in the cell cytoplasm[105]. The two most significant NLRs are NOD1 and NOD2, which detect bacterial molecules produced during peptidoglycan synthesis and/or degradation[114].

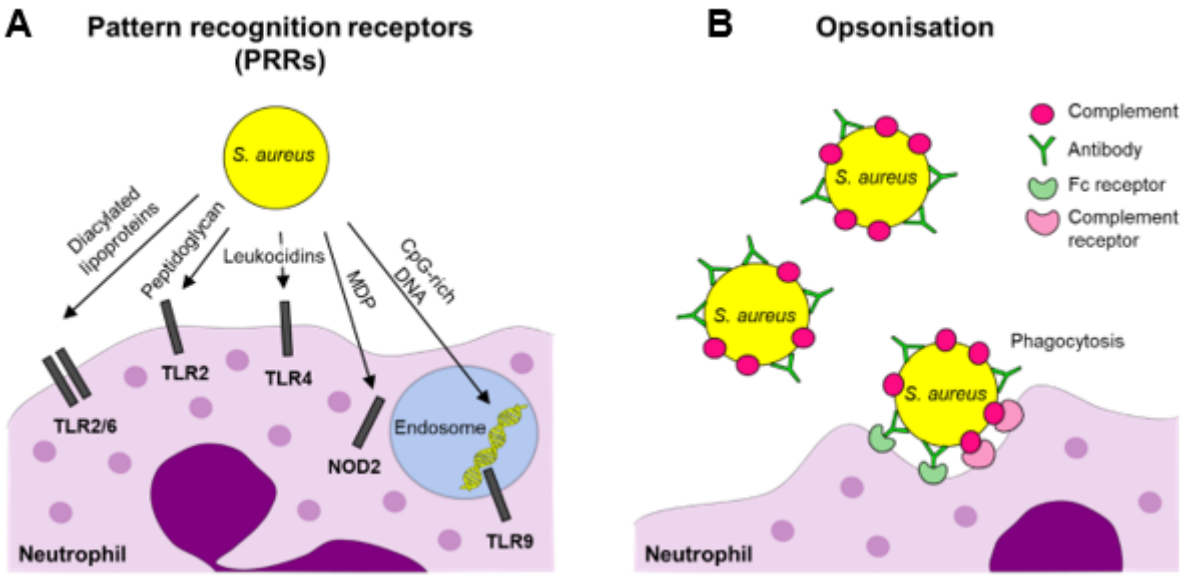

Figure 1.2. Recognition of *S. aureus* in the bloodstream.
Recognition of *S. aureus* by immune cells can occur directly via PRRs **(A)**, or indirectly via opsonisation **(B)**. PRRs include TLRs (such as TLR2, TLR4 and TLR9) and NLRs (such as NOD2), which bind to different pathogen-associated molecular patterns (PAMPs) to induce immune priming and activation. Opsonisation by complement and/or antibodies is required for phagocytosis, which is triggered by the binding of opsonins to their appropriate receptors on the host cell. TLR, toll-like receptor; NLR, NOD-like receptor; MDP, muramyl dipeptide.

NOD1 recognises γ-D-glutamyl-meso-diaminopimelic acid (iE-DAP), which is produced by most Gram-negative bacteria[115,116]. In contrast, NOD2 is activated by muramyl dipeptide (MDP), which is found in all types of peptidoglycan[117,118].

1.2.1.2 Opsonisation of S. aureus

Although PRRs are important for the detection of *S. aureus* by immune cells, the efficiency of phagocytosis is enhanced if bacteria are coated with host serum proteins, such as antibodies and/or complement system components, in a process known as opsonisation (Figure 1.2B)[104].

During *S. aureus* infection, antibodies may be generated against bacterial antigens as part of the adaptive immune response. This response occurs later during the course of infection and is dependent on antigen presentation by APCs, which leads to T cell activation and production of antibodies by B-cells[119]. These antibodies bind to surface antigens, such as *S. aureus* iron surface determinant B (IsdB)[120], via their antigen-binding

fragment (Fab) regions. Meanwhile, the fragment crystallisable (Fc) region of the antibody is recognised by immune cells via Fc receptors, inducing phagocytsis[104]. In addition to opsonisation of *S. aureus*, antibodies can activate the classical complement pathway and also neutralise toxins, such as α-haemolysin (α-toxin, Hla)[121,122]. However, the production of antibodies against *S. aureus* rarely prevent infection, suggesting that the adaptive memory response is not completely effective[119].

The human complement system is made up of more than 30 proteins that rapidly recognise and opsonise pathogens, activating a cascade that enables detection of pathogens even when numbers are low[104,122]. Complement activation occurs though thee different pathways. The classical pathway is initiated by binding of the C1 complex (complement component 1, made up of the subcomponents C1q, C1r and C1s) to antibody-antigen complexes on the surface of bacteria. The alternative pathway is initiated by spontaneous hydrolysis of C3, but due to the inhibition factors H and I in blood plasma, only activates fully on the surface of invading bacteria. The lectin pathway is initiated by the binding of mannose-binding lectin (MBL) or ficolins to carbohydrates on the surface of bacteria, leading to the activation of MBL-associated serine proteases. All thee pathways eventually lead to the formation of C3 convertases, which are enzyme complexes that catalyse the key reaction in complement activation, namely the cleavage of the complement protein C3 into C3a and C3b[122,123]. Activation of complement results in the production of anaphylatoxins (such as C3a) to attract immune cells and promote inflammation, and opsonins (such as C3b, iC3b and C1q) to promote phagocytosis[105].

1.2.2 Neutrophil recruitment and phagocytosis

The most abundant immune cells in the bloodstream are neutrophils, which make up 60% of the leukocyte population and are a critical component of the innate immune response[122]. Neutrophils are derived from pluripotent haematopoietic stem cells in the bone marrow, where they take approximately 6.5 days to mature, after which they are released into the bloodstream[124,125]. Neutrophils circulate in the bloodstream for 10 to 24 hours before migration into infected tissues, and may function for an additional 1 to 2 days before undergoing apoptosis and clearance by macrophages[105,124]. Approximately 10^6 neutrophils are found within 1 ml of human blood, enabling the host to respond rapidly and robustly to infection[126]. In addition, neutrophil production increases upon infection, which provides a large number of neutrophils for a potent immune response[127,128].

Neutrophils are the most important line of defence against *S. aureus* infections, which is highlighted by the recurrent staphylococcal infections in patients with neutropenia (abnormally low number of neutrophils) or disorders of neutrophil function[122,129]. For example, neutrophils derived from individuals with Chédiak-Higashi syndrome or chonic granulomatous disease (CGD) show reduced bactericidal capabilities and individuals are paticularly prone to staphylococcal infection[130,131].

As part of the initial respose to bacterial invasion, neutrophils are recruited to sites of infection by chemokines, anaphylatoxins and other chemoattractants, including molecules secreted or shed by bacteria[132]. Host-derived chemotactic factors include interleukin 8 (IL-8), C-X-C motif chemokine ligand 1 (CXCL1) and the complement component C5a[133]. Chemoattractants derived from bacteria include lipoteichoic acid (LTA) or formylated peptides such as N-formylmethionine, which is required for protein synthesis in bacteria but not in eukaryotes[134,135]. Athough neutrophils are generally short lived, the release of pro-inflammatory cytokines such as interferon-γ (IFN-γ) and tumour necrosis factor-α (TNF-α) leads to a delay in neutrophil apoptosis, likely enhancing the efficiency of pathogen recognition and removal[136].

Once they reach the site of infection, neutrophils bind and ingest *S. aureus* in a process known as phagocytosis, which is the major mechanism for removal of pathogens. Phagocytosis requires opsonisation of *S. aureus* by host serum molecules (section 1.2.1.2 above), and occurs via an active, receptor-mediated process[137]. Direct uptake of the opsonised bacteria is mediated by the binding of distinct complement and Fc receptors on the neutrophil, triggering membrane reorganisation and actin polymerisation[127]. Complement receptors include CR1 (CD35), CR3 (CD11b/CD18) and CR4 (CD11c/CD18), all of which are constitutively expressed on the surface of neutrophils[138].

The most important Fc receptors (FcRs) for inducing phagocytosis of opsonised *S. aureus* are Fcγ receptors (FcγRs), which bind to immunoglobulin G (IgG), the most common type of antibody[104]. Neutrophils express thee types of Fcγ (FcγRI-III). FcγRI (CD64) binds monomeric IgG with high affinity, whereas FcγRII (CD32) binds monomeric IgG with low affinity but has a higher affinity for IgG dimers or aggregates. Meanwhile, FcγRIII (CD16) binds IgG complexes with low affinity and the FcγRIIIb isoform is exclusively and highly expressed on neutrophils, with approximately 150,000 receptors per cell[139]. The efficiency of phagocytosis is maximised by the combined action of PRRs and opsonin receptors[105].

1.2.3 Killing of *S. aureus* by neutrophils

1.2.3.1 The oxidative burst

Phagocytosis of pathogens by neutrophils leads to an oxygen-dependent process known as the oxidative (or respiratory) burst, which is the most important defence mechanism against *S. aureus*. The oxidative burst occurs within the phagosome approximately 20 to 90 minutes after uptake, and involves the rapid generation and release of reactive oxygen species (ROS) (Figure 1.3)[140]. The importance of the oxidative burst is demonstrated by the high incidence of *S. aureus* infections in chonic granulomatous disease (CGD) patients, who lack a functional NADPH oxidase enzyme and cannot generate ROS[141]. In addition, deletion of NADPH oxidase in mice is associated with increased susceptibility to *S. aureus* infections[142], and treatment of

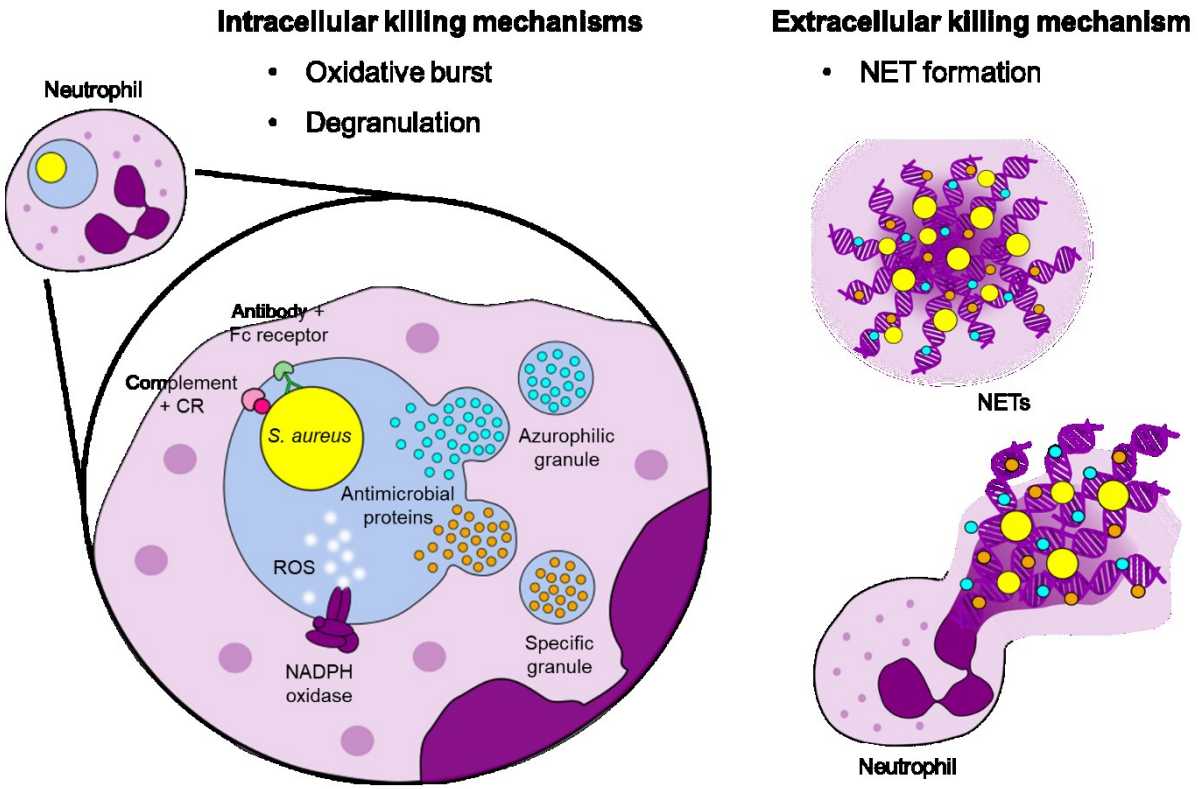

Figure 1.3. Neutrophil killing mechanisms.

Neutrophils are capable of killing *S. aureus* intracellularly by inducing the oxidative burst and degranulation, exposing phagocytosed bacteria to ROS and antimicrobial proteins, respectively. Neutrophils can also form neutrophil extracellular traps (NETs) by releasing chomatin, histones and granule contents into the extracellular environment to trap and kill bacteria. CR, complement receptor.

isolated human neutrophils with the NADPH-oxidase inhibitor diphenyleneiodonium (DPI) has been shown to reduce the killing rate of *S. aureus*[143].

Generation of ROS requires the activity of nicotinamide adenine dinucleotide phosphate (NADPH) oxidase, which is assembled at the phagosomal membrane during phagocytosis[144,145]. This enzyme uses molecular oxygen to produce superoxide ($O_2^{\bullet-}$), which rapidly dismutates to yield hydrogen peroxide (H_2O_2) (Figure 1.4). Although $O_2^{\bullet-}$ and H_2O_2 have limited capacity to kill bacteria directly, they give rise to generate secondary ROS, such as the hydroxyl radical ($^{\bullet}OH$), hypochlorous acid (HOCl) and singlet oxygen ($^1O_2$), all of which are more reactive and therefore effective at killing phagocytosed bacteria[146].

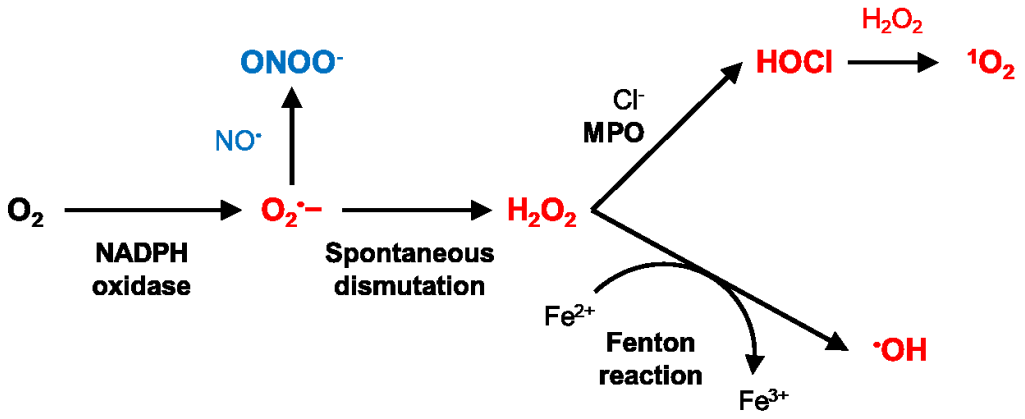

Figure 1.4. Generation of ROS and RNS.

The first step of ROS generation is the reduction of oxygen (O_2) to superoxide ($O_2^{\bullet-}$), catalysed by NADPH oxidase. $O_2^{\bullet-}$ undergoes spontaneous dismutation to form hydrogen peroxide (H_2O_2), which can be used to generate hypochlorous acid (HOCl, catalysed by MPO), singlet oxygen ($^1O_2$) and the hydroxyl radical ($^{\bullet}OH$, via the Fenton reaction). $O_2^{\bullet-}$ can also react with nitric oxide ($NO^{\bullet}$; generated by inducible nitric oxide synthase, iNOS) to generate peroxynitrite ($ONOO^-$) and other RNS. ROS are shown in red and RNS shown in blue. MPO, myeloperoxidase.

The hydroxyl radical is generated from the reaction of H_2O_2 with ferrous iron (Fe^{2+}), via a process called the Fenton reaction (Figure 1.4)[147]. This reaction also generates hydroxide and ferric iron (Fe^{3+}), which can be reduced back to ferrous iron with $O_2^{\bullet-}$, via the Haber-Weiss reaction[148]. The $^{\bullet}OH$ species is the most reactive of all ROS and the only one that can directly damage any biological molecule at diffusion-limited rates, making it a significant contributor to ROS-mediated killing of bacteria[149–151]. Another ROS is HOCl, which is generated from the myeloperoxidase (MPO)-catalysed reaction of H_2O_2 with chloride (Figure 1.4)[148]. Further reaction of HOCl with H_2O_2 leads to the generation of singlet oxygen (Figure 1.4), which has been shown to kill *S. aureus* bacteria *in vitro*[148,152]. However, although MPO deficiency affects at least 1 in 4000 people, these individuals only show an increased susceptibility to *Candida* infections, with no difference in susceptibility to *S. aureus* infection[153]. This contrasts dramatically with CGD patients, which suggests that whilst the oxidative burst is needed for efficient killing of *S. aureus*, MPO is not.

The biological targets of ROS are proteins, lipids and nucleic acids. Examples of protein damage mediated by ROS include peptide bond cleavage, protein carbonylation, and oxidation of amino acid residues (particularly cysteine or methionine residues)[154]. Perhaps most importantly, H_2O_2 is able to diffuse freely across the bacterial cell membrane to oxidise solvent-exposed iron-sulphur (Fe-S) clusters and release free iron, which can react with H_2O_2 to yield the highly-reactive hydroxyl radical (Figure 1.4)[155]. ROS can also attack membrane lipids such as glycolipids and phospholipids in a process known as lipid peroxidation. This process involves the production of fatty acid radicals, which initiate chain oxidation of polyunsaturated phospholipids and can lead to impaired membrane function[156].

However, the most significant impact of the oxidative burst is believed to be upon DNA, because DNA damage can be lethal if not repaired[147,151,157–160]. ROS can react with the base or sugar groups of DNA, producing lesions such as strand breakage, DNA crosslinks, or base alterations that can cause mispairing (e.g. 8-oxo-2'-deoxyguanosine with adenine)[161,162]. Imlay *et al.* (1988) found that even a 10-minute exposure to millimolar levels of H_2O_2 created enough DNA damage to kill bacteria[147].

Although ROS generally eliminate bacteria by causing oxidative damage, they can also kill microbes in an indirect, non-oxidative manner[145]. For example, $O_2^{\bullet-}$ production leads to an increased phagosomal concentration of K^+ to compensate for the negative charge. This promotes the activation of granule enzymes, which then kill bacteria by proteolytic attack[163]. Additionally, quorum-sensing (cell-density dependent) signalling molecules in *S. aureus* can be inactivated by HOCl, leading to a decrease in bacterial virulence and contributing towards clearance of *S. aureus*[164].

In addition to the oxidative burst, neutrophils are able to generate reactive nitrogen species (RNS) that can react with biological molecules and inhibit metabolic processes, using a similar mechanism to ROS[165]. Most RNS are derived from the reaction of $O_2^{\bullet-}$ with nitric oxide ($NO^{\bullet}$), which leads to the production of peroxynitrite ($ONOO^-$) (Figure 1.4). The $NO^{\bullet}$ for this reaction is generated by inducible nitric oxide synthase (iNOS) during the conversion of

L-arginine to L-citrulline[165]. Further reactions with $ONOO^-$ can lead to other types of RNS, such as nitrogen dioxide ($^{\bullet}NO_2$) and dinitrogen trioxide (N_2O_3)[166].

RNS have been shown to protect mice from *S. aureus* infections[167,168]. In addition, iNOS-dependent $NO^{\bullet}$ production can be detected in immune cells exposed to staphylococcal LTA[169], and $NO^{\bullet}$ has been shown to increase killing of phagocytosed *S. aureus* by cytokineplasts (motile anucleate fragments induced from neutrophils, with few granules and no oxidative burst activity)[170]. However, although RNS contribute to the killing of *S. aureus*, they are not essential for clearance of the pathogen[170]. However, since iNOS deficiency has not been demonstrated in humans its role in human immunity is unclear[165].

1.2.3.2 Degranulation

Neutrophils produce a wide variety of antimicrobial molecules that are stored within cytoplasmic granules. Phagocytosis leads to the rapid fusion of these granules with bacteria-containing phagosomes, a process known as degranulation (Figure 1.3)[171]. Thee types of cytoplasmic granules are found within neutrophils: azurophilic granules (also called primary granules), specific (secondary) granules and gelatinase (tertiary) granules[137].

The azurophilic granules contain lysozyme, MPO, bactericidal/permeability-increasing protein (BPI), azurocidin and a number of serine proteases (elastase, proteinase 3, cathepsin G)[105,137]. These granules also contain α-defensins, cationic antimicrobial peptides (AMPs) that comprise up to 50% of the granule protein content and form pores in bacterial membranes[172]. Meanwhile, the specific granules contain an integral membrane component of NADPH oxidase (flavocytochome b_{558}), in addition to lysozyme, collagenase, neutrophil gelatinase-associated lipocalin (NGAL) and human cationic antimicrobial protein 18 (hCAP-18)[173,174]. Specific granules also contain lactoferrin for the sequestration of iron, which is an essential metal required for bacterial growth[175]. Another chelator is calprotectin, which is not stored in the granules, but inhibits growth of *S. aureus* by sequestering manganese and zinc[176]. Finally, the gelatinase granules contain metalloproteases, such as gelatinase and leukolysin[137].

Some of the antimicrobial molecules found within granules are able to kill *S. aureus* (e.g. cathepsin G, hCAP-18)[177,178] and neutralise staphyloccocal toxins (e.g. defensins, elastase)[122,179]. However, unlike other pathogens such as *E. coli* and *Streptococcus pneumoniae*[180,181], *S. aureus* is resistant to many granule proteins (section 1.3.3.2). As a result, the oxidative burst is the key mechanism for the killing of *S. aureus*.

1.2.3.3 Neutrophil extracellular traps (NETs)

In addition to intracellular killing via the oxidative burst and degranulation, neutrophils are able to kill *S. aureus* extracellularly though a mechanism called NETosis[182–184]. During this process, neutrophils expel their nuclear contents together with granule proteins to form networks of extracellular fibres, called neutrophil extracellular traps (NETs) (Figure 1.3). These networks are primarily composed of DNA. NETs bind to bacteria, limiting their spread and dissemination, as well as enhancing the effective concentrations of extruded antimicrobial agents, which promotes killing of attached pathogens[105]. For example, Brinkman *et al.* (2004) showed that NETosis was able to kill around 30% of a *S. aureus* inoculum, even when phagocytosis was blocked (via cytochalasin D, an actin filament inhibitor)[182]. In addition, NETs may neutralise staphylococcal toxins, with histones and BPI capable of degrading α-haemolysin[182].

Although several essential steps in NET formation have been described, the mechanisms for initiation, downstream activation pathways and effector functions are still poorly understood[122]. Experiments performed *in vitro* have found that NETosis can be stimulated by IL-8, platelets, lipopolysaccharide (LPS), and the staphylococcal toxins Panton–Valentine leukocidin (PVL) and leukotoxin GH (LukGH)[182,184–186]. NETosis requires ROS production, because neutrophils from CGD patients are unable to form NETs[187].

The formation of NETs by neutrophils can result in cell death (suicidal NETosis) or vital NET release (vital NETosis), in which neutrophils are still able to perform phagocytosis[188,189]. Suicidal NETosis occurs after a few hours of stimulation and involves ROS production by NADPH oxidase, which activates the protein-arginine deiminase 4 (PAD4) enzyme. This enzyme decondenses chomatin, enabling its association with granular proteins,

and NETs are released though disruption of the cell membrane[188]. Meanwhile, vital NETosis is induced within minutes by *S. aureus* though the joint activation of complement receptors and TLR2[190]. As in suicidal NETosis, PAD4 is activated, which leads to chomatin decondensation. However, NETs are released via vesicles instead, allowing neutrophils to stay alive and maintain their host defensive functions, including chemotaxis, phagocytosis and intracellular killing of bacteria[188–190].

1.2.4 Other defence mechanisms against *S. aureus* in the bloodstream

1.2.4.1 Nutritional immunity

Transition metals such as iron, zinc, and manganese are important cofactors for enzymes involved in key metabolic processes, including respiration and DNA synthesis[191]. It has been estimated that up to one-third of all proteins require a metal cofactor, with the use of each metal varying from cell to cell[192,193]. Consequently, another host defence mechanism against invading pathogens is to sequester these essential metals though a process called nutritional immunity[194]. This limits the availability of these metals in the bloodstream, which restricts bacterial growth[176,195].

The best-studied example of nutritional immunity is the host sequestration of iron. The importance of iron sequestration is highlighted in patients with thalassaemia, who have increased levels of free iron in the blood and are more susceptible to serious infections[196]. Generally, the majority (80%) of iron in the host is complexed to haem and in haemoproteins such as haemoglobin, haptoglobin and myoglobin[197]. Free haem is sequestered by the plasma glycoprotein haemopexin, which transports it to the liver for breakdown and iron recovery[196]. Since iron is insoluble in blood due to the presence of oxygen and neutral pH, it is transported bound to transferrin[197]. Any free iron is rapidly captured by transferrin molecules, which are rarely fully saturated, or taken up by macrophages where it is bound to ferritin for storage[196].

1.2.4.2 Platelets

Platelets (also called thombocytes) are an important component of blood and are required for stopping bleeding after vessel damage[198]. Platelets bind to the site of damage, which stimulates platelet activation and initiation of the coagulation cascade. This results in the conversion of prothombin into thombin, which in turn converts fibrinogen to fibrin. Aggregation of fibrin traps platelets and erythocytes, leading to the formation of a thombus (blood clot)[199].

In addition to their role in vascular repair, platelets contribute to host immunity, expressing receptors such as FcγRIIa and TLRs (e.g. TLR2, TLR4)[200,201]. These enable platelets to recognise several PAMPs, leading to the activation of complement and circulating neutrophils. For example, stimulation of platelet TLR4 increases NET formation[185], while the formation of platelet-neutrophil complexes via platelet P-selectin (CD62P) promotes neutrophil activation[202]. Platelets can also activate immune cells by releasing phospholipid vesicles containing cytokines such as IL-1β[198,203].

In addition to detecting pathogens, platelets contribute to bacterial killing though the release of small, cationic antimicrobial peptides, called platelet microbicidal proteins (PMPs)[204]. These are induced at sites of endovascular infections, via thombin generation or microbe-induced platelet aggregation, and are effective against a broad range of pathogens, including some strains of *S. aureus* and viridans-group streptococci[199,204,205]. Clinical isolates of *S. aureus* that are susceptible to thombin-inducible PMPs (tPMP) *in vitro* are cleared more rapidly from the bloodstream and are less likely to cause endovascular infections[199,204,206]. Upon activation by thombin, tPMPs kill bacteria by disrupting the cell membrane[207]. tPMPs released from platelets include the microbicidal chemokines (kinocidins) platelet factor 4 (PF4), connective tissue activating peptide 3 (CTAP3) and fibrinopeptide B (FpB)[199]. In addition, sub-lytic concentrations of *S. aureus* α-haemolysin can activate platelets and expose the pathogen to tPMPs, suggesting that α-haemolysin production may not benefit *S. aureus* during endovascular infections such as endocarditis[208].

1.3 *S. aureus* evasion of host defences in the bloodstream

S. aureus has evolved an abundant repertoire of secreted and surface-bound molecules with the potential to inhibit neutrophil recruitment, evade phagocytosis and provide protection against host killing mechanisms (Figure 1.5). *S. aureus* is also capable of secreting toxins that have the ability to lyse immune cells. The significant redundancy of these molecules reflects the importance of host defences and their role in the outcome of an infection[105,123].

1.3.1 Inhibition of neutrophil recruitment

Rapid recruitment of neutrophils to the site of infection promotes clearance of the pathogen, which reduces the likelihood of serious damage to the host and dissemination to other parts of the body. Although staphylococcal PAMPs are recognised by the immune system, *S. aureus* also secretes virulence factors that target receptors involved in neutrophil chemotaxis. For example, staphylococcal superantigen-like 10 (SSL10) binds to the C-X-C motif chemokine receptor 4 (CXCR4), inhibiting the action of the chemokine CXCL12[209]. Meanwhile, SSL5 binds to the N-terminal region of formyl peptide receptors 1 and 2 (FPR1 and FPR2), which prevents the detection of formylated peptides[210].

Another secreted molecule is the chemotaxis inhibitory protein of *Staphylococcus* (CHIPS), which is a 14.1-kDa protein produced by approximately 60% of *S. aureus* strains[122,123]. CHIPS prevents neutrophils from responding to both host- and bacteria-derived chemoattractants. Neutrophil activation by host-derived C5a is inhibited by binding of CHIPS to the C5a receptor (C5aR), whereas detection of bacteria-derived formylated peptides is inhibited by CHIPS binding to FPRs[211,212]. A search for homologous proteins to CHIPS led to the discovery of the FPR-like 1 inhibitory protein (FLIPr) and FLIPr-like. Both FLIPr and FLIPr-like can inhibit FPR2, whilst only FLIPr-like can inhibit FPR1[213].

In addition to blocking neutrophil receptors, *S. aureus* produces the cysteine protease staphopain A (ScpA). This protein inhibits neutrophil chemotaxis by cleaving the N-terminal region of CXCR2, which blocks detection of IL-8[214].

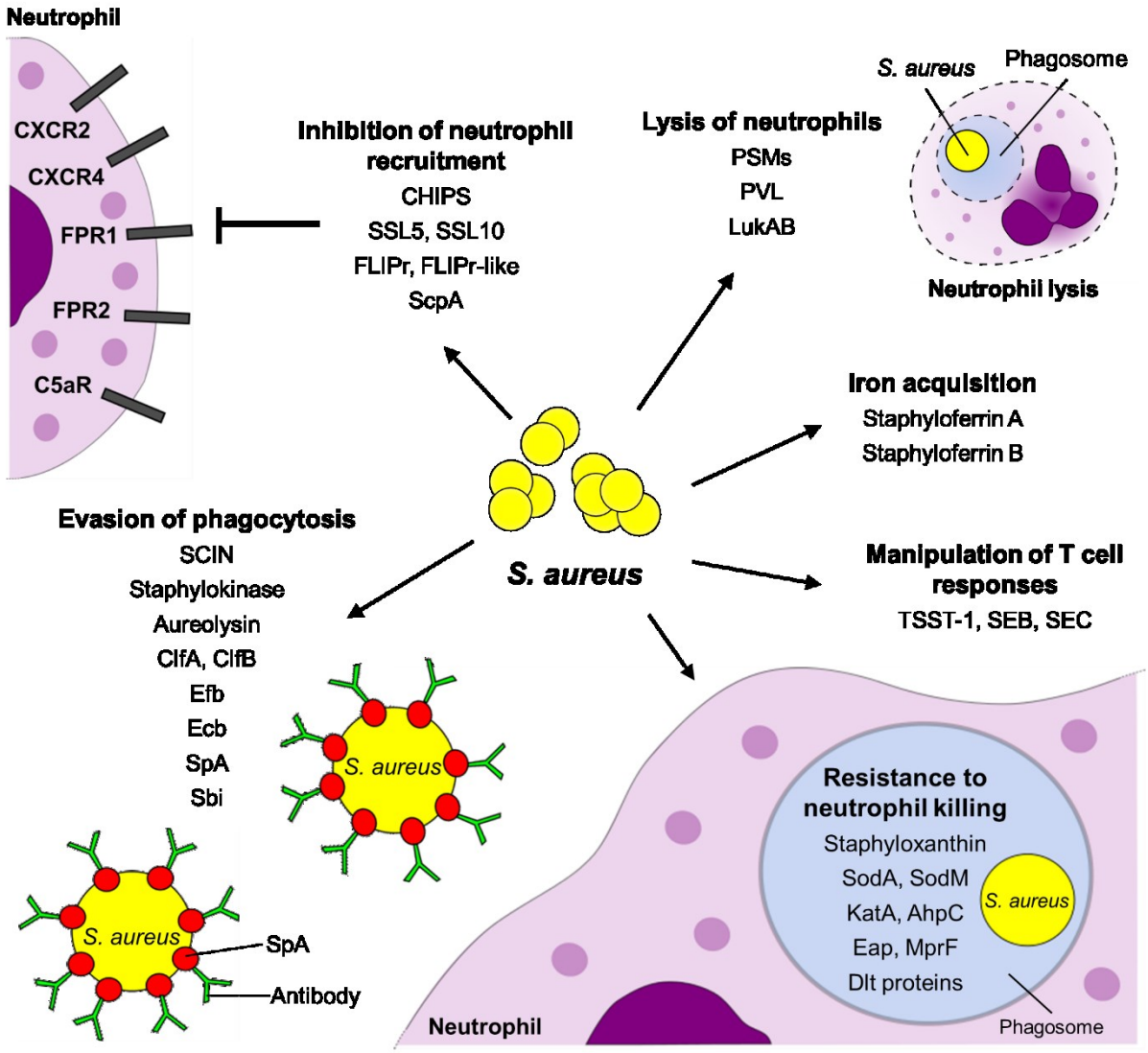

Figure 1.5. *S. aureus* evasion of host defences in the bloodstream.

S. aureus has developed numerous strategies to evade the immune response, including inhibition of neutrophil recruitment by blocking receptors involved in chemotaxis, and disruption of opsonisation and phagocytosis by creating a protective coat of host proteins. In addition, *S. aureus* can resist neutrophil killing by secreting enzymes to detoxify ROS, modifying the cell wall to repel AMPs, and releasing toxins to lyse the host cell. Other strategies include secretion of siderophores for iron acquisition and overstimulation of the immune response via staphylococcal superantigens.

1.3.2 Evasion of phagocytosis

S. aureus can evade phagocytosis by disrupting the binding of complement and antibodies to staphylococcal antigens. The staphylococcal complement inhibitor (SCIN) stabilises C3 convertases, inhibiting cleavage of C3 and the generation of C3a and C3b for opsonisation[215]. Complement can also be targeted without direct binding to C3 convertases. For example, extracellular fibrinogen-binding (Efb) and extracellular complement-binding (Ecb) proteins bind to C3b deposited on the bacterial cell membrane, as well as to C3 to prevent its cleavage[216–218]. In addition, Efb can recruit fibrinogen to form a thick layer on the bacterial surface, blocking recognition by complement receptors[217]. Another secreted molecule is aureolysin, a metalloprotease that cleaves C3 to yield inactive C3a' and C3b'[219].

To prevent phagocytosis mediated by antibodies, *S. aureus* produces staphylococcal protein A (SpA). This protein binds to the Fc region of IgG, coating the bacterial surface with non-specific antibodies (in the wrong orientation) to prevent binding of Fcγ receptors and antigen recognition[105,220]. Another protein that binds to the Fc region of IgG is staphylococcal binding immunoglobulin (Sbi), the loss of which leads to reduced survival of *S. aureus* in whole human blood[221,222]. Sbi can exist in an anchored form where it binds to LTA in the cell wall, or in a secreted form that can bind and inactivate C3[223,224]. *S. aureus* also produces staphylokinase, a serine protease that targets both antibody and complement by cleaving C3b or the Fc region to prevent neutrophil phagocytosis[225].

S. aureus can also evade phagocytosis by generating a protective coat made of capsular polysaccharides or host proteins, which prevents the deposition of complement and antibodies[32,226]. For example, the virulence factors clumping factor A (ClfA), ClfB and the fibronectin-binding proteins (FnBPs) all bind to host extracellular matrix (ECM) proteins present in serum[27]. *S. aureus* can also hijack the coagulation cascade by secreting von-Willebrand factor-binding protein (vWbp) and coagulase (Coa). These two coagulases activate prothombin, leading to the generation of a fibrin-containing pseudocapsule that can act as a mechanical barrier against neutrophils[227]. However, despite the numerous mechanisms used to evade immune uptake, *S. aureus* in blood is still rapidly taken up by neutrophils[4,222,228].

1.3.3 Resistance to neutrophil killing mechanisms

Upon phagocytosis, *S. aureus* adapts to the phagosomal environment by altering its gene expression[69]. Approximately one third of the genome is differentially regulated, with many of these changes, such as the up-regulation of genes involved in oxidative stress resistance and virulence, linked to exposure to oxidative and non-oxidative killing by neutrophils[69,229]. In addition, a report by Schwartz *et al.* (2009) found that approximately 20% of phagocytosed *S. aureus* was still viable inside the neutrophil phagosome after two hours, indicating that *S. aureus* is able to resist neutrophil killing to some extent[230].

1.3.3.1 Evasion of oxidative killing

Survival of *S. aureus* inside the phagosome involves the production of molecules that can neutralise the cytotoxic effects of ROS. Production of staphyloxanthin, the carotenoid pigment responsible for the golden colour of *S. aureus*, functions as an antioxidant and provides resistance to killing by H_2O_2 and singlet oxygen[4]. A mutant defective in staphyloxanthin was shown to be more susceptible to neutrophil killing *in vitro*, and was also less virulent in a mouse subcutaneous abscess model and a systemic infection model, when compared to the pigmented wild-type strain[4,231]. Resistance to singlet oxygen is also provided by surface factor promoting resistance to oxidative killing (SOK), though the mechanism for this is as yet undefined[232].

In addition to staphyloxanthin and SOK, *S. aureus* produces a number of enzymes to degrade and detoxify ROS. The superoxide dismutases, SodA and SodM, convert $O_2^{\bullet-}$ (generated from internal and external sources, respectively) into molecular oxygen and H_2O_2[233], which can be further reduced to water and oxygen by catalase (KatA) or alkyl hydroperoxide reductase (AhpC)[234]. *S. aureus* also produces enzymes in response to RNS. For example, flavohaemoglobin (Hmp) breaks down $NO^{\bullet}$, and L-lactate dehydrogenase (L-LDH) maintains redox-homeostasis and survival within neutrophils by enabling L-lactate production during nitrosative stress[168,235].

S. aureus can also repair biological molecules that are damaged by ROS. Since DNA damage is a key consequence of ROS *in vitro* and believed to be the major mechanism of ROS-mediated bacterial killing[147,151,157–160], *S. aureus* has a number of DNA repair systems (section 1.4). In addition, DNA damage via ROS frequently activates the SOS response pathway, which is a global response to DNA damage that leads to induction of DNA repair (section 1.4.1). Meanwhile, metallo-regulated gene A (MrgA) protects DNA by compacting the nucleoid during oxidative stress[236].

To repair oxidised proteins, *S. aureus* expresses several methionine sulphoxide reductases (MsrA1, MsrA2, MsrA3 and MsrB) that reverse the oxidation of methionine[237,238]. The role of these enzymes in *S. aureus* resistance to oxidative killing was shown by Pang *et al.* (2014), who found that deletion of *msrA1* and *msrB* increased the susceptibility of the pathogen to exogenous H_2O_2 and killing by neutrophils[239]. *S. aureus* has also evolved mechanisms to repair Fe-S clusters, including the cysteine desulphurase enzyme iron-sulphur cluster S (IscS)[240], and the iron-sulphur cluster repair protein ScdA, which can be induced by exposure to H_2O_2[241,242]. In addition, the thioredoxin system in *S. aureus* is enhanced under conditions of oxidative stress to scavenge ROS. This system is comprised of thioredoxin (TrxA), a small disulphide reductase protein important for redox signalling and maintaining a reduced cytoplasm, and the thioredoxin reductase TrxB, which maintains TrxA in a reduced state[243].

Bacteria have evolved multiple transcriptional regulators to detect ROS levels and coordinate the appropriate oxidative stress response. In *S. aureus*, sensing of H_2O_2 is carried out by the peroxide-responsive repressor (PerR)[244,245]. In the presence of H_2O_2, the iron in PerR undergoes Fenton chemistry to form $^{\bullet}OH$, which oxidises histidine residues and leads to de-repression of the PerR regulon[244]. This regulon includes many genes involved in the oxidative stress response, such as *katA, ahpC, mrgA* and *trxA*[245]. In addition, oxidative stress can be sensed by multiple gene regulator A (MgrA) and staphylococcal accessory regulator Z (SarZ). These proteins act as thiol switches, each containing a single cysteine residue that can be oxidised by ROS to disrupt DNA binding and enable transcription[246]. MgrA regulates

~350 genes, including those encoding virulence factors (e.g. protein A), autolysins (e.g. lytic transglycosylase M, *lytM*, which cleaves peptidoglycan), and indirectly regulate other transcriptional regulators (e.g. the general stress-response alternative sigma factor SigB)[246–248]. SarZ regulates ~90 genes, including those involved in metabolism, virulence and oxidative stress resistance, e.g. organic hydroperoxide resistance (*oh*) gene, which is known to confer resistance to peroxides in *Bacillus subtilis*[249,250]. Another regulator is SarA, which has a major role in virulence, but also negatively regulates *sodA, sodM* and *trxB*, possibly by acting as a thiol switch via its single cysteine residue[251,252].

1.3.3.2 Evasion of non-oxidative killing

S. aureus is largely resistant to the enzymes and peptides released during neutrophil degranulation. For example, *S. aureus* is completely resistant to lysozyme, a prominent antibacterial protein present in neutrophil granules. Lysozyme is a muramidase that cleaves the glycosidic bond between *N*-acetylmuramic acid (MurNAc) and *N*-acetylglucosamine in cell wall peptidoglycan, causing cell lysis. However, this cleavage is prevented in *S. aureus* by the *O*-acetylation of MurNAc, which is catalysed by *O*-acetyltransferase A (OatA)[253]. Furthermore, the extracellular adherence protein (Eap) and its two structural homologues, EapH1 and EapH2, inhibit the activity of neutrophil serine proteases, including elastase, proteinase 3 and cathepsin G[254].

Resistance to AMPs is mediated in part by modifications to the bacterial cell wall and membrane. Dlt proteins catalyse the attachment of positively-charged D-alanine into wall teichoic acids[255], whilst multiple peptide resistance factor (MprF) transfers positively-charged L-lysine to phosphatidylglycerol on the outer membrane[256]. These modifications partially neutralise the negative cell surface charge, reducing the binding efficiency of cationic AMPs and repelling them from the bacterial cell surface[123]. Expression of these proteins is regulated by the glycopeptide resistance associated SR (GraSR) two-component system, which works in combination with the accessory regulatory protein GraX and the VraFG transporter to sense the presence of AMPs[257]. Mutants in *dlt* and *mprF* display increased killing by neutrophils *in*

vitro, and reduced virulence in mouse infection models[256,258]. *S. aureus* also secretes proteins that directly bind and degrade AMPs, such as staphylokinase and aureolysin, which cleave α-defensins and the cathelicidin LL-37, respectively[259,260].

In addition to evading killing after phagocytosis, *S. aureus* can escape NETs by secreting nuclease (Nuc), which enables the pathogen to disseminate to other parts of the body[261]. Secretion of the adenosine synthase (AdsA) enzyme leads to conversion of the Nuc-derived DNA degradation products (5′ and 3′ monophosphate nucleotides) into deoxyadenosine, which induces apoptosis in macrophages and thereby protects *S. aureus* from these immune cells[262]. AdsA can also catalyse the dephosphorylation of adenosine mono-, di- and triphosphates to produce adenosine, which is known to inhibit neutrophil degranulation via adenosine receptor (AdoR) signalling[263].

1.3.3.3 S. aureus modulation of neutrophil cell death

S. aureus produces numerous secreted toxins that lyse immune cells by forming pores in the target cell membrane[122]. Toxin production in *S. aureus* is controlled by the *agr* operon, which activates in a quorum-dependent manner to increase production of extracellular proteases and toxins, and decrease expression of cell-surface proteins[264]. In keeping with this, *agr* mutants are more susceptible to killing in whole human blood then wild-type bacteria[265]. Since the *agr* system is inhibited in serum[266], staphylococcal-mediated killing of neutrophils is most likely to occur after phagocytosis, where the enclosed environment of the phagosome promotes *agr* activation[267,268]. CA-MRSA strains exhibit higher levels of *agr* expression compared to HA-MRSA strains, which is believed to contribute to their increased virulence[269].

Toxins regulated by *agr* include leukocidins, phenol soluble modulins (PSMs) and α-haemolysin[270,271]. Leukocidins consist of two different subunits that form octameric pores in the membrane of host target cells[272]. Eight staphylococcal leukocidins have been described, including Panton-Valentine leukocidin (PVL, encoded by the *lukFS-PV* genes), γ-haemolysin AB (HlgAB), γ-haemolysin CB (HlgCB), leukocidin AB (LukAB, also known as LukGH), leukocidin ED (LukED), leukocidin MF' (LukMF', exclusive to bovine-specific *S. aureus*) and

leukocidin PQ (LukPQ, exclusive to equine-specific *S. aureus*)[273,274]. All of the leukocidins have been shown to lyse neutrophils (with LukMF' acting on bovine neutrophils), but only the γ-haemolysins exhibit cytolytic activity towards erythocytes[275–279]. Meanwhile, PSMs are short α-helical peptides that are categorised into two groups based on their size. The shorter α-type PSMs (20-30 amino acids long) are more cytotoxic than the β-type PSMs (44 amino acids long), and are capable of lysing both leukocytes and erythocytes[271]. The *agr* system also mediates the expression of α-haemolysin, which is not cytotoxic to neutrophils, but lyses other immune cells such as macrophages and T cells[280].

After phagocytosis and killing of bacteria, neutrophils undergo apoptosis and are ingested by macrophages in a process called efferocytosis, which removes spent neutrophils and limits inflammation[281,282]. Greenlee-Wacker *et al.* (2014) showed that phagocytosed *S. aureus* is able to inhibit efferocytosis of the neutrophil by upregulating the host CD47 receptor, which transmits a "don't eat me" signal to macrophages[283]. In addition, the *S. aureus* exoprotein expression RS (SaeRS) two-component system promotes accelerated neutrophil death by inhibiting the production of IL-8[284].

1.3.4 Resistance to other immune defences in the bloodstream

1.3.4.1 Iron acquisition

In *S. aureus*, iron levels in the environment are sensed by the ferric uptake regulator (Fur)[285,286]. When iron is present, Fur represses genes involved in iron acquisition and transport, but this is relieved in the blood due to the low levels of free iron[287]. In response to low iron, *S. aureus* secretes haemolysins to lyse erythocytes and release haem[197], which is the preferred iron source of *S. aureus*[288]. Haem can be used directly by membrane proteins or taken up by the iron-regulated surface determinant (Isd) system, which captures haem and transports it into the cytoplasm[289]. Additionally, iron can be acquired from host transferrin using the siderophores staphyloferrin A and staphyloferrin B[290]. When complexed with iron, these siderophores can be taken into the bacterium via the haem-transport system ABC (HtsABC) and staphylococcal iron-regulated ABC (SirABC) transporters, respectively[291].

1.3.4.2 Inhibition of platelet activation

As mentioned in section 1.3.2, *S. aureus* is able to hijack the coagulation pathway to evade phagocytosis, by secreting virulence factors that activate prothombin. *S. aureus* can also inhibit platelet activation and aggregation to stop the release of PMPs and prevent platelet-mediated activation of complement and immune cells[207]. Platelet activation is inhibited by SpA, which binds to PRRs and FcRs on the platelet surface to prevent recognition of *S. aureus*[198,292]. Meanwhile, platelet aggregation is inhibited by the binding of Efb to activated platelets[293]. In addition, *S. aureus* can lyse platelets with α-haemolysin and resist killing by PMPs by making modifications to the cell wall and membrane, similar to those described for AMP resistance (section 1.3.3.2)[199].

1.3.4.3 Manipulation of T-cell responses by staphylococcal superantigens

APCs process and load foreign antigens onto major histocompatibility complex (MHC) molecules to present to antigen-specfic T cells, which generally activates less than 0.01% of the T cell population[294,295]. However, staphylococcal superantigens can bind directly to the MHC class II molecules and to T cell receptors, stimulating up to 30% of the T cell population without the need for antigen processing[123,273]. Excessive T cell expansion is triggered, leading to the overproduction of cytokines (a cytokine storm) and preventing a focused adaptive immune response[296].

S. aureus strains produce up to 23 different superantigens, most of which are regulated by the *agr* system[297]. The thee superantigens most commonly associated with human disease are toxic shock syndrome toxin 1 (TSST-1), staphylococcal enterotoxin B (SEB) and staphylococcal enterotoxin C (SEC)[298]. While enterotoxins are a major cause of food poisoning[299], TSST-1 can lead to toxic shock syndrome (TSS), a serious condition that can result in organ failure and death[300].

1.3.4.4 S. aureus persistence in non-professional phagocytes

Despite being classically considered an extracellular pathogen, *S. aureus* can also invade and persist within non-professional phagocytes (e.g. epithelial and endothelial cells), where the intracellular environment is more habitable than in neutrophils[301]. After invading the host cell via staphylococcal FnBP, the pathogen escapes to the cytoplasm by lysing the phagosome, a process which is mediated by α-haemolysin[302–304]. In the bloodstream, invasion of endothelial cells could promote *S. aureus* survival by facilitating evasion of the immune reponse[305].

S. aureus often persists within host cells in the form of small colony variants (SCVs), which originate by mutations in the electron-transport chain and are selected for by the intracellular environment[306,307]. SCVs have reduced metabolic activity, forming small colonies as a result of slow growth, and show decreased expression of *agr* and *agr*-regulated toxins, which enables survival within the host cell without triggering apoptosis[308]. SCVs can also survive within the lysosome for up to five days[309], possibly due to increased expression of the arginine deiminase pathway to provide protection against acid stress[310].

After leaving the host cell, *S. aureus* can rapidly regain its wild-type phenotype, which can lead to chonic or recurrent infections[301]. For example, SCVs have been associated with persistent bloodstream infections[311,312].

1.4 DNA repair in *S. aureus*

In living cells, DNA is constantly damaged by numerous factors, ranging from environmental agents such as ionising radiation, to endogenous theats produced during cell metabolism[313]. This damage can impair replication and transcription within the cell, affecting cell viability. As a result, prokaryotes and eukaryotes have evolved a wide range of mechanisms to repair DNA lesions[313].

Although DNA repair is vital for bacterial survival and propagation[313,314], relatively little is known about these repair mechanisms in *S. aureus*[248]. Since much of our knowledge of this subject has been derived from studying *E. coli* and *B. subtilis*, these model species are often used to draw inferences into staphylococcal DNA repair, especially as *S. aureus* has homologues of many DNA repair enzymes found in these organisms[248]. This section will describe mechanisms of DNA repair expected to be used by *S. aureus*, with specific reports included where available.

1.4.1 The SOS response

For many bacteria, the SOS response is a global response to DNA damage that leads to cell cycle arrest and the induction of DNA repair[313]. The SOS response pathway can be triggered by numerous DNA-damaging agents, including ultraviolet light, ROS and certain antibiotics (e.g. fluoroquinolones)[315]. In *S. aureus,* the SOS response has been shown to be induced by H_2O_2 and various DNA-damaging antibiotics[242,316–318].

The SOS response is governed by two key proteins: the locus for X-ray sensitivity A (LexA) transcriptional repressor, and recombinase A (RecA) sensor protein (Figure 1.6)[248,319]. In the absence of DNA damage, LexA negatively regulates SOS induction. Upon DNA damage, single-stranded DNA (ssDNA) is formed during the replication of damaged DNA templates or during DNA repair. RecA binds to the ssDNA and polymerises, forming a nucleoprotein filament that activates LexA for self-cleavage, de-repressing SOS genes[248,319]. RecA also activates at least one low-fidelity DNA polymerase (UmuC in *S. aureus*, also known as DNA polymerase V or Pol V), which enables replication of damaged DNA templates[318,320].

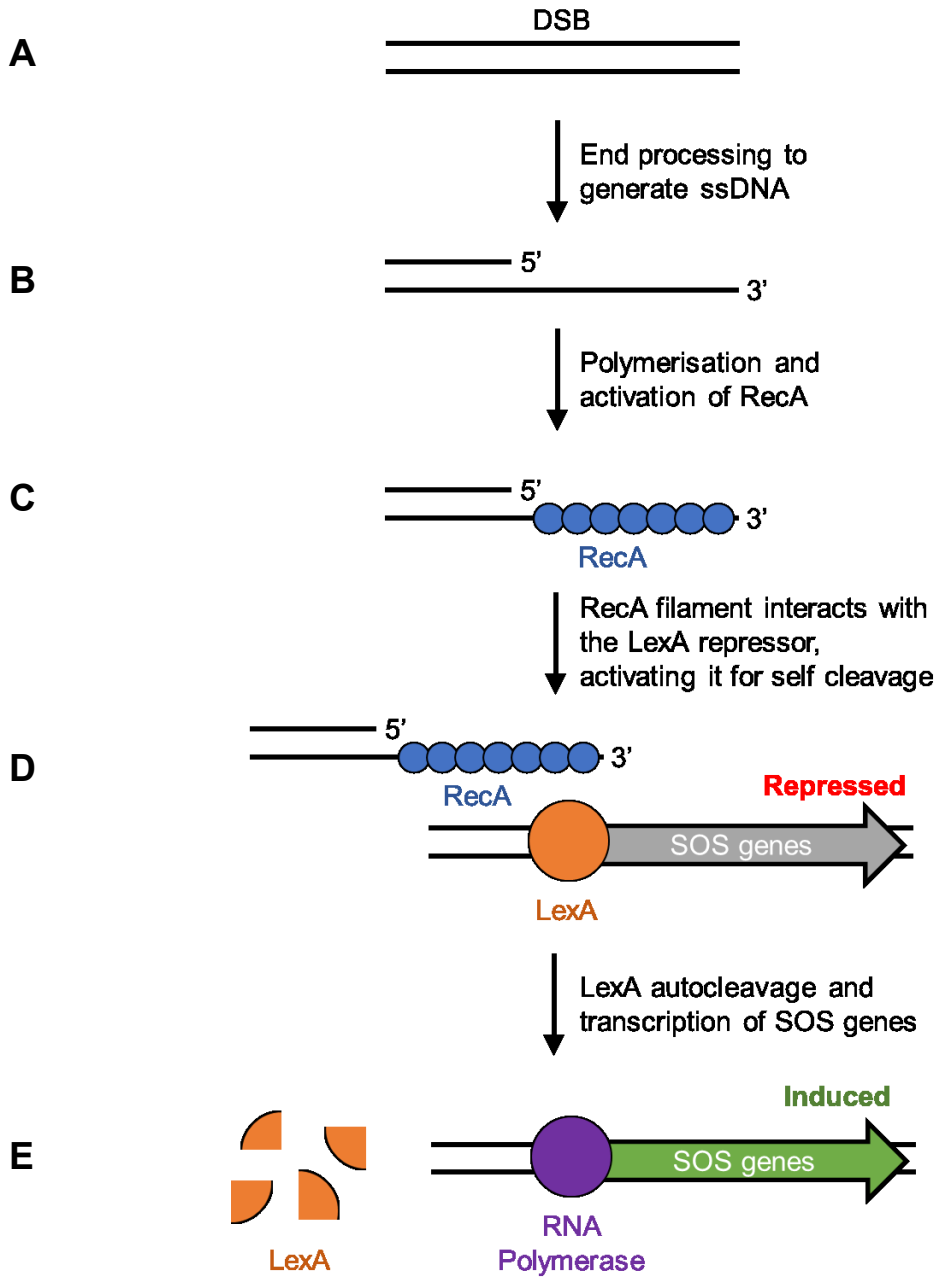

Figure 1.6. Model for activation of the SOS response in *S. aureus*.
In this model, the SOS response is induced by a double-stranded DNA break (DSB), but SOS induction can occur as long as ssDNA is formed during DNA repair or replication of the damaged DNA template **(A)**. The DSB undergoes end processing to produce ssDNA, carried out by the RecBCD or AddAB (also known as RexAB) complexes **(B)**. The RecA protein forms filaments on the ssDNA, leading to RecA activation **(C)**. Activated RecA interacts with the LexA repressor, activating its latent protease activity **(D)**. This results in autocleavage of LexA, inactivating the LexA repressor and leading to de-repression of the SOS genes **(E)**.

Since UmuC lacks proofreading activity, this leads to an increase in the mutation rate[321,322], which has been suggested to promote adaptation at times of environmental stress and contribute to the acquisition of antibiotic resistance[318].

The *S. aureus* SOS regulon consists of 16 genes, identified by Cirz *et al.* (2007) by comparing the global transcriptional response of wild-type and non-cleavable *lexA*-bearing *S. aureus* strains after exposure to ciprofloxacin, a fluoroquinolone antibiotic[318]. These genes include *recA* and *lexA*; *umuC*; genes involved in nucleotide excision repair (NER; section 1.4.3.2) (*uvrA* and *uvrB*); topoisomerase IV genes (*parC* and *parE*); and gene encoding SbcCD endonuclease (*sbcC* and *sbcD*) for processing stalled replication forks. The remaining seven genes consist of four hypothetical genes (SACOL0436, SACOL1375, SACOL1986, and SACOL1999) and the polycistronic operon SACOL2162 to SACOL2160, which encodes a protein of unknown function, a protein involved in cell wall synthesis (UTP—glucose-1-phosphate uridylyltransferase), and a putative haemolysin[318]. The binding of *S. aureus* LexA to the *recA* promoter has also been demonstrated, which is consistent with *recA* regulation in other systems[319,323].

However, the number of genes under LexA-regulated control differs greatly between *S. aureus* and the model organisms *E. coli* and *B. subtilis*, which contain SOS regulons that consist of at least 43 and 63 genes, respectively[319,324]. Genes that are conserved among all thee systems include *recA, lexA,* genes encoding for DNA repair proteins, and at least one error-prone polymerase. For example, SOS-induced error-prone DNA repair is performed by UmuC in *S. aureus*[318]*;* UmuC, DinB (Pol IV) or DnaE (Pol III) in *B. subtilis*[325–327]; and by polymerase B (PolB, or Pol II), DinB or UmuDC in *E. coli*[313].

The SOS response in *S. aureus* has also been shown to affect virulence by promoting horizontal gene transfer of virulence factors and the expression of chomosomal virulence genes[315,323,328–331]. Ubeda *et al.* (2005) found that exposure to ciprofloxacin triggered dissemination of *S. aureus* pathogenicity islands (SaPIs), mobile genetic elements that encode virulence factors, and that this was significantly reduced by inactivation of *recA*[328]. In addition, Goerke *et al.* (2006) showed that increased transcription of staphylokinase (a phage-

encoded virulence factor) in response to ciprofloxacin was strongly linked to up-regulation of *recA*[330]. The SOS response may also affect the ability of *S. aureus* to bind host surfaces, as Bisognano *et al.* (2004) found that purified LexA can bind to the *fnbB* promoter[323].

1.4.2 Direct reversal repair

Bacteria have evolved diverse mechanisms to repair DNA damage caused by endogenous and exogenous agents. These include repair pathways for single-strand damage (section 1.4.30), as well as for double-strand breaks (DSBs) (section 1.4.4). In addition, bacteria have several mechanisms by which damage can be addressed by a single repair protein without breakage of the phosphodiester backbone. Although direct reversal mechanisms only mediate a small set of lesions, these pathways do not require a DNA template and are error free[332].

1.4.2.1 Photoreactivation

Exposure to UV light leads to the formation of pyrimidine dimers, where abnormal covalent bonds form between consecutive thymine or cytosine bases. Two types of pyrimidine dimers can be formed: cyclobutane pyrimidine dimers (CPDs) or pyrimidine pyrimidone (6-4) photoproducts (6-4 PPs). DNA photolyase enzymes can repair these lesions in a process called photoreactivation, which uses blue and near-UV light (350-450 nm) to reverse the damage. Since photolyases are specific to one type of pyrimidine dimer, they are referred to as either CPD photolyases or (6-4) photolyases[332,333].

Photolyases absorb light via chomophoric cofactors. In particular, the flavin adenine dinucleotide (FAD) cofactor is essential for binding to damaged DNA and catalysis[332,333]. CPD photolyases also contain a second chomophore, either methenyltetrahydrofolate (MTHF) or 8-hydroxy-7,8-didemethyl-5-deazariboflavin (8-HDF). The second chomophore is not required for catalysis, but may increase the rate of repair under limiting light conditions[333].

DNA photolyases occur in nearly all living organisms exposed to sunlight, with the exception of placental mammals such as humans, where NER systems are used instead[334–337]. Although (6-4) photolyase has not yet been identified in prokaryotes, the crystal structures

of CPD photolyase from *E. coli* and the marine bacterium *Thermus thermophilus* have been elucidated[338,339], and photoreactivation has been reported in *B. subtilis*[340]*. S. aureus* encodes a putative DNA photolyase (SACOL0751), though its function has not been confirmed[318,341,342].

1.4.2.2 Alkylation damage repair

DNA damage via alkylation and methylation can occur endogenously or in the environment though alkylating agents such as methyl chloride[343]. These agents react with the nitrogen and oxygen atoms of DNA bases to generate covalent adducts that can be cytotoxic. Repair of alkylation damage in bacteria is carried out by multiple partially-redundant mechanisms, including the base excision repair (BER) system (section 1.4.3.1) and two direct reversal repair pathways: O^6-alkylguanine DNA alkyltransferases to reverse O^6-alkylated guanines, and alkylation B (AlkB) family dioxygenases to reverse N-alkyated lesions[332].

In many bacteria, alkylation damage repair is induced by the adaptive response to alkylation damage (Ada response)[313]. In *E. coli,* this is mediated by the N-terminal domain of the Ada protein (N-Ada), which is activated by a DNA methylphosphotriester lesion to induce transcription of Ada response genes: *ada, alkA, alkB* and *aidB*[313,344,345]. AlkA is a DNA glycosylase involved in BER that removes methyl lesions formed on nitrogen moieties (e.g. N^3-methyladenine, N^3-methylguanine)[343,346], whereas Ada and AlkB reverse alkylation damage directly[343,345]. The C-terminus of Ada (C-Ada) repairs O^6-alkylguanine and O^4-alkylthymine base lesions[332,345,347], and AlkB repairs N^1-methyladenine and N^3-methylcytosine lesions[348,349]. Meanwhile, AidB has been proposed to function by preventing alkylation damage[350–352].

The Ada response in *B. subtilis* occurs though a similar process as described for *E. coli,* with the key difference that two separate Ada proteins (AdaA and AdaB) mediate the functions performed by *E. coli* N-Ada and C-Ada, respectively[319]. The *B. subtilis* Ada response also leads to induction of the *adaAB* operon and the *alkA* gene only[353–356], and the lack of AlkB may be compensated for by the BER pathway[357]. However, whilst the Ada response is present in many bacteria[313,319,358], its presence in *S. aureus* is still unknown. A report by Ambur *et al.*

(2009) identifying homologues of selected DNA repair genes found that the *S. aureus* strain EMRSA-16 (MRSA252) did not contain either *ada* or *alkB*[359]. However, another report by Zhang *et al.* (2014) found that the clinical VISA isolate XN108 contains a putative O^6-methylguanine DNA methyltransferase (AdaB)[360].

1.4.3 Single-strand damage repair

When only one strand of DNA is damaged, excision repair mechanisms can remove and replace damaged bases using the undamaged strand as a template[319]. Excision repair mechanisms include base excision repair (BER) (section 1.4.3.1), nucleotide excision repair (NER) (section 1.4.3.2), and mismatch repair (MMR) (section 1.4.3.3). In addition to these mechanisms, the RecF pathway of homologous recombination is used to repair single-strand gaps (section 1.4.4.1).

1.4.3.1 Base excision repair (BER)

BER is the main pathway for repairing non-bulky single-base lesions in DNA, including alkylated and deaminated bases, oxidised bases, abasic sites, and dUTP incorporation during DNA replication[319,361]. BER is initiated by damage-specific DNA glycosylases that recognise lesions and cleave the N-glycosidic bond (Figure 1.7). This removes the damaged base and leads to the formation of abasic or apurinic/apyrimidinic sites (AP sites). The 5' and 3' ends of the AP site are nicked by AP endonucleases and AP lyases, respectively, which enables processing by an exonuclease or deoxyribophosphodiesterase (dRpase). The resultant gap is filled by a repair polymerase (such as Pol I, encoded by the *polA* gene) via short-patch (one nucleotide is replaced) or long-patch (multiple nucleotides are synthesised) pathways, with the remaining nick sealed by DNA ligase[319,362].

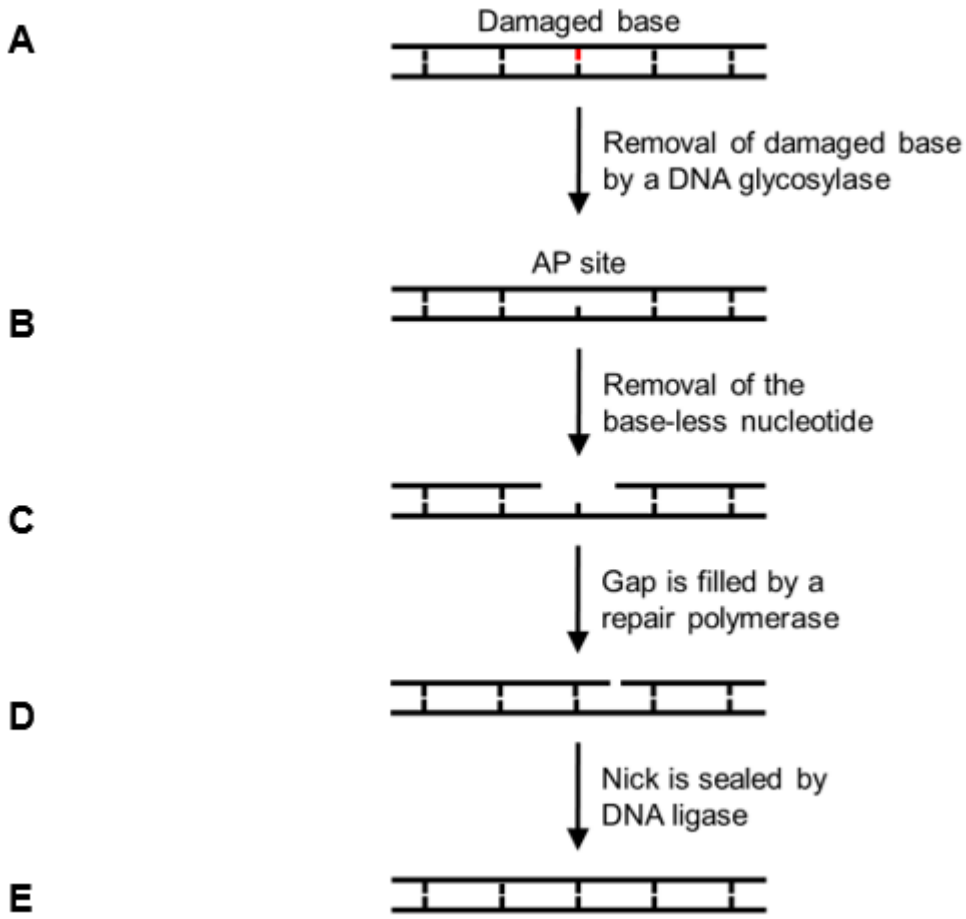

Figure 1.7. Model for the base excision repair (BER) pathway in *S. aureus*.

BER is initiated by specific DNA glycosylases that recognise and remove damaged bases (shown in red) **(A)**, generating abasic or apurinic/apyrimidinic sites (AP sites) **(B)**. Next, 5' and 3' ends of the AP sites are nicked by AP endonucleases and AP lyases, followed by processing by an exonuclease or deoxyribophosphodiesterase (dRpase) to remove the base-less nucleotide **(C)**. This leaves a gap, which is filled by a repair polymerase (such as Pol I) **(D)**. The remaining nick is sealed by DNA ligase **(E)**.

In *E. coli,* AP endonuclease activity is performed by exonuclease III (ExoIII or Xth) and endonuclease IV (EndoIV or Nfo), whereas dRpase activity is carried out by RecJ and exonuclease I (ExoI)[248]. In *B. subtilis*, AP endonuclease activity is encoded by thee genes: *exoA, yqfS* and *yshC*[319,363,364]*.* ExoA and YqfS are homologous to *E. coli* Xth and Nfo, respectively[365,366]. Meanwhile, *yshC* encodes for DNA polymerase X (PolX), a low-processivity DNA polymerase that possesses AP endonuclease activity and acts preferentially on small gaps in DNA[363,367]. As a result, PolX has been suggested as the primary polymerase for repairing small lesions[319]. Although Xth/ExoA is not present within the staphylococcal genome, *S. aureus* contains homologues of Nfo, RecJ, PolX and Pol I[359,368,369].

The most common lesion formed in DNA during oxidative stress is 7,8-dihydro-8-oxoguanine (8-oxoG or GO lesion), which can mispair with adenine and cause G to T transversions[370,371]. In *E. coli*, repair of this lesion is mediated by the GO system via DNA glycosylases[372]. Formamidopyrimidine DNA glycosylase (Fpg, also known as MutM) removes 8-oxoG prior to a mismatch, whereas MutY removes misincorporated adenine from an 8-oxoG-A mismatch[373,374]. The GO system also removes oxidised guanines (8-oxo-dGTP) from the nucleotide pool, preventing their misincorporation into DNA. This function is provided by MutT, which selectively hydrolyses 8-oxo-dGTP to 8-oxo-dGMP, with the concomitant release of pyrophosphate[375].

Removal of 8-oxoG lesions and 8-oxoG-A mismatches in *B. subtilis* and *S. aureus* is performed by homologues of *E. coli* MutM and MutY[376,377]. Canfield *et al.* (2013) showed that *S. aureus mutM* and *mutY* mutants displayed increased mutation frequencies when compared to the wild type, and confirmed MutM and MutY glycosylase activities in the clearance of 8-oxoG-associated DNA lesions[377]. However, a clear functional homologue for MutT has not been identified in either bacterium, though analysis of the *B. subtilis* genome has revealed a putative *mutT* gene and two other possible orthologues (*yycI* and *yjhB*)[364]. Meanwhile, Canfield *et al.* (2013) identified five potential *mutT* homologues in *S. aureus,* but

inactivation of these genes did not increase the mutation frequency as would be expected from a *mutT* mutant[377].

Oxidative stress can also lead to the generation of pyrimidine lesions, such as thymine glycol[378]. In *E. coli*, these lesions are recognised by endonuclease III (EndoIII or Nth) or endonuclease VIII (EndoVIII or Nei), both of which are DNA glycosylases[379–381]. However, less is known about these enzymes in *B. subtilis* and *S. aureus.* Ambur *et al.* (2009) showed that these two species do not contain a homologue of *E. coli* Nei, but do contain homologues of Nth[359]. *B. subtilis* Nth has been shown to nick substrates with AP sites and protect the bacterium against H_2O_2 stress[382,383]. Meanwhile, *S. aureus* Nth (SAUSA300_1343) is induced by H_2O_2 stress[242], and inactivation of this gene has been shown to increase the rate of mutagenesis[384].

Finally, BER is responsible for the removal of misincorporated dUMP during DNA replication[385]. Although dUMP incorporation is rare due to the small pool of dUTP compared to that of dTTP, integration of uracil (instead of thymine) can lead to transition mutations[385]. These dUMP lesions can also occur via deamination of cytosine residues (dCMP to dUMP), which arises spontaneously but is promoted by the presence of $^{\bullet}OH$[313]. Many bacteria (including *E. coli, B. subtilis* and *S. aureus*) counteract dUMP incorporation by removal of dUMP from DNA, which is performed by uracil-DNA glycosylase (UDG, encoded by *ung*)[319,359,385–388]. The function of *S. aureus* UDG was confirmed by Wang *et al.* (2013), via direct testing of the purified protein for uracil-removing activity[388].

1.4.3.2 Nucleotide excision repair (NER)

The NER pathway is responsible for the high-fidelity repair of bulky helix-distorting lesions in DNA, such as thymine dimers or DNA crosslinks[389]. This pathway is conserved in prokaryotes and eukaryotes, and lesions are repaired in 10-15 nucleotide-long segments[319]. This process requires the highly conserved UvrABC endonuclease complex[313]. First, damaged DNA is recognised by a complex of UvrA and UvrB (Figure 1.8). This leads to UvrA dissociation and enables UvrC to complex with UvrB. Then, the UvrBC complex cleaves the phosphodiester backbone, leading to the removal of approximately 10 to 15 nucleotides surrounding the lesion. This removal is facilitated by UvrD (DNA helicase II), which enables release of the nucleotide segment. Finally, the gap is filled by Pol I using the intact strand as a template, and the remaining nick is sealed by DNA ligase[319,390].

The NER pathway is also triggered in response to bulky DNA lesions that cause stalling of RNA polymerase[390]. This subpathway of NER is called transcription-coupled repair (TCR), and involves the mutation frequency decline (Mfd) protein, also known as the transcription repair coupling factor (TRCF). Mfd releases stalled RNA polymerase from the transcribed strand and recruits UvrA, which initiates the rest of the NER pathway as described above[336,390].

Although the majority of studies on NER have focused on *E. coli*, the process is likely to be similar in *B. subtilis* and *S. aureus*, as *uvrABC, uvrD* and *mfd* genes are present in both genomes[359], and the *uvrBA* genes are induced by the SOS response in all thee species[318,319,324]. In addition, *B. subtilis uvrC* has been shown to complement an *E. coli uvrC* mutant[391], and purified *B. subtilis* Mfd protein is able to release stalled RNA polymerase at a crosslinked lesion[392]. Interestingly, a recent paper by Martin *et al.* (2019) also found that *B. subtilis* Mfd can act independently of the NER pathway to protect the bacterium against oxidative damage, by coordinating with MutY[393]. In *S. aureus,* UvrABC has been reported to contribute to nitrosative stress resistance, which has been suggested previously as a role for NER in *E. coli*[394,395].

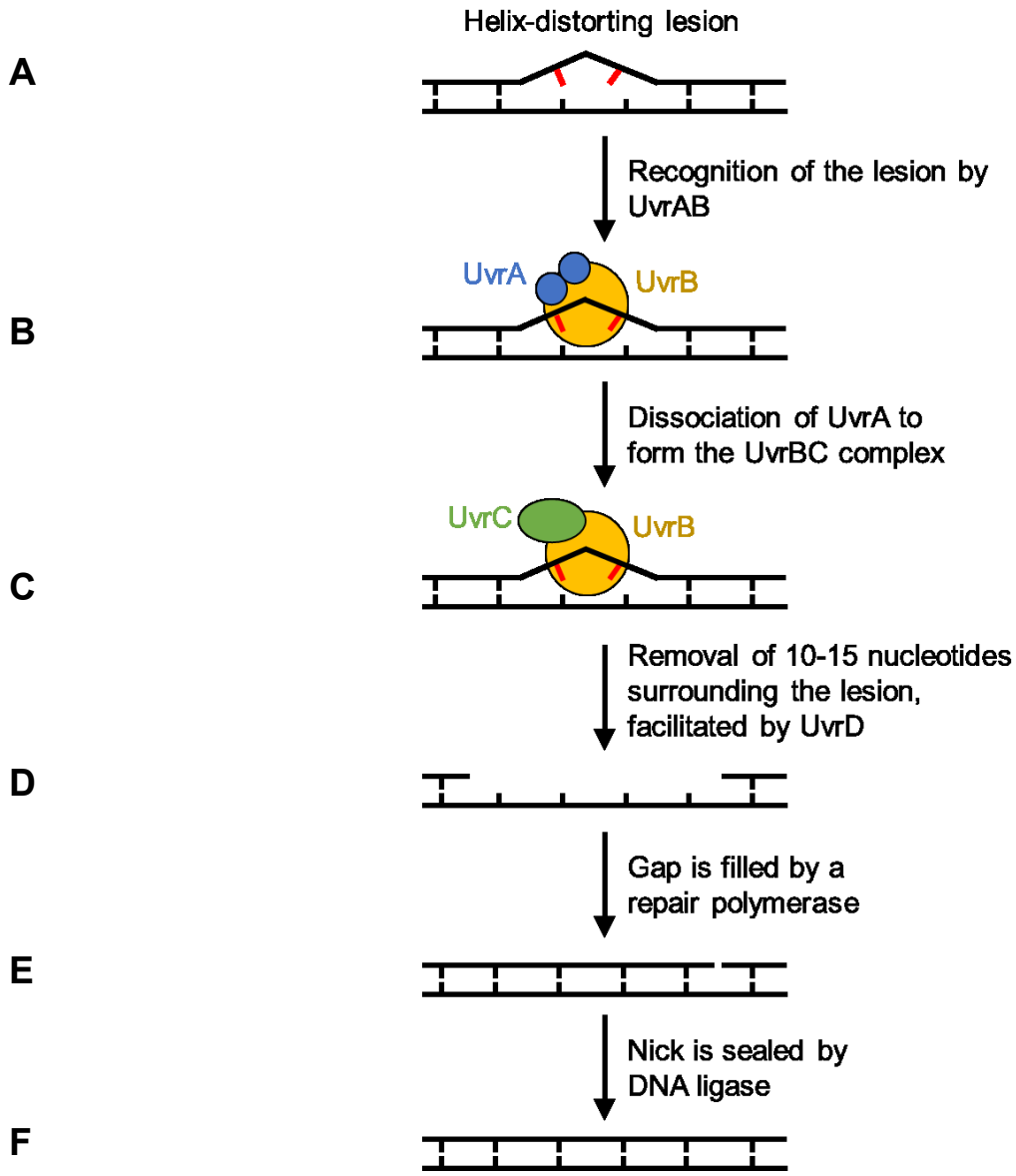

Figure 1.8. Model for the nucleotide excision repair (NER) pathway in *S. aureus*.
The NER pathway repairs bulky helix-distorting DNA lesions, such as thymine dimers and DNA crosslinks **(A)**. In this pathway, damaged DNA is recognised by the UvrAB complex **(B)**. This leads to UvrA dissociation to enable formation of the UvrBC complex **(C)**, which removes approximately 10 to 15 nucleotides surrounding the lesion **(D)**. This removal is facilitated by UvrD (DNA helicase II), which enables release of the nucleotide segment. The resultant gap is filled by Pol I **(E)**, with the nick sealed by DNA ligase **(F)**.

1.4.3.3 Mismatch repair (MMR)

MMR is responsible for correcting replication errors that escape DNA polymerase proofreading activity[396,397]. In Gram-negative bacteria, the replicative DNA polymerase is DnaE (Pol III)[398], but *B. subtilis* and many Gram-positive bacteria contain two replicative Pol III polymerases: DNA polymerase C (PolC) and DnaE[319,398,399]. PolC is the main polymerase, responsible for the majority of leading and lagging strand synthesis, but it cannot extend from the 3'-OH ends of RNA primers, carried out by DnaE before handing over to PolC[400,401]. In Gram-negative bacteria, DnaE is associated with the proofreading ε subunit (DnaQ) to provide 3′-5′ exonuclease activity[402]. However, this subunit is not present in Gram-positive bacteria and high-fidelity DNA replication is enabled by PolC instead, which has endogenous proofreading activity[398]. This corrects the majority of errors that occur during replication. Any remaining errors are corrected by MMR, which is coupled to DNA synthesis and increases the replication fidelity by up to 1000-fold[397,403–405].

In *E. coli,* mismatched bases generated from DNA synthesis are recognised and bound by MutS, which recruits MutL to stabilise the MutS-mismatch complex[396,397]. MutL activates MutH endonuclease to nick the nascent strand carrying the mismatch, identified by its absence of methylation[396,397]. The error-containing region is excised by UvrD helicase and degraded by one of several exonucleases, depending on the polarity of the strand[396]. The remaining gap is filled by Pol III and nick sealed by DNA ligase[396,397]. The daughter strand is then methylated at adenine in the d(GATC) sequence by Dam methylase[319].

Homologues of *E. coli* MutS and MutL are present in the majority of organisms, including prokaryotes such as *B. subtilis* and *S. aureus*[359,397,406–408]. Inactivation of MMR, for example via inactivating mutations, is associated with mutator phenotypes that have been shown to play a role in the adaptation of bacterial populations to stressful environments[409], including for *S. aureus*[377,407,408]. However, homologues of *E. coli* MutH have not been identified in eukaryotes or in most other bacteria[410]. Eukaryotes use a methylation-independent MMR system, where MutL exhibits endonuclease activity and the nascent strand is identified by recognising strand discontinuities near DNA replication forks[319,410,411]. In MutH-less bacteria, it

is hypothesised that MMR resembles eukaryotic systems, because MutL homologues in these bacteria have been shown to exhibit endonuclease activity[412–415]. Although this has not yet been functionally demonstrated with *S. aureus* MutL, Fukui *et al.* (2011) showed that the sequence motifs essential for MutL endonuclease activity are conserved[416]. In addition, d(GATC) sequences in *B. subtilis* and *S. aureus* are not methylated, which supports the use of methylation-independent MMR in these species[417].

1.4.4 Double-strand break (DSB) repair

DNA DSBs can be caused by a variety of factors, including DNA-damaging agents (e.g. ROS and ionising radiation) and replication fork collapse. These DNA lesions are particularly dangerous, because they can interrupt the coding region of a gene, alter chomosome organisation, and lead to mutagenic DNA rearrangements[418]. If not repaired, DSBs can also become substrates for exonucleases, leading to loss of vital genetic information and driving genetic instability[418,419]. In bacteria, DSBs are mainly repaired via homologous recombination, which involves the exchange of genetic material between two homologous DNA sequences[419]. In some bacterial species, a second pathway of DSB repair is present, called non-homologous end joining (NHEJ)[319,420]. This pathway is mutagenic as the two broken DNA ends are directly ligated using minimal or no sequence homology, but unlike homologous recombination, only a single copy of the genome is required[420]. NHEJ is performed by the Ku protein, which binds the DSB ends, and an ATP-dependent DNA ligase (usually Ligase D) to join the broken segments[420].

The NHEJ pathway has been identified in a number of bacteria, including *B. subtilis, M. tuberculosis, M. smegmatis* and *P. aeruginosa*[421–424]. However, it is not present in *S. aureus*, which is believed to rely on homologous recombination[424]. *E. coli* also lacks the NHEJ pathway, though an alternative end-joining (A-EJ) mechanism has been reported[425]. This is a modified version of NHEJ that involves minor processing of the broken ends by the RecBCD complex, followed by direct religation by the essential replicative DNA Ligase A

(LigA). It is not known whether A-EJ is used by *S. aureus*, though homologues of both proteins (RexAB and LigA, respectively) are present in the bacterium[426–428].

1.4.4.1 Homologous recombination

Homologous recombination (also known as recombinational repair) is the major route for DSB repair in bacteria, resulting in high-fidelity DNA repair[419]. This pathway requires a second copy of the genome as a template for repair, meaning that it can only occur when the damaged region has already been copied prior to cell division. This is generally not prohibitive for many bacteria, which often contain multiple copies or partially-replicated copies of the genome[429]. Homologous recombination consists of several steps: (1) break recognition and end resection; (2) loading of RecA and strand invasion; (3) DNA synthesis and branch migration, and (4) Holliday junction resolution (Figure 1.9). Although the details of each step and the components involved may differ between organisms, these steps are conserved in both prokaryotes and eukaryotes[418,426]. In addition to DSB repair, homologous recombination is used to repair single-strand gaps as part of the RecF pathway, which will also be described below.

The homologous recombination pathway is initiated by recognition of the break, followed by end resection, in which broken DNA ends are processed to generate ssDNA[319,430]. In *B. subtilis,* DSBs are specifically recognised by the RecN protein, which binds to the break and works as a scaffold to load repair proteins[430,431], but DSB recognition is poorly characterised in other bacteria[430]. In *E. coli,* RecN is kept at very low levels prior to SOS induction, suggesting that it cannot act before end resection and induction of SOS[430]. The *recN* gene is present in *S. aureus*, but the ability of *S. aureus* RecN to recognise DSB is unknown[318]. After a DSB is identified, the ends are processed by the RecBCD or AddAB (also known as RexAB) helicase-nuclease complexes, which are present in Gram-negative and Gram-positive bacteria, respectively. During this process, RecBCD or AddAB binds to the DSB and unwinds the DNA, simultaneously digesting the strand to generate a 3'-ssDNA overhang[319,429,432]. In the RecF pathway, end resection is performed by the RecQ helicase and RecJ exonuclease, which unwind and degrade the DNA, respectively[433–435].

Next, RecA binds to the 3'-ssDNA overhang and searches for the intact homologous DNA sequence to initiate strand invasion[319,430]. Although mechanisms for RecA loading are well established in *E. coli,* they are poorly understood in many other bacteria. In *E. coli,* RecA loading can be carried out by RecBCD or RecFOR, which are part of the DSB and single-strand gap repair mechanisms, respectively[433,436]. Meanwhile, AddAB is not involved in RecA loading in *B. subtilis,* which is instead carried out by RecFOR[437]. In a report by Alonso *et al.* (1995), the *S. aureus recF* gene was shown to partially restore the activity of a *B. subtilis recF* mutant, indicating that RecF protein function is conserved in *S. aureus*[438]. After binding of RecA to the ssDNA overhang, the recombinase pairs with the homologous DNA sequence and mediates strand invasion, where the broken strand exchanges places with the intact strand. This involves local denaturation of the dsDNA in the region of homology and produces a D-loop structure[319,433]. The steps following RecA loading are the same in both RecBCD and RecF pathways.

After strand invasion, regular DNA synthesis occurs via Pol III using the intact strand as a template to form stable four-stranded DNA structures called Holliday junctions[319,336,433]. These are moved along the DNA in a branch migration process, where base pairs between the two homologous DNA strands are exchanged. In *E. coli,* this process is mediated by the RuvAB protein complex[433,439]. RuvA binds to the Holliday junction and recruits RuvB, which then translocates the junction along the DNA. Finally, the endonuclease RuvC cleaves the Holliday junction to separate the two repaired DNA duplexes, and the nicks at the cleavage site are sealed by DNA ligase[433,439]. Branch migration and resolution can also be catalysed by RecG[433,439]. Although homologues of RuvA, RuvB and RecG proteins are present in many Gram-positive bacteria including *B. subtilis* and *S. aureus*, the RuvC protein is not[319,359,440]. Instead, Holliday junction resolution in Gram-positive bacteria is carried out by the RecU protein, which is absent in most Gram-negative species[441]. In *S. aureus,* deletion of RecU leads to defects in chomosome segregation and DNA damage repair, which is in agreement with the role of a Holliday junction resolvase442

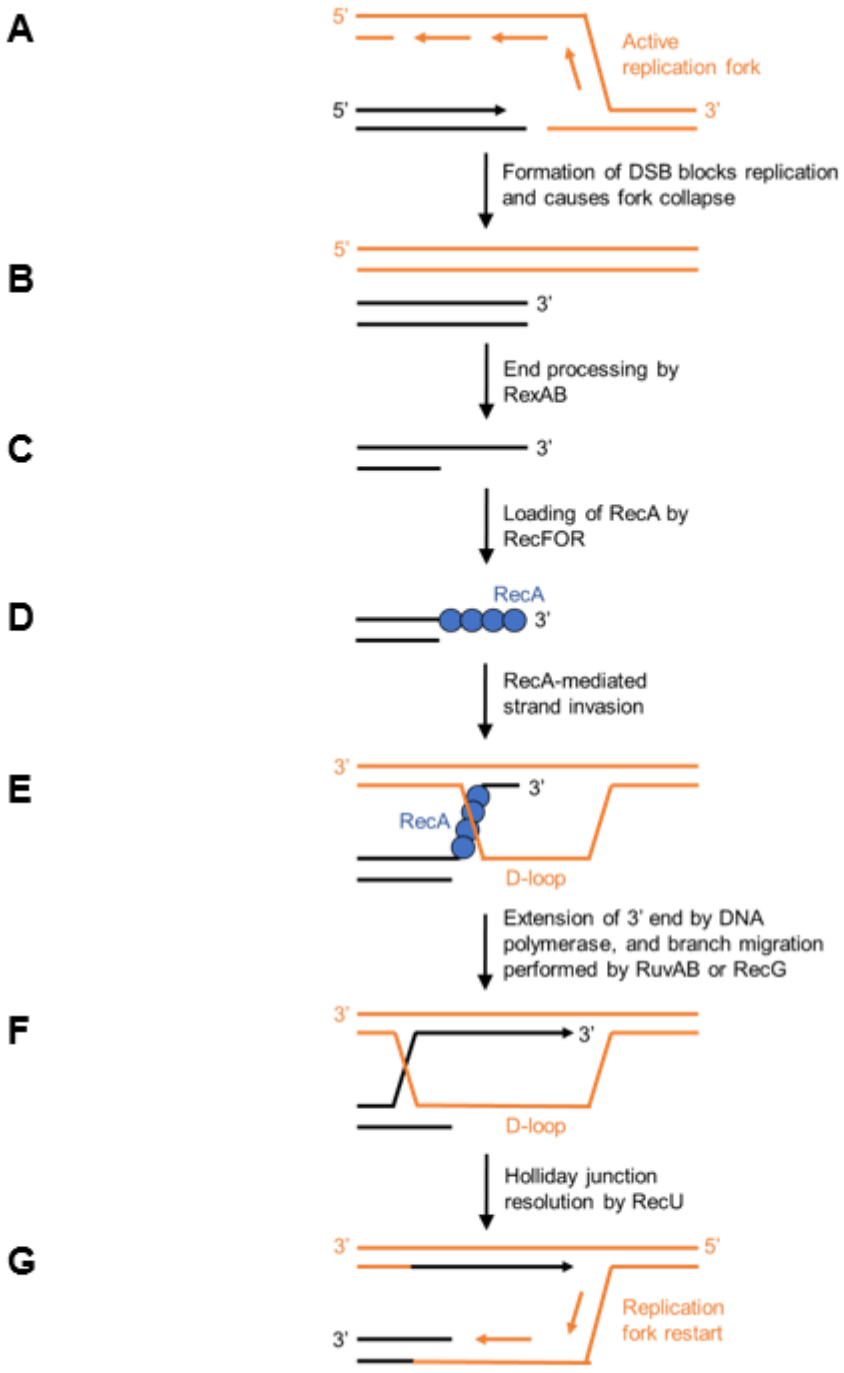

Figure 1.9. Model for DSB repair by homologous recombination in *S. aureus*.

When an active replication fork encounters a single-strand nick **(A)**, this produces a double-strand break (DSB) and the replication fork collapses **(B)**. The DSB is processed by the AddAB complex, generating a 3′-ssDNA overhang **(C)**. RecFOR is recruited to load the RecA recombinase onto the ssDNA region **(D)**. RecA pairs with the homologous DNA sequence and mediates strand invasion, producing a D-loop structure **(E)**. DNA polymerase extends the 3′ end of the filament to form a stable four-stranded DNA structure called a Holliday junction, which is migrated along the DNA by RuvAB or RecG **(F)**. In the final step, this junction is cleaved by RecU and replication restarts **(G)**.

1.5 DNA repair and the oxidative burst

S. aureus infection leads to a complex series of host-pathogen interactions (sections 1.2 and 0) that can result in disease resolution, chonic infection or patient death[105]. Consequently, new therapeutics that favour the host response would greatly benefit patient outcomes. To identify potential targets in *S. aureus*, it is necessary to understand the nature of host-mediated damage and how this damage is repaired by the pathogen.

Despite its many strategies for immune evasion, *S. aureus* is rapidly phagocytosed by neutrophils in human blood and exposed to ROS as part of the oxidative burst[4,222,228]. As mentioned previously, ROS can damage proteins, lipids and DNA in *S. aureus*, playing a major role in immune clearance of the pathogen (section 1.2.3.1). The most significant target of ROS is believed to be upon DNA, because unlike proteins or lipids, which can be newly synthesised if damage is too severe for repair, the repair of DNA is essential for replication[419]. In addition, transcription of DNA is necessary for the replacement of damaged proteins, as well as for making the proteins required for lipid synthesis. As a result, even a single DNA lesion can have mutagenic or lethal consequences[147,151,157–160]. However, although DNA repair mechanisms protect against ROS-mediated DNA damage[160,306,443–447], the role of DNA repair for bacterial survival in the bloodstream is unknown.

1.6 Hypothesis

Since the oxidative burst of neutrophils is a key defence against *S. aureus* infection, the hypothesis is that staphylococcal DNA is a major target of the oxidative burst, such that DNA repair is required for the survival of *S. aureus* when exposed to phagocytic immune cells.

1.7 Aims of the project

1. To determine whether the neutrophil oxidative burst damages DNA in *S. aureus*.
2. To determine whether DNA repair is required for *S. aureus* survival of the oxidative burst, and if so, whether DNA repair is a viable drug target.

2 Materials and Methods

2.1 Bacterial strains, plasmids and growth conditions

2.1.1 Bacterial strains and plasmids

Bacterial strains and plasmids used in this study are listed in Tables 2.1 and 2.2, respectively.

2.1.2 Growth conditions

S. aureus was routinely grown on Tryptic Soy Agar (TSA) or in Tryptic Soy Broth (TSB) (BD Biosciences) with the addition of anhydrotetracycline (AHT; 10 or 100 ng/ml), erythomycin (Erm; 10 µg/ml), chloramphenicol (Cam; 10 µg/ml) and/or kanamycin (Kan; 90 µg/ml) as appropriate. *S. gordonii* and *E. faecalis* were grown in Todd Hewitt Broth (THB; Oxoid) supplemented with 1% (w/v) yeast extract. When appropriate, bacteria were grown on Columbia Blood Agar (CBA; Sigma-Aldrich) plates made with 5% defibrinated sheep blood (E&O Laboratories).

E. coli was routinely grown in Lysogeny Broth (LB) or on LB Agar (LBA; LB containing 1.2% (w/v) Oxoid Technical Agar) (Thermo Fisher Scientific) with the addition of amplicillin (Amp; 100 µg/ml), kanamycin (Kan; 25 or 50 µg/ml) and/or chloramphenicol (Cam; 34 µg/ml) as appropriate. For protein expression, *E. coli* was grown in Terrific Broth (TB; 1.2% (w/v) tryptone, 2.4% (w/v) yeast extract, 0.5% glycerol, 0.17 M KH_2PO_4, 0.72 M K_2HPO_4) and the inducer isopropyl β-D-1-thiogalactopyranoside (IPTG) was added at 1 mM when required.

All agar plates and liquid cultures were incubated at 37 °C for a minimum of 16 h, unless stated otherwise. Agar plates were incubated statically in air (*S. aureus*, *E. coli*) or 5% CO_2 (*S. gordonii*, *E. faecalis*). For liquid cultures, *S. aureus* and *E. coli* were typically grown in 5 ml of broth in 30 ml universal tubes and incubated with shaking at 180 rpm to facilitate aeration. *S. gordonii* and *E. faecalis* were grown in 10 ml broth in 15 ml conical tubes and incubated statically in 5% CO_2. Glycerol stocks were made using a 1:1 ratio of 30% glycerol and overnight culture, and were stored at -80 °C.

Table 2.1. Bacterial strains used in this study

Strain	Description	Source
Staphylococcus aureus		
SH1000	*rsbU*+ derivative of the laboratory strain 8325-4.	[448]
SH1000 *rexB*::Tn	SH1000 with a *bursa aurealis* transposon insertion in *rexB.* Erm^{10}.	[306]
SH1000 *rexB*::Tn *geh*::p*itet*	SH1000 *rexB*::Tn with p*itet* integrated into the genomic *geh* locus.	This study
SH1000 rexB::Tn geh::pitet rexAB	SH1000 *rexB*::Tn complemented with p*itet* *rexAB.*	This study
JE2	A derivative of CA-MRSA USA300 LAC, cured of plasmids, sensitive to Erm.	[368]
JE2 *rexB*::Tn	JE2 with a *bursa aurealis* transposon insertion in *rexB.* Erm^{10}.	[368]
JE2 *rexB*::Tn *geh*::p*itet*	JE2 *rexB*::Tn with p*itet* integrated into the genomic *geh* locus.	This study
JE2 rexB::Tn geh::pitet rexAB	JE2 *rexB*::Tn complemented with p*itet* *rexAB.*	This study
JE2 *sigB*::Tn *geh*::p*itet*	JE2 *sigB*::Tn with p*itet* integrated into the genomic *geh* locus. This was used as a positive control during colony PCR to confirm p*itet* plasmid integration.	Dr Nishanthy Ranganathan (Imperial College London)
SH1000 pCN34	SH1000 carrying empty pCN34.	This study
SH1000 pCN34 *PrecA-gfp*	SH1000 carrying pCN34 *PrecA-gfp.*	This study
JE2 pCN34	JE2 carrying empty pCN34.	This study
JE2 pCN34 *PrecA-gfp*	JE2 carrying pCN34 *PrecA-gfp.*	This study
JE2 *rexB*::Tn pCN34	JE2 *rexB*::Tn carrying empty pCN34.	This study
JE2 *rexB*::Tn pCN34 *PrecA-gfp*	JE2 *rexB*::Tn carrying pCN34 *PrecA-gfp.*	This study
Escherichia coli		
DH5α	Host strain for cloning. Deficiency in *recA1* recombinase prevents unwanted recombination of exogenous DNA.	New England Biolabs (NEB)

	Deficiency in *endA1* endonuclease improves the yield and quality of purified plasmid DNA. The lack of restriction due to mutation in *hsdR* enables transformation with exogenous DNA. The *lacZΔM15* gene on the F' episome allows blue-white colour screening.	
XL1 Blue	Host strain for cloning. *ΔendA1, recA1, hsdR.* The *lacI^{q}ZΔM15* gene on the F´ episome allows blue-white colour screening.	Stratagene
DC10B	DNA cytosine methyltransferase deficient (*Δdcm*). Cloning strain that efficiently bypasses the restriction-modification system of *S. aureus.*	[449]
BL21 (DE3)	Strain used for protein expression. The strain carries the λDE3 prophage encoding T7 RNA polymerase under the control of the *lacUV5* promoter. Induction by IPTG enables expression of cloned genes from the T7 promoter. Deficiency of *ompT* and *lon* proteases improves the stability of expressed proteins.	Stratagene
soluBL21 (DE3)	Strain used for protein expression. Derivative of BL21 (DE3) that can produce soluble protein in most cases where the parent strain yielded no detectable soluble product.	Genlantis
Rosetta 2 (DE3) pLysS	Strain used for protein expression. Derivative of BL21 (DE3) that has been supplied with tRNAs for seven rare codons in *E. coli*. Expresses T7 lysozyme from pLysS, which suppresses basal expression of T7 RNA polymerase prior to induction, Cam^{34}.	Novagen

BW25113	Type strain used in the Keio Knockout Collection. Derivative of the F-, λ-, *E. coli* K-12 strain BD792. *ΔlacZ, hsdR, araBAD, rhaBAD* (cannot metabolise arabinose or rhamnose, so inducible promoters of these sugars can be introduced into this strain if necessary).	[450]
BW25113 *ΔrecB*	BW25113 with the *recB* gene replaced with a kanamycin resistance cassette, Kan[25].	[450]
BW25113 *ΔrecB* (DE3)	BW25113 *ΔrecB* that carries the λDE3 prophage encoding T7 RNA polymerase under the control of the *lacUV5* promoter. This enables expression of cloned genes from the T7 promoter of the pET28b$^+$ vector, via induction by IPTG.	This study
Streptococcus gordonii		
DL1	Wild type.	[451]
DL1 ΔrexAB	Wild-type DL1 with the *rexA* and *rexB* genes deleted.	Dr Angela Nobbs (University of Bristol)
Enterococcus faecalis		
OG1X	Wild type.	[452]
OG1X ΔrexAB	Wild-type OG1X with the *rexA* and *rexB* genes deleted.	Dr Angela Nobbs (University of Bristol)

Table 2.2. Plasmids used in this study

Plasmid	Description	Source
pitet	An integrative shuttle vector used for placing desired genes under the control of a tetracycline-inducible promoter into *S. aureus* for controlled expression. Single-	[453]

	copy in *S. aureus* following integration at the *geh* locus. Amp^{100} in *E. coli*, Cam^{10} in *S. aureus*.	
pitet rexAB	p*itet* containing the *rexAB* operon.	This study
pET28b^{+}	Used for expression of recombinant proteins in *E. coli*. The resulting protein is expressed under the control of a T7 promoter and has an N-terminal 6xHis-tag. Expression is inducible with IPTG, and dependent on the presence of the T7 RNA polymerase. Kan^{50}.	Novagen
pET28b^{+} *rexA*	Plasmid for expressing recombinant, N-terminally His-tagged *S. aureus* RexA.	This study
pET28b^{+} *rexB*	Plasmid for expressing recombinant, N-terminally His-tagged *S. aureus* RexB.	This study
pET28b^{+} *rexAB*	Plasmid for expressing recombinant, N-terminally His-tagged *S. aureus* RexB and N-terminally StrepII-tagged *S. aureus* RexA.	This study
pCN34	A low-copy shuttle vector (20 – 25 copies per cell) used for cloning target genes into *S. aureus* for expression under their native promoters. Amp^{100} in *E. coli*. Kan^{90} in *S. aureus*.	[454]
pCN34 PrecA-gfp	pCN34 carrying the green fluorescent protein (*gfp*) under the control of the *recA* promoter from *S. aureus.*	This study

2.2 DNA techniques

2.2.1 Extraction of plasmid DNA

High-copy plasmid DNA was purified from *E. coli* strains using the QIAprep Miniprep kit (Qiagen), from a 3-5 ml overnight bacterial culture. Purification of low-copy plasmids was performed using the QIAquick Midiprep kit (Qiagen) from 100 ml overnight cultures grown in 500 ml flasks. Plasmid DNA extracted by the Midiprep kit was rehydrated in 150 µl nuclease-free water. DNA concentration was quantified using a NanoVue Plus spectrophotometer (GE Healthcare) and stored at -20 ˚C.

2.2.2 Polymerase chain reaction (PCR)

PCR was carried out to amplify target genes from genomic or plasmid DNA. Phusion DNA polymerase (NEB) was used following the instructions provided. Typical reactions were set up in 0.5 ml microcentrifuge tubes in a PTC-200 Peltier Thermal Cycler (MJ Research), according to the composition and cycling conditions shown in Tables 2.3 and 2.4. Primers were synthesised by Sigma-Aldrich and a full list of primers used in this study is shown in Table 2.5. When appropriate, PCR products were purified using the QIAquick PCR Purification kit (Qiagen), following the instructions provided.

Colony PCR was performed to screen colonies after genetic manipulation and to amplify target genes from genomic DNA. To prepare *S. aureus* DNA for PCR, a single colony was resuspended in 50 µl of nuclease-free water in a 1.5 ml microcentrifuge tube and microwaved on full power for 3 min. The microwave-treated cells were pelleted at 17,000 x *g* for 2 min, and 5 µl of the supernatant was used per PCR reaction. To prepare *E. coli* DNA, a single colony was resuspended into 20 ul of nuclease-free water and heated to 95 ˚C for 15 min. The cells were pelleted at 17,000 x *g* for 2 min, and 1 µl was used per PCR reaction.

Table 2.3. Composition of a PCR reaction

Reaction component	Volume (µl)
Nuclease-free water	15.75
5x Phusion HF buffer	5
10 mM dNTPs	0.5
100 ng/µl Template DNA	1
10 µM Forward primer	1.25
10 µM Reverse primer	1.25
Phusion DNA polymerase	0.25 (1 unit/50 µl PCR)
Total	25

Table 2.4. PCR cycling conditions

Reaction stage	Temperature (˚C)	Duration	Number of cycles
Initial denaturation	98	2 min[a]	1
Denaturation	98	30 s	30
Annealing	45-72	30 s	30
Extension	72	30 s/kb	30
Final extension	72	5 min	1
Hold	4	∞	1

[a] For colony PCR, duration was increased to 10 min.

Table 2.5. Primers used in this study

Primer name	Sequence
Primers for the construction of p*itet rexAB*	
rexB-F AvrII	GGCCCTAGGATGACATTACATGCTTATTTAG
rexA-R PmeI	GCCGTTTAAACCTATAGTTGCAATGTACCAAATTTG
Primers for the construction of pCN34 *PrecA-gfp*	
PrecA-F BamHI	GAGGATCCTATGGTTCAGATGACACAT
PrecA-R 7xT-GFP	CATTTTTTTTCCTCCTAATTGAAATTGC
GFP-F 7xA-PrecA	AGGAAAAAAAATGAGTAAAGGAGAAGAACT
GFP-R KpnI	GCGGGTACCTTATTTGTATAGTTCATCCATG
Primers for the construction of pET28b$^+$ His-*rexB*, His-*rexA* and His-*rexB*-StrepII-*rexA*	
rexB-F BamHI	CCAGGATCCGATGACATTACATGCTTATTTAGG
rexB-R SalI	ATAGTCGACCTATTGCTCACCCCCAAATTC

rexA-F BamHI	CGAGGATCCGATGACAATTCCAGAGAAACC
rexA-R SalI	GCGGTCGACCTATAGTTGCAATGTACC
StrepII rexAB SDM-F	ACAATTCCAGAGAAACCACAAGGCGTGATTTGGACTGACGC GCAATGGC
StrepII rexAB SDM-R	AGCGCTTTTTTCGAACTGCGGGTGGCTCCACATCTATTGCTC ACCCCC
Th rexAB SDM-F	CCCGCAGTTCGAAAAAAGCGCTGGCCTGGTGCCGCGCGGC AGCGGCACAATTCCAGAGAAACCACAAGG
Th rexAB SDM-R	CCTTGTGGTTTCTCTGGAATTGTGCCGCTGCCGCGCGGCAC CAGGCCAGCGCTTTTTTCGAACTGCGGG

Primers for sequencing	
pCL55 Fwd seq	GGATCCCCTCGAGTTCATG
pCL55 Rev seq	CTCGTAGTATCTATACTTCG
pCN34 seq F	GTTATCCCCTGATTCTGTGGATAAC
pCN34 seq R	CCAGAATTATATTCAGAACAGGAAC
T7P	TAATACGACTCACTATAGG
T7T	GCTAGTTATTGCTCAGCGG
rexA midseq1-F	GTTTTAGAAGGTGGCTTTATTGATATACC
rexA midseq2-R	GACGACTACTATCTTCAATTTGTGC
rexB midseq1-F	AGCATCTTGAACAAGAATTTGATGC
rexB midseq2-R	GCTTAGTGTTGTTTCTACAATAGC
rexA midseq3-R	CAGCTTTCAAATCATCAGC
rexB midseq3-F	GGCGATTTTAAACAATTAGACC
StrepII rexA seq-R	GGATAATACGCTCAACTAG

Primers for confirming chomosomal integration of p*itet*	
Lipase geh F	GTTGTTTTTGTACATGGATTTTTAG
Lipase geh R	CTTGCTTTCAATTGTGTTCC
pCL55 R	GCGCATAGGTGAGTTATTAGC

Primers to generate DNA substrate for nuclease, helicase and ATPase activity assays	
Chi F	GCTTAGTTATAGACACGGCAC
Chi R	CCTGGTCTTTTACGTACTGC
Chi control F	TCAGTGAATTAGATGATTCGC
Chi control R	TTCATACGTATGAATGTTATTTGC

2.2.3 Site-directed mutagenesis (SDM)

Site directed mutagenesis (SDM) was performed to introduce a Streptavidin-II (StrepII) tag onto the N-terminus of the recombinant RexA protein to enable its purification and detection. The cloning strategy is described in section 5.3.1. PCR primers for SDM were designed using the QuikChange Primer Design Program (Agilent) and are listed in Table 2.5. PCR reactions were performed using Phusion DNA polymerase as described in section 2.2.2. Products were analysed by agarose gel electrophoresis to confirm size, purified via gel extraction or PCR purification (sections 2.2.6 and 2.2.7), and 1 µg of DNA was incubated with 1 µl (20 units) of DpnI (NEB) at 37 ˚C for 2 h to remove contaminating template DNA. DpnI digests DNA that is methylated on its recognition sequence 5' – GA^{m6}TC – 3'. Since DNA from *dam*+ strains such as *E. coli* XL1 Blue is methylated in this way, DpnI specifically digests the template DNA and leaves the non-methylated PCR product intact. The DpnI-digested product was purified using the QIAquick PCR Purification kit (Qiagen), and transformed into competent *E. coli* XL1 Blue (section 2.2.10). Successful mutagenesis was confirmed by colony PCR (section 2.2.2) and DNA sequencing (section 0).

2.2.4 Restriction digest

Restriction digestion was carried out for cloning and to identify succesfully generated plasmid constructs. Reactions typically consisted of 1 µl of 10x CutSmart Buffer (NEB), 1 µg of DNA, 1 µl (20 units) of restriction enzyme(s) (NEB) and nuclease-free water up to a total volume of 10 µl. Reactions were incubated at 37 ˚C for 2 h. To prevent re-circularisation of the digested vectors, restricted ends were dephosphorylated by the addition of 1 µl (1 unit) of Calf Intestinal Alkaline Phosphatase (NEB), 1 µl of 10x CutSmart buffer, and 8 µl of nuclease-free water to a final volume of 20 µl. Reactions were incubated at 37 ˚C for 1 h. When appropriate, digestion products were analysed by agarose gel electrophoresis (section 2.2.6) and gel extracted (section 2.2.7).

2.2.5 Ligation

Ligations were performed with a 1:3 molar ratio of vector: insert. 50 to 100 ng of the vector was combined with a thee-fold molar excess of insert as calculated using the NEBioCalculator (NEB). Then 2 µl of T4 DNA ligase buffer (NEB), 1 µl (400 units) of T4 DNA ligase (NEB) and nuclease-free water to a total volume of 20 ul were added. The reaction mixture was gently mixed by pipetting up and down. Sticky-ended ligations were incubated at room temperature for 1 h, and blunt-ended ligations were incubated for 2 h. The reaction was then transformed into 50 µl of competent *E. coli* cells (section 2.2.10). Postive clones were identified by colony PCR (section 2.2.2) or restriction digestion (section 2.2.4) of the purified plasmid.

2.2.6 Agarose gel electrophoresis

Agarose gel electrophoresis was used to analyse DNA products from PCR (section 2.2.2) and restriction digest (section 2.2.4). 1% (w/v) agarose gels were made by dissolving agarose (Sigma-Aldrich) in 1x Tris-Borate EDTA (TBE) buffer (1 M Tris-borate, 0.02 M EDTA, pH 8.0) by heating, with SYBR Safe DNA Gel Stain (Invitrogen) added at a 1: 10,000 dilution. Samples were mixed with 6x Purple Gel Loading Dye (NEB) and loaded into the gel alongside 2-Log DNA Ladder (NEB). Gels were run in TBE buffer at 100 V for approximately 40 min or until the dye front had migrated to the bottom of the gel. DNA was visualised, and images captured using a Gel Doc EZ Imager (Bio-Rad).

2.2.7 Gel extraction and PCR purification

DNA products were extracted following agarose gel electrophoresis (section 2.2.6) using the QIAquick Gel Extraction kit (Qiagen). DNA was visualised using a Safe Imager Blue Light Transilluminator (Invitrogen) and the bands of interest were excised using a scalpel. DNA was purified following the protocol accompanying the kit. The QIAquick PCR Purification kit (Qiagen) was used to purify DNA products for downstream applications. Purified DNA was quantified using a NanoVue Plus spectrophotometer (GE Healthcare) and stored at -20 ˚C.

2.2.8 DNA sequencing

DNA samples and primers were prepared for sequencing in separate microcentrifuge tubes, at 30-100 ng/µl for purified plasmid DNA, 10-50 ng/µl for purified PCR product and 10 µM of the appropriate primer (Table 2.5). Sanger sequencing was performed by GATC Biotech using a 3730XL DNA Analyser (Applied Biosystems). Sequencing data were analysed using the Benchling Molecular Biology Suite (Benchling, Inc.).

2.2.9 Preparation of chemically competent *E. coli*

A stationary-phase culture (2 ml) was used to inoculate 100 ml of LB in a 500 ml conical flask and grown to an $OD_{600\ nm}$ of 0.3-0.5. Cells were transferred into 50 ml centrifuge tubes and pelleted by centrifugation at 4000 rpm for 15 min at 4 °C. After discarding the supernatant, the cells were resuspended in 30 ml of ice cold $CaCl_2$ (50 mM) by gentle shaking, and incubated on ice for 20 min. The cells were pelleted again at 4000 rpm for 15 min and finally resuspended in 4 ml of ice-cold $CaCl_2$ (100 mM) containing 15% glycerol. The cell suspension was divided into 100 µl aliquots into pre-chilled microcentrifuge tubes and stored at -80 ˚C until required.

2.2.10 Transformation of competent *E. coli*

Ligation reactions were transformed into $CaCl_2$-competent *E. coli* XL1 Blue or DH5α cells. Briefly, the entire ligation reaction was added to 50 µl of *E. coli* cells before the mixture was incubated on ice for 30 min, heat-shocked for 1 min at 42 °C, and returned to ice for 2 min. LB broth (500 µl) was added and cells were then incubated for 1 h at 37 °C with shaking at 180 rpm. Bacteria were pelleted by centrifugation for 2 min at 7000 rpm, resuspended in 50 µl supernatant, spread on LBA plates containing the appropriate antibiotics and grown overnight at 37 °C in air.

2.2.11 Lysogenisation of *E. coli*

The λDE3 prophage was integrated into an *E. coli* host chomosome to enable expression of target genes cloned into T7 expression vectors, including pET28b$^+$. λDE3 is a recombinant phage that carries the T7 RNA polymerase gene under the control of the *lacUV5* promoter. In

T7 expression vectors, target genes are cloned under the control of the T7 promoter, therefore expression is induced by providing a source of T7 RNA polymerase in the host cell. Commonly used *E. coli* strains for protein expression generally carry the λDE3 prophage and are able to produce T7 RNA polymerase upon induction by IPTG. However, *E. coli* strains that are not typically used for protein expression do not carry the λDE3 prophage and λDE3 would have to be integrated for target gene expression.

Lysogenisation of *E. coli* was performed using the Novagen λDE3 Lysogenisation kit (Merck Millipore), following the manufacturer's instructions. Briefly, the *E. coli* host strain was grown in LB supplemented with 0.2% maltose, 10 mM $MgSO_4$, and any appropriate antibiotics at 37 °C to an OD_{600} of 0.5. Then using the provided stock lysates, lysogens were prepared by co-infection of 1 µl, 3 µl, 5 µl or 10 µl host cells with 10^8 pfu λDE3, 10^8 pfu Helper phage, and 10^8 pfu Selection phage. Several volumes of host cells were tested to produce plates containing 50–200 candidate lysogens as isolated colonies. Since λDE3 has an interrupted *int* gene and cannot integrate into the chomosome by itself, this function is provided by a Helper phage. The Selection phage enables λDE3 lysogens to survive as they have the same immunity, but kills any λDE3 host range mutants. Neither the Helper nor the Selection phages can form lysogens by themselves because they have no *cI* repressor and are virulent as a result. Next, the host-phage mixtures were incubated at 37 °C for 20 min to allow phage to adsorb to host, after which the mixtures were spread onto LBA plates supplemented with antibiotics to select for the host cells. Plates were incubated at 37 °C overnight and surviving colonies were expected to be λDE3 lysogens.

The λDE3 lysogens were verified by plating with a Tester phage, which is a T7 RNA polymerase deletion mutant that can only make plaques on cells containing T7 RNA polymerase (λDE3 lysogens) in the presence of IPTG. Briefly, host strains were grown as described above to an OD_{600} of 0.5. Then 100 µl of host cells were mixed with 100 µl of Tester phage diluted to a titre of 1–2 × 10^3 pfu/ml, in duplicate tubes. The host-phage mixtures were incubated at room temperature for 10 min to allow phage to adsorb to host. Next, 3 ml of molten top agarose (no warmer than 47 °C) was added to each tube and the contents of one

duplicate was poured onto an LB plate, while the other duplicate was poured onto an LB plate supplemented with 0.4 mM IPTG to evaluate induction of T7 RNA polymerase. After the top agarose had hardened, plates were incubated at room temperature overnight. In the presence of IPTG, λDE3 lysogens are expected to produce large plaques surrounded by large halos.

2.2.12 Preparation of electrocompetent *S. aureus*

1 ml of an overnight *S. aureus* culture was added to 100 ml of TSB in a 500 ml conical flask and grown to an $OD_{600\ nm}$ of 0.5-0.6. Cells were transferred into 50 ml centrifuge tubes and pelleted by centrifugation at 4000 rpm for 10 min at 4 °C. After discarding the supernatant the cells were washed twice by repeated rounds of resuspension and centrifugation in an equal volume of sterile 0.5 M sucrose then washed once in half the volume of 0.5 M sucrose and resuspended in 1 ml of 0.5 M sucrose. This bacterial cell suspension was then divided into 100 µl aliquots into pre-chilled microcentrifuge tubes and stored at -80 ˚C until required.

2.2.13 Transformation of electrocompetent *S. aureus*

Plasmid DNA was first transformed into chemically-competent *E. coli* DC10B (~100 ng of DNA transformed using the method described in section 2.2.10), which lacks cytosine methylation to enable bypassing of the staphylococcal restriction-modification barrier[449]. Then plasmid DNA was prepared from *E. coli* DC10B to a concentration of 300 to 800 ng/µl using the QIAprep Midiprep kit (Qiagen) from 100 ml of a stationary-phase culture. Plasmid DNA (20 µl) was dialysed against sterile water for 30 min using 13 mm-0.025 µm filter discs (Merck Millipore) before 15 µl was added to an aliquot of electrocompetent *S. aureus* cells defrosted on ice. Cells were electroporated using a Gene Pulser Electroporation system (Bio-Rad) in 0.1 cm electroporation cuvettes (VWR) at 100 W, 2.5 kV, 25 mF with a desired time constant of 2.1-2.5. Immediately after electroporation, 900 µl of TSB containing 0.5 M sucrose was added to the cuvette. Cells were then transferred into microcentrifuge tubes and incubated for 1 h at 37 °C (180 rpm) in air. Subsequently, cells were centrifuged for 2 min at 7000 rpm, resuspended in 100 µl TSB and spread over TSA plates containing the appropriate antibiotics. Agar plates were incubated for up to 48 h at 37 °C under aerobic conditions.

2.3 Protein techniques

2.3.1 Protein expression from the pET system

The pET system was used for high-level protein expression of recombinant *S. aureus* RexAB protein. This system relies on target gene expression from a T7 promoter, which is specifically recognised by the bacteriophage T7 RNA polymerase. All three expression strains used (Table 2.1) are λDE3 prophage lysogens that carry a chomosomal copy of T7 RNA polymerase gene under the control of the *lacUV5* promoter. *E. coli* soluBL21 (DE3) is a mutant strain of BL21 (DE3) that has been optimised to produce soluble protein in most cases where an insoluble protein is expressed in the parent strain. *E. coli* Rosetta 2 (DE3) pLysS is a BL21 (DE3) derivative that has been supplied with tRNAs for seven rare codons in *E. coli* (AGA, AGG, AUA, CUA, GGA, CCC, and CGG), and expresses T7 lysozyme from pLysS, which suppresses basal expression of T7 RNA polymerase prior to induction. This stabilises pET recombinants with target proteins that affect cell growth and viability.

The pET28b$^+$ vector (Table 2.2) encodes a six-histidine tag (6xHis tag) at the N-terminus of the target protein for nickel affinity chomatography (section 2.3.2.1). The inducer isopropyl β-D-1-thiogalactopyranoside (IPTG) is a molecular mimic of allolactose, which is bound by the LacI repressor to relieve repression of *lacUV5* and to induce the expression of T7 RNA polymerase and as a consequence, the target gene.

Protein expression conditions required optimisation, which involved varying the expression strain (*E. coli* BL21 (DE3), soluBL21 (DE3) and Rosetta 2 (DE3) pLysS), temperature (16, 20, 30 and 37 °C), media (LB and TB) and IPTG induction concentration (0.4 and 1 mM). Expression at 30 °C or 37 °C was carried out for 3 h, and expression at 16 °C or 20 °C was carried out overnight (~20 h).

Plasmids encoding recombinant proteins were transformed (section 2.2.10) into the *E. coli* expression strain, and the transformation plate was used to inoculate 5 ml of medium. After growth at 37 °C (180 rpm) overnight, the culture was used to inoculate centrifuge tubes (50 ml volume) containing 12 ml of fresh media supplemented with the

appropriate antibiotics to a final $OD_{600\ nm}$ of 0.05. The number of centrifuge tubes was dependent on the number of expression conditions to be tested. The cultures were grown at 37 °C (180 rpm) to mid-exponential phase ($OD_{600\ nm}$ of 0.5), at which point a 1 ml pre-induction culture sample was taken and prepared for SDS-PAGE analysis (section 2.3.5). Expression was induced by the addition of IPTG and cultures were shifted to the desired expression temperature. Culture samples were taken every hour post-induction and were prepared for SDS-PAGE analysis.

To determine the solubility of the protein under the expression conditions tested, sonication of bacterial cells was performed. Therefore, the remaining culture was pelleted by centrifugation at 4000 rpm for 10 min at 4 °C, and resuspended in 2 ml of Buffer A (50 mM Tris, 150 mM NaCl, pH 7.5). The cell suspension was sonicated for 2 min (5 sec on-off cycle) at 40% amplitude using a Vibra-cell sonicator (Sonics) until lysed. The lysate was then centrifuged at 17, 000 x *g* for 2 min and the supernatant (soluble fraction) transferred into a clean tube held on ice. The pellet (insoluble fraction) was resuspended in an equal volume of Buffer A to the soluble fraction, and 100 µl samples of both fractions were prepared for SDS-PAGE analysis.

Protein expression samples were analysed by SDS-PAGE to determine the conditions for optimal protein expression. For RexAB protein purification, conditions were optimised to expression in *E. coli* soluBL21 (DE3) cells induced by the addition of 1 mM IPTG, and grown at 20 °C overnight in TB. Expression was scaled up to 1 L or 4 L as desired, and cell pellets were stored at -20 °C until protein purification.

2.3.2 Protein purification

2.3.2.1 Nickel affinity chomatography

Proteins containing 6xHis tags were purified using nickel affinity chomatography. Nickel has a strong affinity for histidine residues and therefore His-tagged proteins bind to the nickel immobilised on the column. This enables them to be separated from other proteins present in the whole cell lysate. His-tagged proteins stay bound to the column until the addition of

imidazole, which acts as a molecular mimic of the imidazole ring side-chain of histidine. At high concentrations, imidazole displaces the His-tagged proteins from the nickel column, resulting in elution of the protein.

Cell pellets containing recombinant proteins that had been stored at -20 °C were thawed fully before resuspension in Buffer A. For 4 L cultures, 175 ml of Buffer A was used. The cell suspension was sonicated for 30 min (10 seconds on, 30 seconds off cycle) at 30% amplitude using a Model 705 Sonic Dismembrator (Thermo Fisher Scientific) until lysed. The lysate was then spun at 32,000 x *g* for 30 min at 4 °C to separate the soluble and insoluble protein fractions. The pellet was resuspended in an equal volume of Buffer A to the soluble fraction, and samples were taken and prepared for SDS-PAGE analysis (section 2.3.5).

While the lysate was being centrifuged, 5 ml of Chelating Sepharose Fast Flow resin (GE Healthcare) was loaded with 0.1 M $NiCl_2$ into a gravity flow column, and equilibrated with 100 ml of equilibration buffer (50 mM Tris, 150 mM NaCl, 20mM imidazole, pH 7.5). The resin was added to the supernatant, and the mixture was left at 4 °C overnight with stirring to enable the His-tagged protein to bind to the nickel-charged resin. The next day, the mixture was poured into a gravity flow column. The column was washed with 40 ml of equilibration buffer and the wash was repeated eight times, making sure to stir the resin after each addition of buffer. To remove weak, non-specific binding to the resin, the column was washed with 20 ml of buffer containing 70 mM imidazole (50 mM Tris, 150 mM NaCl, 70mM imidazole, pH 7.5; 10 ml added each time and stirring the resin in-between). Then the His-tagged protein was eluted with buffer containing 150 mM imidazole (50 mM Tris, 150 mM NaCl, 150mM imidazole, pH 7.5) by adding 10 ml of elution buffer each time. Protein elution was monitored by the addition of sufficient Bradford Reagent (Bio-Rad) to produce chromogenic product, which was used to monitor each fraction until no more protein was detected. Bradford reagent contains the Coomassie Brilliant Blue G-250 dye, which undergoes a colorimetric change from red to blue when protein is present. When no more protein is present, the colour of the reagent remains red-brown. The imidazole concentrations of 70 mM and 150 mM were optimised for RexAB after an initial purification of 1 L culture with stepwise elution at 100, 200 and 300 mM.

Samples were removed during each step and prepared for SDS-PAGE analysis to evaluate the purification. Based on the results of the SDS-PAGE analysis with Coomassie staining, fractions were pooled into an Amicon 100 kDa cut-off concentrator (Merck Millipore) to remove smaller molecular weight proteins, remove imidazole and to concentrate the protein. Concentrators were centrifuged at 2000 x *g* (4 °C), and the pooled fractions were washed 3-4 times with Buffer A to remove the imidazole. Protein samples were aliquoted into microcentrifuge tubes and stored at -80 °C.

2.3.2.2 Strep-Tactin affinity chomatography

Proteins containing Streptavidin-II (StrepII) tags were purified using Strep-Tactin affinity chomatography. This system was designed based on the well-known binding of biotin to streptavidin. The StrepII tag is a short engineered peptide of 8 amino acids (Trp-Ser-His-Pro-Gln-Phe-Glu-Lys) that bind to the biotin-binding pocket of streptavidin when fused to recombinant proteins, serving as a purification mechanism. Strep-Tactin is a streptavidin derivative that is optimised for maximal binding to the StrepII-tag. StrepII-tagged proteins are competitively eluted by the addition of desthiobiotin, which is an inexpensive, stable and reversibly-binding analogue of biotin.

Cell pellets stored at -20 °C were thawed fully before being resuspended in Buffer A. For 1 L cultures, 25 ml of Buffer A was used. The cell suspension was sonicated for 30 min (10 seconds on, 30 seconds off cycle) at 30% amplitube using a Model 705 Sonic Dismembrator (Fisher Scientific) until lysed. The lysate was then spun at 32,000 x *g* for 30 min at 4 °C to separate the soluble and insoluble protein fractions. The pellet was resuspended in an equal volume of Buffer A to the soluble fraction, and samples were taken and prepared for SDS-PAGE analysis (section 2.3.5).

While the lysate was being spun, 5 ml of Strep-Tactin sepharose resin (IBA) was loaded into a gravity flow column, and washed with 100 ml of wash buffer (50 mM Tris-HCl, 1 M NaCl, pH 7.5). Then the supernatant was added to the resin and the mixture was mixed for 2 h to enable the StrepII-tagged protein to bind to the Strep-Tactin resin. After collecting the

flow though, the column was washed with 200 ml of wash buffer, by adding 25 ml each time and making sure to stir the resin after each addition of buffer. The StrepII-tagged protein was eluted with 25-30 ml of buffer containing desthiobiotin (50 mM Tris, 150 mM NaCl, 2.5 mM D-desthiobiotin, pH 7.5) by adding 5 ml of the buffer each time. Samples were removed during each step and prepared for SDS-PAGE analysis to evaluate the purification. Based on the results of the SDS-PAGE analysis, selected fractions were pooled and stored at -80 °C. The Strep-Tactin resin was regnerated by the addition of regeneration buffer (50 mM Tris, 150 mM NaCl, 1 mM EDTA, 1 mM HABA (2- [4'-hydroxy-benzeneazo] benzoic acid), pH 7.5). The resin was stored at 4 °C.

2.3.3 Bicinchoninic acid (BCA) assay for protein quantification

The bicinchoninic acid (BCA) protein assay was used to quantify the total protein concentration. In the assay, peptide bonds reduce cupric (Cu^{2+}) ions in a copper solution to the cuprous (Cu^{1+}) ion. This is followed by the chelation of BCA with the cuprous ion, resulting in a purple colour. The BCA/copper complex is water-soluble and has a strong linear absorbance at 562 nm with increasing protein concentrations.

The total protein concentration was quantified using the Pierce BCA protein assay kit (Thermo Fisher Scientific), following the manufacturer's instructions. Briefly, a standard curve was prepared by diluting bovine serum albumin (BSA) in Buffer A and 25 µl of each concentration was pipetted into a clean, flat-bottomed 96-well plate. The protein was diluted 1/5, 1/10 and 1/20 in Buffer A up to 25 µl in each well, and 25 µl of storage buffer was used as a blank. Then 1 ml of proprietary BCA reagent was added to each sample, and the 96-well plate was incubated at 37 °C for 30 min. After cooling for 5 min at room temperature, the absorbance at 562 nm was measured using an Infinite M200-PRO microplate reader (Tecan).

2.3.4 Polyclonal antibody production

The purified recombinant *S. aureus* RexAB protein complex (section 5.3.3) was sent to Covalab for rabbit immunisation. The complex was used for antibody production to enable detection of the native protein complex in *S. aureus* whole cell extracts. In addition, the

individual RexA and RexB subunits were discovered to be unstable in solution when protein purification was attempted (sections 5.3.2.1 and 5.3.2.2). Two rabbits were immunised with the protein following a 53-day protocol with thee injections and thee bleeds. Injections were performed at 0, 14, and 28 days. Bleeds were taken pre-immunisation, 39 days after immunisation and after termination at 53 days (final bleed). This produced one polyclonal antibody against the recombinant *S. aureus* RexAB complex.

2.3.5 SDS-Polyacrylamide Gel Electrophoresis (SDS-PAGE)

Sodium dodecyl sulphate (SDS)-polyacrylamide gel electrophoresis (PAGE) was used for protein analysis. SDS is a detergent that denatures proteins and imparts a uniform negative charge so that the rate of migration though the gel is inversely related to the molecular weight. Heating of samples further promotes protein denaturation. Gels were prepared as per the composition listed in Table 2.6. Ammonium persulphate (10%) (APS; Sigma-Aldrich) and tetramethylethylenediamine (TEMED; Sigma-Aldrich) were added immediately prior to casting to polymerise the mixture. Running gel mixture (5 ml) was pipetted between clean Mini-PROTEAN glass plates (Bio-Rad) and the gel was levelled with 1 ml of isopropanol. After the running gel had polymerised, the isopropanol was poured out and the gel surface washed with distilled water. Residual water was blotted with filter paper. Then, the stacking gel mixture was prepared and pipetted on top. An appropriate well comb was inserted and the stacking gel was left to set.

Samples (10 µl) were loaded into the wells of the SDS-PAGE gel alongside 5 µl of PageRuler Plus Prestained Protein Ladder (Thermo Fisher Scientific). SDS-PAGE running buffer (0.025 M Tris, 0.192 M glycine, 0.1% SDS, pH 8.5) was added to the inner chamber of the Mini-PROTEAN Tetra Cell buffer tank (Bio-Rad) until full and then to the outer chamber until half full. Gels were run at 100 V for 10 min, then 200 V for 35 min (400 mA) or until dye front had migrated to the bottom of the gel.

Table 2.6. Composition of SDS-polyacrylamide running and stacking gels

Component	Running gel 8% (10 ml, for one gel)	Stacking gel 4.5% (4 ml, for two gels)
30% Acrylamide/Bis	2.6 ml	600 µl
1.5 M Tris-HCl pH 8.8 + 0.3% SDS	2.5 ml	-
0.5 M Tris-HCl pH 6.8 + 0.4% SDS	-	1 ml
Distilled water	4.9 ml	2.4 ml
10% (w/v) APS	100 µl	40 µl
TEMED	10 µl	4 µl

2.3.5.1 SDS-PAGE sample preparation

Protein samples for SDS-PAGE analysis were prepared via the protein purification processes described above from *E. coli* and *S. aureus* cultures. For samples taken during protein purification, an equal volume of 2x Laemmli buffer (4% SDS, 20% glycerol, 10% 2-mercaptoethanol, 0.02% bromophenol blue and 0.125 M Tris-HCl, pH 6.8) was added and the mixture was heated at 95 °C for 5 min. For *E. coli* samples, 1 ml of the culture was centrifuged for 2 min at 17,000 x *g*. Then the pellet was resuspended in 5 µl of distilled water for every 0.1 $OD_{600\ nm}$ to correct for differences in optical density between samples. The same volume of 2x Laemmli buffer was added, and the sample was heated at 95 °C for 5 min.

For *S. aureus*, 100 ml of overnight culture was centrifuged for 10 min at 4000 rpm and the pellet resuspended in 1.6 ml of distilled water. Lysostaphin solution (200 µl, 2 mg/ml) (Sigma-Aldrich) was added and the mixture incubated at 37 °C for 30 min. Next, 20 µl of DNase (NEB) was added and the sample incubated at 37 °C for a further 30 min. After centrifugation at 17,000 x *g* for 2 min, the supernatant was loaded into an Amicon Ultra-2 100 kDa filter to concentrate the sample by centrifugation for 30 min at 4000 rpm. Finally, an equal volume of 2x Laemmli buffer was added and the mixture boiled at 95 °C for 10 min.

All samples were stored at -20 °C and were spun at 17,000 x *g* for 1 min before being resolved by SDS-PAGE analysis (see section above).

2.3.5.2 Coomassie blue staining

Coomassie blue was used to visualise protein bands. Developed SDS-PAGE gels were removed from between glass plates and placed in distilled water for 10 min on a rocking platform. Then the water was discarded and the gel was immersed in 20 ml of Bio-Safe Coomassie stain (Bio-Rad) for 45 min on a rocking platform to resolve protein bands. Stained gels were washed with distilled water for 1 h before being imaged on a Gel Doc EZ Imager (Bio-Rad).

2.3.6 Western blotting

Western blotting was used to detect specific proteins in cell extracts to assess protein expression and/or purification. The SDS-PAGE gel was removed from the glass plates and placed in Towbin buffer (25 mM Tris, 192 mM glycine, 20% (v/v) methanol, pH 8.3) for 10 min. Meanwhile, eight gel-sized sheets of Whatmann filter paper were soaked in Towbin buffer, and a gel-sized sheet of nitrocellulose membrane was wetted in Towbin buffer and rinsed briefly with distilled water. The blot was assembled on a Trans-Blot Turbo transfer system (Bio-Rad), with four sheets of filter paper at the bottom, followed by the blot, then the gel, and finally the remaining four sheets of filter paper were placed on top. A roller was used over the assembled blot to remove any trapped air bubbles. The proteins in the gel were transferred onto the membrane by running the Trans-Blot system at 10 V (1 A) for 1 h.

The membrane was then blocked in TBST (20 mM Tris, 150 mM NaCl, 0.1% Tween 20, pH 7.5) containing 5% skimmed milk powder or 3% bovine serum albumin (BSA; as appropriate for the antibody to be used) for 1 h at room temperature, or overnight at 4 °C. For *S. aureus* cell extracts, TBST containing 5% skimmed milk powder and 3% human serum albumin (HSA) at 1/200 dilution was used to prevent non-specific binding of the antibodies . The membrane was washed thee times in TBST for 10 min each, and incubated for 1 h with the primary antibody diluted appropriately in TBST containing 5% skimmed milk powder, 3% BSA and/or 1/200 HSA. The membrane was then washed thee times in TBST for 10 min each, and incubated with the secondary antibody in TBST containing 5% skimmed milk

powder, 3% BSA and/or 1/200 HSA. After the incubation, the membrane was washed for a final thee times in TBST for 10 min each, and 1 ml of premixed Amersham ECL Prime western blotting detection reagent (GE Healthcare) was pipetted onto the surface of the membrane to enable chemiluminescent detection of protein bands. The blot was imaged after 5 min of incubation with the detection reagent, using a ChemiDoc Touch imaging system (Bio-Rad).

To detect His-tagged proteins, mouse anti-His horseradish peroxidase (HP)-conjugated antibody (Sigma-Aldrich) was used at 1/2000 dilution in TBST containing 5% skimmed milk powder. To detect StrepII-tagged proteins, Strep-Tactin conjugated to alkaline phosphatase (IBA) was used at 1/4000 dilution in TBST containing 3% BSA. For detecting the RexAB protein in staphyloccocal cell extracts, rabbit polyclonal anti-RexAB (Covalab; section 2.3.4) was used at 1/10,000 dilution (unless stated otherwise) in TBST containing 5% skimmed milk powder and 1/200 HSA as the primary antibody, and goat anti-rabbit IgG-HP (Cell Signaling Technology) was used at 1/2000 dilution as the secondary antibody.

2.4 Determination of enzyme activity

2.4.1 Catalase activity

Catalase is an enzyme that breaks down H_2O_2 into oxygen and water. To determine the level of catalase activity, overnight *S. aureus* cultures were washed thee times with PBS and 10^7 CFU were added to 100 µM H_2O_2 (diluted in PBS) to a total volume of 1 ml and incubated at 37 °C in the dark. At the start of the incubation and after 15 min, 200 µl of sample was removed and centrifuged at 17,000 x *g* for 3 min, and 20 µl of the supernatant was added to a 96-well plate. PBS containing no bacteria was used as a negative control.

Catalase activity was determined indirectly by measuring the concentration of H_2O_2 using the Pierce Quantitative Peroxide Assay kit (aqueous-compatible formulation) (Thermo Fisher Scientific). Following the manufacturer's instuctions, reagents A and B were mixed at a ratio of 1:100 and 200 µl was added to each sample in the 96-well plate. The plate was then incubated for 30 min at room temperature and the absorbance was measured at 595

nm using an iMark microplate reader (Bio-Rad). The H_2O_2 concentration was determined using a standard curve of known concentrations (up to 1 mM).

2.4.2 Nuclease activity

Nucleases are able to degrade nucleic acid by hydrolysing the phosphodiester bonds between nucleotides. The nuclease activity of the RexAB protein complex was measured to confirm the presence of nuclease activity in the recombinant protein and to determine the activity of compounds as nuclease inhibitors. Since staphylococcal RexAB is believed to recognise a seven-nucleotide motif (otherwise known as the crossover hotspot instigator (Chi, χ) site) that leads to inhibition of degradation[455], Chi recognition was also tested via the DNA substrate used. Staphylococcal DNA was amplified from the whole genome by colony PCR (section 2.2.2) using the primer pairs listed in Table 2.5. This created two 1 kb DNA fragments, one with a staphyloccocal Chi site in the middle ("Chi F" and "Chi R" primers) and one without ("Chi control F" and "Chi control R" primers, as a negative control). After PCR purification (section 2.2.7), these DNA fragments were used as the DNA substrate in the assay.

Reactions were set up in nuclease assay buffer (25 mM Tris-acetate pH 7.5, 2 mM Mg acetate, 1 mM DTT) as per the composition in Table 2.7. The DMSO content was maintained at 1% (v/v) when compounds were being tested. Samples were incubated at 37 °C in a heat block. At the start of the incubation and at 5, 15, 30, 60 and 120 min, 5 µl of the reaction mixture was removed and pipetted into pre-prepared microcentrifuge tubes containing 20 µl of STEB buffer (40 % (w/v) sucrose, 100 mM Tris-HCl, 10 mM EDTA, 0.5 mg/ml bromophenol blue, pH 8) to stop the reaction. Chloroform/isoamyl alcohol (24:1, 20 µl) was added to each tube, vortexed for 10 s and centrifuged for 2 min at 17,000 x *g* to remove the protein and any compounds tested for inhibitory activity. The aqueous (upper blue) phase was loaded onto a 1% (w/v) agarose gel prepared in TBE buffer and electrophoresis was carried out at 85 V for 1 h. The gel was then stained with SYBR Safe DNA gel stain (Invitrogen) at 1/10,000 dilution in TBE buffer for 2 h with rocking, and visualised using a Gel Doc EZ

Imager (Bio-Rad). Band intensity was quantified using ImageJ software[456]. Values were normalised to the no-compound, no-ATP control at 0 h.

Table 2.7. Composition of the nuclease activity assay

Reaction component	Volume (µl)	Final concentration
5x nuclease assay buffer	12	1x (25 mM Tris-acetate pH 7.5, 2 mM Mg acetate, 1 mM DTT)
DNA (Chi^0 or Chi^+, 100 ng/µl)	3	5 ng/µl
ATP (10 mM) or nuclease-free water	6	1 mM
RexAB (500 nM)	6	50 nM
Nuclease-free water	27	-
Total	60	

2.4.3 Helicase activity

DNA helicases separate double-stranded DNA into single strands using energy derived from ATP hydrolysis. The helicase activity of RexAB was measured to confirm the presence of this activity in recombinant RexAB and to determine the activity of compounds as helicase inhibitors. The DNA substrate was created by colony PCR amplification of the staphylococcal genome using the primer pair “Chi F” and “Chi R” listed in Table 2.5, and PCR purification of the resulting DNA fragment (section 2.2.2).

Reactions were set up in helicase assay buffer (25 mM Tris-acetate pH 7.5, 0.25 mM Mg acetate, 1 mM DTT) as per the composition in Table 2.8. The DMSO content was maintained at 1% (v/v) when compounds were being tested. Samples were incubated at 37 °C in a heat block. At the start of the incubation and at 5, 15, 30, 60 and 120 min, 5 µl was removed and pipetted into pre-prepared microcentrifuge tubes containing 20 µl of STEB buffer (40 % (w/v) sucrose, 100 mM Tris-HCl, 10 mM EDTA, 0.5 mg/ml bromophenol blue, pH 8) to stop the reaction. 20 µl of chloroform/isoamyl alcohol (24:1) was added to each tube, vortexed for 10 s and centrifuged for 2 min at 17,000 x *g* to remove the protein and any compounds used for inhibition. The aqueous (upper blue) phase was then loaded onto a 1% (w/v) agarose gel prepared in TBE buffer and electrophoresis was carried out at 85 V for 1 h. The gel was

stained for 2 h on a rocking platform with SYBR Green II (Sigma-Aldrich) at 1/10,000 dilution in TBE buffer to detect dsDNA and ssDNA. The gel was visualised using a Gel Doc EZ Imager (Bio-Rad) and band intensity was quantified using ImageJ software[456]. Values were normalised to a ssDNA control, which was set up similarly to Table 2.8 but without the RexAB, and the mixture was instead heated at 95 °C for 2 min to denature the dsDNA and allow the single-stranded DNA binding protein (SSB) to bind and stabilise the two ssDNA strands.

Table 2.8. Composition of the helicase activity assay

Reaction component	Volume (µl)	Final concentration
5x helicase assay buffer	12	1x (25 mM Tris-acetate pH 7.5, 0.25 mM Mg acetate, 1 mM DTT)
DNA (Chi$^+$, 100 ng/µl)	3	5 ng/µl
ATP (10 mM) or nuclease-free water	6	1 mM
E. coli single-stranded DNA binding protein (SSB, 661.4 µM) (Sigma-Aldrich)	0.2	2 µM
RexAB (200 nM)	6	20 nM
Nuclease-free water	32.8	-
Total	60	

2.4.4 ATPase activity

ATPase activity involves the release of an inorganic phosphate (P_i) from an organic phosphorylated substrate, such as ATP. This dephosphorylation reaction releases energy, which is often used to drive other chemical reactions. This assay was used to measure ATPase activity in recombinant RexAB and to determine the activity of compounds as inhibitors of ATPase activity in RexAB.

Reactions were set up similarly to the nuclease activity assay (section 2.4.2) with the difference that no DTT was added in the assay buffer to prevent interference with the P_i detection reagent. The DMSO content was maintained at 1% (v/v) when compounds were being tested. Samples were incubated at 37 °C in a heat block. At the start of the incubation and at 5, 15, 30, 60 and 120 min, 5 µl samples were removed and heated at 95 °C for 5 min to stop the reaction, and then diluted 1/10 in nuclease-free water in a 96-well plate to a total

volume of 50 µl (T = 120 min samples were diluted 1/20). The 96-well plate was incubated at 37 °C for 10 min to equilibrate to the same temperature, before using the PiColorLock Gold Phosphate Detection System assay kit (Expedeon) to detect P_i, following the manufacturer's instructions. The PiColorLock assay is based on the change in absorbance of the dye malachite green when it reacts with P_i to form a green P_i -dye complex.

After equilibration, 12.5 µl Gold mix was added to each well of the plate, incubated at room temperature for 5 min, and finally 5 µl of stabiliser solution was added. Then the plate was left for 30 min at room temperature and the absorbance was measured at 595 nm using an iMark microplate reader (Bio-Rad). The P_i concentration was determined using a standard curve of known concentrations (up to 50 µM).

2.4.5 Topoisomerase IV activity

E. coli topoisomerase IV is a type II topoisomerase that relaxes supercoiled DNA. To determine the topoisomerase IV-inhibitory activity of compounds an *E. coli* Topoisomerase IV Relaxation Assay Kit (Inspiralis) was used, following the manufacturer's instructions and maintaining a constant DMSO content of 1% (v/v). Supercoiled pQE80L (Table 2.2) was prepared via plasmid purification (section 2.2.1) and used as the substrate for the reaction. The relaxed and supercoiled forms of the plasmid were visualised by agarose gel electrophoresis (section 2.2.6). Electrophoresis was carried out at 85 V for 2 h or until the dye front had migrated to the bottom of the gel. The gel was then stained with SYBR Safe DNA gel stain (Invitrogen) at 1/2500 dilution in TBE buffer for 1.5 h with rocking, and visualised using a Gel Doc EZ Imager (Bio-Rad). Band intensity was quantified using ImageJ software (2) and the fraction of relaxed plasmid was determined as the density of the relaxed bands compared to the total density. Values were normalised to the no-compound control and background corrected against the no-enzyme control.

2.4.6 Gyrase activity

DNA gyrase is a type II topoisomerase that introduces negative supercoils into DNA by hydrolysing ATP. It is present in all bacteria but not in higher eukaryotes. To determine the

gyrase-inhibitory activity of compounds, an *E. coli* gyrase supercoiling assay kit (Inspiralis) was used, following the manufacturer's instructions and maintaining a constant DMSO content of 1% (v/v). Relaxed pBR322 substrate (provided in the kit) was supercoiled by the gyrase and the two forms of the plasmid were visualised by agarose gel electrophoresis (section 2.2.6). Electrophoresis was carried out at 85 V for 2 h or until the dye front had migrated to the bottom of the gel. The gel was then stained with SYBR Safe DNA gel stain (Invitrogen) at 1/2500 dilution in TBE buffer for 1.5 h with rocking, and visualised using a Gel Doc EZ Imager (Bio-Rad). Band intensity was quantified using ImageJ software[456] and the fraction of supercoiled plasmid was determined as the density of the supercoiled band compared to the total density. Values were normalised to the no-compound control and background corrected against the no-enzyme control.

2.5 Growth profiling

To measure growth of *S. aureus*, bacterial cultures were first grown overnight in TSB at 37 °C (180 rpm), then subcultured 1/50 into a flat-bottomed 96-well plate (200 µl total volume) and placed into a POLARstar Omega plate reader (BMG Labtech). Bacteria were grown for 17 h at 37 °C (700 rpm) in air, and absorbance at 600 nm was measured every 30 min.

For *S. gordonii* and *E. faecalis*, overnight cultures were grown in THB containing 1% yeast extract at 37 °C (static, in 5% CO_2), subcultured 1/50 into a flat-bottomed 96-well plate (200 µl total volume) and placed into an Infinite M200-PRO microplate reader (Tecan). Bacteria were grown for 17 h at 37 °C (static, in 5% CO_2), and absorbance at 600 nm was measured every 30 min.

2.6 *recA* promoter fluorescent reporter assay

Promoter-reporter gene constructs were used to directly assess expression from the *recA* promoter in response to DNA damage, by linking promoter activity to green fluorescent protein (GFP) production (section 3.2). Strains carrying the reporter construct were grown overnight

in TSB containing the appropriate antibiotics, then diluted 1/10 into a flat-bottomed 96-well plate containing fresh TSB with the DNA damaging agent (200 µl total volume per well) and placed into an Infinite M200-PRO microplate reader (Tecan).

Cultures were grown for 17 h at 37 °C (700 rpm), and both absorbance at 600 nm ($OD_{600\ nm}$) and GFP fluorescence intensity (FI) were measured every 30 min. To account for differences in FI caused by variation in the total number of bacteria in each sample, fluorescence values were corrected for culture density as measured by $OD_{600\ nm}$, and *recA*-promoter activity was expressed as $FI/OD_{600\ nm}$.

2.7 Haemolytic activity

The haemolytic activity of *S. aureus* culture supernatants was determined essentially as described previously[457]. Bacterial cultures were set up in 5 ml TSB supplemented with AHT and/or antibiotic as appropriate, and incubated overnight at 37 °C (180 rpm). 1 ml of the culture was pelleted for 5 min at 17,000 x *g* and the supernatant was pipetted undiluted into microcentrifuge tubes or at a 1/10 dilution in TSB, to a total volume of 400 µl. An equal volume of 2% Defibrinated Sheep's Blood (E&O) prepared in PBS was then added and the mixture incubated statically for 1 h at 37 °C. Fresh TSB containing 2% Defibrinated Sheep's Blood was used as a negative control, and the supernatant from the wild-type strain was used as a positive control. After centrifugation for 5 min at 500 x *g* (room temperature), 200 µl of supernatant was transferred into a flat-bottomed 96-well plate and the absorbance of released haemoglobin was measured at 540 nm using a POLARstar Omega plate reader (BMG Labtech).

2.8 Staphyloxanthin extraction and quantification

To extract and quantify staphyloxanthin from *S. aureus*, overnight cultures grown in TSB were first harvested by centrifugation at 17,000 x *g* for 2 min. Staphyloxanthin was extracted by incubating bacteria in methanol at 42 °C for 30 min. Cells were pelleted by centrifugation at

17,000 x *g* for 2 min, and 100 µl of supernatant was transferred into a flat-bottomed 96-well plate. The released staphyloxanthin was quantified by measuring the absorbance at 462 nm using a POLARstar Omega plate reader (BMG Labtech).

2.9 Determination of minimum inhibitory concentration (MIC)

Minimum inhibitory concentrations (MICs) were determined using the serial broth dilution protocol described by Wiegand *et al.* (2008)[458]. Overnight cultures were grown in appropriate media at 37 °C (180 rpm or static, as appropriate), diluted to a concentration of 1 x 10^5 CFU/ml and incubated in flat-bottomed 96-well plates with a range of antibiotic concentrations for 17 h at 37 °C under static conditions (aerobic or 5% CO_2). The range of antibiotic concentrations was generated by two-fold serial dilutions in media starting from the highest concentration of antibiotic and resulted in a final volume of 100 µl. The MIC was defined as the lowest concentration at which no growth was observed (zero turbidity).

Chequerboard MIC assays were performed to test the effect of two antibiotics or compounds simultaneously. Unless specified otherwise, compounds were obtained from MolPort. The two antibiotics or compounds were first prepared separately in flat-bottomed 96-well plates by two-fold serial dilutions in media (one with dilutions running down the plate and the other going across) starting with double the highest concentration to be tested and ending with a row/column containing no antibiotic or compound. This resulted in a final volume of 95 µl in each well. Then, a further two-fold dilution was carried out by removing 95 µl from the final column (lowest concentration) of one plate, mixing with the same column on the second plate, and pipetting the doubly-diluted media back into the first plate. This was repeated across the entire plate with the highest concentration diluted last, resulting in two chequerboard 96-well plates, one of which was stored overnight at 4 °C for the second replicate. Overnight cultures were prepared as for a standard MIC assay and 5 µl of bacteria was added to each well for a final concentration of 1 x 10^5 CFU/ml. Chequerboard MIC assays were incubated for

17 h at 37 °C under static conditions, and absorbance was measured at 600 nm (2 x 2 readings) using an Infinite M200-PRO microplate reader (Tecan).

2.10 Determination of minimum bactericidal concentration (MBC)

The minimum bactericidal concentration (MBC) was determined by subculturing broth dilutions from the wells of MIC assays that inhibited the growth of a bacterium (i.e. concentrations at or above the MIC). The broth dilutions were plated onto agar without the antibacterial agent, and the CFU counts were enumerated. The MBC was defined as the lowest concentration of antibiotic required for a 1000-fold reduction in CFU counts compared to the inoculum[459].

2.11 Determination of bacterial survival

2.11.1 Antibiotic survival

Antibiotic survival assays were performed to measure the rate at which *S. aureus, S. gordonii* and *E. faecalis* strains were killed by an antibiotic. Aliquots of stationary-phase bacterial cultures (1 ml) were centrifuged for 2 min at 17,000 x *g* and the recovered cells washed twice with fresh media. The washed bacteria were adjusted to a final concentration of 10^8 CFU/ml in fresh media before the antibiotic was added. Cultures were incubated at 37 °C and bacterial viability determined by CFU counts at 0, 2, 4 and 6 h.

2.11.2 Whole blood survival

To assess bacterial survival in whole human blood, stationary-phase cultures were washed twice with PBS and adjusted to 10^6 CFU/ml. Aliquots of the bacterial suspension (10^4 CFU in 10 µl) were added to the wells of a sterile 96-well flat-bottomed plate and incubated with 90 µl of freshly-donated human blood (collected in EDTA-treated tubes; BD Biosciences) or PBS (for 0 h time point). Before the addition of bacteria, blood was treated for 15 min with diphenyleneiodonium (DPI; 50 µM, Sigma-Aldrich), or for 45 min with L-N_5-(1-iminoethyl)ornithine (L-NIO; 100 µM, Sigma-Aldrich), N_G-monomethyl-L-arginine (L-NMMA;

100 µM, Sigma-Aldrich), or cytochalasin D (10 µM, Sigma-Aldrich) as needed. An equivalent volume of DMSO was tested as a solvent control. For experiments involving DPI in combination with L-NIO or L-NMMA, all blood was treated for 45 min. Plates were then sealed with Parafilm and incubated for 6 h at 37 °C with shaking at 180 rpm. CFU counts were enumerated by serial dilution and plating onto CBA plates, which stopped the killing. Survival was calculated as a percentage of the number of bacteria in the inoculum.

2.11.3 Hydrogen peroxide survival

To assess bacterial survival in hydrogen peroxide (H_2O_2), stationary-phase cultures were washed twice with PBS and adjusted to 10^6 CFU/ml. 10 µl of the bacterial suspension (10^4 CFU) was added to wells in a sterile 96-well flat-bottomed plate, and 90 µl of freshly diluted H_2O_2 (10 mM in PBS) or PBS (for 0 h time point) was added. The 96-well plate was incubated for 1 h at 37 °C (static) in the dark. CFUs were enumerated by serial dilution and plating onto CBA, which contains catalase to prevent any further killing after plating. Survival was calculated as a percentage of the number of bacteria in the inoculum.

2.11.4 Neutrophil survival

Neutrophils (freshly-isolated human PMNs) were adjusted to 5 x 10^6 cells/ml in Hanks' Balanced Salt Solution (HBSS) containing 10% human serum, 0.1 mM calcium and 0.1 mM magnesium (Thermo Fisher Scientific). Overnight bacterial cultures were washed in PBS and 1 x 10^6 CFU was added to the neutrophil suspension (MOI 1:5) to a total volume of 1 ml. Neutrophils were treated for 10 min prior to the addition of bacteria with diphenyleneiodonium (DPI; final concentration of 50 µM) or an equivalent volume of DMSO (solvent control for DPI) as needed. The bacterial and neutrophil suspension was then incubated at 37 °C with tumbling. At each time point (0.5, 1, 2, 3 h), 50 µl of the suspension was transferred to a 96-well plate and serially diluted in ten-fold steps in PBS up to 10^3 dilution. Aliquots of each dilution (and undiluted) were then plated onto CBA and incubated for 24 h at 37 °C before colonies were counted. Survival was calculated for each time point as a percentage of the number of bacteria in the inoculum.

2.11.5 Murine infection model

Animal experiments were conducted Dr Thomas Clarke (Imperial College London). Mice were infected via the intraperitoneal route with wild-type or *rexAB* mutant JE2 or SH1000. Stationary-phase bacterial cultures were washed twice with PBS and adjusted to 10^7 CFU/ml. 0.4 ml of the bacterial suspensions were injected into the peritoneal cavity of each mouse (5 mice for each strain, 20 in total). After 6 h, the animals were humanely sacrificed by cervical dislocation and death confirmed by severing the femoral artery.

The peritoneal cavity was washed with PBS to release bacteria and CFU counts were determined by plating onto TSA. The murine sample size was determined prior to the experiment using power analysis[460]. Tubes containing the bacterial suspensions were blinded before starting the experiment. Mice were randomly allocated to group cages and each group was randomly allocated to a treatment. Following Home Office regulations, any animals that displayed two or more of the following symptoms were humanely killed using a Schedule 1 method and excluded from the study: shivering, hunched posture, reduced movement, cyanosis, circling or difficulty breathing.

2.12 Isolation of neutrophils

Neutrophils were isolated from human blood for use in neutrophil survival assays and flow cytometry experiments. Whole human blood (15 ml) freshly collected in EDTA-treated tubes (BD Biosciences) was layered over 20 ml of room temperature Polymorphprep (Alere Limited). Cells were centrifuged at 500 x *g* for 45-60 min (brake off, 30 °C) until a clear separation of red blood cells (RBCs), peripheral blood mononuclear cells (PBMCs) and polymophonuclear leukocytes (PMNs, or neutrophils) was seen. The PBMCs were discarded and the PMNs were transferred to a fresh 50 ml centrifuge tube. HBSS (Thermo Fisher Scientific) was added to the PMNs to a total volume of 50 ml and the cells wre pelleted at 500 x *g* for 10 min (brake off, 30 °C). The cells were resuspended in 3 ml of HBSS, counted using a haemocytometer and

adjusted to 5 x 10^6 cells/ml in HBSS containing 10% human serum, 0.1 mM calcium and 0.1 mM magnesium (Thermo Fisher Scientific).

2.13 Flow cytometry

2.13.1 Preparation of samples for cell analysis

Bacteria containing the *PrecA-gfp* reporter construct (section 3.2) were prepared and added to neutrophils as described for the neutrophil survival assay (MOI 1:5) (section 2.11.4). The bacterial and neutrophil suspension was incubated at 37 °C with tumbling. At each time point (0.5, 1, 2, 3 h), 500 µl of the suspension was transferred to a fresh microcentrifuge tube and spun at 500 x *g* for 10 min. The pellet was resuspended in 4% paraformaldahyde in PBS (PFA; Affymetrix). Samples were left in 4% PFA at room temperature for a least 1 h to fix the cells, before centrifugation at 500 x *g* for 10 min and resuspension of the pellet in PBS.

2.13.2 Analysis of fluorescent reporter-containing bacteria incubated with neutrophils

Flow cytometry experiments were conducted by Dr Jessica Rowley (Imperial College London). Samples were analysed on the FACS Aria flow cytometer (BD Biosciences) and at least 100,000 events were captured for all samples. Green fluorescence (from GFP-expressing bacteria) was detected at 488/530 (30) nm. Data were analysed by Kam Pou Ha using FlowJo software (Version 10).

2.14 Computational analyses

2.14.1 Alignment of amino acid sequences

Multiple sequence alignments were generated using Clustal Omega via the EMBL-EBI web server (https://www.ebi.ac.uk/Tools/msa/clustalo). Parameters were left in their default settings with the exception of alignment “order”, which was set to consider the input order. The output format was set to “ClustalW with character counts”, which provides the alignment with base/residue numbering.

2.14.2 Phyre2 structural modelling

Protein structure was predicted using the Phyre2 protein fold recognition server, which is a protein homology/analogy recognition engine (http://www.sbg.bio.ic.ac.uk/phyre2).

Phyre2 uses multiple algorithms and programs to build a structural model for the input query sequence in a four-stage process. In the first stage, closely-related homologues are gathered by scanning the query sequence against a curated sequence database in which no sequences share greater than 20% identity, by creating and comparing Hidden Markov Model profiles. The resulting multiple-sequence alignment is used to predict the secondary structure using PSIPRED, which is a program that uses neural network machine learning to predict the presence of α-helices, β-sheets and coils. In the second stage, the alignment and the secondary structure prediction are combined and scanned against a database of known protein structures ("fold library") whose profiles have been calculated using the same approach as stage one. The top-scoring alignments are used to construct crude backbone models that generally contain insertions and deletions (indels) and do not contain side chains[461].

In the third stage, indels are corrected by a process called loop modelling, in which the crude model is compared against the query sequence and a library of fragments of known protein structures is generated, taking into account the sequence, distance between endpoints, and geometry of flanking regions of each indel. Fragments are then fitted to the crude model, the fitted fragments are ranked and the top-scoring model is selected. Finally, amino-acid side chains are fitted to the backbone to generate the final 3D model[461]. The model was viewed using the PyMOL Molecular Graphics System Version 2.3 (Schödinger).

2.14.3 I-TASSER structural modelling

In addition to the Phyre2 structural modelling above, the iterative theading assembly refinement (I-TASSER) server was also used for protein structure prediction. The server was accessed at the following URL: https://zhanglab.ccmb.med.umich.edu/I-TASSER/.

I-TASSER uses a similar multi-step protocol to generate a structural model for the query sequence. Initially, the query sequence is matched against a non-redundant sequence

database to identify homologues using Position-Specific Iterated Basic Local Alignment Search Tool (PSI-BLAST), and the resulting multiple-sequence alignment is used to predict the secondary structure using PSIPRED. Then the query sequence, assisted by the alignment and the predicted secondary structure, is scanned against a protein structure database using LOMETS, which is a server that combines seven programs for identifying template proteins from solved structure databases. Continuous fragments from the top-scoring alignments are generated from the template structures and used to assemble structures of the sections that aligned well. The fragment assembly simulation is repeated using these structures to remove steric clashes and the most probable structures are selected as input for REMO, which is an algorithm that generates 3D models by optimising the hydrogen-bonding network. Finally, the function of the query protein is derived by structurally matching the predicted model against proteins of known structure and function in the Research Collaboratory for Structural Bioinformatics Protein Data Bank (RCSB PDB) library[462]. The model was viewed using the PyMOL Molecular Graphics System Version 2.3 (Schödinger).

2.15 Statistical analyses

Results are expressed as the mean of at least thee independent experiments, with the standard deviation of the mean indicated by error bars. Statistical significance was assessed using either a one-way analysis of variance (ANOVA) followed by the Dunnett's test, or a two-way ANOVA followed by Sidak's or the Tukey test as appropriate. ANOVA testing was performed as it takes into account the variances within different groups to reduce false-positives when making multiple comparisons. For murine experiments, CFU counts are expressed as the value obtained from each animal, median values are shown for comparisons, and significance was assessed using the Mann-Whitney test. $P < 0.05$ was considered significant between data points (GraphPad Prism 8 for Windows).

3 DNA repair is required for survival of *S. aureus* during infection

3.1 Introduction

Staphylococcus aureus is an opportunistic pathogen responsible for a wide range of human infections, including those of the skin and soft tissues, bones, joints and bloodstream[8,17]. Treatment can be ineffective due to the emergence of antibiotic-resistant or tolerant strains[59], necessitating the development of new therapeutic approaches. One such approach is to increase the sensitivity of *S. aureus* to host defences.

In the host, interactions between *S. aureus* and immune cells greatly influence infection outcomes. Phagocytosis of *S. aureus* by neutrophils leads to the oxidative burst, in which reactive oxygen species (ROS) are rapidly generated and released within the phagosome[140]. The neutrophil oxidative burst is the most important defence mechanism against *S. aureus*, demonstrated by the high incidence of *S. aureus* infections in chonic granulomatous disease (CGD) patients who cannot generate ROS[141]. ROS cause oxidative damage to a variety of biomolecules, leading to lipid and protein peroxidation, oxidation and deamination of DNA bases, and DNA strand breakage[154]. Of these, the most significant impact is believed to be upon DNA, because DNA damage can be lethal if not repaired[147,151,157–160]. However, although DNA is believed to be the major target of the oxidative burst, this has not been shown experimentally in *S. aureus*.

DNA damage in bacteria triggers the SOS response, which is a global regulatory pathway that causes cell cycle arrest and the induction of DNA repair[313]. In *S. aureus,* induction of the SOS pathway leads to the transcription of 16 genes[318]. These genes include the low-fidelity DNA polymerase UmuC (Pol V), which enables replication of damaged DNA templates, and RecA, which is a key regulator of the SOS response and mediates the repair of DSBs[157,445,463]. Previous approaches used to study the SOS response involve treatment of bacterial cultures with a DNA-damaging agent followed by direct quantification of SOS genes

via reverse transcription quantitative PCR (RT-qPCR) or detection of the gene product by Western blotting[317,318,331,464,465], or by using a reporter gene construct[444,466–469]. For example, McCool *et al.* (2004) quantified SOS expression in *E. coli* by fusing the promoter of the *sulA* gene, which is induced 100-fold during the SOS response, to the green fluorescent protein (*gfp*) reporter gene[470].

The hypothesis to be tested in this chapter is that the neutrophil oxidative burst targets staphylococcal DNA such that DNA repair is necessary for survival of the pathogen. To assess whether the observed phenotypes are conserved across both methicillin-sensitive and methicillin-resistant *S. aureus* (MSSA and MRSA, respectively), experiments were performed in two distinct genetic backgrounds (SH1000 and JE2). SH1000 is a well-characterised MSSA strain that is sensitive to first-line β-lactam antibiotics, whereas JE2 is a community-associated MRSA (CA-MRSA) strain of the USA300 LAC lineage, originally isolated from a skin and soft tissue infection (SSTI) in a Los Angeles County (LAC) prison inmate[368]. USA300 is the most prevalent strain in the United States[471], where it is responsible for more than a third of *S. aureus* bacteraemia cases[472].

Aim: To determine whether staphylococcal DNA is a target of the neutrophil oxidative burst and to assess the importance of DNA repair for the survival of *S. aureus* during infection and when exposed to DNA-damaging antibiotics.

3.2 Construction of the *recA*-promoter fluorescent reporter

To determine whether the oxidative burst causes DNA damage in *S. aureus*, a fluorescent reporter system was constructed to measure SOS induction via a fluorescent signal. To do this, the *gfp* gene was placed under the control of a promoter that is activated as part of the SOS response. The *umuC* promoter was initially chosen, because Cirz *et al.* (2007) found that *umuC* (SACOL1400) showed the greatest upregulation (24.8-fold after 30 min) in *S. aureus* after treatment with ciprofloxacin, a well-characterised DNA-damaging antibiotic that triggers the SOS response[318]. However, attempts to transform either of the shuttle vectors pCL55 or pCN34 containing the *PumuC-gfp* construct into *S aureus* were unsuccessful (data not shown). Therefore, the *S. aureus recA* promoter was then chosen due to its regulation via the SOS response, of which it is itself a key regulator.

The *recA* promoter was amplified from wild-type JE2 genomic DNA (provided by Dr Kimberley Painter) using primers specific for the *recA* promoter region (Table 2.5)[467]. Then, overlapping extension PCR was used to fuse the promoter to the gene for green fluorescent protein (*gfp*), amplied from an existing *agr*-P3*gfp* reporter construct[266]. The shuttle vector pCL55 was initially used for the cloning as it integrates a single copy of the gene into the *S. aureus* genome and does not require antibiotic for selection[473]. However, after unsuccessful attempts at staphylococcal transformation (data not shown), it was decided to use the pCN34 shuttle vector. This is a low-copy plasmid (20-25 copies per cell) that does not integrate into the genome[454]. Considering the large difference in SOS induction between *recA* (4.9-fold compared to baseline) and *umuC* (24.8-fold) as measured by Cirz *et al.* (2007), having multiple copies of the plasmid would boost the *recA* signal and thereby promote signal strength[318].

After sequencing the pCN34 *PrecA-gfp* reporter system (Figure 3.1) to confirm that the construct was correct, the plasmid was transformed into *E. coli* DC10B to ensure that the DNA would not be methylated and therefore targeted by staphylococcal restriction systems[449]. The pCN34 *PrecA-gfp* plasmid was then transformed into wild-type SH1000 and JE2 strains, which was confirmed by colony PCR using the pCN34 sequencing primers listed

in Table 2.5 (Figure 3.2). As a control for the effects of the plasmid and its selection, unmodified pCN34 was introduced into wild-type *S. aureus* strains. Next, the growth of all strains was assessed using a microplate reader to test whether the reporter construct conferred a growth defect. However, any differences in growth were minimal or below the limits of detection between wild-type strains containing empty pCN34 or the pCN34 *PrecA-gfp* reporter construct (Figure 3.3A, B).

To test whether the reporter system produced a signal in response to DNA damage, bacteria were exposed to the DNA-damaging antibiotic ciprofloxacin, a well-known trigger of the SOS response. These data showed a dose-dependent fluorescent signal in response to the antibiotic for the *PrecA-gfp* reporter strains (Figure 3.3C-F) with a peak at around 4 h to indicate ciprofloxacin-induced SOS induction, which is indicative of DNA damage. The signal gradually increased after stationary phase, most likely suggesting SOS induction from internal DNA damage caused by nutrient limitation and metabolic stress[286,474]. Taken together, these results showed that a promoter-reporter system to measure SOS induction had been successfully generated.

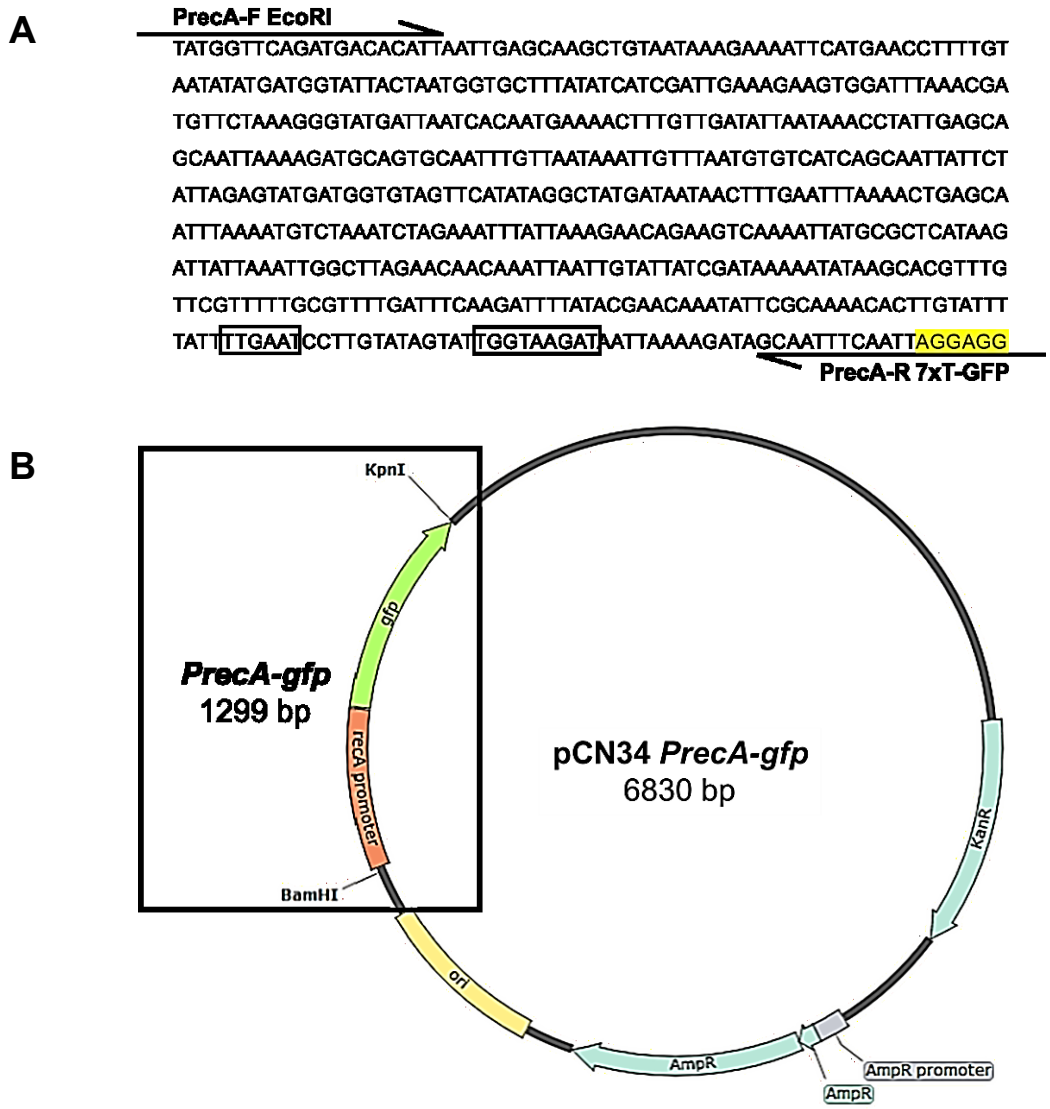

Figure 3.1. Schematic representation of the pCN34 *PrecA-gfp* reporter system.

The *recA* promoter region with predicted -10 and -35 promoter elements in boxes and the ribosome binding sequence (RBS) highlighted in yellow **(A)**. Primers used for amplification and their respective binding sites are indicated. Diagram of the pCN34 plasmid showing BamHI and KpnI restriction sites used for cloning and the *PrecA-gfp* insert **(B)**. Ori, origin of replication; AmpR, amplicillin resistance gene; KanR, kanamycin resistance gene. Plasmid map created with SnapGene.

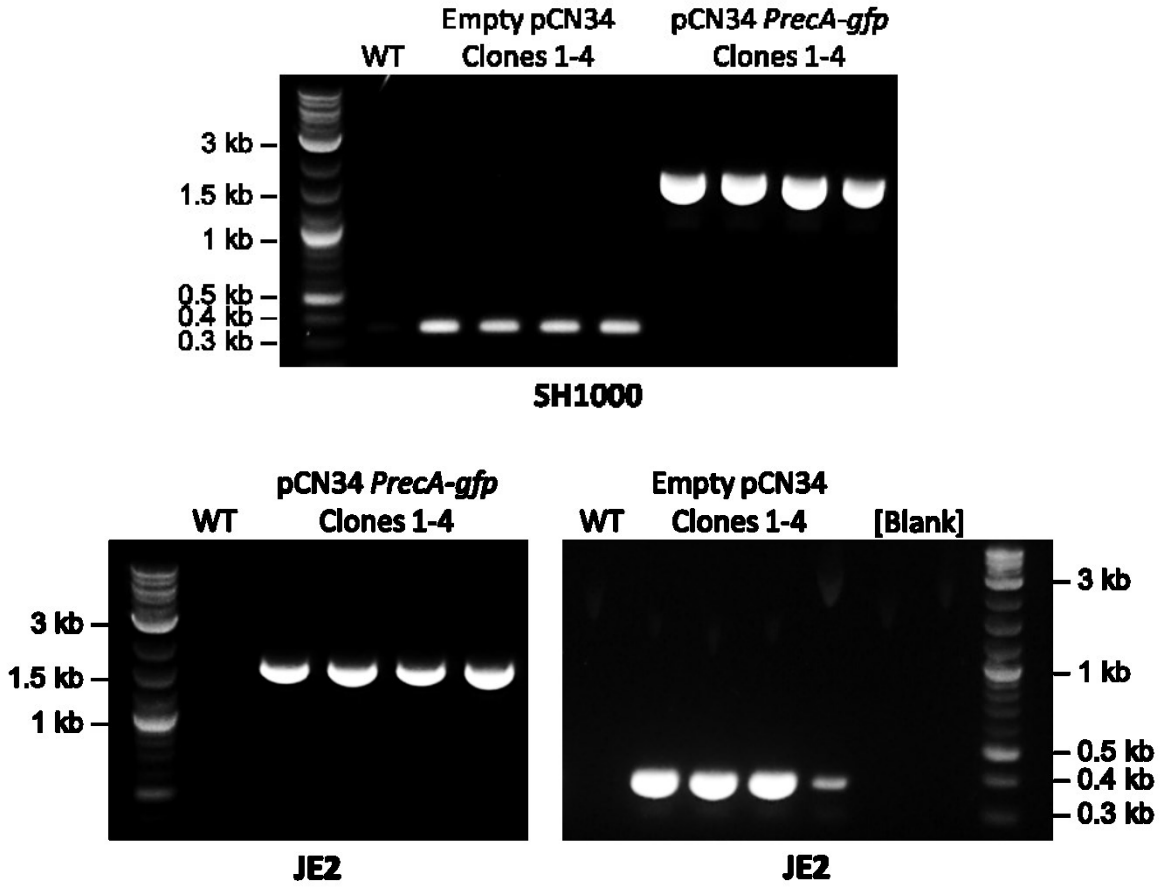

Figure 3.2. Gel electrophoresis images confirming the transformation of empty pCN34 or pCN34 *PrecA-gfp* into wild-type *S. aureus* SH1000 and JE2.

Colony PCR was used to amplify DNA from wild-type and reporter strains, using primers flanking the insert. PCR products were analysed on a 1% (w/v) agarose gel next to a 2-log DNA ladder (NEB) to confirm the presence of the empty pCN34 (PCR product size of 377 bp) or pCN34 *PrecA-gfp* (1663 bp). For all strains, clone 1 was selected for future experiments.

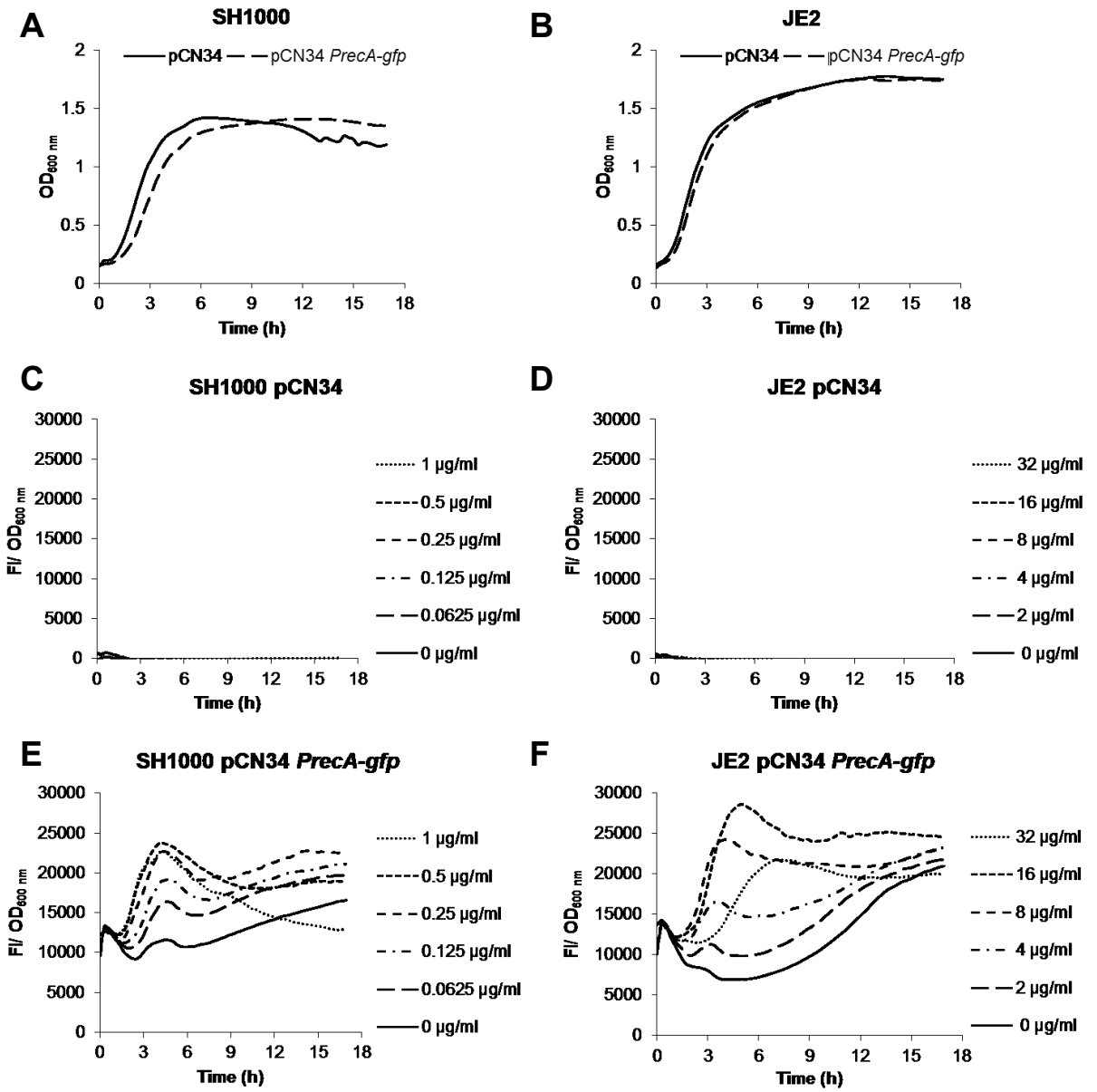

Figure 3.3. pCN34 *PrecA-gfp* reporter system successfully generates a dose-dependent fluorescent signal in response to ciprofloxacin-induced DNA damage.

Growth of wild-type SH1000 **(A)** and JE2 **(B)** strains was assessed by taking $OD_{600\,nm}$ readings every 30 min over 17 h. Reporter strains were exposed to a range of ciprofloxacin concentrations and *recA* expression was measured for SH1000 containing empty pCN34 **(C)**, JE2 containing empty pCN34 **(D)**, SH1000 pCN34 *PrecA-gfp* **(E)**, and JE2 pCN34 *PrecA-gfp* **(F)**. Expression is shown relative to cell density ($FI/OD_{600\,nm}$) for each strain over time. Graphs represent the mean of three biological replicates with error bars omitted for clarity.

3.3 The neutrophil oxidative burst triggers the SOS response pathway in *S. aureus*

To determine whether the oxidative burst damages DNA and triggers the SOS response, wild-type SH1000 and JE2 strains carrying the *PrecA-gfp* reporter were incubated with purified human neutrophils and *recA* expression was measured using flow cytometry. To study the role of the oxidative burst, some of the neutrophils were pre-treated with diphenyleneiodonium (DPI), which prevents ROS production by inhibiting NADPH oxidase[475]. As a solvent control, additional neutrophils were incubated with DMSO. At the beginning of the assay (0 h) and after 0.5, 1, 2 and 3 h, cells were washed in PBS and fixed with 4% PFA. Bacteria- and neutrophil-only samples were prepared to inform with the gating strategy. Flow cytometry of prepared samples was carried out by Dr Jessica Rowley (Imperial College London).

To measure phagocytosis, cells were first gated on cell size (side scatter, SSC) and granularity (forward scatter, FSC) to differentiate between bacteria and neutrophils (Figure 3.4A, C, F). Then, the number of free bacteria was determined by gating for GFP-positive cells, because *PrecA-gfp* produces a low level of GFP even in the absence of DNA damage (Figure 3.4B). This was compared to the number of bacteria associated with neutrophils, which was determined by gating the neutrophils for single cells and then calculating the number of GFP-positive cells (Figure 3.4D, E, G, H). The percentage of phagocytosis was determined as the number of phagocytosed bacteria divided by the total number of free and phagocytosed bacteria. Since the MOI was 0.2 (1 bacterium to 5 neutrophils), it was assumed that there would be no more than one bacterium phagocytosed per neutrophil, making the number of GFP-positive neutrophils proportional to the number of phagocytosed bacteria. The median fluorescence intensity (FITC median) of the GFP-positive cells in this gate (Figure 3.4E, H) was used to measure the degree of SOS induction. Inital flow cytometry experiments were also performed on *S. aureus* strains containing empty pCN34 to optimise the gating strategy for GFP-positive cells (data not shown). Flow cytometry

plots from one representative experiment are shown for all samples in Figure 3.5, with the first time point adjusted to 0.083 h (5 min) to account for the sample processing time.

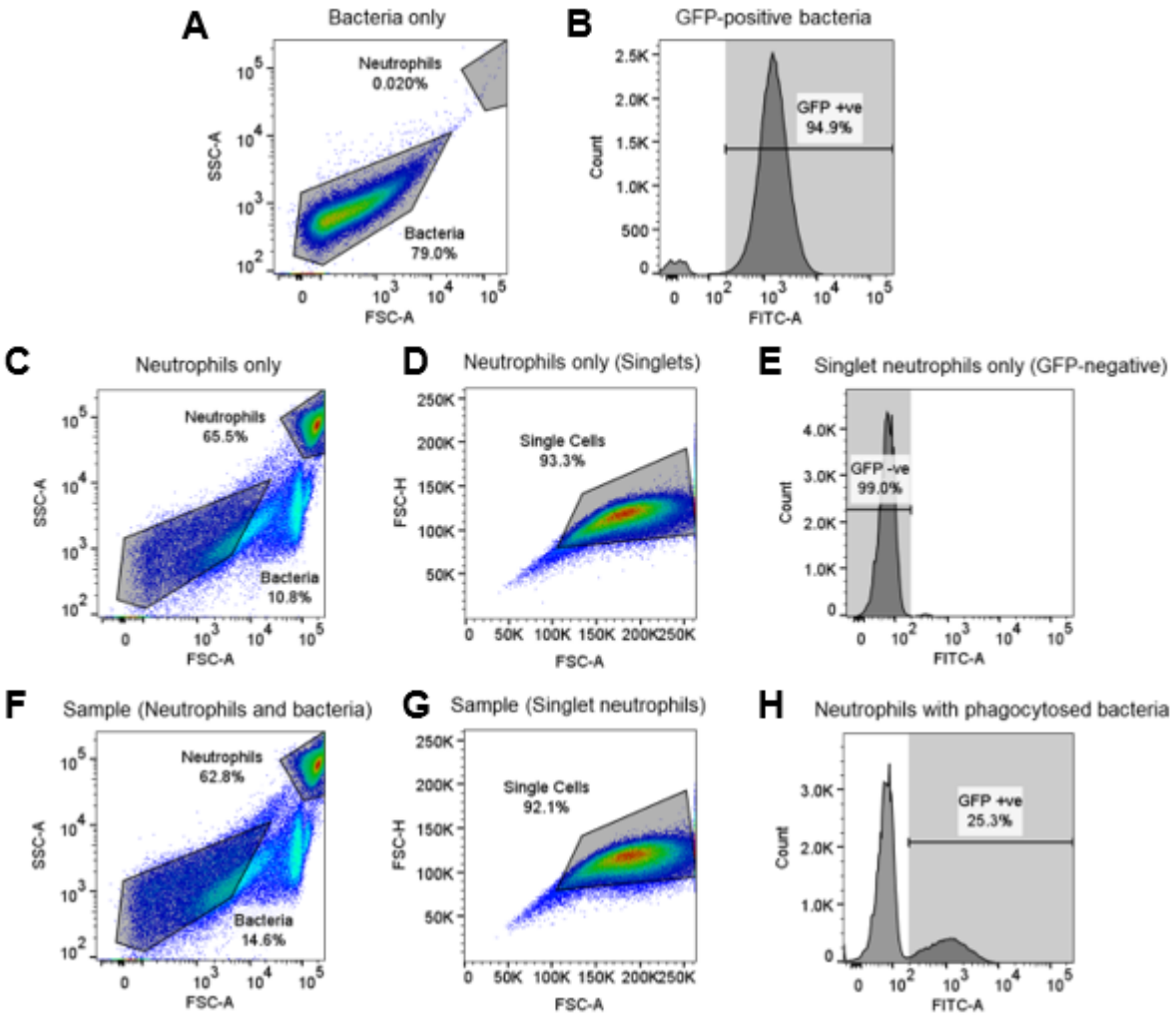

Figure 3.4. Gating strategy for flow cytometry analysis.

(A-B) Bacteria-only control gated by forward scatter (FSC-A) and side scatter (SSC-A) to differentiate between bacteria and neutrophils (A). Then, cells were gated by GFP expression (FITC-A) to determine the number of free bacteria (B) since *recA* (hence, *gfp*) is expressed at a low level even in the absence of DNA damage. **(C-E)** Neutrophil-only control gated by forward and side scatter (C), then gated to isolate single cells (D), and subsequently by GFP expression (E). **(F-H)** Gating strategy used for each sample and time point. Neutrophils and bacteria were gated by forward and side scatter (F), then to isolate single cells (G). Numbers of phagocytosed bacteria were compared to total number of bacteria to calculate percentage phagocytosis at each time point. To quantify DNA damage, neutrophils containing phagocytosed GFP-positive bacteria were isolated and the median GFP value was determined at each time point (H). Relative GFP detection was used to compare induction of SOS in *S. aureus* when incubated with DMSO- or DPI-treated neutrophils.

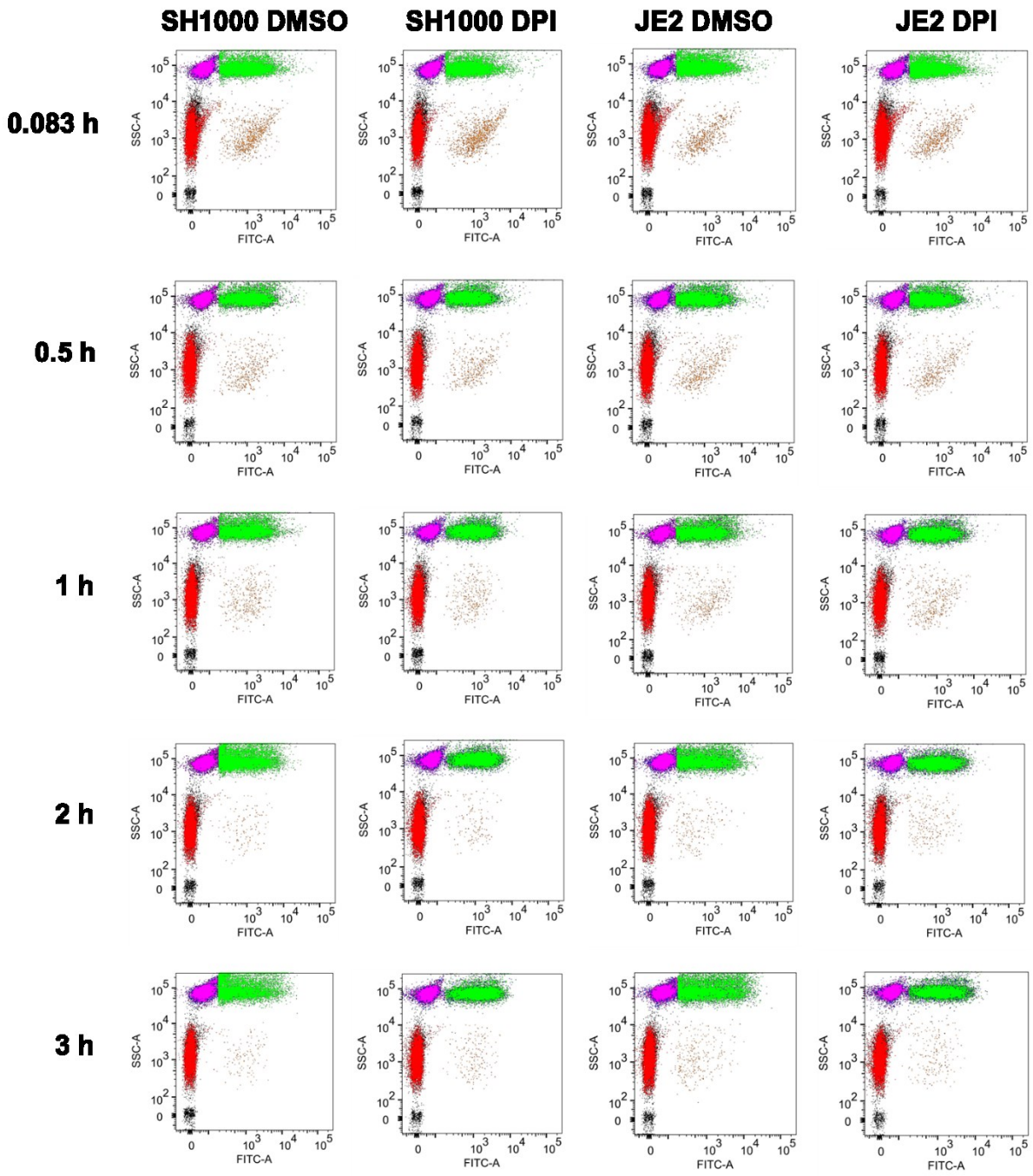

Figure 3.5. Flow cytometry plots of wild-type SH1000 and JE2 after incubation with DPI- or DMSO-treated neutrophils.

Samples were taken at 0.083 (0 h + 5 min sample processing time), 0.5, 1, 2 and 3 h incubation. Bacteria and neutrophils were differentiated by their SSC, and GFP-positive cells were gated on with a FITC greater than ~110 units. Colours refer to each gated population following the key in Figure 3.4. Phagocytosed bacteria (green), single cells of neutrophils (pink), neutrophils (blue), free bacteria (orange), bacteria (red), ungated (black). One representative image is shown for each time point for each sample.

Wild-type SH1000 or JE2 strains containing the *PrecA-gfp* reporter were rapidly phagocytosed when incubated with neutrophils, with over 90% of the bacteria being internalised within 5 min and over 99% by 30 min (Figure 3.6A, B). This occurred at similar levels with both DMSO- and DPI-treated neutrophils, indicating that inhibition of NADPH oxidase activity does not affect phagocytosis. During the first 30 min, there was also an increase in GFP-mediated fluorescence for SH1000 and JE2 strains incubated with DMSO-treated neutrophils (Figure 3.6C, D), indicating that the oxidative burst of neutrophils triggered SOS induction in response to DNA damage.

However, there also appear to be triggers of SOS that are independent of the oxidative burst. After 1 h, strains incubated with DPI-treated neutrophils continued to increase in fluorescence (Figure 3.6E, F), suggesting DNA damage from other sources, such as nutrient limitation and metabolic stress[286,474]. By contrast, GFP-mediated fluorescence from strains incubated with DMSO-treated neutrophils either decreased as for SH1000 (Figure 3.6E), or slowly plateaued as for JE2 (Figure 3.6F), possibly due to killing of the bacteria accompanied by bleaching of intraphagosomal GFP[230].

Results from these flow cytometry experiments show that neutrophil-mediated killing of *S. aureus* leads to DNA damage and the induction of the SOS DNA repair pathway. Furthermore, this DNA damage is caused, at least in part, by the neutrophil oxidative burst.

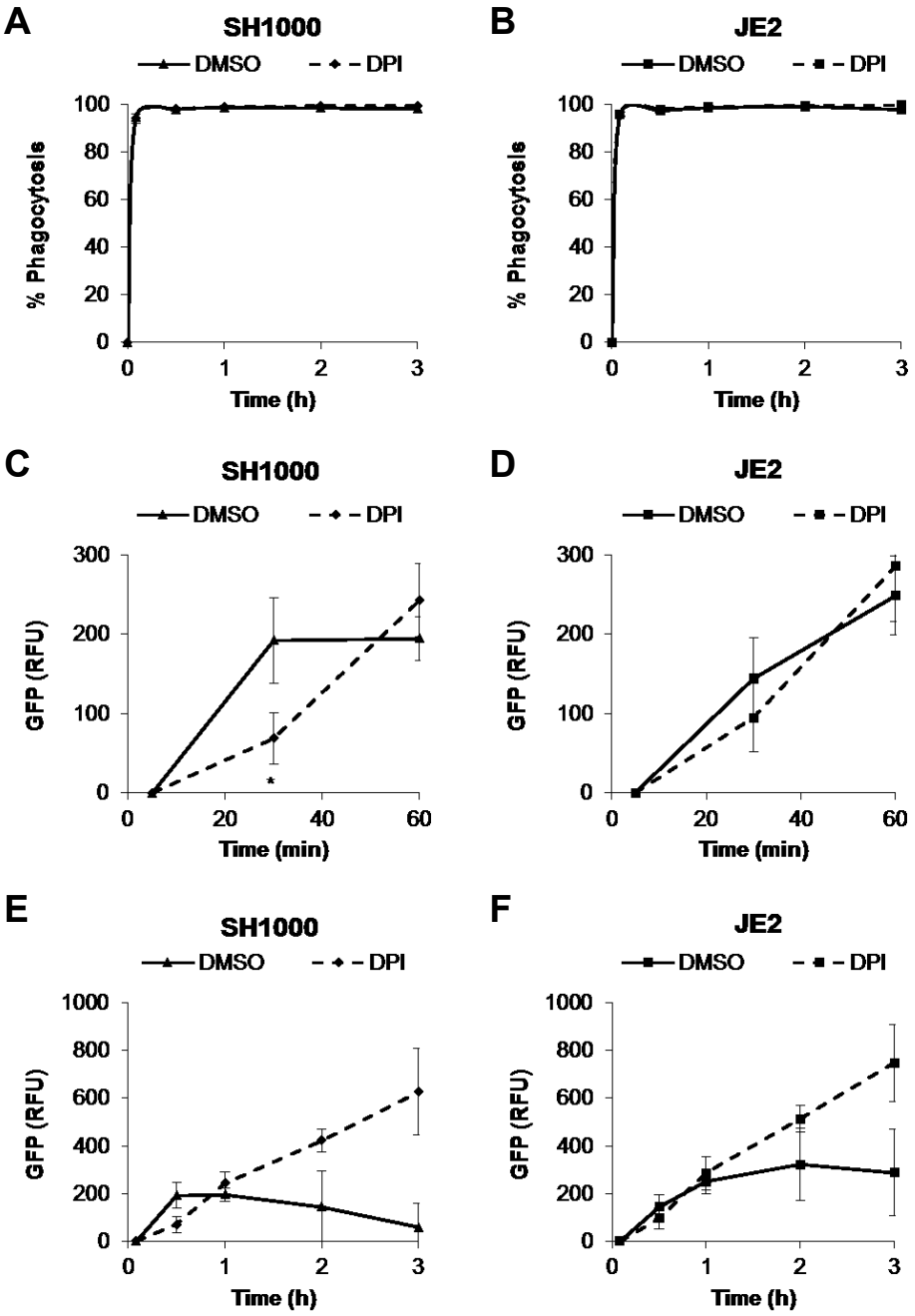

Figure 3.6. The neutrophil oxidative burst induces *recA* expression in *S. aureus*.
Percentage of phagocytosed bacteria over time for wild-type SH1000 **(A)** and JE2 **(B)**. The percentage of phagocytosed cells was calculated from the number of free and phagocytosed bacterial events. Expression of *recA* was determined from GFP intensity via the FITC-A median. Median GFP fluorescence of neutrophils associated with GFP-positive SH1000 or JE2 for up to 1 h **(C, D)** and for up to 3 h **(E, F)**. Results represent the mean of four experiments with different donors. Error bars indicate the standard deviation. *, $P < 0.05$ (two-way ANOVA with Sidak's test, compared to DMSO-treated neutrophils).

3.4 DNA repair is required for survival of *S. aureus* in whole human blood

To understand how *S. aureus* repaired DNA that was damaged by the oxidative burst, 19 mutants defective for proteins predicted to be involved in DNA repair were identified from the Nebraska Transposon Mutant Library (NTML) and screened by Dr Andrew Edwards (Imperial College London). The NTML library is a collection of 1,952 sequence-defined *bursa aurealis* transposon mutants in the *S. aureus* USA300 LAC strain JE2[368]. This strain has been cured of two plasmids normally found in LAC, p01 (a 3.1-kb cryptic plasmid) and p03 (a 27-kb plasmid that confers erythomycin resistance), to eliminate incompatibilities with the *bursa aurealis* transposon and to ensure that it did not insert preferentially into plasmid DNA[476]. The *bursa aurealis* transposon contains an erythomycin resistance cassette to enable screening for successful colonies and for maintaining the insertion mutants[368].

To identify proteins important for repairing oxidative damage to DNA, zone-of-inhibition assays were performed using H_2O_2-soaked paper discs. This revealed 11 mutants with increased susceptibility to H_2O_2, including *recA, recF, rexA, rexB, nth, sbcC, sbcD* and four genes controlled by the SOS regulon (designated here as *sos4, 5, 6, 7*) whose products have no ascribed function (Figure 3.7A). Next, the mutants were assessed for their ability to survive in whole human blood. The *ex vivo* whole human blood model of infection was employed because *S. aureus* is a major cause of bacteraemia and blood contains a high number of neutrophils, as well as opsonins and other immune factors such as platelets[4,477]. In this model, *S. aureus* is rapidly phagocytosed by neutrophils present in the blood and is exposed to the oxidative burst[4,222,228]. Strains with transposon insertions in *recA, recF, rexA, rexB, sos5* and *sos7* displayed significantly reduced survival in blood. In particular, survival of the *rexA* and *rexB* mutants was reduced to below 5% of the inoculum, compared to over 60% for the wild type (Figure 3.7B). Zone-of-inhibition and blood survival assays were performed by Dr Edwards.

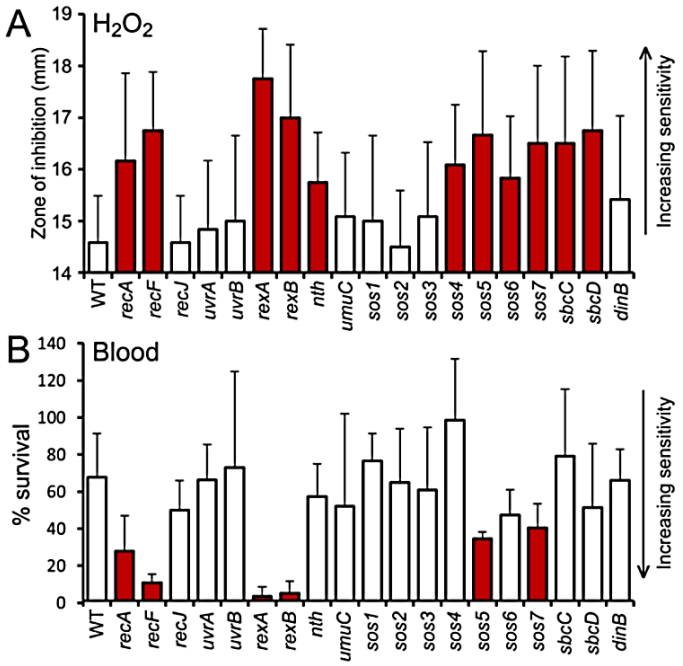

Figure 3.7. DNA repair is required for staphylococcal survival in human blood.

S. aureus JE2 wild-type (WT) and DNA repair mutants were grown on agar plates overlaid with paper discs containing 50 mM of H_2O_2 and the zone of inhibition was measured **(A)**. A larger zone of inhibition indicates greater sensitivity to H_2O_2. Survival of the strains in whole human blood after 2 h was determined by CFU counts **(B)**. Results represent the mean of at least three experiments with different donors. Error bars indicate the standard deviation. Values significantly different from WT are shaded red ($P < 0.05$ (one-way ANOVA with Dunnett's test, compared to the wild type). These experiments were carried out by Dr Andrew Edwards (Imperial College London).

3.5 Complementation and characterisation of *rexAB* mutants

The *rexA* and *rexB* genes form a two-gene operon (*rexAB*) in the staphylococcal genome. To confirm that these genes were required for maximal staphylococcal survival of the oxidative burst, *rexB* mutants in SH1000 and JE2 backgrounds were complemented with a plasmid containing the *rexAB* operon under the control of an anhydrotetracycline (AHT)-inducible promoter (Figure 3.8). The transposon insertion in *rexB* contains a terminator sequence that prevents transcription of *rexA*, the second gene in the operon, therefore mutants are defective for both *rexB* and *rexA.* Reintroducing the gene at a second locus ensured that the observed phenotype was not a result of compensatory spontaneous mutations or polar effects of the transposon insertion. The shuttle vector pCL55-*itet* (p*itet*) was used for complementation as it stably integrates as a single copy into the *S. aureus* genome and does not require antibiotic selection. Furthermore, the vector contains an AHT-inducible promoter, which enables gene expression levels to be controlled[453].

After sequencing the p*itet rexAB* vector to confirm that the construct was correct, the plasmid was transformed into SH1000 and JE2 *rexB* mutants via *E. coli* DC10B. Empty p*itet* was also introduced into wild-type strains as a plasmid control. Since p*itet* introduces itself ectopically into the chomosomal lipase gene (*geh*) locus, this provided a convenient method to confirm integration via colony PCR. Two reactions were performed per strain to confirm either the presence of the intact *geh* gene ("gehF" and "geh" primers) or the presence of integrated plasmid ("gehF" and "pCL55-R" primers). JE2 *sigB*::Tn p*itet* was provided by Dr Nishanthy Ranganathan (Imperial College London) as a positive control strain, which has been confirmed for successful integration by both colony PCR and DNA sequencing. Gel analysis of the colony PCR reactions confirmed successful integration of empty p*itet* and p*itet rexAB* into the *rexB* mutants (Figure 3.9).

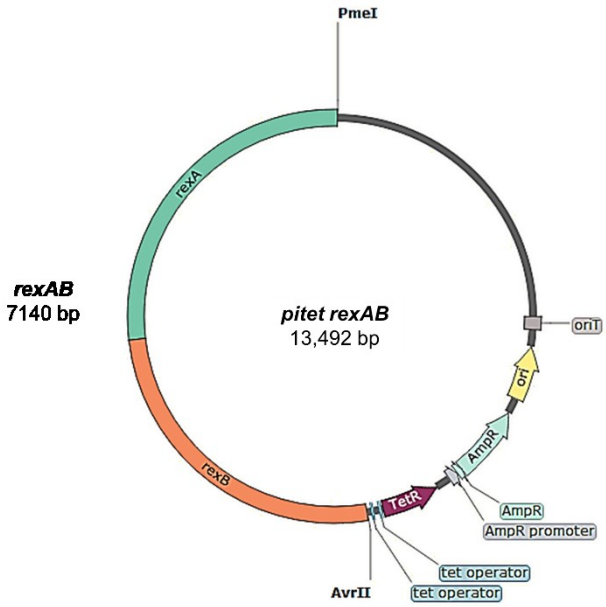

Figure 3.8. Schematic representation of the p*itet rexAB* complementation system.
Diagram of the p*itet* plasmid showing AvrII and PmeI restriction sites used for cloning and the *rexAB* insert. Ori, origin of replication; oriT, origin of transfer; AmpR, amplicillin resistance gene; TetR, tetracycline resistance gene. Plasmid map created with SnapGene.

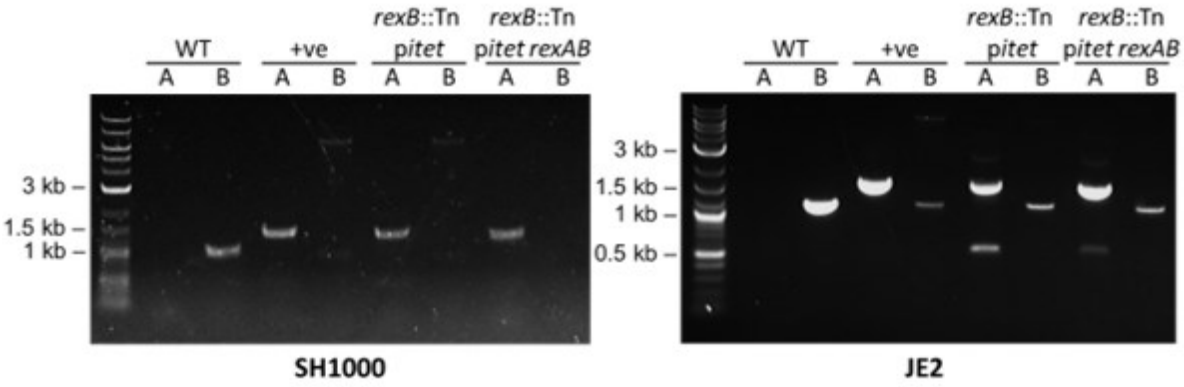

Figure 3.9. Gel electrophoresis images confirming the integration of empty p*itet* or p*itet rexAB* into *S. aureus* SH1000 and JE2 *rexB*::Tn mutants.
Colony PCR was used to amplify DNA from wild-type and complemented strains. Two PCR reactions were performed for each strain: “gehF” and “pCL55-R” primers (reaction A) produce a 1.5 kb fragment if the plasmid has integrated into the genome, and “gehF” and “geh” primers (reaction B) lead to a 1 kb fragment if the plasmid has not integrated. The positive control strain used in both gels was JE2 *sigB*::Tn p*itet* provided by Dr Nishanthy Ranganathan (Imperial College London). PCR products were analysed on a 1% agarose gel next to a 2-log DNA ladder (NEB) to confirm the presence of integrated p*itet.*

Several factors have been shown to affect survival of *S. aureus* incubated in human blood or exposed to oxidative stress, including the production of catalase, staphyloxanthin pigment and toxins[4,231,234,265]. Therefore, phenotypic characterisation of the strains was carried out next to assess whether the *rexAB* mutants were defective for any of these, which could confound the analysis of the role of *rexAB* in mediating staphylococcal survival in human blood.

Growth profiles were determined for the strains by measuring optical density (OD) at 600 nm over 17 h in the presence of increasing concentrations of the inducer AHT. This would assess whether changes in *rexAB* gene expression affected bacterial growth. Wild-type strains were also tested and compared to the *rexB* mutants and complemented strains. This revealed small differences in growth between wild-type *S. aureus* SH1000 and JE2 (Figure 3.10A, B). Wild-type SH1000 reached stationary phase faster than wild-type JE2 (5 h compared to 7 h), but the final cell density was higher in JE2 ($OD_{600\ nm}$ of 3.3, compared to 2.3). The *rexB* mutants grew more slowly than the wild type, with the $OD_{600\ nm}$ half that of the wild type in both backgrounds at mid-exponential phase (at 3 h, Figure 3.10A, B). However by the end of the incubation, growth of JE2 *rexB*::Tn eventually reached wild-type levels. Therefore, loss of RexAB causes a slight growth defect relative to the wild type strains. The complemented strains grew at the same rate regardless of the presence or absence of AHT (Figure 3.10C, D), suggesting leaky expression of the *rexAB* operon and that increasing *rexAB* gene expression beyond this basal level did not affect growth.

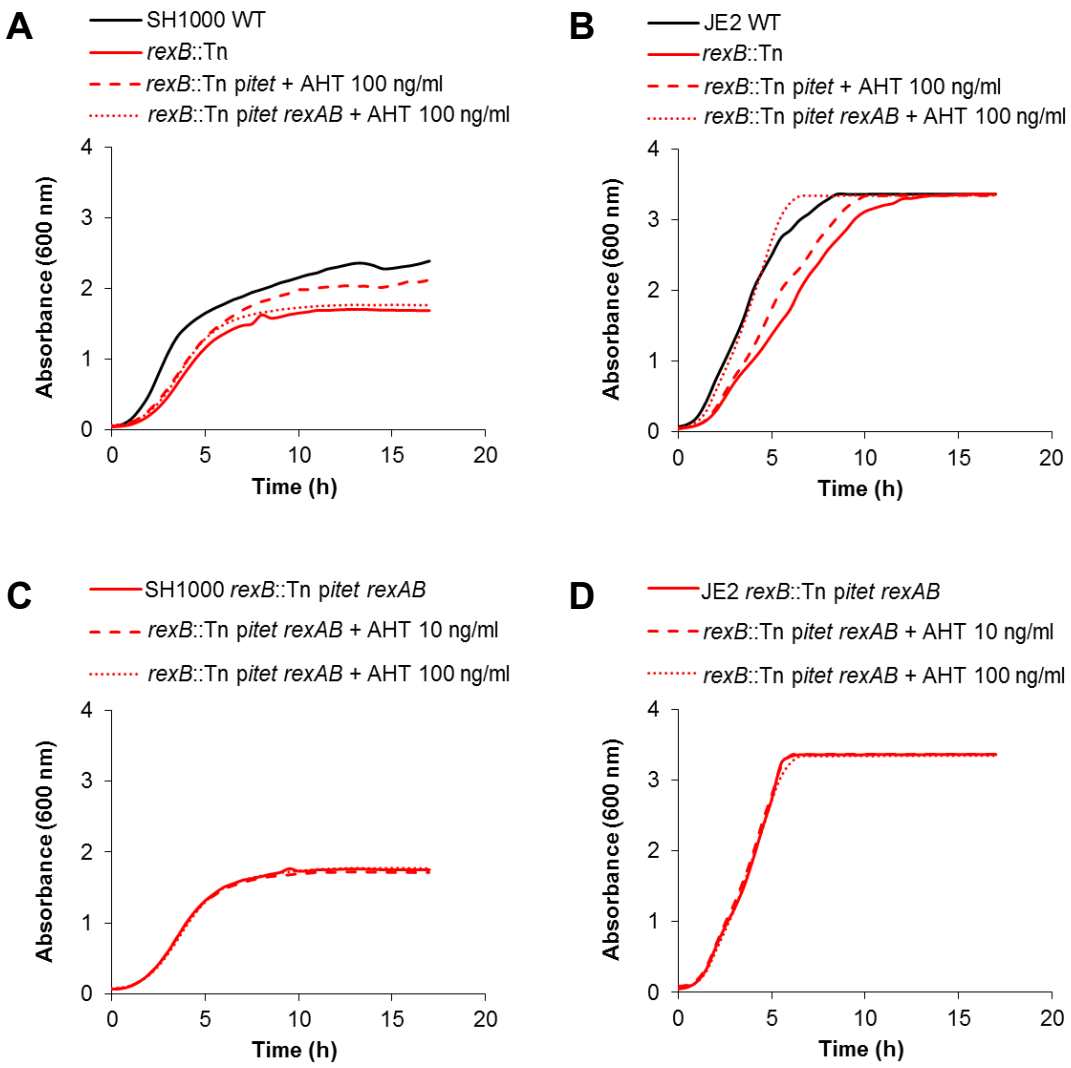

Figure 3.10. Growth profiles of *S. aureus* wild type and *rexAB* mutants.

Growth was assessed by taking $OD_{600\ nm}$ readings every 30 min for 17 h. Growth is shown for wild type and *rexAB* mutants (complemented strains induced with 100 ng/ml of AHT) **(A, B)**, and for different AHT concentrations **(C, D)**. The *rexAB* mutant (*rexB*::Tn) was complemented with the wild-type gene (p*itet rexAB*) or transformed with plasmid only as a control. The inducer anhydrotetracycline (AHT) was added at 10 or 100 ng/ml. Graphs represent the mean of three experiments. Error bars were omitted for clarity.

Toxin production in *S. aureus* is controlled by the *agr* operon, induction of which leads to production of leukocidins and PSMs that are capable of lysing immune cells[271,275–279]. To determine whether *agr* expression was affected by loss of RexAB, haemolysin production was measured as an indicator of *agr* operon activity. This revealed that there was no difference in haemolysis with undiluted culture supernatant for *rexAB* mutants in both SH1000 and JE2 backgrounds (Figure 3.11A, B). However, SH1000 mutants displayed significantly reduced haemolysis compared to the wild-type when the culture supernatant was diluted 1/10 with fresh medium ($P < 0.05$; Figure 3.11A). No difference in haemolysis was observed between JE2 wild type and mutant strains with undiluted or diluted culture supernatant (Figure 3.11B).

Staphyloxanthin is a pigment produced by *S. aureus* that confers its characteristic golden colour and can function as an antioxidant to protect against neutrophil killing[4]. To determine whether loss of RexAB could affect its production, staphyloxanthin was extracted from the strains and pigment levels compared. This analysis revealed that no differences in staphyloxanthin levels were observed between wild type and mutants in either strain (Figure 3.11C, D). Therefore, loss of RexAB does not affect staphyloxanthin production in *S. aureus*.

Finally, catalase activity was measured. This enzyme provides protection against ROS by breaking down H_2O_2 into molecular oxygen and water[172]. Bacteria were incubated with a fixed concentration of H_2O_2 for 15 min, then the level of catalase activity was determined by measuring the concentration of H_2O_2 that remained. This revealed that no significant differences were observed between wild-type and mutant strains in both SH1000 and JE2 (Figure 3.11E, F). Therefore, loss of RexAB does not affect catalase activity in *S. aureus.*

To summarise, p*itet* containing the wild-type *rexAB* operon was successfully transformed into SH1000 and JE2 *rexB* mutants and no significant differences were found between the wild type and *rexAB* mutant for growth, staphyloxanthin activity and catalase activity. However, there were slight differences in growth of the mutant between SH1000 and JE2 backgrounds. Haemolytic activity was also significantly different between SH1000 wild-type and mutant strains, but this was not observed in the JE2 background. Therefore, both

strains will be used in future assays to determine whether the phenotypes observed for the *rexAB* mutant are conserved across genetic backgrounds.

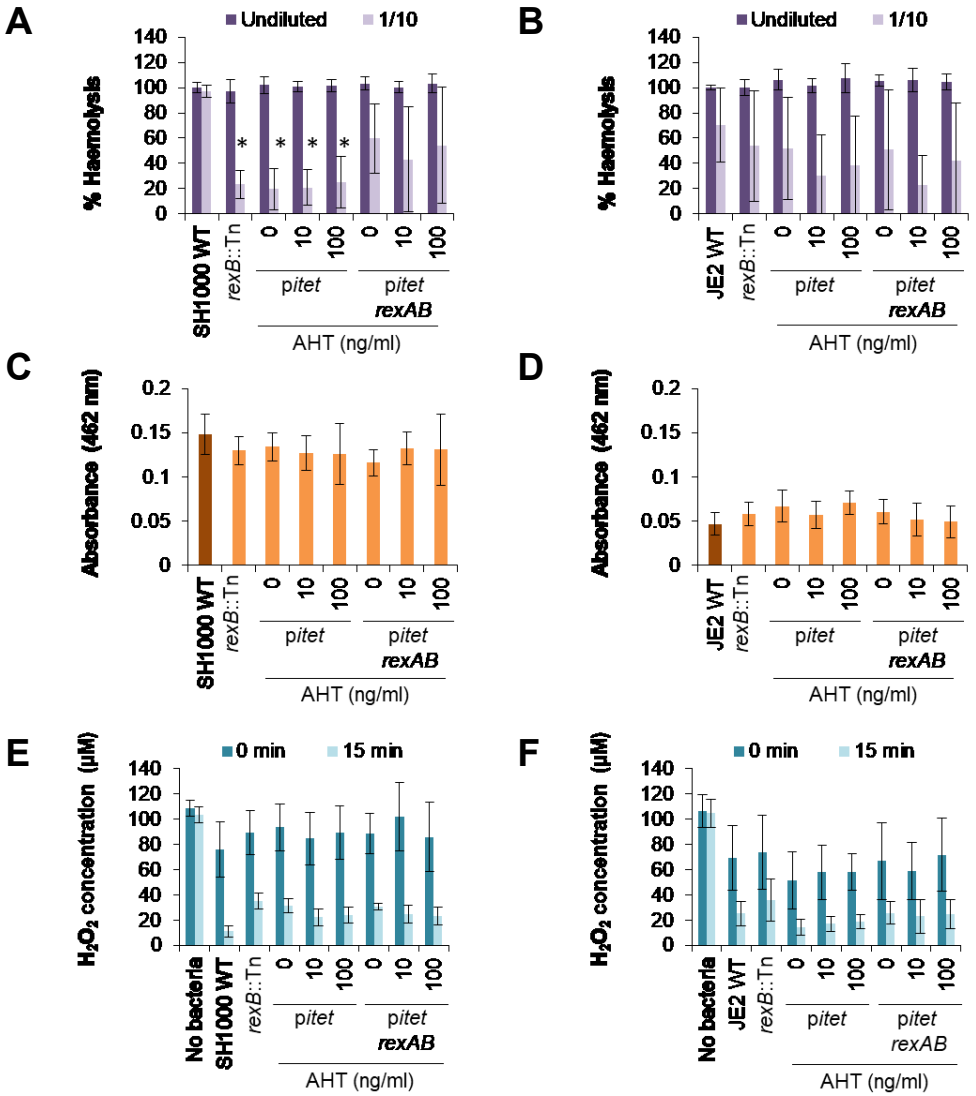

Figure 3.11. Phenotypic characterisation of *S. aureus* wild type and *rexAB* mutants. Wild-type and mutant strains from SH1000 and JE2 were characterised for haemolytic activity **(A, B)**, staphyloxanthin levels **(C, D)** and catalase activity **(E, F)**. Overnight cultures were induced with 10 or 100 ng/ml of AHT. Percentage haemolysis of sheep's blood by culture supernatants was adjusted and compared to the wild type (with the neat dilution set to 100%). Staphyloxanthin was extracted by treating bacterial pellets with methanol and absorbance was measured at 462 nm. Catalase activity was measured by incubating bacteria in 100 µM of H_2O_2 for 15 min (37 °C) in the dark, then quantifying the concentration of H_2O_2 using the Thermo-Fisher Pierce Pierce Quantitative Peroxide Assay kit. Graphs represent the mean of three independent experiments. Error bars indicate the standard deviation. *, $P < 0.05$ (one-way ANOVA with Dunnett's test, compared to the corresponding wild type).

3.6 Loss of RexAB increases susceptibility of *S. aureus* to DNA-damaging antibiotics

To assess the role of RexAB in the repair of DNA damage, the minimum inhibitory concentration (MIC) of each strain for ciprofloxacin, mitomycin C or hydrogen peroxide (H_2O_2) was determined, as all of these are genotoxic and cause DNA double-strand breaks (DSBs). Ciprofloxacin causes DSBs by inhibiting DNA gyrase during DNA replication[478], mitomycin C crosslinks DNA to cause stalling of replication forks[479], and H_2O_2 is a simple mimic of the oxidative burst, generating lesions that also result in stalled replication[306]. In addition to these well established genotoxic stresses, oxacillin was included in assays because it inhibits cell wall synthesis and is not believed to damage DNA[480]. MIC assays were carried out using the well-established serial broth dilution method in 96-well plates, where the MIC is defined as the lowest concentration at which no growth is observed.

For both ciprofloxacin and mitomycin C, the MICs of *rexB*::Tn mutants were reduced at least 16-fold in the SH1000 background and by 8-fold in JE2 when compared to the wild type (Figure 3.12A-D). The wild-type phenotype was restored in *rexB*-defective mutants complemented by the reintroduction of the wild-type *rexAB* genes in both cases, whilst p*itet* alone had no effect on the MIC for either antibiotic (Figure 3.12A-D). Therefore RexAB contributes to the repair of ciprofloxacin- or mitomycin C-induced DNA damage. The MIC of ciprofloxacin was also found to be 32-fold higher in wild-type JE2 (16 µg/ml; Figure 3.12B) compared to wild-type SH1000 (0.5 µg/ml; Figure 3.12A), which supports the previously reported fluoroquinolone resistance of the MRSA JE2 strain[68].

For H_2O_2, the MICs of the *rexAB* mutant was reduced 4-fold in the SH1000 background when compared to the wild type (Figure 3.12E), but no significant difference was found in the JE2 strain (Figure 3.12F). Complementation restored the wild-type phenotype in the SH1000 *rexB* mutant. (Figure 3.12E). Unexpectedly, the MICs of oxacillin for the SH1000 *rexAB* mutants were reduced 2-fold when compared to the wild type (Figure 3.12G). However,

no significant differences were found in the JE2 background, which is resistant to oxacillin (Figure 3.12H).

Taken together, the MIC data indicated that *rexAB* mutants are more sensitive to DNA-damaging antibiotics when compared to wild-type *S. aureus,* indicating that RexAB plays an important role in repairing DNA damage from multiple sources. Furthermore, complementation with wild-type *rexAB* genes restored the wild-type phenotype in the *rexAB* mutants, confirming the role of RexAB in DNA repair. However, different concentrations of the inducer AHT led to the same phenotype in the complemented strains, suggesting that leaky expression was sufficient to fully restore the wild-type phenotype and extra transcription was not protective. It is also possible that AHT did not induce gene expression beyond basal levels.

To further investigate the inducibility of *rexAB* expression in the complemented strains, a different approach was used to determine the antibiotic susceptibility of the staphylococcal strains. Bacteria were incubated in the presence of ciprofloxacin over 6 h and CFU counts were determined every 2 h. This approach enables bacterial growth and/or death to be measured, whereas MIC assays only examine inhibition of bacterial growth. For these assays, ciprofloxacin was added at a fixed concentration of 5 µg/ml, which is 10x MIC for wild-type SH1000 and 0.3x MIC for wild-type JE2. At 10x MIC of ciprofloxacin, survival of all SH1000 *rexAB* mutants and complemented strains was reduced by a similar amount, which was significantly lower than wild type (Figure 3.13A). Although wild-type JE2 grew well at 0.3x MIC, the growth of the *rexAB* mutant was inhibited (Figure 3.13B), suggesting that JE2 requires RexAB to maintain its resistance to ciprofloxacin. In addition, induction with AHT led to dose-dependent restoration of growth, which suggested that the inducible system is functional since AHT did not affect the survival of the *rexB*::Tn mutant transformed with empty p*itet* (Figure 3.13B). However, growth in the induced strains still did not reach wild-type levels (Figure 3.13B), suggesting that complementation does not fully restore the phenotype. Nevertheless, these results concur with the MIC data that loss of RexAB sensitises both an MSSA (SH1000) and an MRSA (JE2) strain to ciprofloxacin. Therefore, RexAB is required in *S. aureus* for repairing damage caused by DNA-damaging antibiotics.

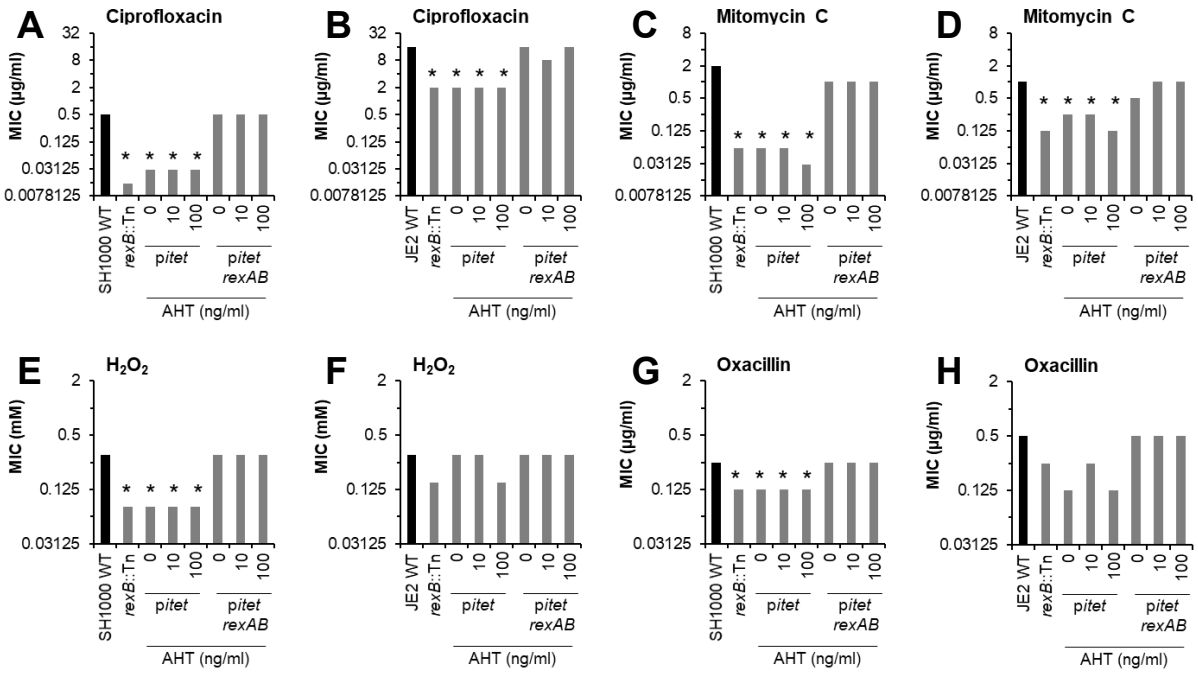

Figure 3.12. MIC data for *S. aureus* wild type and *rexAB* mutants.

MIC assays were performed using the serial broth dilution method in 96-well plates for ciprofloxacin **(A, B)**, mitomycin C **(C, D)**, H_2O_2 **(E, F)** and oxacillin **(G, H)** for SH1000 and JE2. The MIC was defined as the lowest concentration at which no growth was observed after static incubation at 37 °C for 17 h. The inducer AHT was added at 10 or 100 ng/ml. Graphs represent the median of three independent experiments. *, $P < 0.05$ (one-way ANOVA with Dunnett's test, compared to the corresponding wild type).

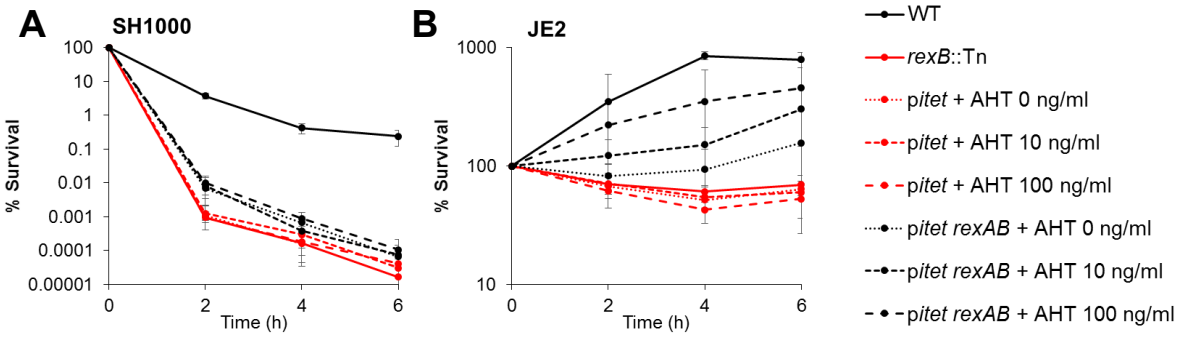

Figure 3.13. Complementation of *rexB*::Tn mutants with wild-type *rexAB* is incomplete.

Percentage survival over 6 h incubation with 5 µg/ml of ciprofloxacin is shown for SH1000 **(A)** and JE2 **(B)**. Ciprofloxacin, at 5 µg/ml, is equal to 10x MIC for wild-type SH1000 and 0.3x MIC for wild-type JE2. The inducer AHT was added at 10 or 100 ng/ml. Graphs represent the mean of three independent experiments. Error bars indicate the standard deviation. *, $P < 0.05$ (two-way ANOVA with Tukey's test, compared to the corresponding wild type).

3.7 RexAB is required for maximal survival of *S. aureus* when challenged with H_2O_2

H_2O_2 is a type of ROS that is produced by neutrophils during the oxidative burst, and is able to diffuse across the bacterial cell membrane to cause oxidative damage inside the cell[146]. To test the contribution of RexAB to survival of oxidative stress, wild-type and mutant strains were exposed to H_2O_2 (10 mM) for 1 h and survival was determined by CFU counts. Although this concentration of H_2O_2 is much higher than the levels predicted in the phagosome (2 μM)[481], a single phagosome generally contains only one or a few bacteria[482], compared to 10^4 CFU in the assay. Therefore, a higher concentration of H_2O_2 was necessary to prevent inactivation of H_2O_2 by catalase and peroxidase enzymes. Bacteria were incubated at 37°C in the dark due to the light sensitivity of H_2O_2, then serially diluted and plated onto CBA, which prevented further killing due to the presence of catalase within the medium.

After challenging the bacteria with H_2O_2 for 1 h, survival of wild-type SH1000 and JE2 was reduced to 34% and 50% of the inoculum respectively (Figure 3.14). Survival of *rexB*::Tn mutants was significantly lower compared to the wild type in both SH1000 (13%) and JE2 (7%), and complementation with a wild-type copy of *rexAB* led to restoration of the wild-type phenotype (Figure 3.14). When *rexB*::Tn mutants were transformed with empty p*itet* plasmid as a control, survival was unaffected compared to the original mutant (Figure 3.14). Therefore, these results indicated that RexAB plays an important role in repairing DNA damage caused by H_2O_2. Futhermore, although RexAB may not be required for maintaining bacterial growth in the presence of H_2O_2 (section 3.6 above), it is still necessary for bacterial survival in response to H_2O_2-induced oxidative stress. As for the MIC assays, there was no difference in survival of complemented strains at differing AHT concentrations (Figure 3.14).

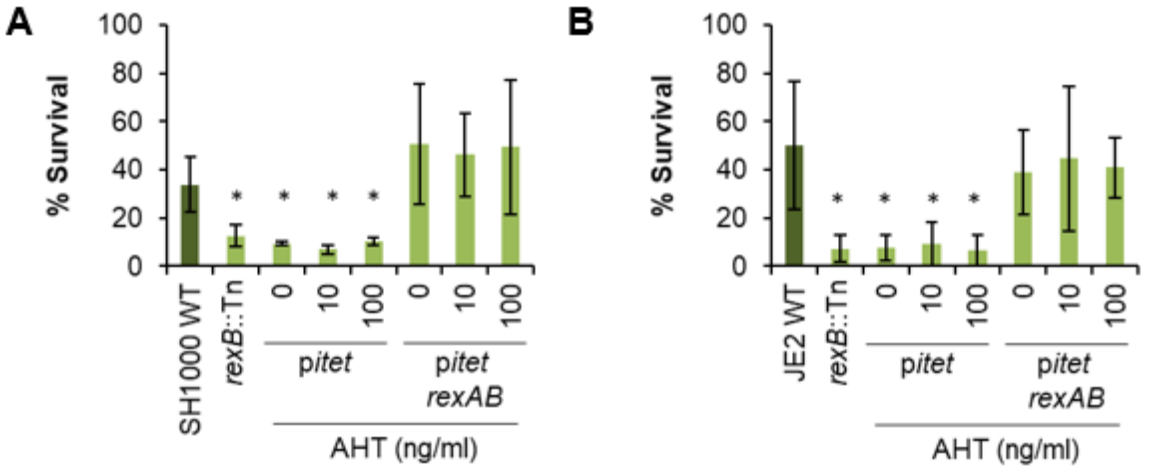

Figure 3.14. Loss of RexAB reduces survival of *S. aureus* when challenged with H_2O_2. Percentage survival after 1 h incubation with 10 mM of H_2O_2 is shown for SH1000 **(A)** and JE2 **(B)**. The inducer AHT was added at 10 or 100 ng/ml. Graphs represent the mean of three independent experiments. Error bars indicate the standard deviation. *, $P < 0.05$ (one-way ANOVA with Dunnett's test, compared to the corresponding wild type).

3.8 RexAB is required for survival of *S. aureus* in human blood

Having confirmed that RexAB contributed to DNA repair, its role in infection was determined using an *ex vivo* whole human blood model of bacteraemia. This is an established method previously shown to efficiently assess survival of *S. aureus* in the bloodstream[265], in which bacteria are incubated with freshly-donated whole human blood and survival enumerated by plating for CFU[4,222,477]. In addition, this system includes components in human blood that are absent in neutrophil assays but contribute to bacterial killing, such as platelets[483]. Therefore, this model was used to assess the importance of DNA repair during bloodstream infection. The incubation time of 6 h was chosen because this is long enough to observe killing of *S. aureus* and neutrophils have been shown to lose viability after this point[265,484]. Four independent experiments were performed using blood from a new donor each time to account for differences in immune response to *S. aureus* and the presence of reactive IgG between individuals. For example, variables such as age, lifestyle habits and having had any prior *S. aureus* infections would be expected to affect the efficiency of the immune system, including the ability of immune cells to recognise and kill *S. aureus*.

After incubation for 6 h, the percentage survival of the SH1000 and JE2 wild-type strains had dropped to 15% and 20% of the inoculum respectively, which showed that the killing of *S. aureus* by blood phagocytes is highly effective (Figure 3.15). Survival of *rexAB* mutants was reduced to 2% of the inoculum in both strain backgrounds, which is a 7-fold reduction for SH1000 when compared to the wild type (Figure 3.15A) and a 10-fold reduction for JE2 (Figure 3.15B). The *rexB*::Tn mutants transformed with empty p*itet* survived at the same levels as the *rexB*::Tn mutant without plasmid (Figure 3.15). By contrast, complementation of the *rexB*::Tn mutant with the *rexAB* operon restored survival to wild-type levels, regardless of whether expression was induced with AHT or not. This confirmed that the reduced survival of *rexAB* mutants was due to the loss of RexBA, rather than polar effects of the transposon insertion. Furthermore, leaky expression from the AHT-inducible promoter in the absence of the antibiotic was sufficient to restore the wild-type survival phenotype. Therefore, RexAB is required for the survival of *S. aureus* in whole human blood. Combined, these findings provided evidence that bacterial DNA repair contributes to staphylococcal survival in the bloodstream.

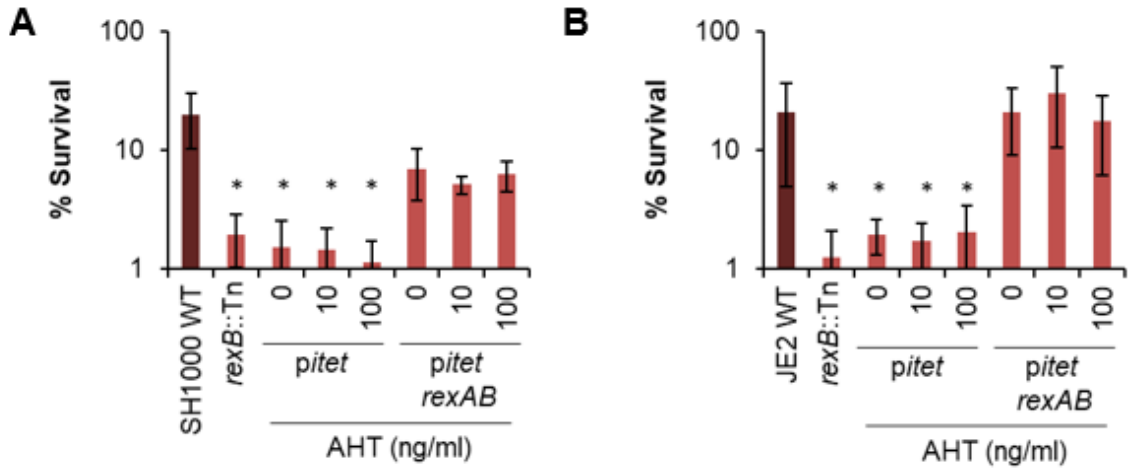

Figure 3.15. RexAB influences susceptibility of *S. aureus* to killing in whole blood. Percentage survival after 6 h incubation in whole human blood is shown for SH1000 **(A)** and JE2 **(B)**. The inducer AHT was added at 10 or 100 ng/ml. Graphs represent the mean of three independent experiments. Error bars indicate the standard deviation. *, $P < 0.05$ (one-way ANOVA with Dunnett's test, compared to the corresponding wild type).

3.9 RexAB repairs DNA damage caused by the oxidative burst

The key host defence against staphylococcal infection is the oxidative burst of neutrophils, in which ROS are produced to kill phagocytosed bacteria[140]. To determine whether the enhanced killing of *rexAB* mutants in blood was due to the oxidative burst, the inhibitor diphenyleneiodonium (DPI) was used to block activity of NADPH oxidase, which is responsible for the production of ROS by neutrophils[475]. Blood was treated with DPI or DMSO (the solvent DPI is dissolved in) as a control, for 15 min before the addition of bacteria.

After 6 h incubation, survival of the wild-type strains were enhanced in DPI-treated blood when compared to DMSO-treated blood, demonstrating that ROS production is required for immune killing of *S. aureus* and confirming that the assay was functional (Figure 3.16A, B). In addition, survival of *rexAB* mutants in blood treated with DPI compared to DMSO was significantly increased by 5-fold for SH1000 and 4-fold for JE2 (Figure 3.16A, B), such that survival of the mutants was restored to wild-type levels. This was observed on the blood-agar plates used for CFU enumeration, in which incubation with DPI-treated blood led to bacterial colonies that were larger and more numerous compared to blood treated with DMSO only (Figure 3.16C, D). This was also seen for *rexB*::Tn mutants complemented with the wild-type *rexAB* operon, in which the number and size of colonies were restored to wild-type levels. These results demonstrate that most of the killing of the *rexAB* mutants in blood is due to ROS production, and that RexAB is important for protecting *S. aureus* against the oxidative burst of phagocytes in blood.

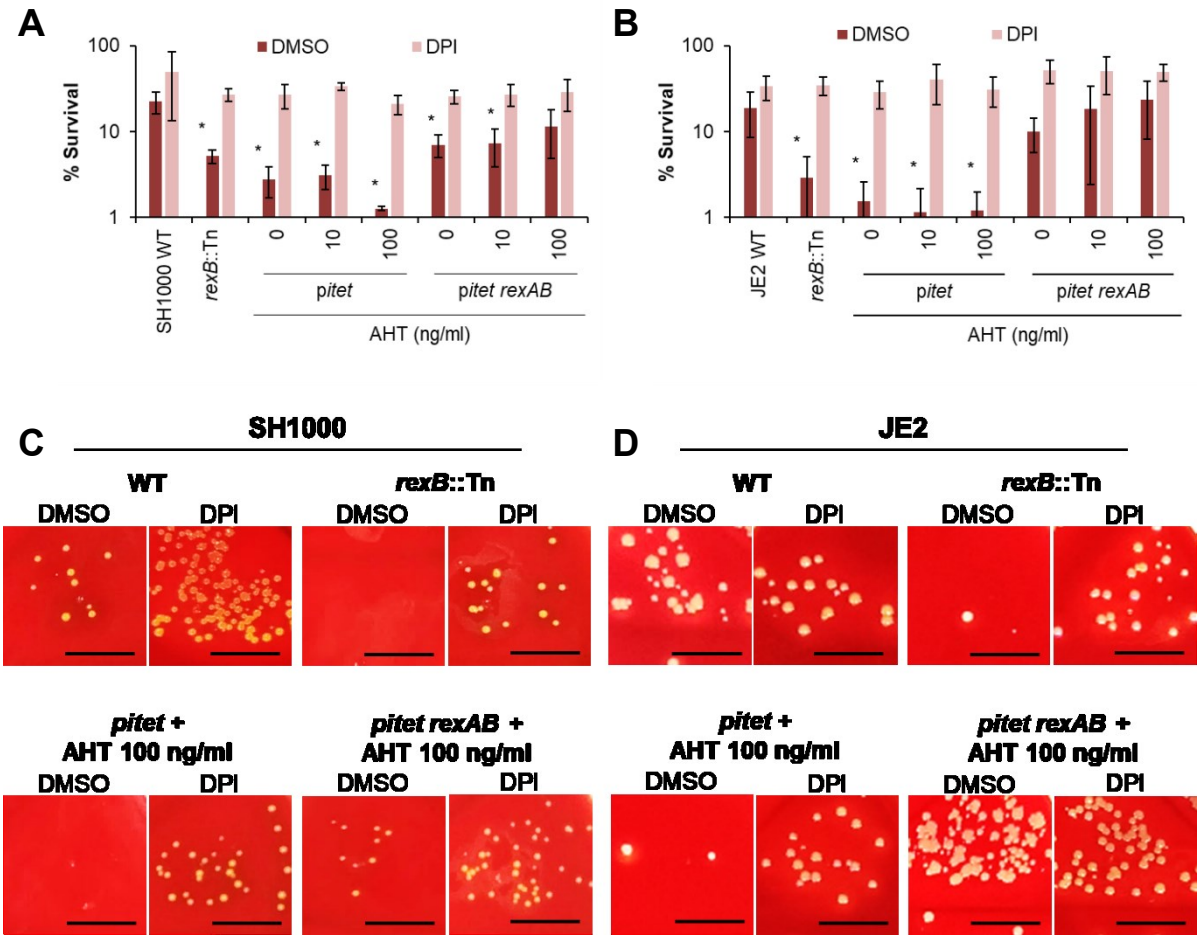

Figure 3.16. Killing of *S. aureus* in human blood is due to the production of ROS. Percentage survival **(A, B)** and representative images of bacteria plated at 1/10 dilution **(C, D)** after 6 h incubation in blood are shown for SH1000 and JE2. Whole human blood was incubated for 15 min with the NADPH-oxidase inhibitor DPI, or DMSO as a control, before the addition of bacteria. Graphs represent the mean of three independent experiments. Error bars indicate the standard deviation. *, $P < 0.05$ (one-way ANOVA with Dunnett's test, compared to the corresponding wild type). Scale bars on the bottom right of each image represent one centimetre.

3.10 Loss of RexAB increases susceptibility of *S. aureus* to killing by purified neutrophils

Neutrophils are the main defence against *S. aureus* found in the bloodstream[122]. However, since other components in blood have been shown to promote neutrophil activity and staphylococcal killing[4,477], it was decided to examine the survival of *S. aureus* during incubation with purified neutrophils.

Neutrophils were isolated from freshly-donated whole human blood using Polymorphprep, which enables the separation of erythocytes, PMNs and mononuclear cells from blood via a density gradient. Since neutrophils are the second most abundant type of cell found in blood at approximately 10^6 cells/ml, they were isolated at a concentration of 10^7 cells/ml (3 ml total volume) from 30 ml of whole human blood[485]. Neutrophils were adjusted to 5 x 10^6 cells/ml in HBSS containing calcium and magnesium to activate the cells, and pre-treated either with DPI to prevent ROS production, or with DMSO as a solvent control. Then bacteria were added (1 x 10^6 CFU/ml) and the suspension was incubated with tumbling at 37 °C for 3 h, with samples taken periodically and plated onto CBA to measure survival.

Over the incubaton period of 3 h, killing was observed for all strains under both DPI- and DMSO-treated conditions (Figure 3.17A,B), likely due to mechanisms that are not dependent on ROS, such as killing by nitric oxide or AMPs. However, survival of the *rexB*::Tn mutant was reduced by up to 7-fold for SH1000 and over 6-fold for JE2, when compared to the wild type (Figure 3.17A,B). Furthermore, representative images of the blood-agar plates show that the colony number of the *rexB*::Tn mutant was reduced when compared to DPI-treated blood and the DMSO-treated wild type (Figure 3.17C). Therefore, these results confirm that neutrophils are a key defence against *S. aureus* in blood, that neutrophil-mediated killing involves the oxidative burst, and that RexAB is required to repair DNA damage and promote *S. aureus* survival of the oxidative burst.

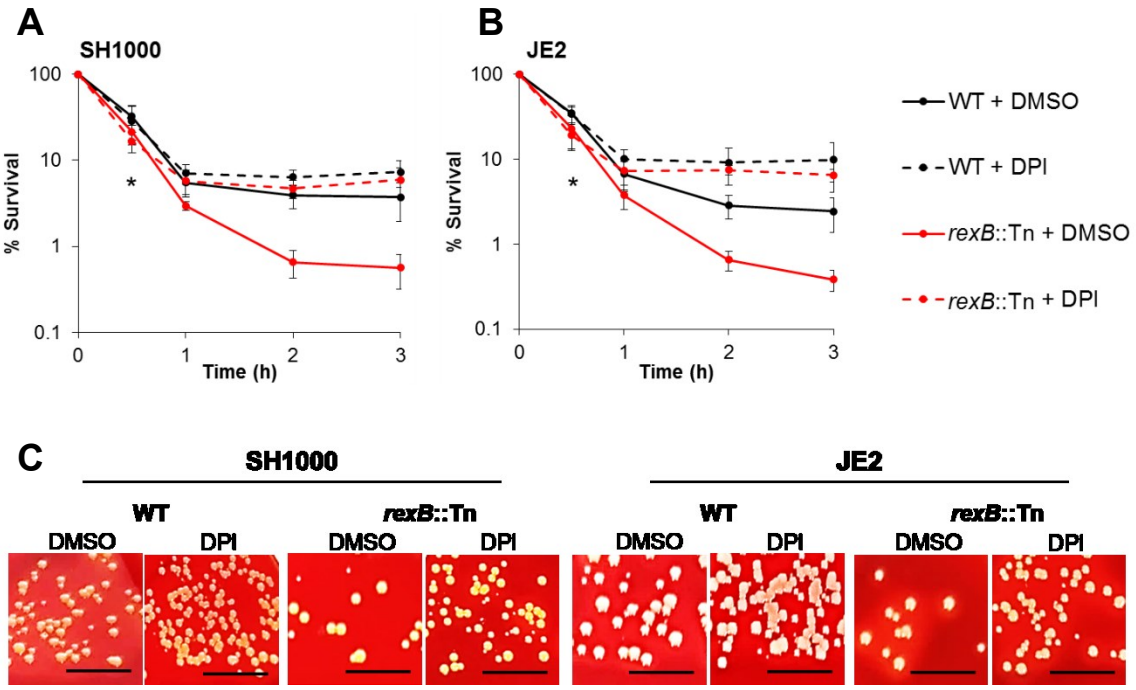

Figure 3.17. RexAB influences susceptibility of *S. aureus* to neutrophil killing.
Percentage survival **(A, B)** and representative images of bacteria plated at 1/10 dilution after 3 h incubation with neutrophils are shown for SH1000 and JE2 **(C)**. Neutrophils were incubated for 10 min with the NADPH-oxidase inhibitor DPI, or DMSO as a control, before the addition of bacteria. Graphs represent the mean of four independent experiments. Error bars indicate the standard deviation. *, $P < 0.05$ (two-way ANOVA with Tukey's test, "*rexB*::Tn + DMSO" and "*rexB*::Tn + DPI" compared to their corresponding wild types at 0.5 h). Scale bars on the bottom right of each image represent one centimetre.

3.11 RexAB is required for survival of *S. aureus* in a mouse model of infection

Having established that RexAB promotes staphylococcal survival in whole blood and during incubation with neutrophils, its role in infection was assessed using a mouse model of acute invasive infection. Mice were infected via the peritoneal cavity with wild-type or *rexB*::Tn mutant *S. aureus* SH1000 or JE2. After 6 h, the mice were sacrificed and the intraperitoneal cavity washed with PBS to recover bacteria, which were quantified by determining CFU counts. All animal handling was performed by Dr Thomas Clarke (Imperial College London). Survival of *rexB*::Tn mutants in both genetic backgrounds was significantly attenuated *in vivo*, with a 4-fold lower CFU counts for SH100 and 3-fold lower CFU counts for JE2 when compared to the respective wild types (Figure 3.18). This confirms that DNA repair via RexAB contributes towards survival of *S. aureus* during infection.

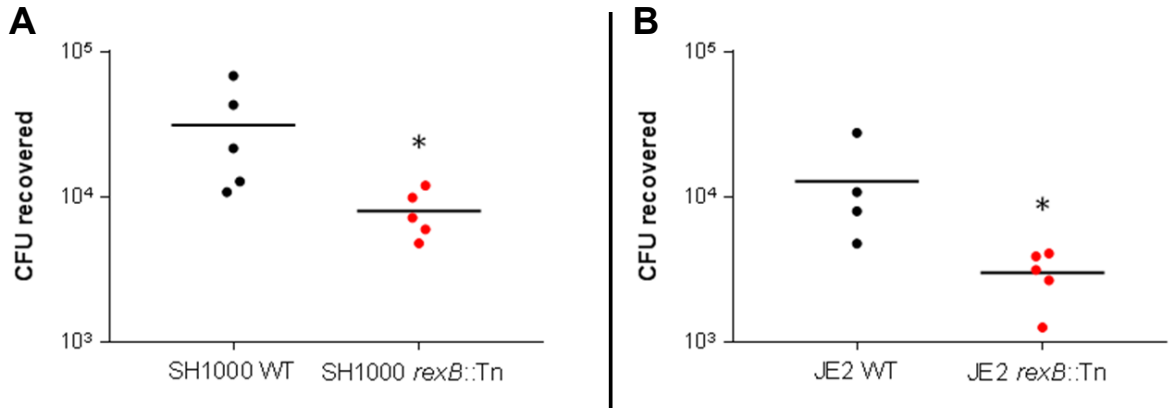

Figure 3.18. RexAB influences susceptibility of *S. aureus* strains *in vivo*.
CFU counts of wild type or *rexAB* mutant after 6 h in the peritoneal cavity of mice, shown for SH1000 **(A)** and JE2 **(B)**. Each filled circle represents a single mouse, five mice were tested for each group and median values are indicated. *, $P < 0.05$ (two-tailed Mann-Whitney test, compared to the wild type).

3.12 RexAB protein level is too low to be detectable in *S. aureus*

Previous data have shown that RexAB is required for survival of *S. aureus* during exposure to DNA-damaging antibiotics (section 3.6) and during infection (section 3.11 above). However, the level of expression that is required for RexAB function is unknown. The use of a tetracycline-inducible plasmid (p*itet*) for expressing the wild-type *rexAB* operon in the *rexB*::Tn mutants led to incomplete restoration of the wild-type phenotype (Figure 3.13), and increasing concentrations of the inducer AHT did not always lead to a dose-dependent effect (section 3.6). Therefore, to directly measure RexAB expression levels in *S. aureus*, a custom polyclonal antibody was generated by Covalab against the purified *S. aureus* RexAB complex (section 2.3.4) and used in a Western blot to detect RexAB protein expression in *S. aureus* cell extracts.

Whole cell extracts were prepared from *S. aureus* overnight cultures by treating the bacteria with lysostaphin to lyse cells and with DNase to reduce sample viscosity, while correcting for differences in $OD_{600\ nm}$ between overnight cultures. Samples were run on an SDS-PAGE gel and either analysed by Coomassie blue staining or by Western blot, in which the polyclonal anti-RexAB antibody was used as the primary antibody. After binding of the primary antibody to RexAB, a secondary HP-conjugated antibody was used for detection of antibody-protein complexes by enhanced chemiluminenscence (ECL). Human serum albumin was added at 1/200 dilution to prevent non-specific binding, which would lead to a background signal. RexAB expression was compared between wild type, *rexB*::Tn mutant and *rexB*::Tn mutants complemented with either empty p*itet* or p*itet* containing the wild-type *rexAB* operon induced with 100 ng/ml of AHT. Recombinant RexAB was run as a positive control for the anti-RexAB antibody, as well as to provide approximate running positions for RexA and RexB proteins.

During SDS-PAGE sample preparation, the anionic detergent SDS denatures proteins and applies a negative charge in proportion to mass, enabling protein mixtures to be separated based on size. This process denatures RexAB from its native form as a heterodimeric complex into its constituent subunits RexA and RexB, which appear as two

discrete bands on the SDS-PAGE gel (Figure 3.19A). These subunits were successfully detected by the polyclonal anti-RexAB antibody using the recombinant RexAB positive control, which confirmed that the antibody was functional (Figure 3.19B).

For wild-type JE2, two bands were detected on the Western blot at a similar molecular weight to RexA and RexB (Figure 3.19B). However, the intensity of the second band was much stronger than the first band (Figure 3.19B), which was unexpected because as a native heterodimer, band intensities for the RexA and RexB subunits should be roughly equal. In addition, no other bands at a similar size were detected in any of the other samples, including wild-type SH1000 and the mutants complemented with the wild-type *rexAB* operon. Together, these results suggest that accurately detecting the expression of RexAB at wild-type levels is extremely difficult by Western blot, and that expression of this protein is very low in *S. aureus*. Nevertheless, although RexAB could not be accurately detected, data from this chapter clearly indicate that the protein is being expressed in both wild type and p*itet rexAB*-complemented strains, as loss of RexAB increased the susceptibility of *S. aureus* to killing by both DNA-damaging antibiotics (section 3.6) and the immune response (sections 3.8 to 3.11).

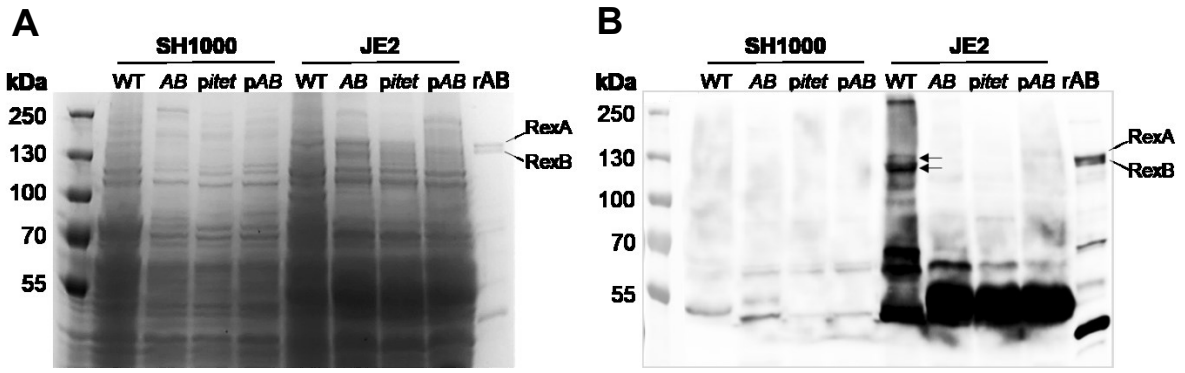

Figure 3.19. SDS-PAGE and Western blot analysis of concentrated *S. aureus* whole cell extracts from wild type, *rexAB* mutant and complemented strains

S. aureus whole cell lysates prepared from wild type, *rexAB* mutant and complemented strains were analysed by SDS-PAGE **(A)** and anti-RexAB Western blot **(B)**. Recombinant RexA (144 kDa) and RexB (138 kDa) protein bands are indicated. Arrows indicate bands at the approximate size of RexAB. The molecular weight of the marker bands in kDa are indicated. WT = wild type; *AB* = *rexB*::Tn mutant; p*itet* = *rexB*::Tn p*itet* + AHT 100 ng/ml; p*AB* = *rexB*::Tn p*itet rexAB* + AHT 100 ng/ml; rAB = recombinant RexAB.

3.13 Discussion

The aim of this chapter was to determine whether staphylococcal DNA was a target of the neutrophil oxidative burst and assessed the role of DNA repair in bacterial survival during infection. It was found that DNA repair via the RexAB complex was required for *S. aureus* survival of the oxidative burst, and that loss of RexAB significantly reduced survival *in vivo*.

The neutrophil oxidative burst was shown to damage bacterial DNA and trigger the SOS response in *S. aureus*, which occurred soon after phagocytosis (at 30 min), corresponding with the time at which the maximum generation of ROS occurs in neutrophils[69,486]. These data demonstrate that ROS generated by phagocytic immune cells damage the DNA of phagocytosed bacteria, previously only shown for macrophages[466,469]. Although other studies have examined the transcriptome of *S. aureus* in human blood[228] or with purified neutrophils[69], these did not detect significant differences in SOS expression via *recA* expression. However, Voyich *et al.* (2005) observed up-regulation of multiple oxidative stress response genes, including catalase (*katA*) and superoxide dismutase (*sodA, sodM*)[69]. Therefore, it is possible that variation in transcriptomic data may have obscured smaller differences in SOS expression. Alternatively, the high MOI used in those studies (ratio of 10 bacteria: PMN, compared to 5 PMN: bacteria in this study) promoted neutrophil lysis rather than bacterial killing[69,486], which may have led to the differences observed.

Nevertheless, DNA was hypothesised to be a target based on previous studies with ROS. Oxidative DNA damage by ROS leads to a wide variety of lesions that, if not repaired, can cause cell death[157,161,447,487,488]. For example, Imlay *et al.* (1988) found that a ten-minute exposure to millimolar levels of H_2O_2 created enough DNA damage to kill bacteria[147]. Furthermore, ROS induce the SOS response because they directly damage DNA[306,443–445]. The flow cytometry data presented here confirmed that DNA is damaged by ROS using the NADPH oxidase inhibitor DPI, and show that DNA damage also occurs at physiological concentrations of ROS using relevant immune cells. Interestingly, some degree of SOS

induction also occurred in the presence of DPI, which indicates DNA damage from other sources, such as nutrient limitation and metabolic stress[286,474].

Despite expressing multiple immune evasins to avoid phagocytosis, previous studies have shown that *S. aureus* is rapidly taken up by neutrophils[4,222,228,265]. The results in this chapter confirm these findings, showing that the majority of bacteria were phagocytosed within 5 min. Killing of *S. aureus* within blood was also mostly due to the oxidative burst, as has been shown previously for purified neutrophils[181,230]. However, killing of wild-type *S. aureus* could not be fully prevented with DPI. This may be due to incomplete blocking of NADPH oxidase activity or other killing mechanisms that are not dependent on ROS, including nitric oxide, AMPs and various proteases[166,489,490]. For example, *S. aureus* is completely resistant to lysozyme, but can be lysed by other proteases such as cathepsin B, cathepsin D, cathepsin G and elastase[177].

RexAB is proposed to be a member of the RecBCD/AddAB family of DNA repair enzymes based on sequence similarity[426,427,491]. These enzymes process DNA DSBs for recombinational repair and have been well-characterised in other bacterial species, particularly in *E. coli* for RecBCD, which is more commonly found in Gram-negative bacteria, and in *B. subtilis* AddAB for Gram-positive bacteria[429]. Inactivation of RecBCD and AddAB enzymes in other bacterial species have been found to increase sensitivity to DNA-damaging agents, including ciprofloxacin, mitomycin C and H_2O_2[427,446,463,492], which also applied to *S. aureus* RexAB. However, it was found that complementation of the *S. aureus* SH1000 *rexAB* mutant only partially restored the wild-type phenotype when exposed to a bactericidal concentration of ciprofloxacin. Furthermore, growth of the complemented JE2 strains was not fully restored to wild-type levels when exposed to an inhibitory concentration of ciprofloxacin, even at the highest concentration of AHT added for *rexAB* gene induction. Although the wild-type phenotype of the complemented strains was fully restored in the other assays, future experiments could aim to rule out spurious mutations in both the mutants and complemented strains by performing whole-genome sequencing of these strains and comparing them to the wild-type genome.

In addition, although exposure to oxacillin was not expected to have an impact on the *S. aureus rexAB* mutant, the oxacillin MIC was significantly reduced when compared to the wild-type methicillin-sensitive SH1000 strain, suggesting that DNA was being damaged. As a β-lactam antibiotic, oxacillin is expected to act on the peptidoglycan cell wall, leading to cell death via autolysis rather than on DNA[480], but induction of the SOS response by β-lactams has been documented[331,468]. In *S. aureus,* Maiques *et al.* (2006) found that SOS induction was also triggered by the β-lactam antibiotics ceftriaxone and cloxacillin, which are used extensively in the treatment of staphylococcal infections[331]. These results suggest that β-lactam antibiotics cause DNA damage. Whilst it is not yet known how this damage occurs, previous reports have suggested that disruption of metabolic processes results in production of ROS, which can in turn damage DNA[493–501]. Since the MIC assays examined the effect of oxacillin on bacterial growth, further experiments could determine whether DNA repair is required for bacterial survival, by exposing wild type *S. aureus* and *rexAB* mutants to bactericidal concentrations of oxacillin. SOS induction of oxacillin and other β-lactams could also be confirmed directly using the *S. aureus* pCN34 *PrecA-gfp* reporter strains described in section 3.2 above.

The increased susceptibility of *rexAB* mutants to killing in whole blood, with purified neutrophils or in a mouse systemic infection model demonstrate that DNA damage caused by the oxidative burst is lethal if not repaired. Oxidative damage to the deoxyribose sugar backbone can lead to strand breaks, whereas damage to DNA bases leads to generation of 8-oxo-2′-deoxyguanosine, thymine glycol and hydroxymethyl urea, among other products, which can lead to strand breaks during DNA replication[165]. The key role of RexAB in DNA repair also identifies DSBs as a potentially lethal type of DNA damage generated by neutrophil ROS. In partial support of this, Schlosser-Silverman *et al.* (2000) have reported the formation of DNA strand breaks in phagocytosed *E. coli* bacteria, induced by macrophage ROS[466].

Loss of recombinational DNA repair has also been shown to reduce survival of other bacterial species *in vivo*, though this has mainly focused on RecA[502–504]. Amundsen *et al.* (2008) reported that *addAB* and *recA* mutants in *Helicobacter pylori* displayed a reduced capacity for stomach colonisation in mice[463]. Loss of AddAB also impaired the colonisation of chicken intestines by *Campylobacter jejuni*[505], and loss of RecBC in *Salmonella enterica* was unable to establish an infection in mice[506]. These mutants also showed comparable sensitivity to ciprofloxacin and mitomycin C, but loss of RecA led to greater sensitivity to UV damage than the loss of AddAB, which was suggested by the authors to indicate an additional RecA-dependent DNA repair pathway[463]. In *E. coli*, the existence of hybrid pathways, with interchangeable parts of the RecBCD and RecF complexes, have been documented[507,508]. The RecF pathway is generally used to repair single-stranded gaps, in which the RecQ helicase and RecJ exonuclease create an exposed 3'-ssDNA tail. Then RecA is loaded onto this 3'-ssDNA tail via the RecFOR complex[434–436]. In the absence of RecBCD, the RecF pathway is activated and can compensate for RecBCD function[508,509].

Although the steps involved in AddAB-mediated DSB repair are less well defined, it has been shown that in the absence of AddAB and RecJ nucleases, RecA loading is impaired in *B. subtilis*[431]. Furthermore, RecOR cannot compensate for AddAB activity in *H. pylori*[510]. These studies suggest that in contrast to *E. coli* RecBCD model, the RecF pathway cannot compensate for loss of AddAB function. The screen of *S. aureus* DNA repair mutants in whole human blood found that loss of RecF significantly reduced survival, though not as much as RexAB (*recR* and *recO* genes are present in *S. aureus*, but mutants were not available from the NTML library). Nevertheless, results from blood survival, neutrophil survival and *in vivo* assays demonstrate that loss of RexAB is not compensated for by another pathway. In addition, complementation with the wild-type *rexAB* operon confirmed that reduced survival was specific to RexAB function. Together, these data indicate that there is little to no redundancy in the staphylococcal DSB repair pathway, making it vulnerable to external inhibition and making RexAB a potential target for novel therapeutics. Further work could determine whether clinical isolates are equally as susceptible to DNA damage via the

oxidative burst, by measuring survival during bloodstream infection or against DNA-damaging agents using the *ex vivo* whole blood model and antibiotic survival assays, and examining SOS induction levels using the fluoresecent SOS reporter.

DSBs occur naturally as a result of normal cellular processes, including oxidative metabolism and during chomosome replication, or due to exposure to DNA-damaging agents[511,512]. Since the accumulation of DSBs during growth will lead to cell death if not repaired, several reports have shown that *recBCD* or *addAB* mutants often display a considerable reduction in cell growth and viability[492,513–515]. For example, Halpern *et al.* (2004) found that growth of *rexA* and *rexB* mutants in *Streptococcus pneumoniae* were severely impaired and viability was just 20% of the wild type[492]. In contrast, Amundsen *et al.* (2008) found that growth was comparable between mutants (*addA* and *addB*) and the wild type in *H. pylori*[463]. Although *S. aureus rexAB* mutants experienced a slightly longer lag phase, growth eventually reached levels comparable to the wild type. These bacteria may produce higher levels of antioxidants to prevent DNA damage caused by oxidative metabolism, and/or have high DNA replication fidelity, both of which would limit the formation and subsequent accumulation of DSBs. For example, *S. aureus* produces the golden pigment staphyloxanthin, which acts as an antioxidant to quench singlet oxygen and free radicals[4]. It is possible that cell growth and viability are only severely affected when DSBs are caused by external sources of DNA damage, such as exposure to DNA-damaging agents or the oxidative burst of phagocytes.

In summary, results from this chapter have shown that staphylococcal DNA is damaged by the neutrophil oxidative burst and that this damage is repaired, at least in part, by RexAB, which makes a significant contribution to bacterial survival in host tissues. RexAB provided protection from the DNA-damaging agents ciprofloxacin, mitomycin C and H_2O_2. The aim of the next chapter will be to determine whether RexAB plays a similarly important role in the survival of other Gram-positive pathogens during bloodstream infection.

4 RexAB is required for survival of the Gram-positive pathogens *Streptococcus gordonii* and *Enterococcus faecalis* during interactions with neutrophils

4.1 Introduction

Infective endocarditis (IE) is a serious infection of the inner lining of the heart (endocardium) and the heart valves. Despite advances in diagnostics, antibiotic therapy and surgical approaches, IE remains a frequently fatal infection, with a mortality rate of 25%[516]. The vast majority (80-90%) of cases of IE are caused by Gram-positive bacterial pathogens such as *S. aureus,* viridans streptococci or *Enterococcus* species[517]. Whilst *S. aureus* is most frequently associated with IE in high-income countries and is reported in up to 30% of cases[516,517], streptococcal IE caused by the oral viridans group, which include *S. sanguinis, S. oralis* and *S. gordonii*, is more common in low-income countries[518]. *Enterococcus* species account for 10% of all cases, with most isolates designated as *E. faecalis*[516,517,519].

Since the normal valvular endocardium is generally resistant to bacterial colonisation, IE tends to develop only after damage to heart valves or in the case of a congenital heart defect, both of which provide a suitable site for bacterial attachment[520]. The pathogenesis of IE is described in Figure 4.1. After the valvular surface is perturbed, IE pathogens that enter the bloodstream via the oral cavity (viridans streptococci), wounds or intravenous catheters (staphylococci or enterococci) attach to the heart valves via specific surface proteins that bind host molecules[521]. Some bacteria bind to components of damaged endothelium, such as fibronectin, collagen and laminin, while others bind directly to activated endothelial cells from an inflammatory endothelial lesion[522–524]. For example, *S. aureus* clumping factor (Clf) and coagulase bind to fibrinogen on the surface of activated endothelial cells[525].

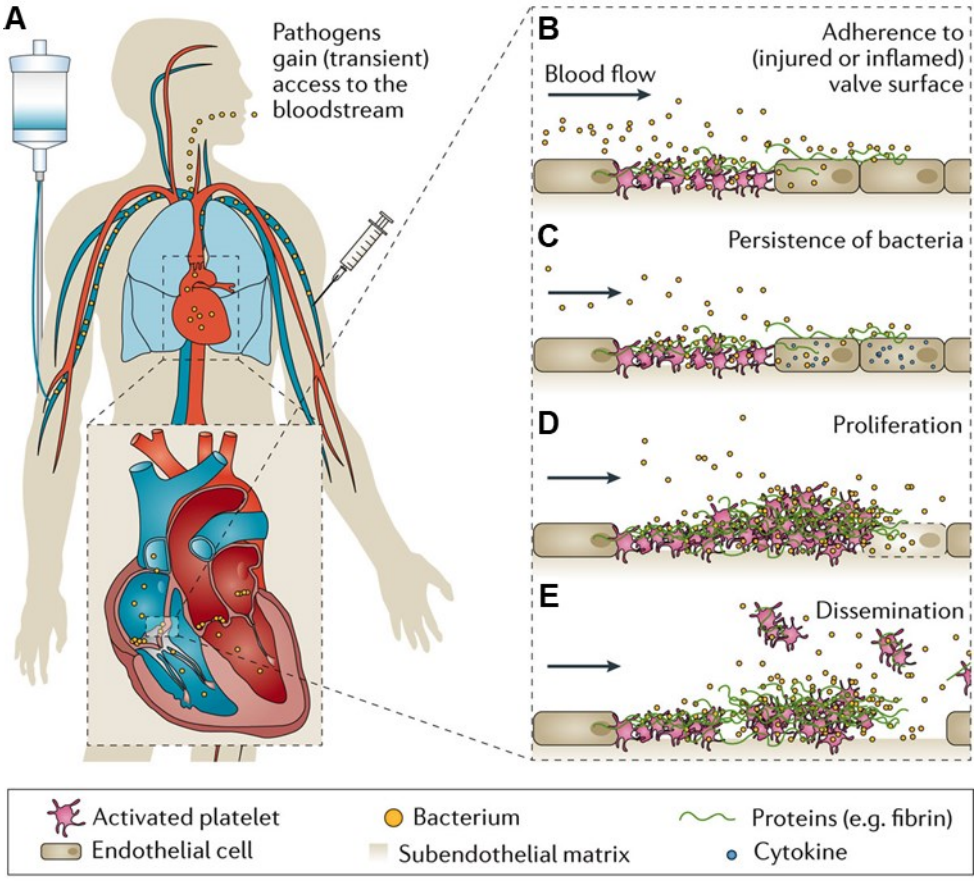

Figure 4.1. Pathogenesis of infective endocarditis.

Pathogens gain access to the bloodstream via wounds, intravenous catheters or the oral cavity **(A)**. Pathogens bind to and persist on the surface of a damaged heart valve **(B, C)**. Bacterial proliferation leads to the formation of an infected mass or "vegetation" **(D)**, which can detach and disseminate in the bloodstream **(E)**. IE, infective endocarditis. Figure taken from Holland *et al.* (2016)[521].

Bacterial colonisation leads to a potent host immune response involving the release of tissue factor and cytokines, multiple cycles of fibrin-platelet deposition and bacterial proliferation, and the development of large vegetations (abnormal growths) on the heart valves[526,527]. Vegetation particles can detach and disseminate in the bloodstream, leading to further complications caused by blocked arteries, such as strokes, aneurysms or abcesses at remote sites[521,528,529].

Phagocytic immune cells such as granulocytes and monocytes provide a key defence against bacterial pathogens that enter the bloodstream[122,530]. However, the host immune response often fails to clear the IE infection and antibiotic therapy is required for up to 6 weeks[519,531]. The high frequency of infections caused by bacterial strains resistant to first line antibiotics, such as penicillin-resistant streptococci or vancomycin-resistant enterococci, present additional therapeutic challenges[521,532,533]. Therefore, there is an urgent need to understand how these pathogens survive the host response in order to develop new approaches to eliminate bacterial pathogens from the bloodstream.

In the previous chapter, DNA was identified as a target of the phagocyte oxidative burst in *S. aureus* and DNA repair shown to be required for staphylococcal survival in human blood, enabling bacteria to overcome oxidative damage. In particular, loss of the RexAB repair complex significantly increased sensitivity of *S. aureus* to the oxidative burst of blood phagocytes and to H_2O_2. A similar LexA-regulated DNA repair system appears to be present in enterococci[534,535], and while streptococci lack the LexA-regulated SOS response[536], both pathogens encode *rexAB* (*addAB*)[426,537] and are able to perform DNA double-strand break (DSB) repair by homologous recombination[491]. Therefore, it was hypothesised that DNA repair is also important in streptococci and enterococci, and that inactivation of RexAB sensitises both these pathogens to oxidative killing by phagocytes in blood.

To understand whether these IE pathogens require DNA repair mechanisms to survive in the bloodstream, *rexAB* deletion mutants were obtained from Dr Angela Nobbs (University of Bristol) in *Streptococcus gordonii* strain DL1 and *Enterococcus faecalis* strain OG1X. *S. gordonii* DL1 has been previously shown to display pathogenicity in the rat

endocarditis model and causes IE due partly to its ability to avoid phagocytic killing[538]. Meanwhile, OG1X is a commonly-used laboratory strain of *E. faecalis* that possesses a selectable streptomycin resistance marker and was originally derived from the human oral isolate OG1[539,540]. Similar assays to Chapter 3 were used in this chapter to determine the importance of RexAB for survival of *S. gordonii* and *E. faecalis* when exposed to DNA-damaging antibiotics, when challenged with H_2O_2 and in the *ex vivo* whole human blood model. Further experiments sought to identify how these pathogens were killed in the bloodstream.

Aim: To assess the importance of RexAB for the survival of the Gram-positive pathogens *S. gordonii* and *E. faecalis* when exposed to DNA-damaging antibiotics, H_2O_2-induced oxidative stress, and in whole human blood.

4.2 Characterisation of growth in wild type and *rexAB* mutants

Differences in growth between wild type and *rexAB* mutants may affect bacterial survival in human blood or when exposed to oxidative stress or antibiotics. Therefore, growth profiles were first determined for *S. gordonii* and *E. faecalis* strains by measuring absorbance at 600 nm over 17 h. As seen in Figure 4.2A, *S. gordonii ΔrexAB* has a small growth defect when compared to the wild type, but this difference is minimal and the final $OD_{600\ nm}$ measurements differ only slightly. As for *E. faecalis*, growth of the *rexAB* mutant was initially slower than wild type, but eventually caught up to wild-type levels after 17 h (Figure 4.2B). Therefore, loss of RexAB led to slightly slower growth when compared to the wild type.

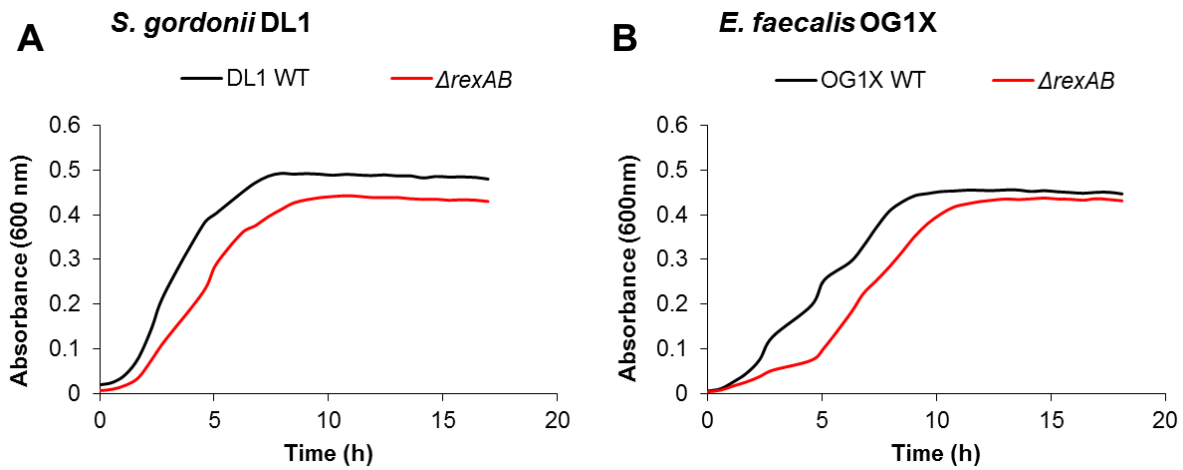

Figure 4.2. Growth profiles of *S. gordonii* and *E. faecalis* wild type and *rexAB* mutants. Growth was assessed by taking $OD_{600\ nm}$ readings every 30 min for 17 h, for *S. gordonii* DL1 **(A)** and *E. faecalis* OG1X **(B)**. Graphs represent the mean of three experiments in duplicate. Error bars were omitted for clarity.

4.3 Loss of RexAB increases susceptibility of *S. gordonii* and *E. faecalis* to DNA-damaging antibiotics

To assess the role of RexAB in repairing DNA damage in *S. gordonii* and *E. faecalis*, the MICs of ciprofloxacin, mitomycin C and H_2O_2 were determined for wild-type and mutant strains as described in Chapter 3.

As for *S. aureus*, the MICs of ciprofloxacin and mitomycin C were significantly reduced in the *S. gordonii rexAB* mutant, by 4-fold for ciprofloxacin and 2-fold for mitomycin C, relative to the wild type (Figure 4.3A, B). An even greater difference was observed for *E. faecalis,* in which the MICs of ciprofloxacin and mitomycin C were reduced by 8-fold in the *rexAB* mutant when compared to the wild type (Figure 4.3D, E). However, although the MIC of H_2O_2 was reduced by 2-fold in the *E. faecalis rexAB* mutant when compared to the wild type*,* no significant difference was found in *S. gordonii* (Figure 4.3C, F). Therefore, *S. gordonii* and *E. faecalis rexAB* mutants are more sensitive to ciprofloxacin- and mitomycin C-mediated DNA damage when compared to the wild type, but only *E. faecalis ΔrexAB* is more sensitive to H_2O_2-mediated DNA damage. This suggests that RexAB is required for DNA damage repair in both pathogens.

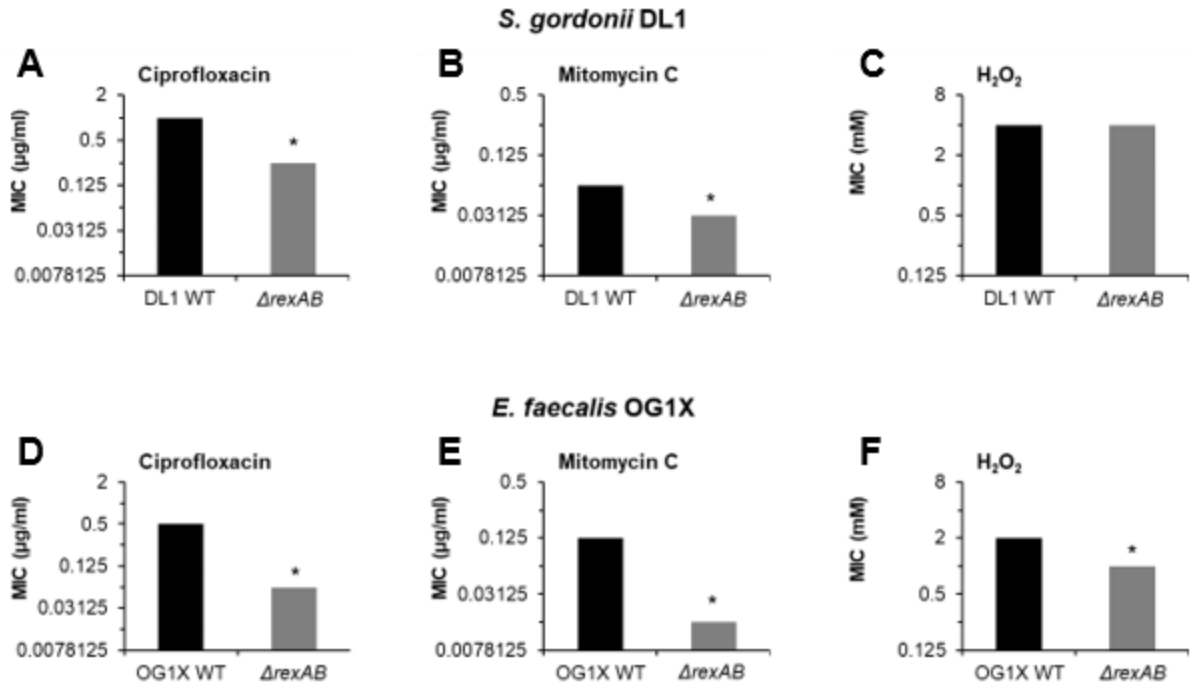

Figure 4.3. MIC data for *S. gordonii* and *E. faecalis* wild type and *rexAB* mutants.
MIC assays were performed using the serial broth dilution method in 96-well plates for ciprofloxacin, mitomycin C and H_2O_2 for *S. gordonii* DL1 **(A-C)** and *E. faecalis* OG1X **(D-F)**. The MIC was defined as the lowest concentration at which no growth was observed after static incubation at 37 °C for 17 h. Graphs represent the median of three independent experiments. *, $P < 0.05$ (paired t test compared to the corresponding wild type).

To investigate antibiotic susceptibility of the strains further, killing kinetics of wild type and *rexAB* mutants were determined for ciprofloxacin as described in the previous chapter. Ciprofloxacin was added at 5 µg/ml, which is 5x MIC for wild-type *S. gordonii* DL1 and 10x MIC for wild-type *E. faecalis* OG1X. Survival at each time point was measured as a percentage of the inoculum at the start of the assay. Over 6 h, there was a decrease in the CFU of both wild-type strains, indicating that both bacterial species are susceptibile to killing by ciprofloxacin (Figure 4.4). *S. gordonii* was more sensitive to ciprofloxacin killing than *E. faecalis,* with a final percentage survival of 0.42% after 6 h compared to 38% for OG1X. Survival of the *rexAB* mutants in both *S. gordonii* and *E. faecalis* was also reduced at all time points when compared to the wild type (Figure 4.4). After 6 h, survival of *ΔrexAB* was reduced by 2.5-fold when compared to wild type *S. gordonii*, and by up to 240-fold for *E. faecalis*.

Therefore, both *S. gordonii* and *E. faecalis* require DNA repair via RexAB for survival of ciprofloxacin-induced DNA damage.

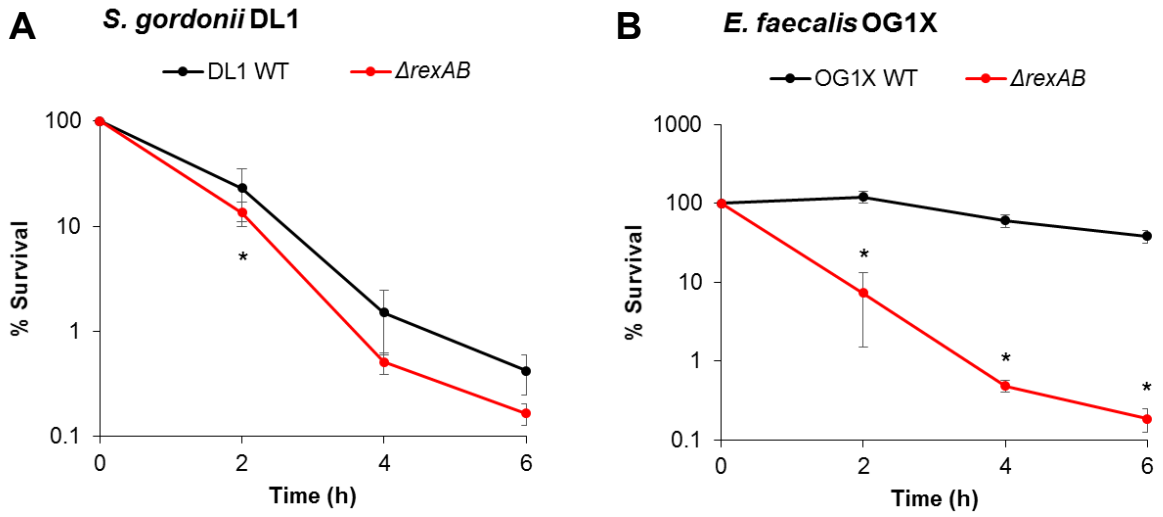

Figure 4.4. *S. gordonii* and *E. faecalis rexAB* mutants are more susceptible to killing by ciprofloxacin.

Percentage survival over 6 h incubation with 5 µg/ml of ciprofloxacin is shown for *S. gordonii* DL1 **(A)** and *E. faecalis* OG1X **(B)**. Ciprofloxacin, at 5 µg/ml, is equal to 5x MIC for wild-type *S. gordonii* and 10x MIC for wild-type *E. faecalis*. Graphs represent the mean of three independent experiments. Error bars indicate the standard deviation. *, $P < 0.05$ (two-way ANOVA with Sidak's test, compared to the corresponding wild type).

4.4 RexAB is not required for survival of *S. gordonii* and *E. faecalis* when challenged with H_2O_2

H_2O_2 is a type of ROS that can diffuse across the bacterial cell membrane to cause oxidative damage[146]. To assess the role of RexAB for survival of *S. gordonii* and *E. faecalis* under oxidative stress, wild type and *rexAB* mutants were exposed to H_2O_2 and survival was determined after 1 h by CFU counts. For both wild-type *S. gordonii* and *E. faecalis,* survival was reduced to 4.3% and 30% of the inoculum respectively (Figure 4.5). However, no significant differences between wild type and *rexAB* mutants were found in *S. gordonii* or *E. faecalis*. Therefore, these results indicate that although these pathogens are susceptible to killing by H_2O_2, RexAB is not involved in the survival of either *S. gordonii* or *E. faecalis* in response to H_2O_2-induced oxidative stress.

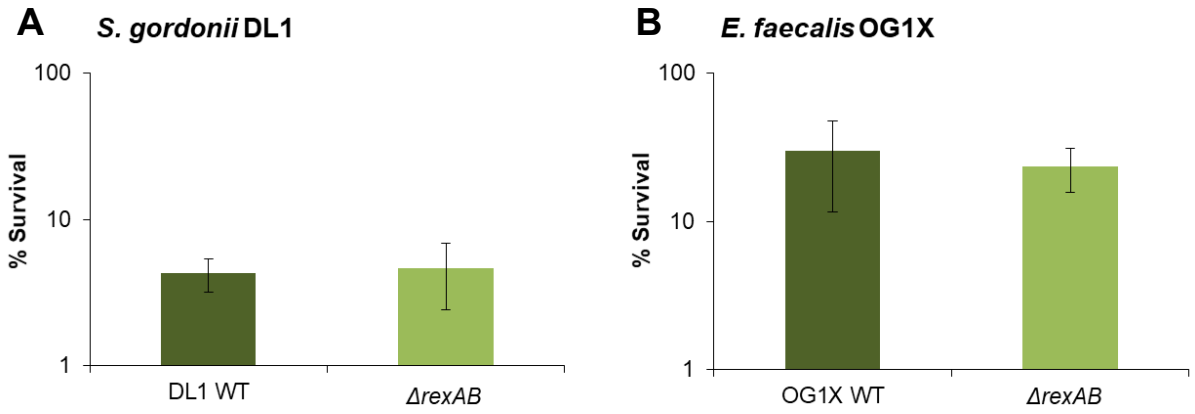

Figure 4.5. Loss of RexAB does not affect survival of *S. gordonii* and *E. faecalis* when challenged with H_2O_2.

Percentage survival after 1 h incubation with 10 mM of H_2O_2 is shown for *S. gordonii* DL1 **(A)** and *E. faecalis* OG1X **(B)**. Graphs represent the mean of three independent experiments. Error bars indicate the standard deviation. No significance was observed (paired t test, compared to the corresponding wild type).

4.5 RexAB promotes the survival of *S. gordonii* and *E. faecalis* in whole human blood, independently of the oxidative burst

Previous data showed that RexAB was required for survival of *S. aureus* in whole human blood by providing protection against the neutrophil oxidative burst (sections 3.8 and 3.9). To determine whether RexAB was similarly important for the survival of *S. gordonii* and *E. faecalis* in the bloodstream, the *ex vivo* whole human blood model was employed. To assess whether loss of RexAB made *S. gordonii* and *E. faecalis* more susceptible to oxidative burst killing, whole human blood was pre-treated for 15 min with the inhibitor DPI to block ROS production[475]. After the addition of bacteria, survival was measured every 2 h by plating onto CBA.

Over 6 h, the percentage survival of wild-type *S. gordonii* initially dropped to 2% of the inoculum, but eventually increased to 5% at the 6 h time point (Figure 4.6A). This indicates that killing of *S. gordonii* by blood phagocytes is effective in the short term, but bacterial numbers eventually start to recover. In contrast to *S. gordonii*, incubation of wild-type *E. faecalis* in whole human blood did not affect bacterial survival at all (Figure 4.6B-D), indicating that *E. faecalis* is naturally resistant to phagocytic killing under these conditions. However, the survival of *rexAB* mutants from both species was reduced when compared to the wild type at all time points, with a 5.5-fold reduction for *S. gordonii* after 6 h when compared to the wild type (DMSO-treated blood, Figure 4.6A) and up to a 3-fold reduction for *E. faecalis* (DMSO-treated blood, Figure 4.6B). Therefore, RexAB promotes the survival of both *S. gordonii* and *E. faecalis* in human blood.

By contrast to *S. aureus*, treatment of blood with DPI did not significantly enhance the survival of the *rexAB* mutants of either species, which remained significantly reduced when compared to the wild type at most of the time points (Figure 4.6). In fact, incubation of *S. gordonii* with DPI-treated blood reduced survival in both wild-type and *rexAB* mutant strains, suggesting that ROS production may actually benefit *S. gordonii*, though reasons for this are unclear. Nevertheless, results from blood survival assays demonstrate that RexAB is

important for survival of *S. gordonii* and *E. faecalis* in the bloodstream, but killing of the *rexAB* mutants in blood is not mediated by the production of ROS.

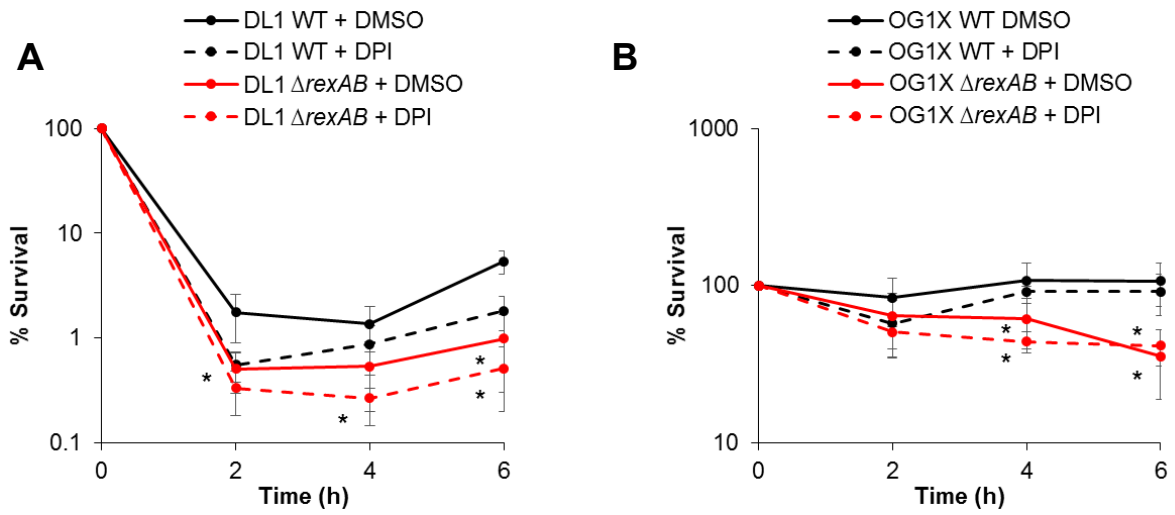

Figure 4.6. RexAB influences susceptibility of *S. gordonii* and *E. faecalis* to killing in whole human blood.

Percentage survival over 6 h incubation in whole human blood is shown for *S. gordonii* DL1 **(A)** and *E. faecalis* OG1X **(B)**. Whole human blood was incubated for 15 min with the NADPH-oxidase inhibitor DPI, or DMSO as a control, before the addition of bacteria. Graphs represent the mean of three independent experiments. Error bars indicate the standard deviation. *, $P < 0.05$ (two-way ANOVA with Sidak's test, compared to the corresponding wild type).

4.6 Killing of *rexAB* mutant in whole human blood is due to production of RNS in *S. gordonii*, but not for *E. faecalis*

In addition to the oxidative burst, another antimicrobial system used by neutrophils is the generation of reactive nitrogen species (RNS), including nitric oxide ($NO^{\bullet}$), nitrogen dioxide ($^{\bullet}NO_2$) and peroxynitrite ($ONOO^-$)[165] (section 1.2.3.1). Nitric oxide is formed by inducible nitric oxide synthase (iNOS) during the conversion of L-arginine to L-citrulline, and reacts with superoxide to generate peroxynitrite and other RNS, which can damage DNA[166].

To assess whether RNS were responsible for killing *S. gordonii* and *E. faecalis* mutants lacking in RexAB, the NOS inhibitors L-NIO and L-NMMA were used. Both inhibitors have been previously shown to be highly effective in blocking NOS activity in human neutrophils, and function by acting as analogues of L-arginine[541]. A combination of RNS and ROS inhibitors was also tested to determine whether both were needed for maximal killing. In addition, the actin-polymerisation inhibitor cytochalasin D was used to determine whether killing of *rexAB* mutants required phagocytosis by immune cells[542]. Blood was treated for 45 min with inhibitor(s) or DMSO as a solvent control before the addition of bacteria. Then bacteria were incubated in pre-treated blood for 6 h and survival was measured by plating onto CBA.

Survival of the *S. gordonii rexAB* mutant in blood treated with DPI alone was reduced relative to the wild type (Figure 4.7A), correlating with results from the previous assay (Figure 4.6A) and indicating that ROS are not involved in *ΔrexAB* killing. For blood treated with L-NIO or L-NMMA, no significant differences in survival were observed between wild type and *rexAB* mutant, and this was similarly observed for NOS inhibitors in combination with DPI (Figure 4.7A), suggesting *ΔrexAB* killing involves RNS. When blood was treated with cytochalasin D, survival of both wild type and *rexAB* mutant increased and survival of the *rexAB* mutant was comparable to the wild type, indicating that phagocytosis is involved in killing of the *S. gordonii rexAB* mutant within blood (Figure 4.7A).

For *E. faecalis,* survival of the *rexAB* mutant remained significantly reduced in DPI- and L-NIO/L-NMMA-treated blood when compared to the wild type (Figure 4.7B), indicating that neither ROS nor RNS are involved in killing of the *rexAB* mutant within blood. Interestingly, no significant difference was seen for cytochalasin D-treated blood, though survival of the mutant was increased when compared to the DMSO control (40% in cytochalasin D vs. 20% in DMSO, Figure 4.7B). These results suggest that killing of the *E. faecalis rexAB* mutant within blood is not due to ROS or RNS, though other mechanisms requiring phagocytosis may be partly involved.

Taken together, these results indicate that neutrophils employ diverse killing mechanisms for *S. gordonii*, *E. faecalis* and *S. aureus*. Whilst killing of *S. aureus* requires ROS, the killing of *S. gordonnii* is dependent upon RNS and an unknown factor is needed to kill *E. faecalis*. However, regardless of the killing mechanism employed, mutants lacking *rexAB* were significantly more susceptible than wild-type strains to neutrophil-mediated killing.

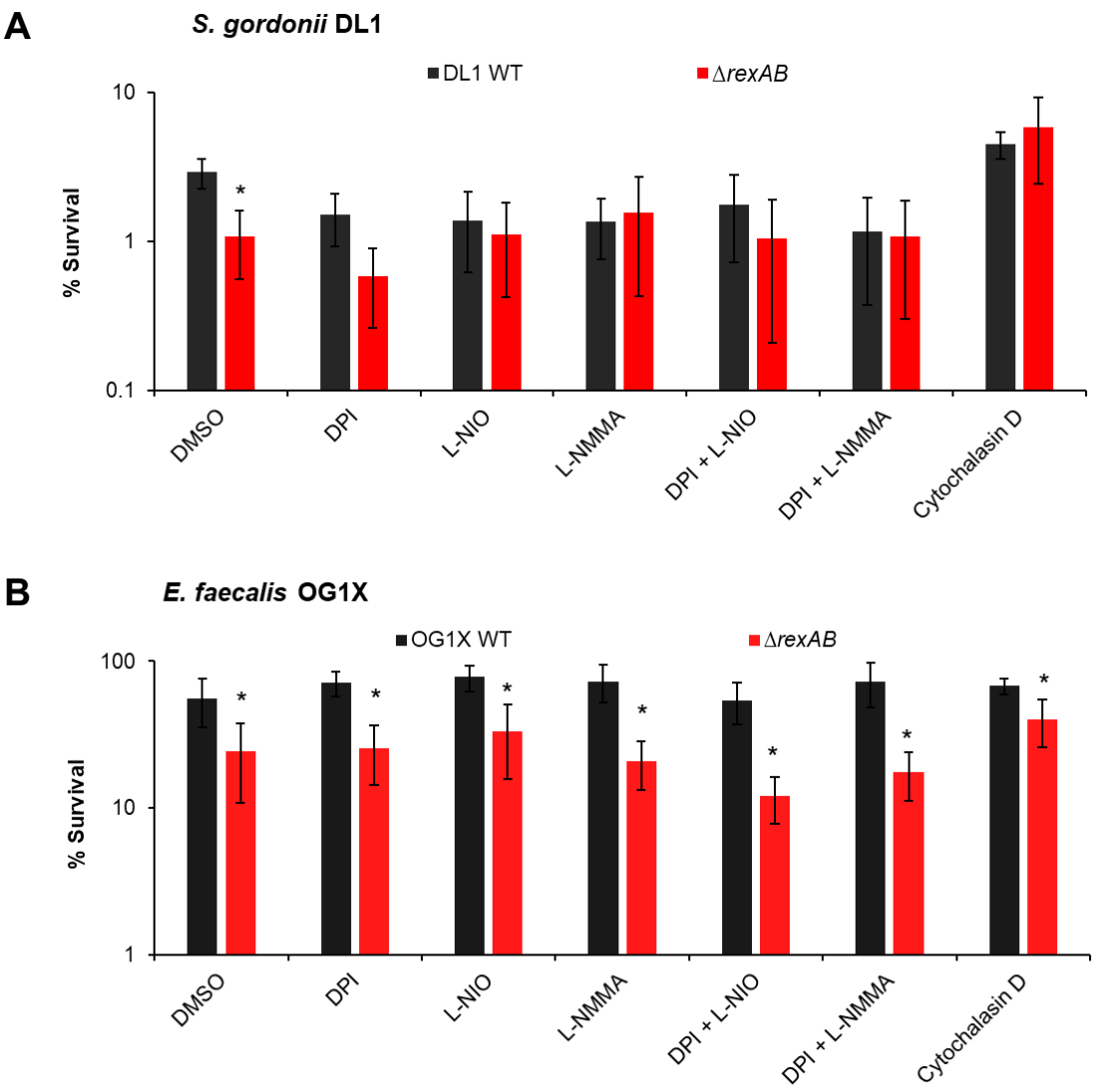

Figure 4.7. Killing of *rexAB* mutant in human blood is due to production of RNS in *S. gordonii*, but not for *E. faecalis*.

Percentage survival after 6 h incubation in blood is shown for *S. gordonii* DL1 **(A)** and *E. faecalis* OG1X **(B)**. Whole human blood was incubated for 45 min with the NADPH-oxidase inhibitor DPI, the NO synthase inhibitors L-NIO or L-NMMA, the phagocytosis inhibitor cytochalasin D, or DMSO as a control, before the addition of bacteria. Graphs represent the mean of four independent experiments. Error bars indicate the standard deviation. *, $P < 0.05$ (two-way ANOVA with Sidak's test, compared to the corresponding wild type).

4.7 Discussion

The objective of this chapter was to assess the role of DNA repair via RexAB in the survival of Gram-positive pathogens *S. gordonii* and *E. faecalis* in the bloodstream and in the presence of DNA-damaging agents. It was found that loss of RexAB increased sensitivity of *S. gordonii* and *E. faecalis* to DNA-damaging antibiotics, supporting the role of this complex in DNA repair. RexAB was also required for survival of these pathogens in blood, supporting findings from the previous chapter that neutrophil killing leads to DNA damage and that DNA repair is necessary for survival during bloodstream infection.

Blood survival assays with the NADPH oxidase inhibitor DPI showed that killing of *rexAB* mutants of *S. gordonii* or *E. faecalis* was not caused by the oxidative burst. This was supported by *in vitro* experiments with H_2O_2, which found that oxidative stress induced by this ROS did not enhance killing of the mutants relative to the wild-type in either pathogen. These results are in keeping with previous findings that ROS are not important for neutrophil-mediated killing of either *S. gordonii* or *E. faecalis*[181,265]. Streptococci are killed by neutrophils via mechanisms involving granule serine proteases[181], while the absence of the electron transport chain in *E. faecalis* reduces its sensitivity to oxidative stress, leading to increased survival in the bloodstream[265]. This is in contrast to *S. aureus,* where the most important host defence is the oxidative burst of neutrophils[141].

Although it was shown that immune killing of *S. gordonii* and *E. faecalis* did not require ROS*, rexAB* mutants still displayed reduced survival in blood. This indicated that DNA damage was occuring, resulting in DSBs. To determine whether this damage was caused by neutrophil-derived RNS, the NOS inhibitors L-NIO and L-NMMA were used in the *ex vivo* whole blood model to block RNS production. Results showed that killing of the *rexAB* mutant in *S. gordonii* was due to DNA damage via RNS, which is in agreement with previous reports that DNA repair via this complex is required for survival against RNS-mediated macrophage killing in *Bacillus cereus*[543] and nitrosative stress resistance in *Salmonella enterica*[544].

In contrast to *S. gordonii*, it was found that RNS had no effect on killing of the *rexAB* mutant in *E. faecalis*, suggesting that DNA damage occurs via a mechanism separate from oxidative or nitrosative stress. When the actin-polymerisation inhibitor cytochalasin D was used, survival of the *rexAB* mutants increased slightly but was still significantly lower than wild-type levels, which suggested that killing of the mutant did not require phagocytic uptake by immune cells. This was unexpected, because previous reports have shown that neutrophil-mediated killing of enterococci requires complement opsonisation and phagocytosis[545,546]. It is possible that the low concentration of cytochalasin D used in this study led to granule exocytosis, as has been shown previously for doses less than or equal to 10 μM[547], which could have enabled killing in the absence of phagocytosis. This is especially as neutrophils can trap and kill pathogens extracellularly via the formation of NETs[182–184], which has been previously linked to the killing of *E. faecalis* in urinary tract infections[548]. To determine whether NETs are involved in killing of *E. faecalis* in the bloodstream, whole blood survival assays could be performed with neutrophils pre-treated with phorbol 12-myristate 13-acetate (PMA) to induce NET formation[549]. This could be confirmed via treatment with deoxyribonuclease (DNase) to degrade extracellular DNA, the primary component of NETs.

Nevertheless, the mechanism by which immune-mediated DNA damage occurs in *E. faecalis* is still unclear. A previous study has shown that *E. faecalis* is highly susceptible to killing by neutrophil-derived proteases[178], but whether these proteases have an effect, if any, on bacterial DNA is unknown. The thee major neutrophil serine proteases (elastase, cathepsin G and proteinase 3) are located in the primary granules and are able to kill bacteria directly[550], and/or by activating or generating AMPs[551]. Future work could investigate the role of proteases in immune killing of the *E. faecalis rexAB* mutant by performing blood or neutrophil survival assays after degranulating the primary granules using PMA[552]. Another experiment could be to inhibit neutrophil granule proteases with the serine protease inhibitors 4-(2-Aminoethyl)benzenesulfonylfluoride (AEBSF) or diisopropylfluorophosphate (DFP)[181].

To summarise, the work presented in this chapter has shown that DNA repair via RexAB is important for survival of the Gram-positive pathogens *S. gordonii* and *E. faecalis* in

whole human blood. In *S. gordonii*, immune-mediated DNA damage was caused by production of RNS. However, this was not the case for *E. faecalis,* in which neither ROS nor RNS had any effect on killing of the *rexAB* mutant. Nevertheless, loss of RexAB function sensitised both pathogens to immune-mediated killing.

5 *S. aureus* RexAB is a member of the RecBCD/AddAB enzyme family

5.1 Introduction

DSBs can occur as a result of DNA-damaging agents, stalled replication forks or replication past single-strand nicks, and is lethal if not repaired prior to cell division[419]. The two main pathways of DSB repair in bacteria are homologous recombination and non-homologous end joining (NHEJ), which only occurs in a few bacterial genera[421–424]. Repair by NHEJ is of low fidelity because DNA ends are joined together with minimal or no sequence homology. In contrast, homologous recombination results in high-fidelity DNA repair and is the preferred method when a second copy of the affected locus is available as a template. For many bacteria, multiple copies or partially-replicated copies of the genome are present within the cell, which facilitates repair[429]. The NHEJ pathway is not present in *S. aureus,* which is believed to rely on homologous recombination for DSB repair[424].

The process of homologous recombination can be divided into several stages, described in further detail in section 1.4.4.1. The first stage is end resection, in which DSBs are processed to create ssDNA that is bound by RecA. Then, RecA mediates the exchange of an intact strand and broken strand, and DNA synthesis occurs using the intact strand as a template. Finally, the two repaired DNA duplexes are separated from each other[433].

In bacteria, processing of DSBs is mediated by the RecBCD/AddAB family of enzymes. This family consists of thee members: RecBCD, AddAB and AdnAB. These multisubunit complexes use different combinations of helicase and nuclease activities to resect DNA ends, resulting in a 3' ssDNA extension onto which RecA is loaded[429]. RecBCD and AddAB enzymes have been well studied, mostly using *E. coli* RecBCD and *B. subtilis* AddAB, respectively. The third member of the family, AdnAB, was identified more recently in mycobacterial species[553]. Since less is known about AdnAB compared to the other two family members, this introduction will focus on RecBCD and AddAB enzymes.

RecBCD/AddAB complexes initiate recombinational repair by binding to free DNA ends and unwinding the DNA using their helicase activity (Figure 5.1A, B), located in the RecB and RecD, or AddA subunits[554,555]. Then, the enzyme translocates along the DNA, using its nuclease activity to degrade both strands until a crossover hotspot instigator (Chi or χ) site is reached (Figure 5.1C). Nuclease activity is located in the RecB or AddA subunits. When a Chi site is encountered, structural changes are induced in the complex that lead to attenuated cleavage of DNA in the 3'-5' direction (Figure 5.1D)[432]. Recognition of the Chi site is polar, only occurring when the enzyme is travelling though the DNA from the 3' end[429]. The Chi sequence recognised by *E. coli* RecBCD is eight bases long (5′-GCTGGTGG-3′)[556,557], whereas the Chi site for *B. subtilis* AddAB is shorter at five bases long (5′-AGCGG-3')[558], and *S. aureus* RexAB is predicted to recognise a seven-nucleotide Chi site (5′-GAAGCGG-3′)[455]. Chi sequences are specific to a bacterial species, although those recognised by RecBCD homologues do share some similarity[429,455].

Although recognition of Chi leads to attenuated 3'-5' nuclease activity, degradation continues in the 5'-3' direction, resulting in the production of a 3' single-strand overhang (Figure 5.1E)[432]. Chi recognition also enhances 5'-3' nuclease activity in RecBCD, leading to faster degradation of the 5' strand[559], but this does not occur in AddAB[560]. Finally, RecA protein is loaded onto the 3' overhang for the next step of recombination (Figure 5.1F). In the case of RecBCD, this is performed by the RecB subunit[561,562]. However, it is still unclear whether AddAB is involved in RecA loading[563].

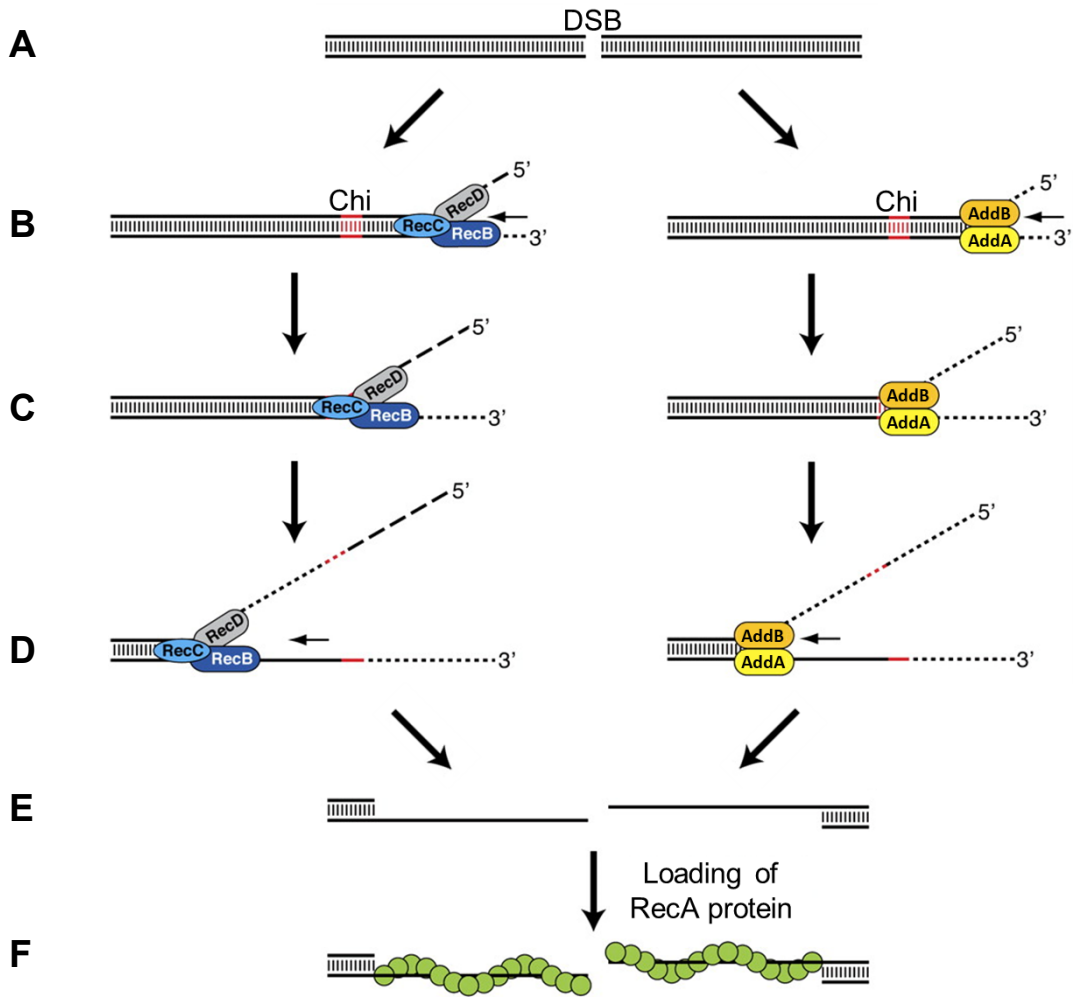

Figure 5.1. Processing of DNA ends by RecBCD/AddAB enzymes.

DNA damage can lead to a double-strand break (DSB) **(A)**, which can be lethal if not repaired. RecBCD or AddAB complexes bind to the broken end and unwind the DNA **(B)**. A Chi (crossover hotspot instigator) site is denoted in red. RecBCD or AddAB translocates along the DNA, degrading both DNA strands **(C)**. Degradation is performed by the RecB subunit in RecBCD, or AddA and AddB subunits in AddAB. When a Chi site is encountered in the 3' strand, this induces changes that attenuate degradation of the 3'-5' nuclease **(D)**, resulting in a 3' overhang **(E)**. The RecA protein is loaded onto the 3' overhang to form a filament (green circles) **(F)**, for the next step of the recombinational repair pathway. Adapted from Niu *et al.* (2009)[564].

RecBCD and AddAB enzymes have similar biochemical properties and both lead to the formation of a RecA filament, but there are significant differences in the structure of these two protein complexes. The most obvious difference is in their subunit composition. RecBCD consists of thee subunits, whereas AddAB only has two (Figure 5.2A)[554,565]. In addition, these subunits have different combinations of helicase and nuclease activities, reflected in their domain structures (Figure 5.2B).

In RecBCD, the RecB subunit contains an N-terminal helicase domain with 3'-5' directionality, which is followed by a nuclease domain (Figure 5.2B) that is also responsible for loading RecA onto the 3' ssDNA overhang[561 565]. The RecD subunit contains the second RecBCD helicase domain, but has 5'-3' specificity. RecC contains an inactive helicase domain[565], but is responsible for recognising Chi sites[566,567]. In contrast, AddAB has a single helicase domain located in the AddA subunit, and two homologous nuclease domains located at the C-terminal of each subunit (Figure 5.2B). The AddA subunit is therefore functionally equivalent to RecB, containing a 3'-5' helicase domain followed by a nuclease domain[554]. The AddB subunit contains a nuclease domain and is responsible for Chi recognition. Each nuclease cleaves a different DNA strand, with the AddA subunit displaying 3'-5' nuclease activity, while AddB has 5'-3' activity[560]. DNA degradation occurs symmetrically in AddAB but not in RecBCD, which is consistent with the fact that the AddAB enzyme contains two nuclease domains, while RecBCD contains only one[568].

Meanwhile, the third member of the RecBCD/AddAB enzyme family, AdnAB, consists of two subunits, each displaying both helicase and nuclease activities[553]. The arrangement and cleavage activity of AdnAB corresponds to those of AddAB (with AdnA and AdnB being equivalent to AddB and AddA, respectively), in that both helicase subunits move along the same DNA strand, but each nuclease subunit cleaves a different strand[429,569].

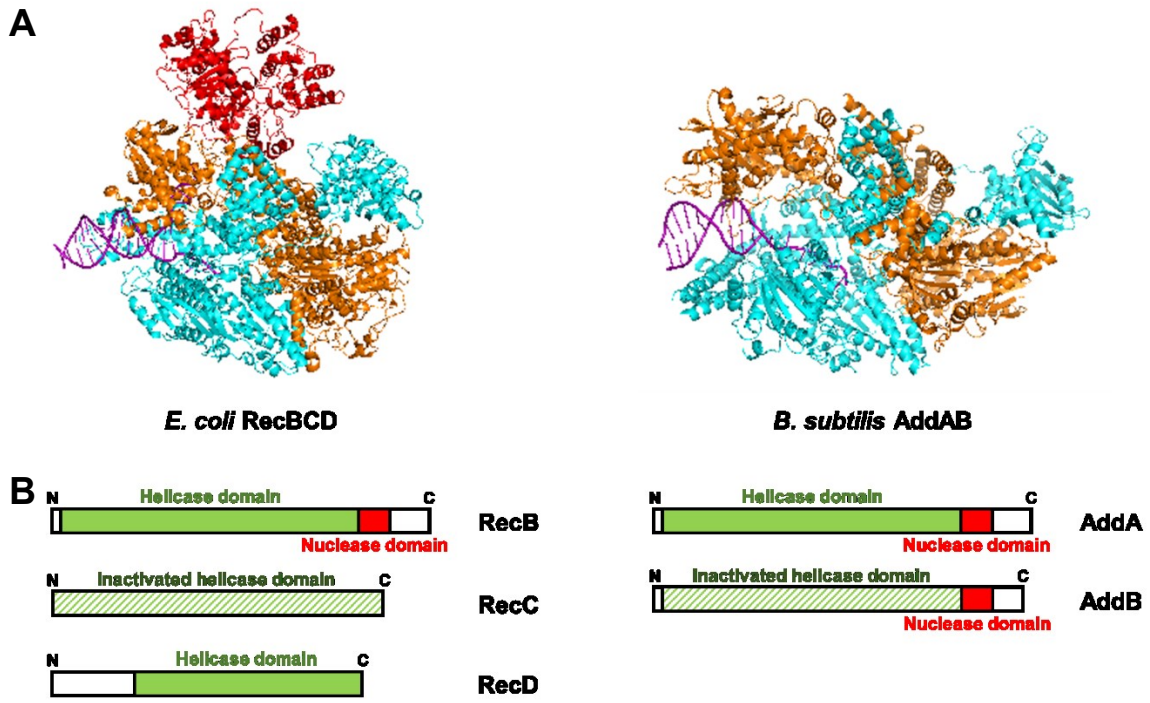

Figure 5.2. Structure of RecBCD and AddAB proteins.

Crystal structures of *E. coli* RecBCD and *B. subtilis* AddAB complexed with DNA (purple) **(A)**. RecBCD is shown in cyan (RecB), orange (RecC) and red (RecD). AddAB is shown in cyan (AddA) and orange (AddB). Protein structures were visualised with PyMOL. PDB 1W36 and 3U4Q were used for the *E. coli* RecBCD and *B. subtilis* AddAB structures, respectively. Protein domains in RecBCD and AddAB complexes **(B).** RecB, RecD and AddA proteins contain a helicase domain (solid green) with seven motifs for ATP-binding and helicase activities, whereas RecC and AddB proteins have an inactivated helicase domain (striped green). RecB, AddA and AddB proteins possess an additional short C-terminal nuclease domain (red). Adapted from Cromie (2009)[537].

Although RecBCD is most often present in Gram-negative bacteria and AddAB in Gram-positive bacteria, this is not always the case. Zuñiga-Castillo *et al.* (2004) found that AddAB was present in members of the Gram-negative α-proteobacteria and in *Ralstonia solanacearum* (β-proteobacterium)[427]. This was supported by an extensive analysis of homologous recombination systems by Rocha *et al.* (2005), in which AddAB proteins were shown to be distributed in both Gram-positive and Gram-negative bacteria (Firmicutes and in most α-and β-proteobacteria)[426]. The exceptions were *Bacillus halodurans*, *Neisseria*

meningitidis and *Chomobacterium violaceum*, which contain RecBCD. Another exception is *H. pylori* from the Gram-negative ϵ-proteobacteria class, which expresses AddAB[463].

Previous studies have identified *S. aureus* RexAB as a member of the AddAB enzyme family via sequence homology[426,427], but direct testing of *S. aureus* RexAB to confirm enzyme function has not been performed. In addition, most of what is known of AddAB is based on experiments in *B. subtilis*[429], with the assumption that the enzyme is similar in other species. However, it is possible that the enzyme may function slightly differently in some species. For example, the mycobacterial RecBCD complex is involved in single-strand annealing but not homologous recombination[570]. Therefore, to assess *S. aureus* RexAB as an AddAB family member, enzyme function of *S. aureus* RexAB was directly tested. In addition, since AddAB is required for RecA activation and subsequent induction of the SOS DNA repair pathway in response to DSBs (sections 1.4.1 and 1.4.4.1), SOS induction levels were compared between wild-type *S. aureus* and *rexAB* mutants. This chapter describes the expression and purification of the recombinant *S. aureus* RexAB protein complex, and the establishment of assays to measure AddAB enzyme activity and SOS induction. *S. aureus* RexAB was hypothesised to be a functional member of the AddAB enzyme family.

Aim: To determine whether staphylococcal RexAB is a functional member of the AddAB enzyme family by confirming homology to AddAB proteins in other bacterial species, measuring AddAB enzyme activity of recombinant *S. aureus* RexAB, and assessing whether *S. aureus* RexAB is required for SOS induction.

5.2 *S. aureus* RexAB is structurally homologous to *B. subtilis* AddAB

Previous studies have reported *S. aureus* RexAB as a homologue of the *B. subtilis* AddAB enyzme on the basis of sequence homology[426,427]. AddAB is a heterodimeric complex that consists of an AddA protein subunit containing active helicase and nuclease domains, and an AddB subunit containing an active nuclease domain only (Figure 5.2B). Functional helicase and nuclease motifs have been identified in the protein domains of both subunits[571–573]. To confirm sequence homology of *S. aureus* RexAB to the AddAB protein family, a multiple sequence alignment was generated of these AddAB motifs in *S. aureus* RexAB and AddAB proteins from *B. subtilis, Streptococcus pyogenes, Streptococcus pneumoniae* and *E. faecalis*.

The AddAB motifs associated with enzyme function were well conserved across the bacterial species examined, with the majority of residues either identical or similar (140 out of 190 in total, 74%; Figure 5.3). In particular, the AddA helicase domain motifs contained 103 residues that were either identical or similar (out of 127 in total, 81%), with 64 identical residues (50%) and 39 similar residues (31%). As for the nuclease domain motifs, 22 residues were either identical or similar in AddA (out of 35, 63%), and 15 residues in AddB (out of 28, 54%), of which the lower similarity was partly due to the shorter motif in the streptococcal species. The sequence similarity of these AddAB motifs is in contrast to the low sequence identity when full-length protein is compared between species (29-38% sequence identity for AddA and 18-30% for AddB, unless between streptococcal species where it increases to 49% and 42%, respectively; Table 5.1). This demonstrates that regions of the sequence relating to enzyme function are conserved across AddAB proteins.

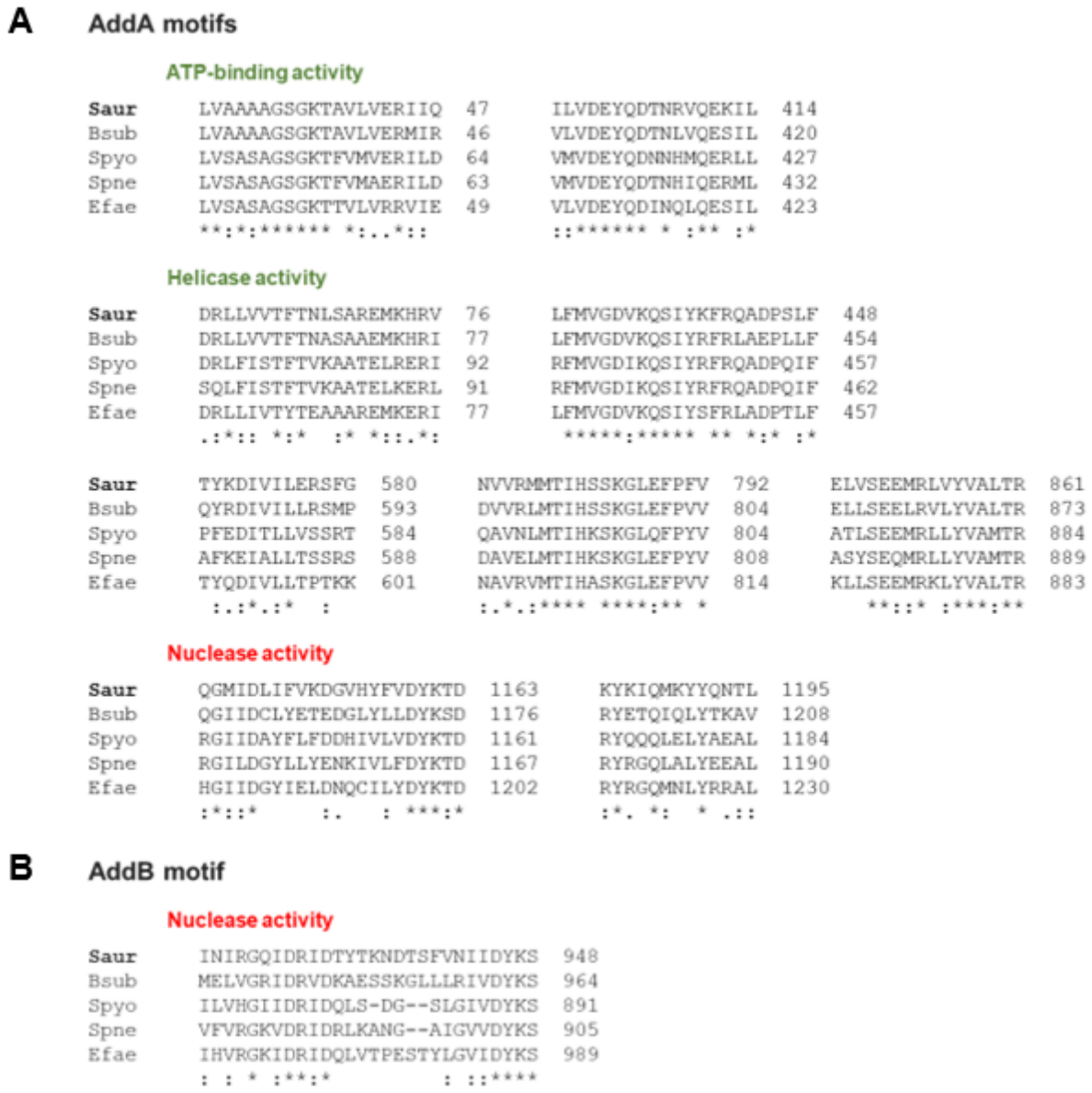

Figure 5.3. **Conserved functional motifs in *S. aureus* RexAB and AddAB homologues**. Multiple sequence alignment of conserved motifs from AddA **(A)** and AddB **(B)**. Motifs present in the helicase domain are indicated in green, and those present in the nuclease domains are indicated in red. Identical residues are indicated by '*', highly similar and less similar residues are indicated by ':' and '.' respectively. Residue positions are indicated on the right-hand side. Alignment was generated by Clustal Omega. Saur, *S. aureus*; Bsub, *Bacillus subtilis*; Spyo, *Streptococcus pyogenes*; Spne, *Streptococcus pneumoniae*; Efae, *Enterococcus faecalis.*

Table 5.1. Percentage identity of full-length AddA and AddB protein sequences between species.

Percent identity matrices for AddA (RexA in *S. aureus*) and AddB (RexB in *S. aureus*) were generated by Clustal Omega.

AddA

	S. aureus	*B. subtilis*	*S. pyogenes*	*S. pneumoniae*	*E. faecalis*
S. aureus		38.12	29.10	28.96	33.45
B. subtilis	38.12		30.98	30.19	40.95
S. pyogenes	29.10	30.98		48.79	31.28
S. pneumoniae	28.96	30.19	48.79		34.01
E. faecalis	33.45	40.95	31.28	34.01	

AddB

	S. aureus	*B. subtilis*	*S. pyogenes*	*S. pneumoniae*	*E. faecalis*
S. aureus		30.38	18.90	17.95	24.56
B. subtilis	30.38		20.70	21.31	29.28
S. pyogenes	18.90	20.70		41.80	23.87
S. pneumoniae	17.95	21.31	41.80		23.62
E. faecalis	24.56	29.28	23.87	23.62	

Next, the structural homology of *S. aureus* RexAB to *B. subtilis* AddAB was examined. Since the crystal structure of *S. aureus* RexAB has not yet been determined, homology modelling was performed using the Phyre2 and I-TASSER platforms. These programs use sequence and protein structure databases of existing proteins to predict the structure of a query sequence[461,462]. Comparisons of homology models to crystal structures show that they can be geometrically very close to experimental structures, and are excellent substitutes when crystal structures are not available[574]. The 3D models produced for *S. aureus* RexA and RexB are shown in Figure 5.4. The Phyre2 and I-TASSER models were near identical, with only slight variations in the loop regions. Homology modelling found that *S. aureus* RexA and RexB displayed the greatest similarity to *B. subtilis* AddA and AddB respectively, and crystal structures of these proteins were used by both platforms as templates for the 3D models. For *S. aureus* RexA, 1110 residues (91% of the sequence) were modelled

with 100% confidence to the *B. subtilis* AddA template (PDB 3U4QA and 3U44A), and for *S. aureus* RexB, 1115 residues (96%) were modelled with 100% confidence with *B. subtilis* AddB as the template (PDB 3U44B). Superimposition of *S. aureus* RexA and RexB models onto corresponding crystal structures of *B. subtilis* AddA and AddB showed that the structures were very similar (Figure 5.5).

After assembly of the 3D model, I-TASSER additionally matches the model against known proteins in the Protein Data Bank (PDB), a global database of the 3D structures of large biological molecules[462]. This process reports proteins with the closest structural similarity to the predicted model, and derives the protein function by identifying ligand-binding sites. The top identified structural analogue of *S. aureus* RexA was *B. subtilis* AddA (PDB 4CEHA, 92% confidence) and RexA was predicted to bind ADP as a helicase-nuclease enzyme (PDB 4CEIA: *B. subtilis* AddA, 58% confidence). For *S. aureus* RexB, the confidence of the function prediction was much lower, at 24% as a helicase (PDB 2IS4: *E. coli* UvrD) and 8% as a nuclease (PDB 3U44B: *B. subtilis* AddB), most likely due to sequence-specific differences in the ligand-binding sites. Nevertheless, the top structural analogue was *B. subtilis* AddB (PDB 3U44B, 96% confidence), aligning with previous results. Taken together, the sequence alignment and homology modelling data indicate that *S. aureus* RexAB is sequentially and structurally homologous to *B. subtilis* AddAB.

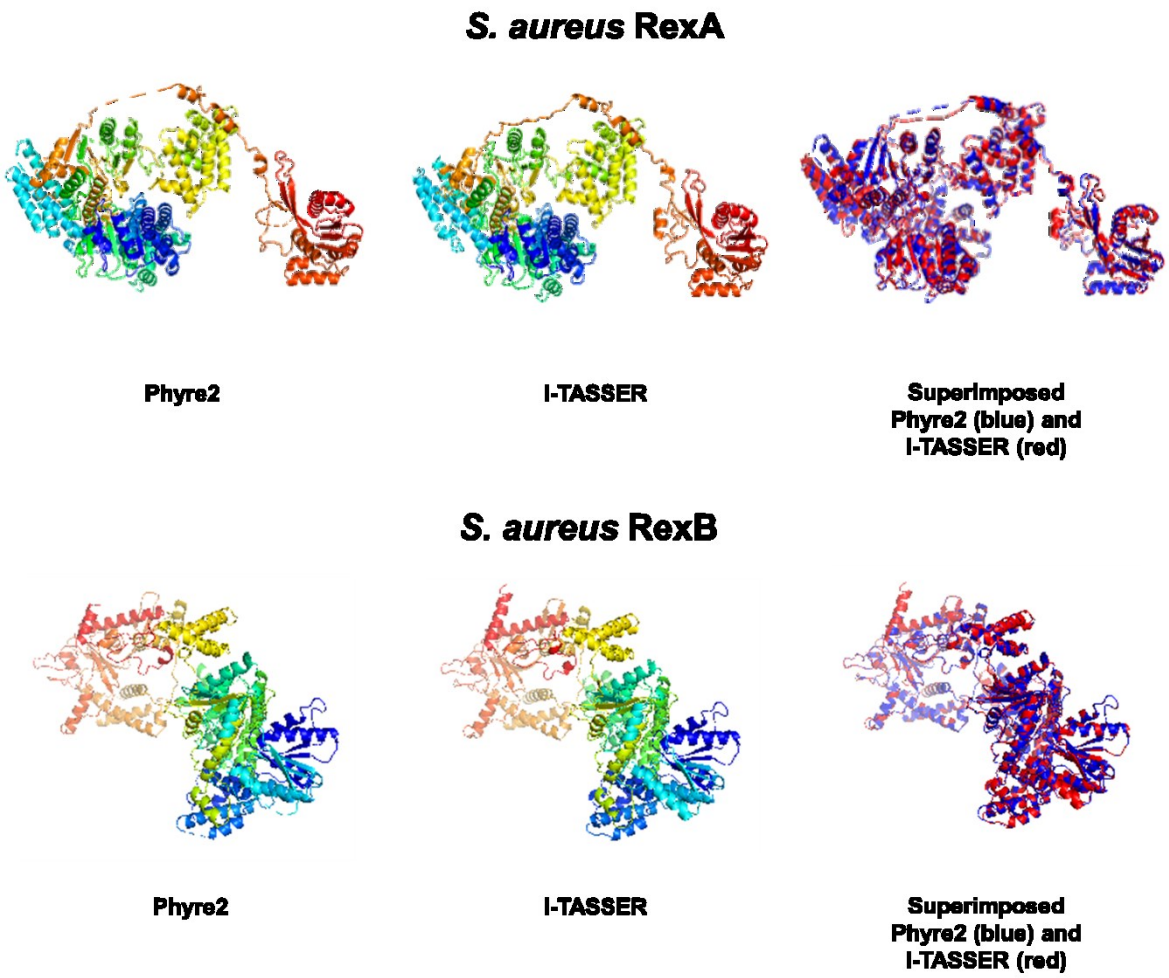

Figure 5.4. Structural modelling of *S. aureus* RexA and RexB.

Ribbon representation of *S. aureus* RexA and RexB proteins as predicted by Phyre2 and I-TASSER, and with Phyre2 and I-TASSER models superimposed onto each other. Individual structures of RexA and RexB are coloured from blue to red from N- to C-terminals. When superimposed, Phyre2 models are shown in blue and I-TASSER shown in red. Protein structures were visualised with PyMOL.

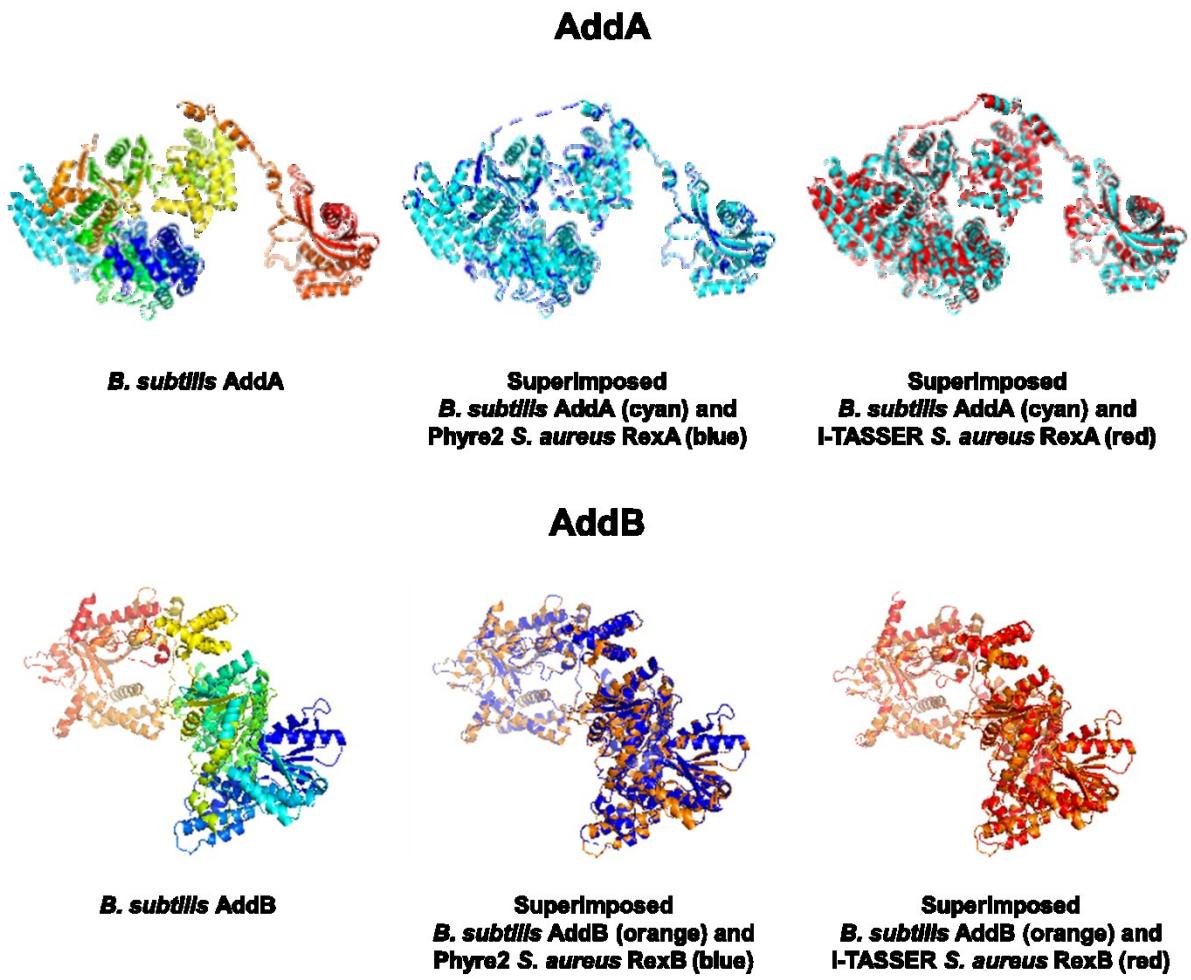

Figure 5.5. Predicted models of *S. aureus* RexA and RexB superimposed onto individual AddA and AddB subunits of the *Bacillus subtilis* AddAB crystal structure. Ribbon representation of *B. subtilis* AddA and AddB proteins individually, and superimposed with Phyre2 and I-TASSER models of *S. aureus* RexA and RexB. Individual *B. subtilis* AddA and AddB structures are coloured from blue to red from N- to C-terminals. When superimposed, *B. subtilis* AddA is shown in cyan, AddB in orange, Phyre2 models in blue and I-TASSER models in red. Protein structures were visualised with PyMOL. PDB 3U4Q was used for the *B. subtilis* AddAB structure[554,575].

5.3 Expression and purification of *S. aureus* RexAB

Whilst sequence homology provided evidence that RexAB is a member of the AddAB family, confirmation required a demonstration of relevant enzymatic activity. AddAB proteins display helicase and nuclease activities, which require energy released from ATP hydrolysis[429]. Previous studies have successfully purified recombinant *B. subtilis* AddAB protein and measured its helicase and/or nuclease activities[560,576]. To enable helicase, nuclease and ATPase activities to be determined for *S. aureus* RexAB, recombinant RexAB was expressed and purified before assays for helicase, nuclease and ATP hydrolysis were undertaken.

5.3.1 Cloning strategy for RexAB expression

RexAB is a large heterodimeric protein (276 kDa) formed of AddA and AddB protein subunits, each greater than 130 kDa in size. Since the separate components of a complex are often not soluble due to hydrophobic regions that mediate binding between subunits, two approaches were considered to obtain the RexAB complex. In the first approach, the complex would be co-expressed from one plasmid, a technique used previously to express *B. subtilis* AddAB[560]. In the second approach, each protein subunit would be expressed individually and then mixed to allow formation of the complex. This would also enable the enzyme activity of each subunit to be tested if the proteins were soluble. Both approaches were tested in parallel to determine which was most useful. The pET expression system was chosen for *S. aureus* RexAB expression as it had been used previously by Chedin *et al.* (2006) to successfully express the *B. subtilis* AddAB complex[576].

The *rexA*, *rexB*, or *rexAB* genes were cloned into the pET28b$^+$ vector under the control of the inducible promoter to enable controllable expression of the target protein with an N-terminal 6xHis tag (Figure 5.6). This tag was followed in the recombinant protein by a thombin site, which was included in the event that the tag impeded protein function and had to be removed. To ensure that both RexA and RexB from the *rexAB* plasmid could be detected by Western blot, SDM (section 2.2.3) was performed to insert a StrepII-tag and a thombin site in front of the *rexA* gene (Figure 5.6). This enabled expression of RexA and RexB proteins to

be detected individually, and provided another method for protein purification by using the StrepII tag. The expression plasmids (hereafter referred to as pET28b$^+$ *rexA,* pET28b$^+$ *rexB* and pET28b$^+$ *rexAB*) were sequenced to confirm that the *rexA, rexB* and *rexAB* genes, StrepII-tag and thombin site had been inserted correctly.

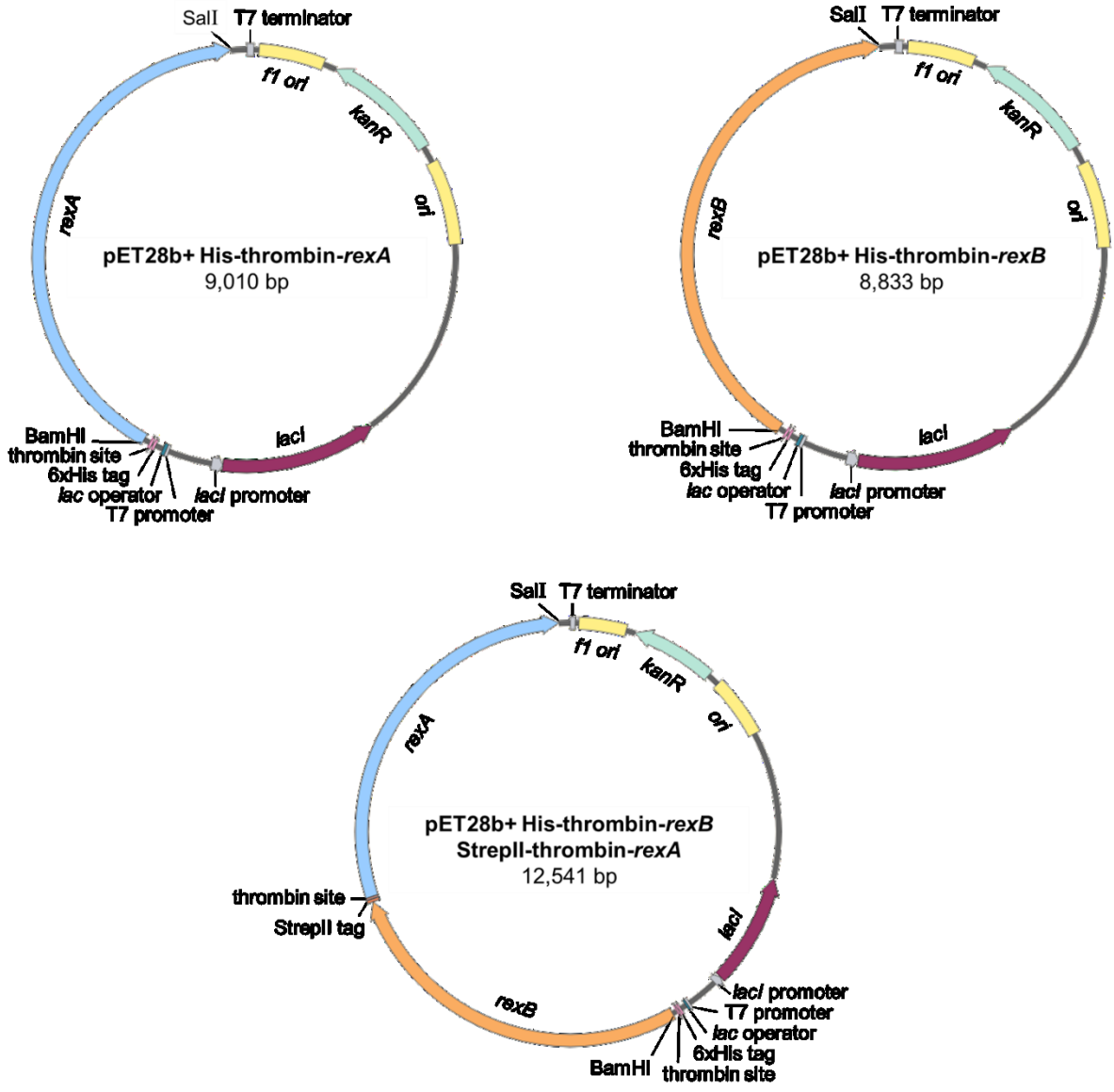

Figure 5.6. Schematic representation of pET28b$^+$ expression plasmids.

Diagram of the final pET28b$^+$ plasmids used for RexA, RexB or RexAB protein expression. BamHI and SalI restriction sites were used to clone *rexA, rexB* or *rexAB* into the pET28b$^+$ vector following a His tag and thombin site. Then SDM was conducted to insert a StrepII tag and a second thombin site before the *rexA* gene to create pET28b$^+$ His-thombin-*rexB* StrepII-thombin-*rexA*. *ori*, origin of replication; *f1 ori*, f1 origin of replication; *kanR*, kanamycin resistance gene; *lacI*, lac repressor. Plasmid maps created with SnapGene.

5.3.2 Optimisation of protein expression and purification conditions

To maximise the production of soluble protein, expression conditions for RexA, RexB and RexAB were optimised. The pET28b$^+$ *rexA, rexB* and *rexAB* constructs were transformed into *E. coli* expression strains (BL21, Rosetta 2 pLysS and/or soluBL21; all contain the λDE3 prophage to enable expression from a pET vector) and expression was tested at various temperatures (16 °C, 30 °C and 37 °C). The inducer IPTG was initially added at 0.4 mM for these tests, but after no protein products were detected by SDS-PAGE analysis and Western blot (data not shown), the concentration was increased to 1 mM, which successfully induced the protein. All further work on expression optimisation was carried out at IPTG concentration of 1 mM. This enabled the strain background and temperature to be determined for the expression of each recombinant protein.

Next, to determine whether RexAB could be successfully purified as a complex and whether it was possible to purify RexA and RexB protein subunits individually, 1 L cultures of the *E. coli* expression strains were grown under the optimised protein expression conditions and strain backgrounds for each protein, and nickel affinity chomatography and/or Strep-Tactin affinity chomatography were performed. This enabled technical aspects of the purification to be optimised prior to a final scale up to a 4 L culture and subsequent purification.

5.3.2.1 Expression and purification of RexA

To optimise expression of RexA protein, the pET28b$^+$ *rexA* construct was transformed into *E. coli* BL21 (DE3) and Rosetta 2 (DE3) pLysS strains, and expression was performed at 16 °C, 30 °C or 37 °C. BL21 (DE3) is an *E. coli* strain that is routinely used for the expression of proteins from pET vectors. Rosetta 2 (DE3) pLysS is a derivative of BL21 (DE3) that has been supplied with tRNAs for codons that are rarely used in *E. coli* but are present in other species, such as *S. aureus*. This strain also expresses T7 lysozyme from pLysS, which suppresses basal expression of T7 RNA polymerase prior to induction, stabilising recombinants with target proteins that may affect cell growth and viability.

Overnight cultures of the transformed cells were used to inoculate 12 ml of fresh media supplemented with appropriate antibiotics to a final $OD_{600\ nm}$ of 0.05. The cultures were grown to mid-exponential phase ($OD_{600\ nm}$ of 0.5), then expression was induced by the addition of IPTG and cultures were shifted to the desired expression temperature. Expression at 30 °C and 37 °C was carried out for 3 h, and expression at 16 °C was carried out for 20 h. Culture samples were taken regularly post-induction. To determine protein solubility, bacterial cells were sonicated after the expression process and the cell lysate was centrifuged to separate supernatant (soluble fraction) from the pellet (insoluble fraction). All samples were analysed by SDS-PAGE and Western blot to detect the His-tagged RexA protein.

RexA was successfully expressed in BL21 (DE3) at the thee temperatures tested, 16 °C, 30 °C and 37 °C (Figure 5.7A). Expression levels and solubility were both temperature-dependent, with higher levels of RexA solubility and protein expression at lower temperatures. For example, RexA was more soluble when expressed at 16 °C than at 37 °C (lanes 13 and 14, compared to lanes 5 and 6; Figure 5.7A). By comparison, expression in Rosetta 2 pLysS occured at much lower levels than in BL21 (Figure 5.7B). In this strain, soluble RexA of the correct mass was only faintly detected at 16 °C by Western blot (lane 13; Figure 5.7B) and not detected at all at 37 °C (lane 5; Figure 5.7B), most likely due to substantial protein degradation, as evidenced by the significant reactivity of anti-His antibodies with multiple low-molecular weight proteins (Figure 5.7B). Therefore, out of the conditions tested, RexA was expressed most successfully in *E. coli* BL21 (DE3) at 16 °C for 20 h.

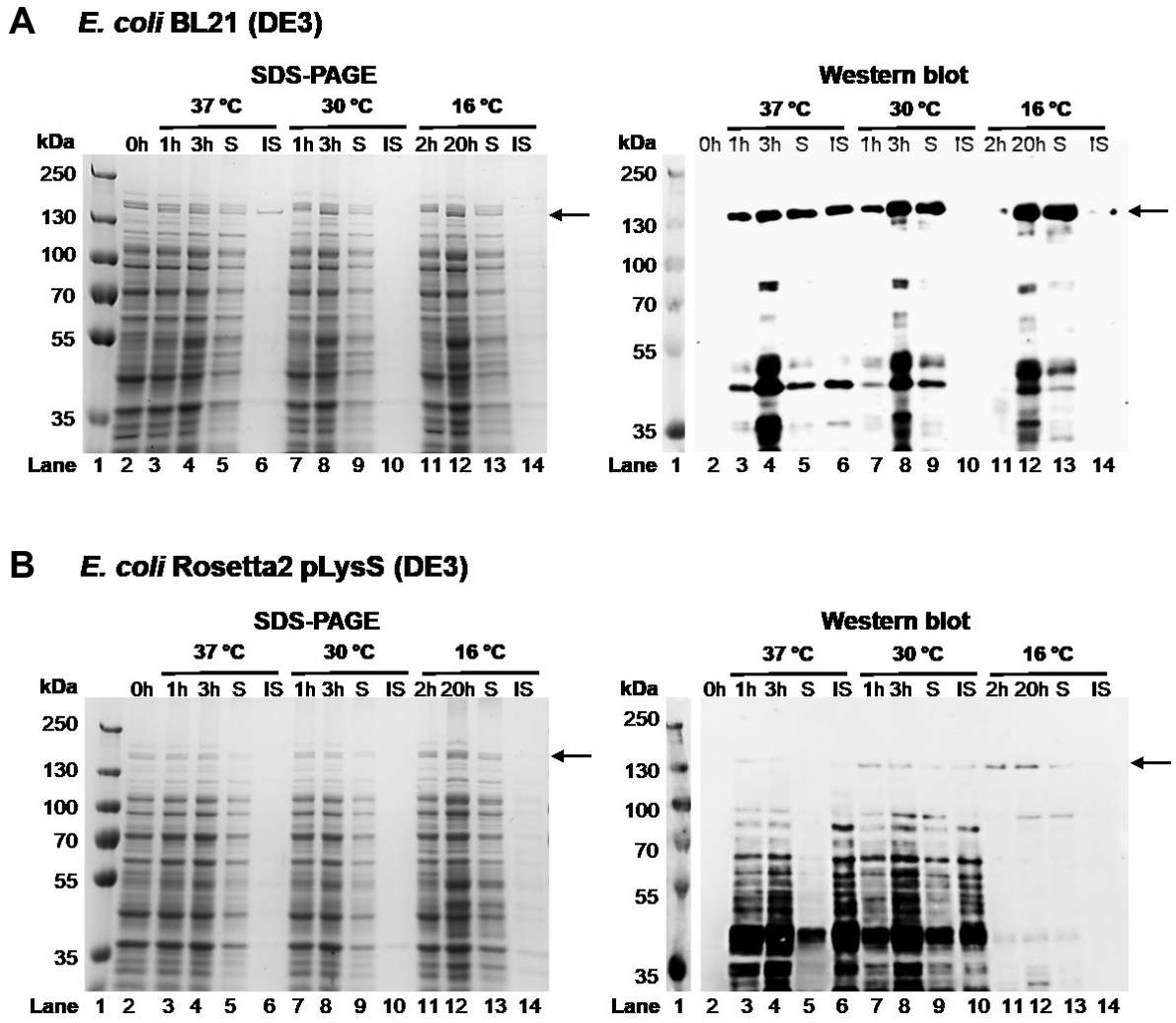

Figure 5.7. Expression of His-tagged RexA in *E. coli* strains BL21 (DE3) and Rosetta 2 (DE3) pLysS at different temperatures.

SDS-PAGE and anti-His Western blot analysis of RexA expression from *E. coli* strains BL21 (DE3) **(A)** and Rosetta 2 (DE3) pLysS **(B)**. Expression was induced by the addition of 1 mM IPTG. Protein bands for His-RexA (145 kDa) are indicated by the arrows. The molecular weight of the marker bands in kDa are indicated. 0h = uninduced; 1h = 1 h post induction; 2h = 2 h post induction; 3h = 3 h post induction; 20h = 20 h post induction; S = soluble fraction; IS = insoluble fraction.

To determine whether RexA could be purified successfully as a monomer, His-tagged RexA was expressed in *E. coli* BL21 (DE3) at 16 °C for 20 h, then nickel affinity chomatography was performed. This purification technique relies on the ability of nickel to bind to histidine residues. His-tagged proteins bind to the nickel column, which enables them to be separated from other proteins in the whole cell lysate. The addition of imidazole displaces the bound proteins by mimicking the side-chain of histidine. To optimise the imidazole concentration for elution, stepwise elution was performed at 100 mM, 200 mM and 300 mM. Elution buffer was added in small volumes (10 ml) and each fraction was tested with Bradford reagent until no more protein was detected. Samples taken during the process were analysed by SDS-PAGE and Western blot to detect His-tagged RexA.

His-tagged RexA was detected in the soluble fraction (lanes 3 and 4; Figure 5.8) and was eluted at 100 mM and 200 mM of imidazole (lanes 8 and 9; Figure 5.8). However, although a strong band was observed at the expected size of His-tagged RexA (145 kDa), many other bands were also present. These bands only appeared after induction with IPTG, indicating that these were likely to be degradation products of the target protein. Therefore, RexA is mostly soluble in the absence of RexB and can be purified to some degree, but appears to be unstable.

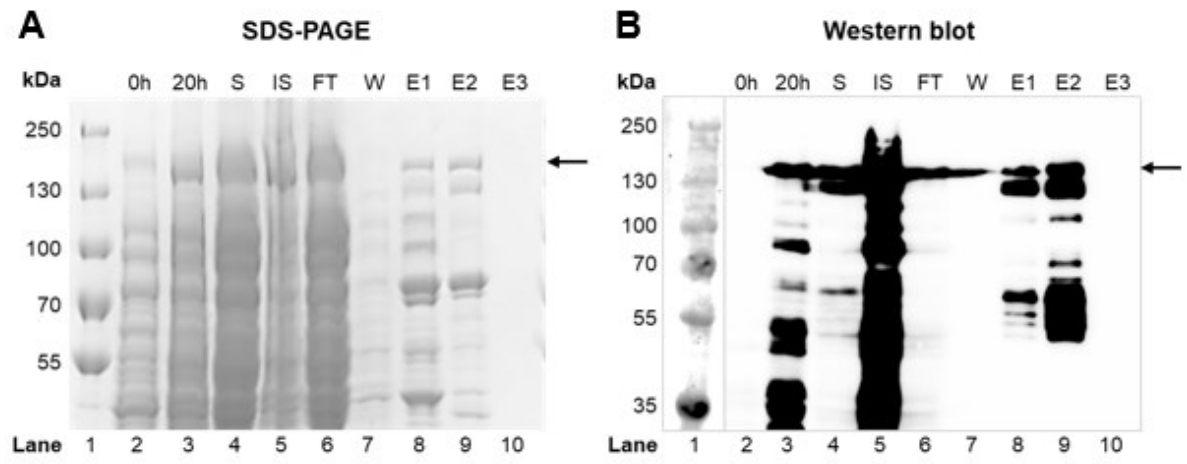

Figure 5.8. RexA purification via nickel affinity chomatography.

Analysis of RexA purification by SDS-PAGE **(A)** and anti-His Western blot **(B)**. Expression was carried out in *E. coli* BL21 (DE3) cells at 16 °C for 20 h, induced by the addition of 1 mM IPTG. Protein bands for His-RexA (145 kDa) are indicated by the arrows. The molecular weight of the marker bands in kDa are indicated. 0h = uninduced; 20h = 20 h post induction; S = soluble fraction; IS = insoluble fraction; FT = flow though; W = wash; E1-3 = stepwise elution at 100 mM, 200 mM and 300 mM imidazole, respectively.

5.3.2.2 Expression and purification of RexB

To optimise expression of RexB protein, the pET28b$^+$ *rexB* construct was transformed into *E. coli* BL21 (DE3) and Rosetta 2 (DE3) pLysS, and expression was tested at 16 °C, 30 °C and 37 °C. As shown in Figure 5.9A, RexB was not expressed at all in BL21 (DE3) and no protein bands were detected in either the SDS-PAGE or Western blot. In Rosetta 2 (DE3) pLysS, RexB was very faintly detected at 3 h post-induction at 30 °C and 37 °C (lanes 8 and 4 respectively in the Western blot; Figure 5.9B), but expression levels were too low to be detected when lysed and separated into soluble and insoluble fractions (lanes 5, 6, 9, 10 in the Western blot; Figure 5.9B). However, RexB protein was successfully expressed at 16 °C for 20 h by SDS-PAGE and Western blot (lane 12; Figure 5.9B). Furthermore, the expressed protein was found to be soluble under these conditions (lane 13; Figure 5.9B). Therefore, out of the *E. coli* strains and temperatures tested, RexB was expressed most successfully in *E. coli* Rosetta 2 (DE3) pLysS at 16 °C for 20 h.

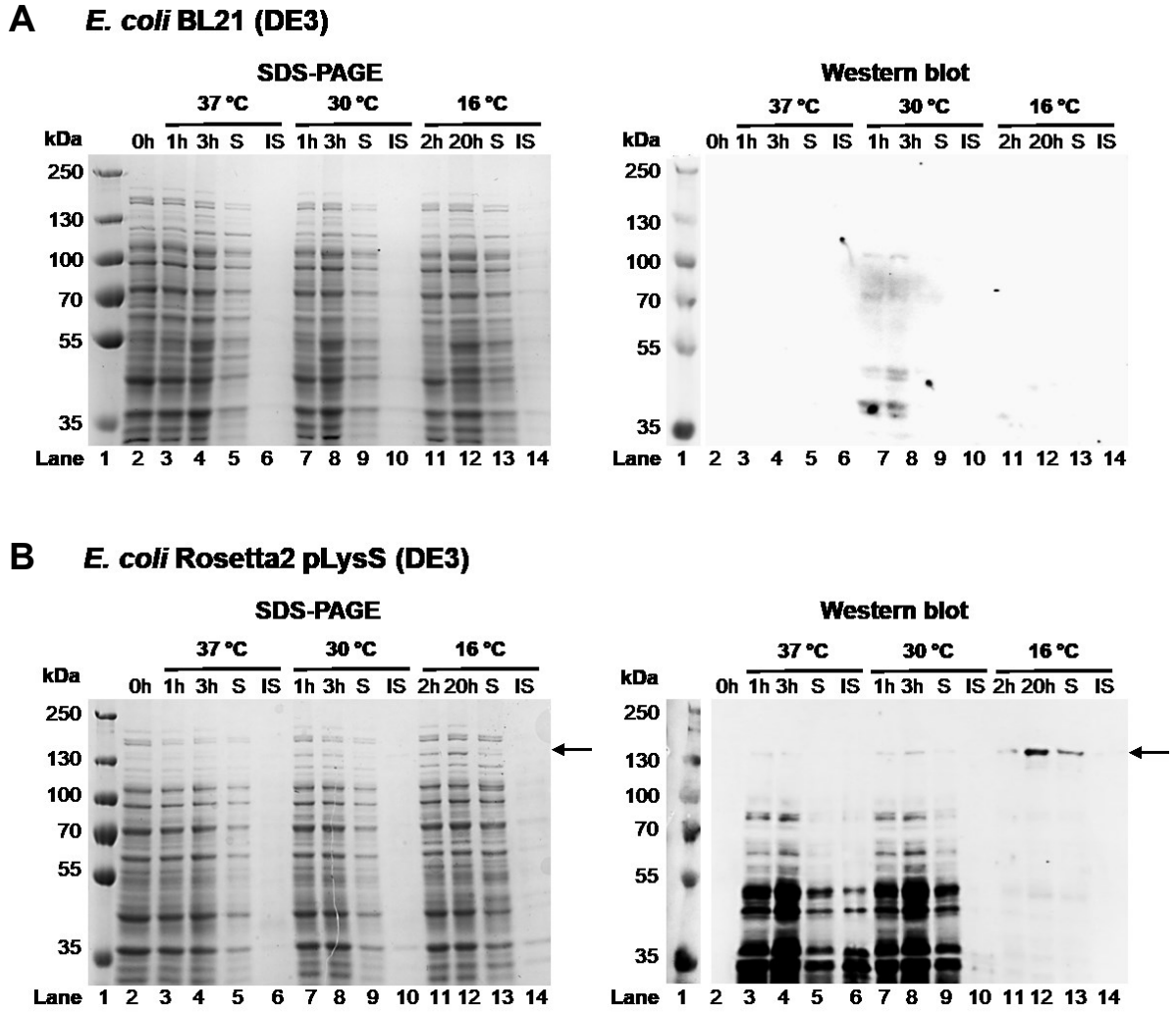

Figure 5.9. Expression of His-tagged RexB in *E. coli* strains BL21 (DE3) and Rosetta 2 (DE3) pLysS at different temperatures.

SDS-PAGE and anti-His Western blot analysis of RexB expression from *E. coli* strains BL21 (DE3) **(A)** and Rosetta 2 (DE3) pLysS **(B)**. Expression was induced by the addition of 1 mM IPTG. Protein bands for His-RexB (138 kDa) are indicated by the arrows. The molecular weight of the marker bands in kDa are indicated. 0h = uninduced; 1h = 1 h post induction; 2h = 2 h post induction; 3h = 3 h post induction; 20h = 20 h post induction; S = soluble fraction; IS = insoluble fraction.

Next, nickel affinity chomatography was performed on His-tagged RexB as described above for His-tagged RexA. RexB was expressed after incubation for 20 h at 16 °C, and was detected in the whole cell lysate by both SDS-PAGE and Western blot (lanes 3 and 4; Figure 5.10). However, no protein was present in the eluted fractions and so the purification was considered unsuccessful (lanes 10-12; Figure 5.10). Upon closer examination of the Western blot, it was found that this was because the RexB protein was highly insoluble (lanes 5 and 6; Figure 5.10B). This aligns with the finding by Yeeles *et al.* (2009) that *B. subtilis* AddB (RexB homologue) was highly insoluble when over-expressed in the absence of AddA [577]. Although the data in Figure 5.9 indicated that expression of RexB was soluble, this was only possible in small volumes (12 ml) and not at the larger quantities required for purification. Therefore, RexB cannot be purified on its own and appeared, therefore, to require co-purification with RexA.

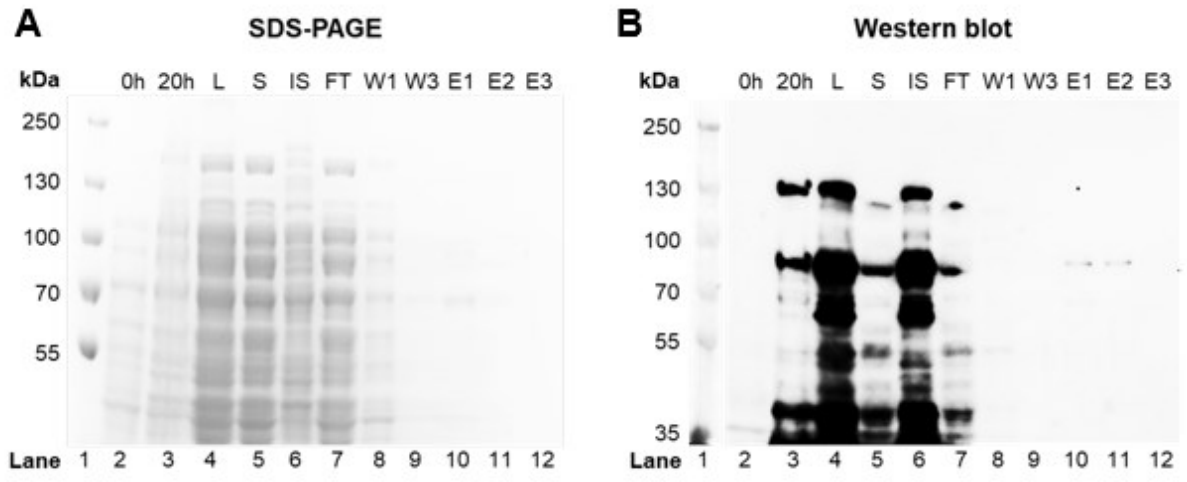

Figure 5.10. RexB purification via nickel affinity chomatography.
Analysis of RexB purification by SDS-PAGE **(A)** and anti-His Western blot **(B)**. Expression was carried out in *E. coli* Rosetta 2 (DE3) pLysS cells at 16 °C for 20 h, induced by the addition of 1 mM IPTG. Protein bands for His-RexB (138 kDa) are indicated by the arrows. The molecular weight of the marker bands in kDa are indicated. 0h = uninduced; 20h = 20 h post induction; S = soluble fraction; IS = insoluble fraction; FT = flow though; W = wash; E1-3 = stepwise elution at 100 mM, 200 mM and 300 mM imidazole, respectively.

5.3.2.3 Expression and purification of RexAB

Similarly to RexA and RexB, expression of RexAB was tested in *E. coli* BL21 (DE3) and Rosetta 2 (DE3) pLysS strains at 16 °C, 30 °C and 37 °C. However, the RexAB complex was not expressed at all in BL21 (DE3) and no protein bands were detected in either the SDS-PAGE or Western blot (Figure 5.11A). Furthermore, the complex was poorly expressed in Rosetta 2 (DE3) pLysS. At 30 °C, a faint band corresponding to His-tagged RexB was detected after 1 h of induction (lane 7; Figure 5.11B), but this was no longer present after the cells were lysed and separated into soluble and insoluble fractions (lanes 9 and 10; Figure 5.11B). At 16 °C, bands corresponding to RexA and RexB were detected after 20 h by SDS-PAGE analysis (lane 12; Figure 5.11B), but the corresponding band in the Western blot was faint and soluble protein was hardly detectable (lanes 12 and 13 respectively; Figure 5.11B).

Since neither BL21 (DE3) nor Rosetta 2 (DE3) pLysS were suitable for RexAB expression, the pET28b$^+$ *rexAB* construct was transformed into a third *E. coli* expression strain. *E. coli* soluBL21 (DE3) is a derivative of BL21 (DE3) for expressing proteins that are difficult to solubilise. Expression was carried out as described previously. As shown in Figure 5.11C, RexAB was successfully expressed in soluBL21 (DE3) at all the temperatures tested and soluble protein was maintained after cell lysis (lanes 5, 9 and 13). The protein complex was most successfully expressed at 16 °C for 20 h, reflected in the higher levels of His-tagged RexB detected by Western blot compared to expression at 30 °C and 37 °C (lane 13, compared to lanes 5 and 9 respectively; Figure 5.11C). In addition, both RexA and RexB protein subunits were detected by SDS-PAGE analysis at 16 °C, but not at 30 °C or 37 °C (lane 12, compared to lanes 4 and 8; Figure 5.11C). Therefore, from the *E. coli* strains and temperatures tested, RexAB was expressed best in *E. coli* soluBL21 (DE3) at 16 °C for 20 h.

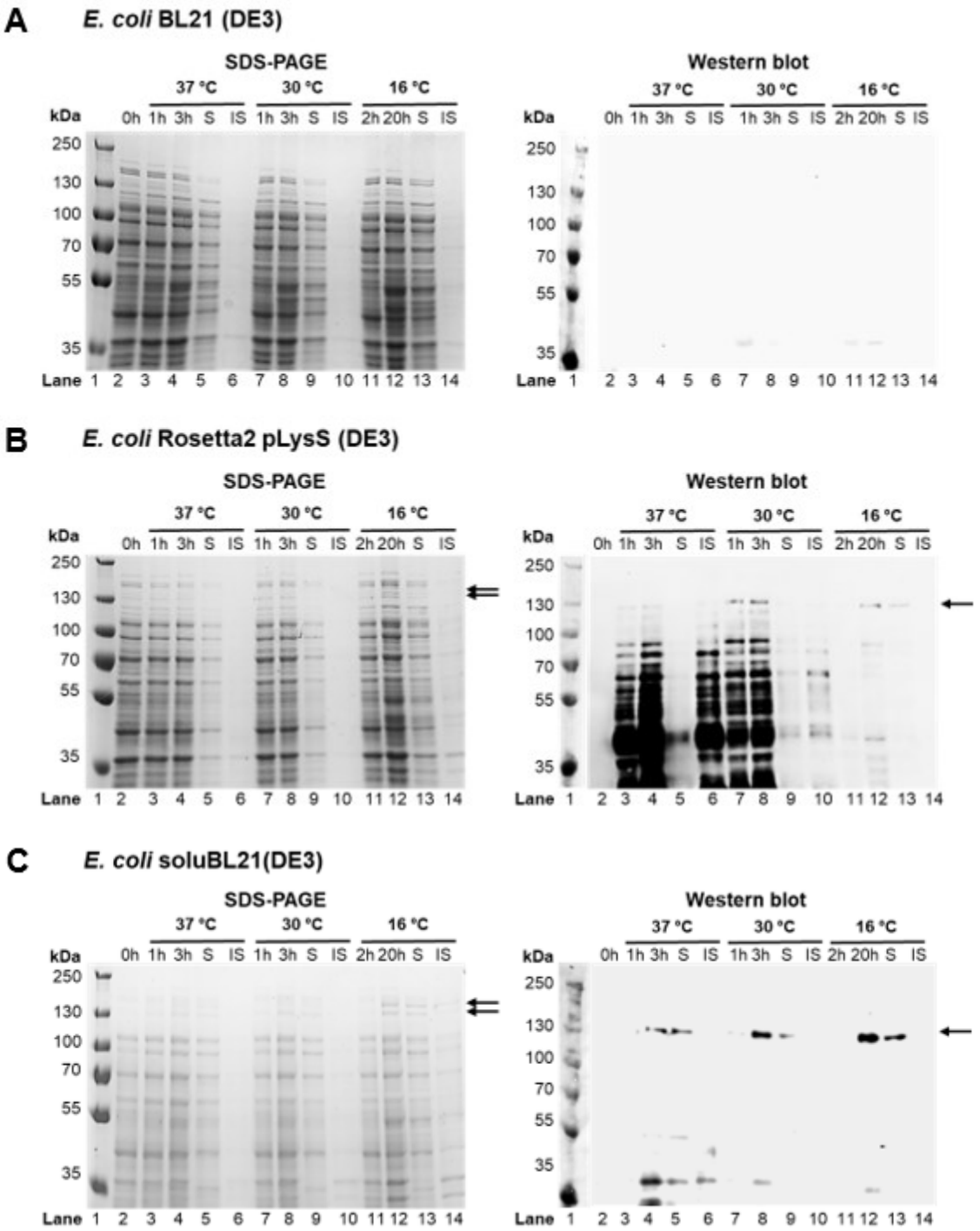

Figure 5.11. Expression of RexAB in *E. coli* strains BL21 (DE3) and Rosetta 2 (DE3) pLysS at different temperatures.

SDS-PAGE and Western blot analysis of RexAB expression from *E. coli* strains BL21 (DE3) **(A)**, Rosetta 2 (DE3) pLysS **(B)** and soluBL21 (DE3) **(C)**, induced by the addition of 1 mM IPTG. StrepII-RexA (144 kDa) and His-RexB (138 kDa) are indicated by the arrows. His-RexB is detected in the Western blot. Molecular weight of marker bands are indicated in kDa. 0h = uninduced; 1h = 1 h post induction; 2h = 2 h post induction; 3h = 3 h post induction; 20h = 20 h post induction; S = soluble fraction; IS = insoluble fraction.

To determine whether RexAB could be purified as a complex and to optimise the purification technique, two methods for RexAB purification were tested. Expression from the pET28b^{+} *rexAB* construct led to the production of StrepII-tagged RexA and His-tagged RexB. These protein tags enabled purification of RexAB by Strep-Tactin affinity chomatography via the StrepII tag, or nickel affinity chomatography via the His tag. Therefore, provided that RexAB was expressed as a protein complex within *E. coli* soluBL21 (DE3) cells, it was possible for both RexA and RexB subunits to be eluted together during the purification.

Strep-Tactin affinity chomatography relies on the binding of biotin to streptavidin. The StrepII tag binds to the biotin-binding pocket of streptavidin, which enables purification of the recombinant protein. Strep-Tactin is a streptavidin derivative that is optimised for maximal binding to the StrepII-tag. StrepII-tagged proteins are competitively eluted by adding the biotin-analogue desthiobiotin. Purification was performed in a gravity-flow column and protein eluted with 2.5 mM of desthiobiotin. Elution buffer was added in volumes of 5 ml and each fraction tested with Bradford reagent until no more protein was detected. Samples were analysed by SDS-PAGE and Western blot to detect StrepII-tagged RexA and His-tagged RexB.

Although RexA and RexB proteins were soluble and detected by SDS-PAGE and Western blot (lane 5; Figure 5.12), no corresponding bands were detected in the eluted fraction (lane 10), indicating that the purification of RexAB by Strep-Tactin affinity chomatography was unsuccessful. Upon closer examination, SDS-PAGE and Western blot data showed that RexA and RexB were detected in the flow though and in the first wash step (lanes 7 and 8; Figure 5.12), but not in subsequent steps (lanes 9 and 10). This revealed that the StrepII-tagged protein had not bound to the Strep-Tactin column, which could have been due to the StrepII tag being hidden by protein folding in the formation of the RexAB complex.

When nickel affinity chomatography was performed using the same method described for His-tagged RexA (section 5.3.2.1 above), RexAB protein bound to the nickel column via the His-tagged RexB was eluted successfully (lanes 10-13; Figure 5.13). His-tagged RexB and StrepII-tagged RexA were both detected by Western blot in the eluted fractions, indicating that the protein subunits were expressed as a complex and purified

together (1:1 ratio, based on Figure 5.13A). Step-wise elution with increasing imidazole concentrations showed that the protein eluted around 100 to 200 mM, therefore it was decided that 150 mM would be used to elute RexAB in subsequent experiments. It was noted that a few bands of lower molecular weight were present in the eluted fractions on the SDS-PAGE gel (lanes 10 and 11; Figure 5.13A). It was decided to remove these in the final purification using a 100 kDa cut-off filter. Since nickel affinity chomatography was successful for purification of RexAB, this technique was used in future experiments.

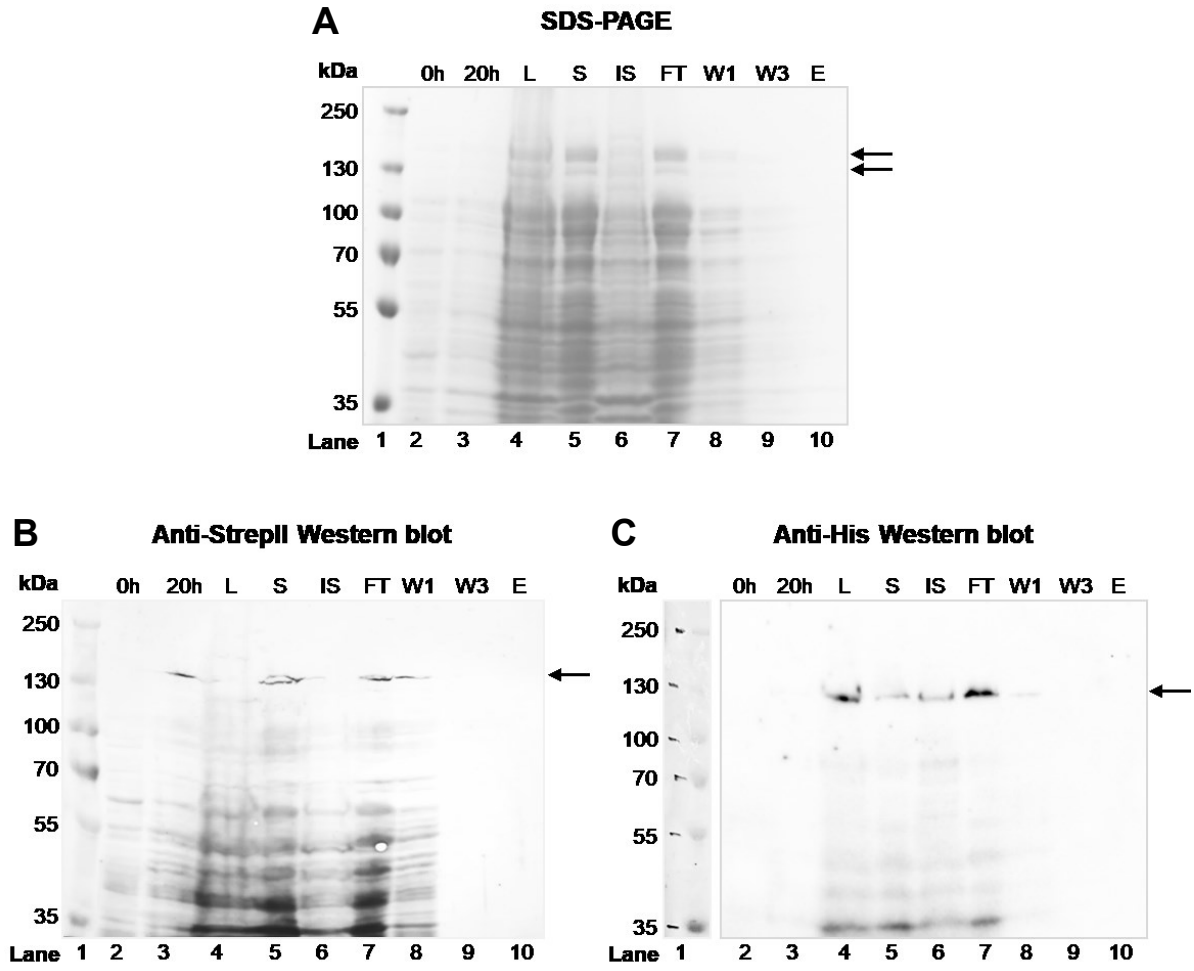

Figure 5.12. RexAB purification via Strep-Tactin affinity chomatography.
Analysis of RexAB purification by SDS-PAGE **(A)**, anti-StrepII Western blot **(B)** and anti-His Western blot **(C)**. Expression was carried out in *E. coli* soluBL21 (DE3) cells at 16 °C for 20 h, induced by the addition of 1 mM IPTG. Protein bands for StrepII-RexA (144 kDa) and His-RexB (138 kDa) are indicated by the arrows. The molecular weight of the marker bands in kDa are indicated. 0h = uninduced; 20h = 20 h post induction; S = soluble fraction; IS = insoluble fraction; FT = flow though; W = wash; E = elution.

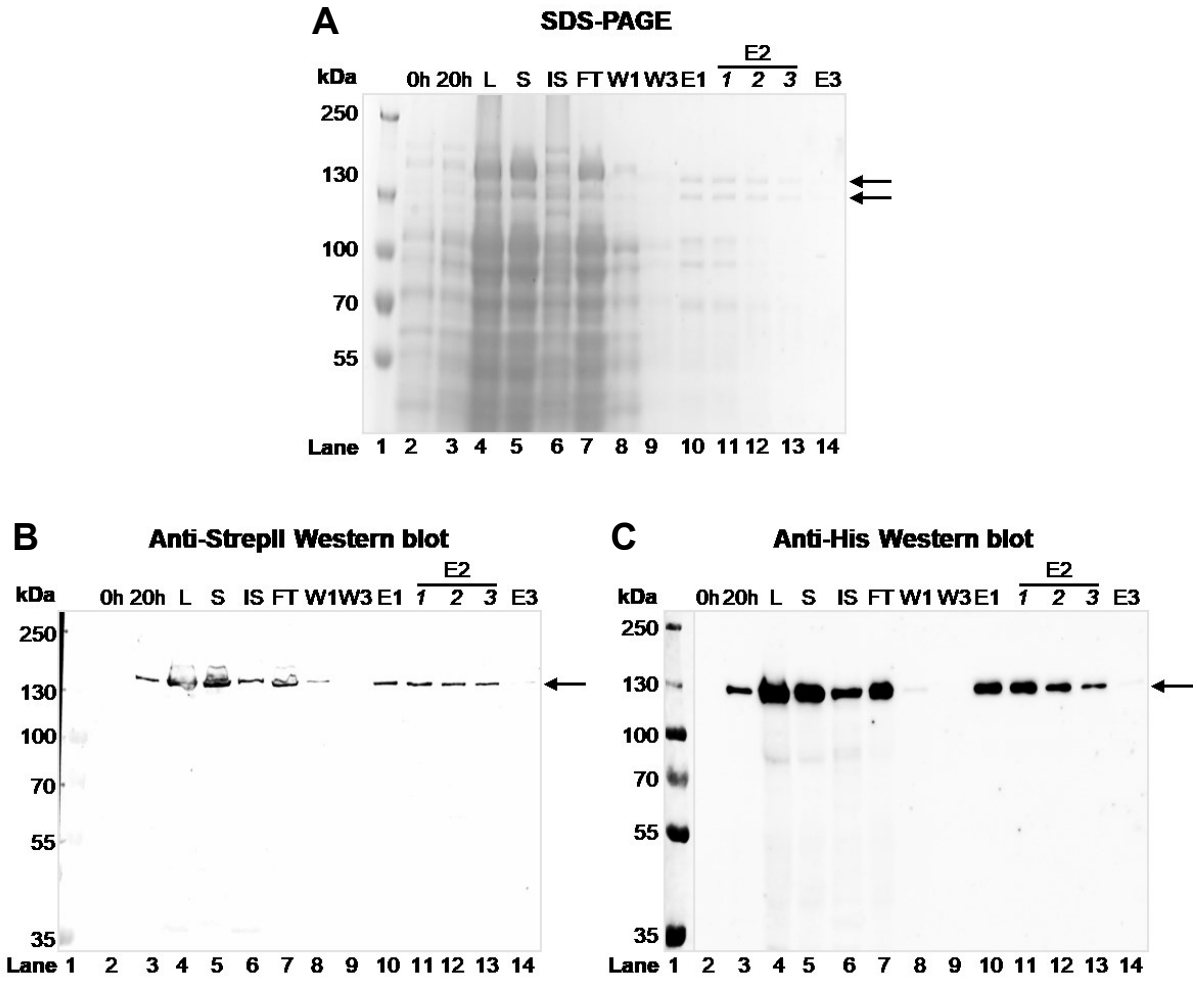

Figure 5.13. RexAB purification via nickel affinity chomatography.

Analysis of RexAB purification by SDS-PAGE **(A)**, anti-StrepII Western blot **(B)** and anti-His Western blot **(C)**. Expression was carried out in *E. coli* soluBL21 (DE3) cells at 16 °C for 20 h, induced by the addition of 1 mM IPTG. Protein bands for StrepII-RexA (144 kDa) and His-RexB (138 kDa) are indicated by the arrows. The molecular weight of the marker bands in kDa are indicated. 0h = uninduced; 20 h post induction; S = soluble fraction; IS = insoluble fraction; FT = flow though; W = wash; E1-3 = stepwise elution at 100 mM, 200 mM and 300 mM imidazole, respectively.

Although the expression conditions of RexAB had been optimised to growth of *E. coli* soluBL21 (DE3) in LB at 16 °C for 20 h, a shortage of incubator space at 16 °C meant that further testing was carried out to determine whether RexAB expression was possible at 20 °C. In addition, Terrific broth (TB) was tested in comparison with LB to account for the reduced expression of RexAB at higher temperatures. TB is a highly enriched medium designed to improve purification yields of plasmid DNA or recombinant proteins from *E. coli* strains. It contains increased concentrations of peptone, yeast extract and glycerol as a carbon source, and a phosphate buffer solution that slows down the acidification of culture broth at high bacterial concentrations. This supports higher cell densities and a longer period of exponential growth compared to LB[578].

Expression of RexAB in TB at 20 °C was comparable to that in LB at 16 °C when analysed by SDS-PAGE (lanes 13 and 3 respectively; Figure 5.14A). In addition, both RexA and RexB proteins remain soluble at 20 °C as indicated by the corresponding Western blots, though the protein band for soluble RexB does appear to be stronger in LB at 16 °C (lanes 4 and 14 for LB at 16 °C and TB at 20 °C, respectively; Figure 5.14B, C). Nevertheless, expression of RexAB in TB at 20 °C was possible. Therefore, protein expression would be performed in *E. coli* soluBL21 (DE3) cells at 20 °C for 20 h, induced by the addition of 1 mM IPTG.

To summarise, it was found that the RexAB protein needed to be purified as a complex because neither RexA nor RexB were very stable as individual subunits (due to degradation or insolubilty, respectively). Furthermore, purification was not possible via Strep-Tactin affinity chomatography, possibly due to the StrepII tag being hidden by protein folding, but purification was possible via nickel affinity chomatography. Optimised expression conditions for RexAB was determined to be with *E. coli* soluBL21 (DE3) in TB at 20 °C for 20 h, induced by the addition of 1 mM IPTG.

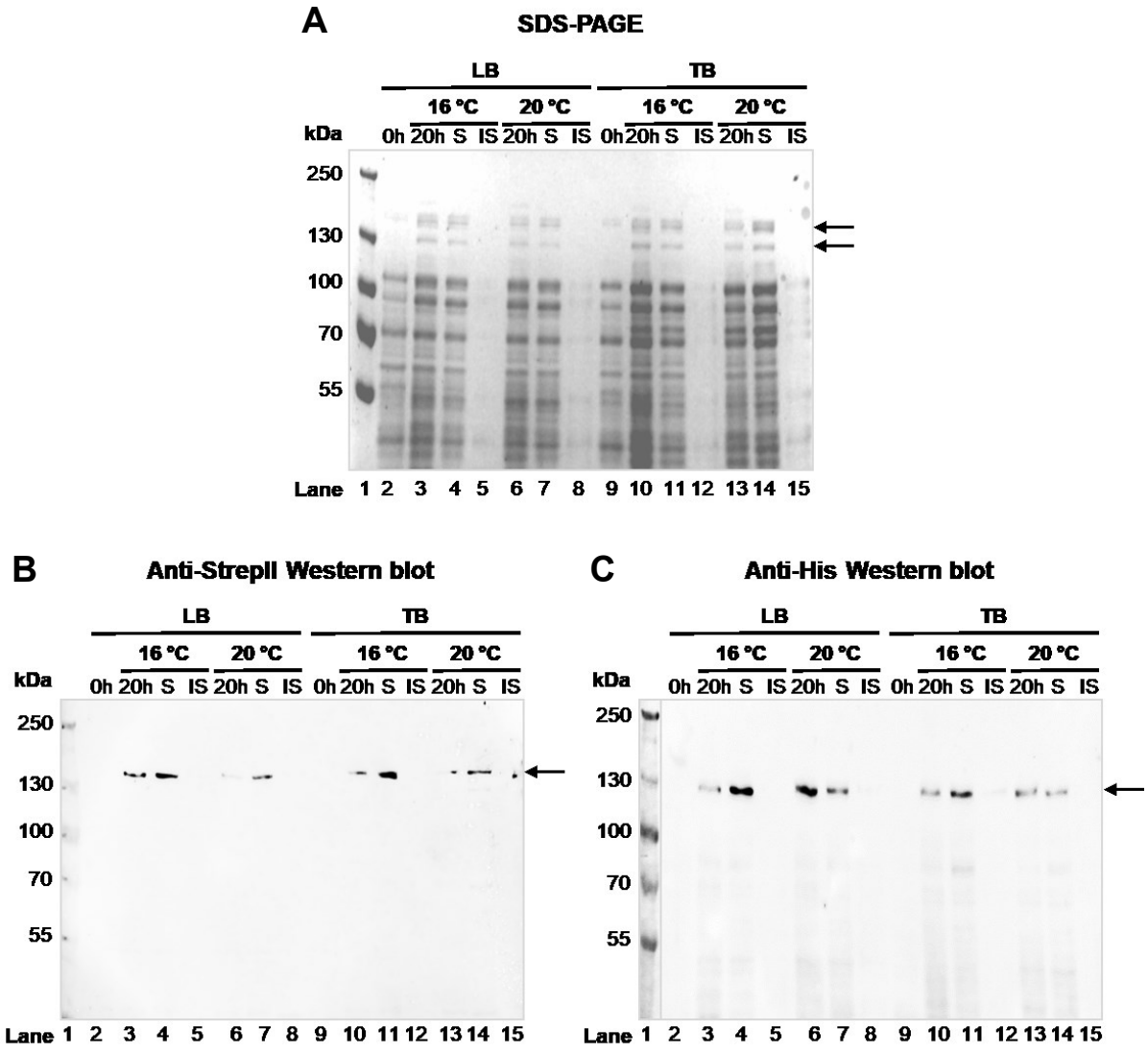

Figure 5.14. Comparison of RexAB expression in LB and TB at 16 °C and 20 °C.

RexAB expression from *E. coli* soluBL21 (DE3) cells grown in Lysogeny broth (LB) or Terrific broth (TB) at 16 °C or 20 °C, analysed by SDS-PAGE **(A)**, anti-StrepII Western blot **(B)** and anti-His Western blot **(C)**. Expression was induced by the addition of 1 mM IPTG. Protein bands for StrepII-RexA (144 kDa) and His-RexB (138 kDa) are indicated by the arrows. The molecular weight of the marker bands in kDa are indicated. 0h = uninduced; 20h = 20 h post induction; S = soluble fraction; IS = insoluble fraction.

5.3.3 Final expression and purification of RexAB

Expression of RexAB was performed with *E. coli* soluBL21 (DE3) cells grown in TB at 20 °C for 20 h, induced by the addition of 1 mM IPTG, followed by purification of the recombinant protein as a complex via nickel affinity chomatography. Whilst bacterial culture volumes of 1 L were used during the optimisation process, 4 L of culture was used in the final expression to produce a larger quantity of purified protein.

After expression at 20 °C for 20 h, protein bands corresponding to RexA and RexB appeared in the appropriate Western blots (lane 3; Figure 5.15B, C). RexAB was found predominantly in the soluble fraction (lane 5; Figure 5.15A), from which purification via nickel affinity chomatography was performed as described in section 0. All eluted fractions (lanes 10-14; Figure 5.15) were then concentrated and purified further using an Amicon 100 kDa cut-off filter, which removed imidazole and contaminants smaller than 100 kDa in size (lane 15; Figure 5.15). Finally, the purified protein was aliquoted and stored at -80 °C. Protein concentration was determined via BCA protein assay.

Although a 100 kDa cut-off filter was used to remove all lower molecular weight degradation products, the purification process did lead to some additional degradation of the RexAB complex, particularly after elution (lane 15; Figure 5.15). The additional bands were found to contain either a His tag or a StrepII tag by Western blot, confirming that these were degradation products of the recombinant protein (lane 15; Figure 5.15B, C). In addition, it was noted that the protein complex began to precipitate whilst using the 100 kDa cut-off filter, so further handling of the protein was minimised by storing at 80 °C as quickly as possible. In summary, purification of the RexAB complex was successfully achieved, but susceptibility of the purified complex to degradation was an issue (discussed further in section 5.9). RexAB was purified to a final concentration of 7 μM of intact complex.

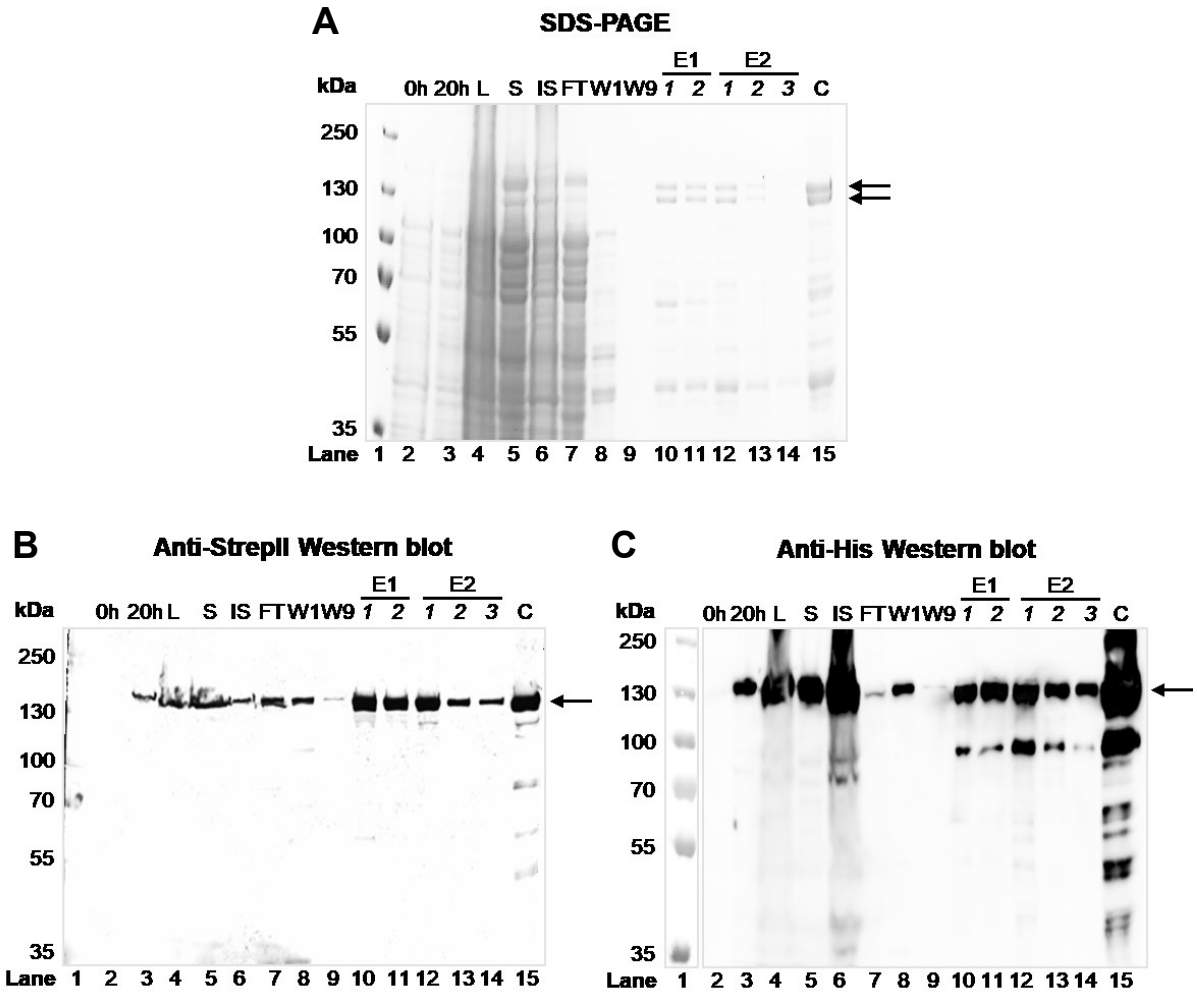

Figure 5.15. SDS-PAGE and Western blot analysis of RexAB purification via nickel affinity chomatography.

RexAB expression from *E. coli* soluBL21 (DE3) cells grown in TB at 20 °C for 20 h, analysed by SDS-PAGE **(A)**, anti-StrepII Western blot **(B)** and anti-His Western blot **(C)**. Expression was induced by the addition of 1 mM IPTG. Protein bands for StrepII-RexA (144 kDa) and His-RexB (138 kDa) are indicated by the arrows. The molecular weight of the marker bands in kDa are indicated. T0 = uninduced; T20 = 20 h post induction; L = cell lysate; S = soluble fraction; IS = insoluble fraction; FT = flow though; W = wash; E1, E2 = stepwise elution at 70 mM and 150 mM imidazole, respectively; C = concentrated using a 100 kDa cut-off filter.

5.4 *S. aureus* RexAB has nuclease activity

Members of the RecBCD/AddAB family process the ends of DSBs via their helicase and nuclease activities, both of which require energy from ATP hydrolysis[429]. To determine whether *S. aureus* RexAB had the functional properties of an AddAB protein complex, enzyme assays were performed to measure nuclease, helicase and ATPase activities using recombinant *S. aureus* RexAB.

To assess the presence of nuclease activity, RexAB was incubated in the presence of a dsDNA substrate at 37 °C for 2 h, with or without ATP. Reactions were performed under conditions of high free Mg^{2+} using a buffer containing 2 mM of magnesium acetate, which has been shown previously to activate nuclease activity in AddAB enzymes[560]. Since staphylococcal RexAB is predicted to recognise a seven-nucleotide Chi motif (5′-GAAGCGG-3′)[455], which then attenuates degradation of one DNA strand, Chi recognition was tested using dsDNA substrates in which the predicted Chi site was either present (Chi^+) or absent (Chi^0). Samples were taken over 2 h and analysed by agarose gel electrophoresis. Gels were stained with SYBR Safe to detect dsDNA and band intensity of the remaining dsDNA substrate was quantified. Values were normalised to the no-ATP control at the start of the incubation.

DNA was degraded over time in the presence of ATP for both Chi^0 and Chi^+ substrates (Figure 5.16). In the absence of ATP, degradation was minimal. This indicated that the recombinant protein complex displayed nuclease activity, and that this activity required ATP hydrolysis. Interestingly, DNA degradation was detected at the first time point (up to 27% for Chi^0 at 0 min; Figure 5.16A), indicating that nuclease activity occurs quickly after the addition of ATP, even during the time taken to stop the reaction (< 1 min).

To detect ssDNA fragments produced in the presence of the Chi^+ site, the experiment was also performed with the addition of SSB to stabilise ssDNA strands and the gel was stained with SYBR Green II to detect both dsDNA and ssDNA. However, no new bands were observed (data not shown), possibly due to the ssDNA-SSB product being too

faint to detect on the agarose gel, or that the size of the ssDNA-SSB complex was comparable to dsDNA substrate alone. Nevertheless, results showed that *S. aureus* RexAB was able to degrade dsDNA in the presence of ATP, demonstrating its function as a nuclease.

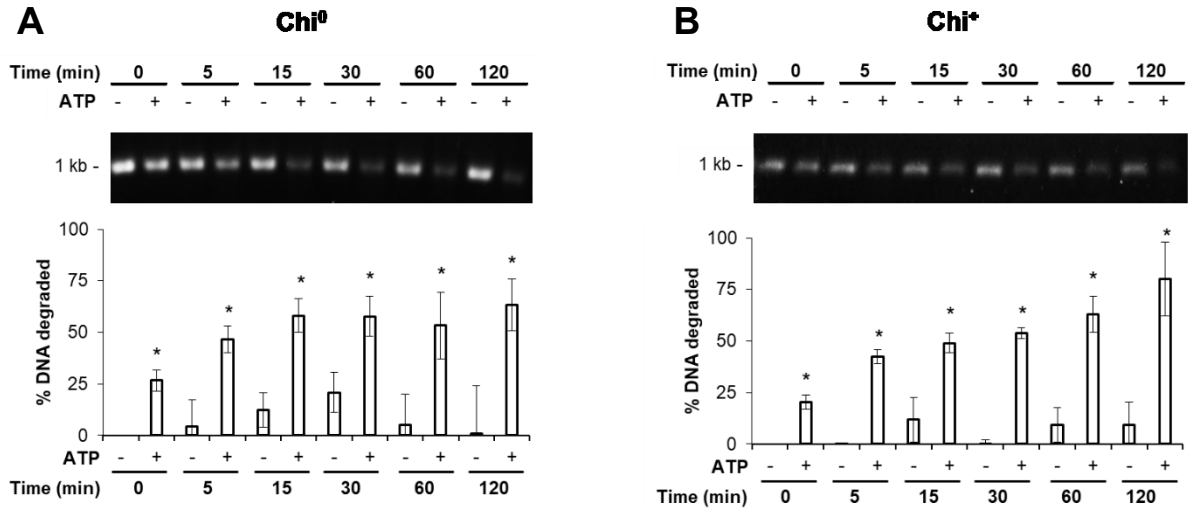

Figure 5.16. Degradation of dsDNA by the RexAB complex.

Nuclease activity was determined by incubating RexAB protein and DNA substrate Chi^0 **(A)** or Chi^+ **(B)** with or without ATP at 37 °C. Samples were taken over 2 h and analysed by agarose gel electrophoresis. Gels were stained using SYBR Safe to detect dsDNA. Band intensity of the DNA substrate was quantified. Graphs represent the mean of four independent experiments. Error bars indicate the standard deviation. *, $P < 0.05$ (two-way ANOVA with Sidak's test, compared to the corresponding ATP control).

5.5 *S. aureus* RexAB has helicase activity

To determine the presence of helicase activity, RexAB was incubated with the Chi^+ dsDNA substrate under conditions of low free Mg^{2+} (0.25 mM magnesium acetate), which suppressed nuclease activity and enabled measurement of DNA unwinding and ssDNA formation over time[560,568]. Reactions were performed with or without ATP, and SSB was included in the reaction mixture to bind and stabilise ssDNA products. Samples were taken over 2 h and analysed by agarose gel electrophoresis. Gels were stained with SYBR Green II to detect both dsDNA and ssDNA, and band intensities of remaining dsDNA substrate and ssDNA-SSB product were quantified. For dsDNA unwinding, values were normalised to the no-ATP control at the start of the incubation. For ssDNA formation, values were normalised to a ssDNA control, in which the dsDNA substrate was heat-denatured in the presence of SSB to provide the maximum possible band intensity for the ssDNA-SSB product.

In the presence of ATP, it was found that the dsDNA substrate was quickly unwound by recombinant RexAB (Figure 5.17A), and this was accompanied by an increase in the formation of ssDNA over time (Figure 5.17B). In addition, minimal DNA unwinding or ssDNA formation were detected in the absence of ATP, indicating that enzyme activity required energy from ATP hydrolysis (Figure 5.17A, B). These data suggest that recombinant staphylococcal RexAB displays helicase activity.

The presence of helicase activity was confirmed by performing the same assays without SSB. Since SSB is required to stabilise and prevent reannealing of ssDNA strands, detection of unwound dsDNA in the absence of SSB would indicate incomplete suppression of nuclease activity. However, neither dsDNA unwinding nor ssDNA formation were detected (Figure 5.17C, D), confirming that the assays measured helicase activity only and that *S. aureus* RexAB exhibits helicase activity.

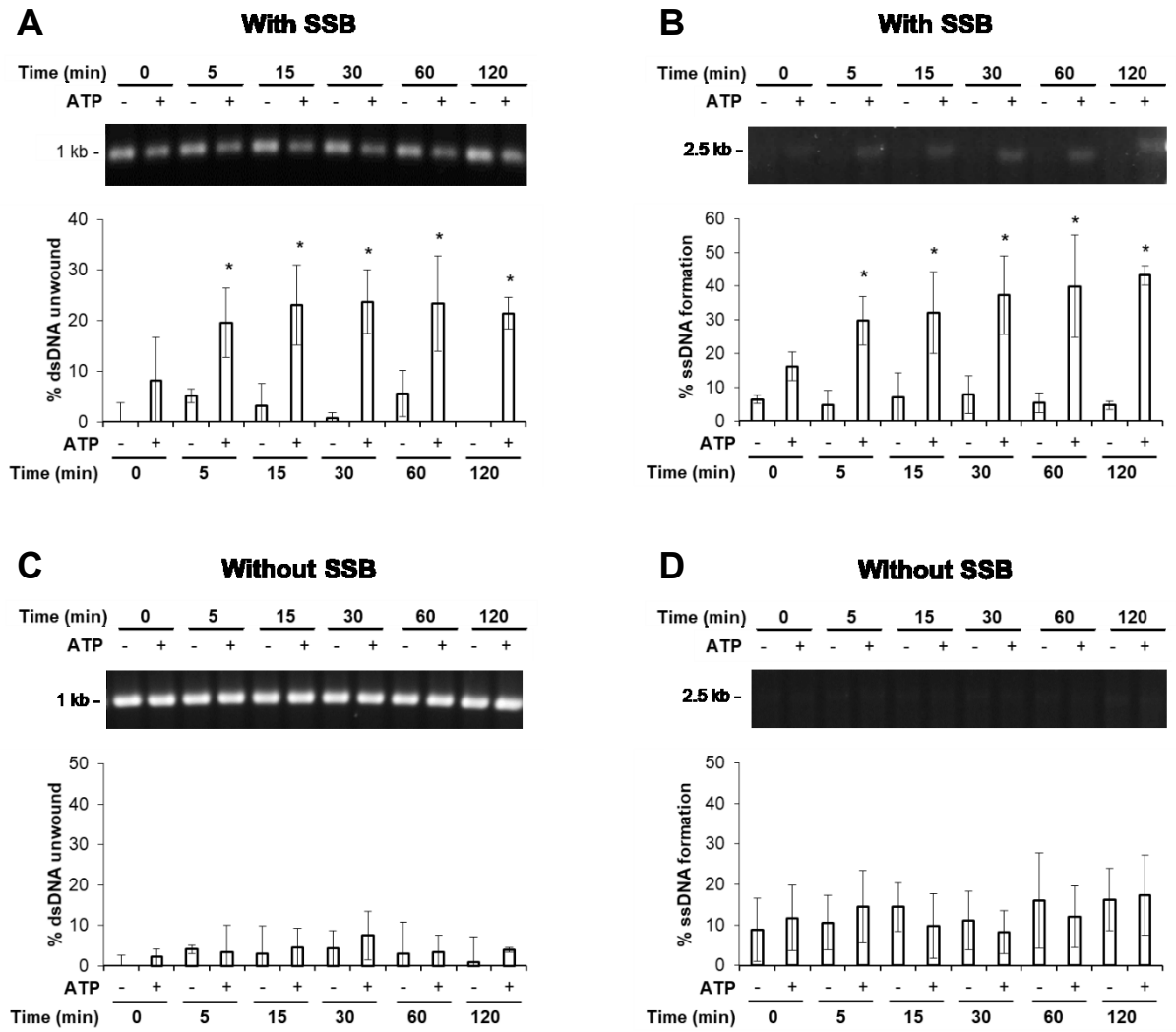

Figure 5.17. DNA unwinding and formation of ssDNA by the RexAB complex.

Helicase activity was determined by measuring unwinding of dsDNA **(A)** and formation of ssDNA **(B)** after RexAB protein and DNA substrate (Chi^+) were incubated with or without ATP at 37 °C. *E. coli* single-stranded DNA binding protein (SSB) was used to prevent reannealing of DNA. An equivalent assay was performed without SSB as a control **(C, D)**. Samples were taken over 2 h and analysed by agarose gel electrophoresis. Gels were stained using SYBR Green II to detect dsDNA and ssDNA. Band intensities of dsDNA substrate and ssDNA-SSB product were quantified. Graphs represent the mean of four independent experiments. Error bars indicate the standard deviation. *, $P < 0.05$ (two-way ANOVA with Sidak's test, compared to the corresponding ATP control).

5.6 *S. aureus* RexAB has ATPase activity

To determine the presence of ATPase activity, the release of P_i by RexAB during DNA degradation was measured over time. Recombinant RexAB was incubated with the dsDNA substrate with or without ATP, similar to the nuclease activity assay above (section 5.4), but no DTT was added in the assay buffer to prevent interference with the P_i detection reagent. Both Chi^0 and Chi^+ substrates were tested to determine whether presence of the Chi^+ site led to a change in the extent of ATP hydrolysis. P_i was measured using the Expedeon PiColorLock Gold Phosphate Detection System. This is a colorimetric technique based on a change in absorbance of malachite green when it reacts with P_i, which leads to the formation of a green P_i-dye complex. Samples were read at the wavelength 595 nm in a microplate reader, and the P_i concentration was determined using a standard curve of known P_i concentrations.

The concentration of P_i increased over time in the presence of recombinant RexAB, DNA substrate and ATP, indicating that ATP hydrolysis was taking place. The release of P_i was accompanied by DNA degradation, which was confirmed by agarose gel electrophoresis (data not shown). It was found that the presence of a Chi site in the DNA substrate led to decreased P_i release when compared to the Chi^0 substrate (610 μM vs. 651 μM; Figure 5.18), suggesting reduced DNA unwinding or degradation by RexAB. This aligns with the function of the Chi site, which leads to attenuated ATP-dependent nuclease activity on one DNA strand[554]. It was also noted that RexAB was able to hydrolyse ATP in the absence of DNA substrate, though at reduced levels. These results demonstrate that *S. aureus* RexAB displays ATPase activity.

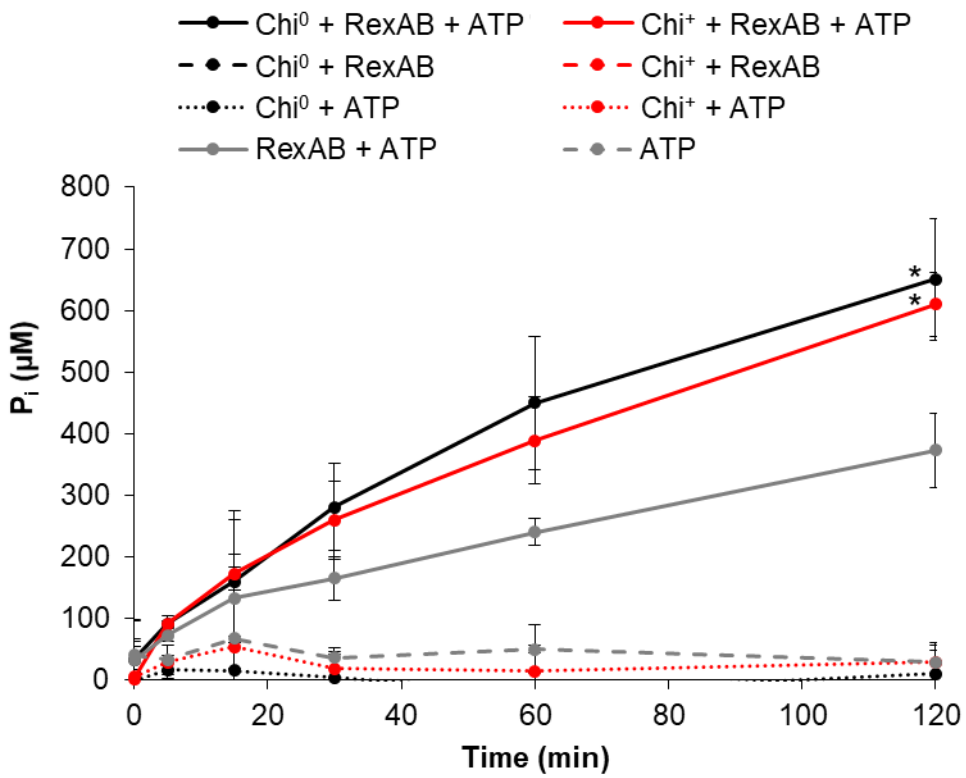

Figure 5.18. Hydrolysis of ATP by the RexAB complex.

ATPase activity was determined by incubating RexAB protein and DNA substrate (Chi^0 or Chi^+) with or without ATP at 37 °C. The concentration of inorganic phosphate (P_i) in the samples was quantified over 2 h using the Expedeon PiColorLock Gold Phosphate Detection System assay kit and use of a standard curve. Graph represents the mean of four independent experiments. Error bars indicate the standard deviation. *, $P < 0.05$ (two-way ANOVA with Dunnett's test, "Chi^0 + RexAB + ATP" and "Chi^+ + RexAB + ATP" compared to the "RexAB + ATP" control).

5.7 *S. aureus* RexAB is required for SOS induction

AddAB enzymes process the ends of DSBs to create a 3' ssDNA overhang, which the RecA protein then binds to enable recombinational DNA repair[429]. Activation of RecA also leads to expression of the SOS regulon[445,467]. As a result, AddAB proteins are required for successful induction of SOS. To confirm that RexAB was a functional AddAB family member, the role of *S. aureus* RexAB in triggering the SOS response was determined by comparing levels of SOS induction between wild-type and *rexAB* mutant strains.

To measure SOS induction, the *PrecA-gfp* reporter construct from section 3.2 was employed. This construct generates a fluorescent signal in response to DNA damage, which is based on the expression of *recA*, one of the 16 genes of the *S. aureus* SOS regulon[318]. The construct was transformed into the JE2 *rexB*:Tn mutant and successful transformation was confirmed via colony PCR (Figure 5.19A). The empty vector was also transformed into the mutant as a control strain. Transformation of the *PrecA-gfp* construct was also attempted in the SH1000 *rexB*::Tn mutant, but this was unsuccessful. Growth curves of JE2 *rexB*::Tn pCN34 *PrecA-gfp* and JE2 *rexB*::Tn containing the empty pCN34 vector showed that the presence of the *PrecA-gfp* reporter construct did not affect growth (Figure 5.19B). To confirm that the empty vector did not lead to fluoresence in the mutant, JE2 *rexB*::Tn pCN34 was exposed to a range of ciprofloxacin concentrations and the GFP signal was monitored over 17 h. Ciprofloxacin is a well-characterised DNA-damaging antibiotic known to trigger the SOS response[318], and was used in section 3.2 to confirm the functionality of the *PrecA-gfp* reporter. As shown in Figure 5.19C, no GFP signal was detected in the JE2 *rexAB* mutant containing empty pCN34, demonstrating that the *PrecA-gfp* reporter construct was required for fluorescence.

Finally, wild-type and *rexB*::Tn strains containing the *PrecA-gfp* reporter were exposed to a number of DNA damaging agents and SOS induction was measured. Exposure to ciprofloxacin led to a dose-dependent induction of the SOS response in wild-type JE2, reflected by the peak at 4-5 h (Figure 5.20), which confirmed previous results (section 3.2)[318].

However, no SOS induction was observed in the *rexAB* mutant. This was also observed with the DNA-damaging antibiotic mitomycin C (Figure 5.20), indicating that RexAB is required for triggering SOS in response to these antibiotics.

Exposure to H_2O_2 did not induce SOS in either the wild type or mutant strains (Figure 5.20). This was likely due to the high inoculum used in these assays when compared to the H_2O_2 survival assays performed in section 3.7 (10^{-1} vs. 10^{-4} dilution of overnight bacterial cultures). Since *S. aureus* produces catalase, the high numbers of bacteria used in this reporter assay would have led to H_2O_2 being degraded before DNA damage could occur, which was supported by the observation of air bubbles forming during assay preparation. Therefore, the effect of ROS on SOS induction was tested using paraquat, which generates superoxide radicals[488]. As shown in Figure 5.20, exposure to paraquat triggered the SOS response in the wild type but not in the *rexAB* mutant, indicating that RexAB is required for the induction of SOS in response to ROS-mediated DNA damage. Taken together, these results show that RexAB is required for triggering the SOS response in *S. aureus*.

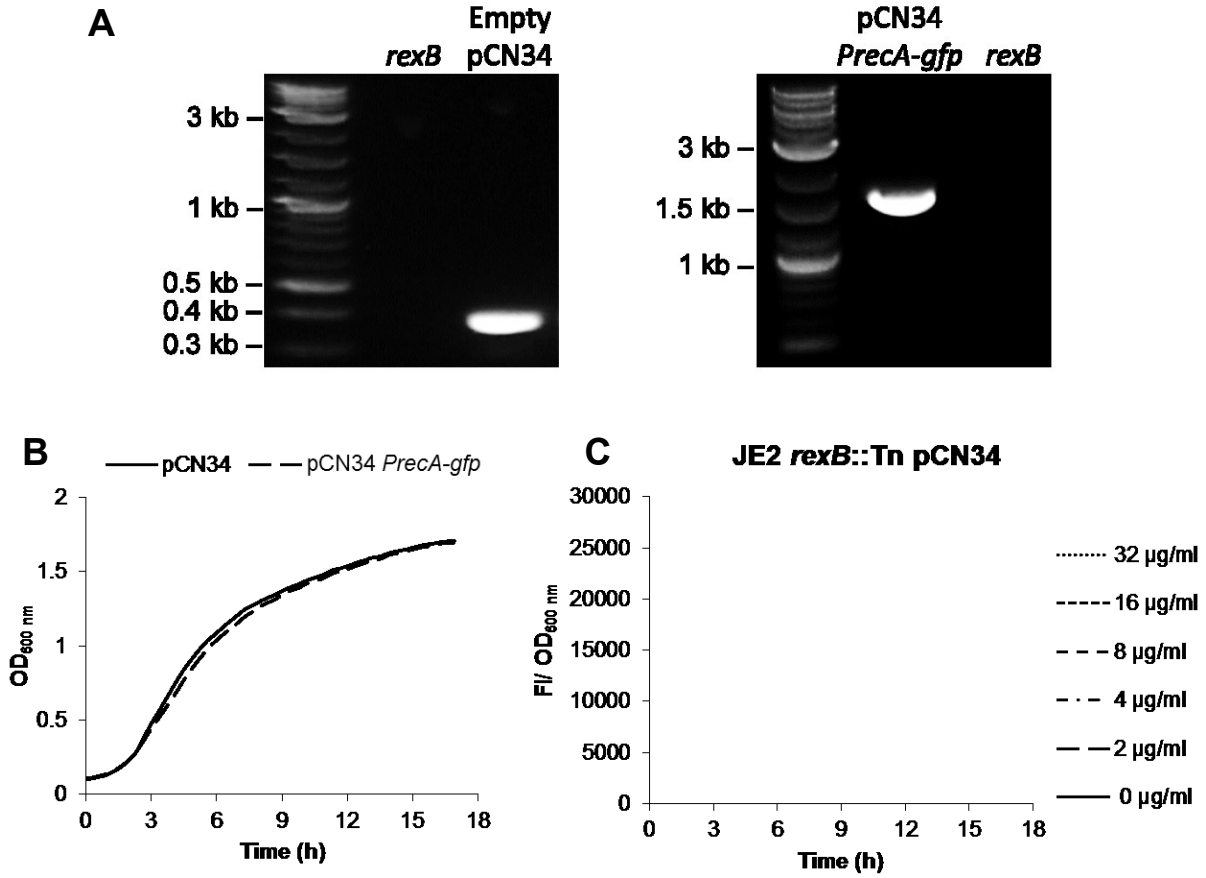

Figure 5.19. Transformation of empty pCN34 or pCN34 *PrecA-gfp* into the *S. aureus* JE2 *rexB*::Tn mutant.

Colony PCR was used to amplify DNA from JE2 *rexB*::Tn (*rexB*), *rexB*::Tn pCN34 (empty pCN34) and *rexB*::Tn pCN34 *PrecA-gfp* (pCN34 *PrecA-gfp*) to confirm successful transformation, using “pCN34 seq F” and “pCN34 seq R" primers **(A)**. PCR products were analysed on a 1% agarose gel next to 2-log DNA ladder (NEB) to confirm the presence of empty pCN34 (PCR product size of 377 bp) or pCN34 *PrecA-gfp* (1663 bp). Growth of JE2 *rexB*::Tn pCN34 and *rexB*::Tn pCN34 *PrecA-gfp* was assessed by taking $OD_{600\ nm}$ readings every 30 min for 17 h **(B)**. *S. aureus* JE2 *rexB*::Tn pCN34 was exposed to a range of ciprofloxacin concentrations and *recA* expression was measured over 17 h to confirm that the empty vector did not lead to fluoresence in the mutant **(C)**. Expression is shown relative to cell density ($FI/OD_{600\ nm}$) over time. Graphs represent the mean of three biological replicates with error bars omitted for clarification.

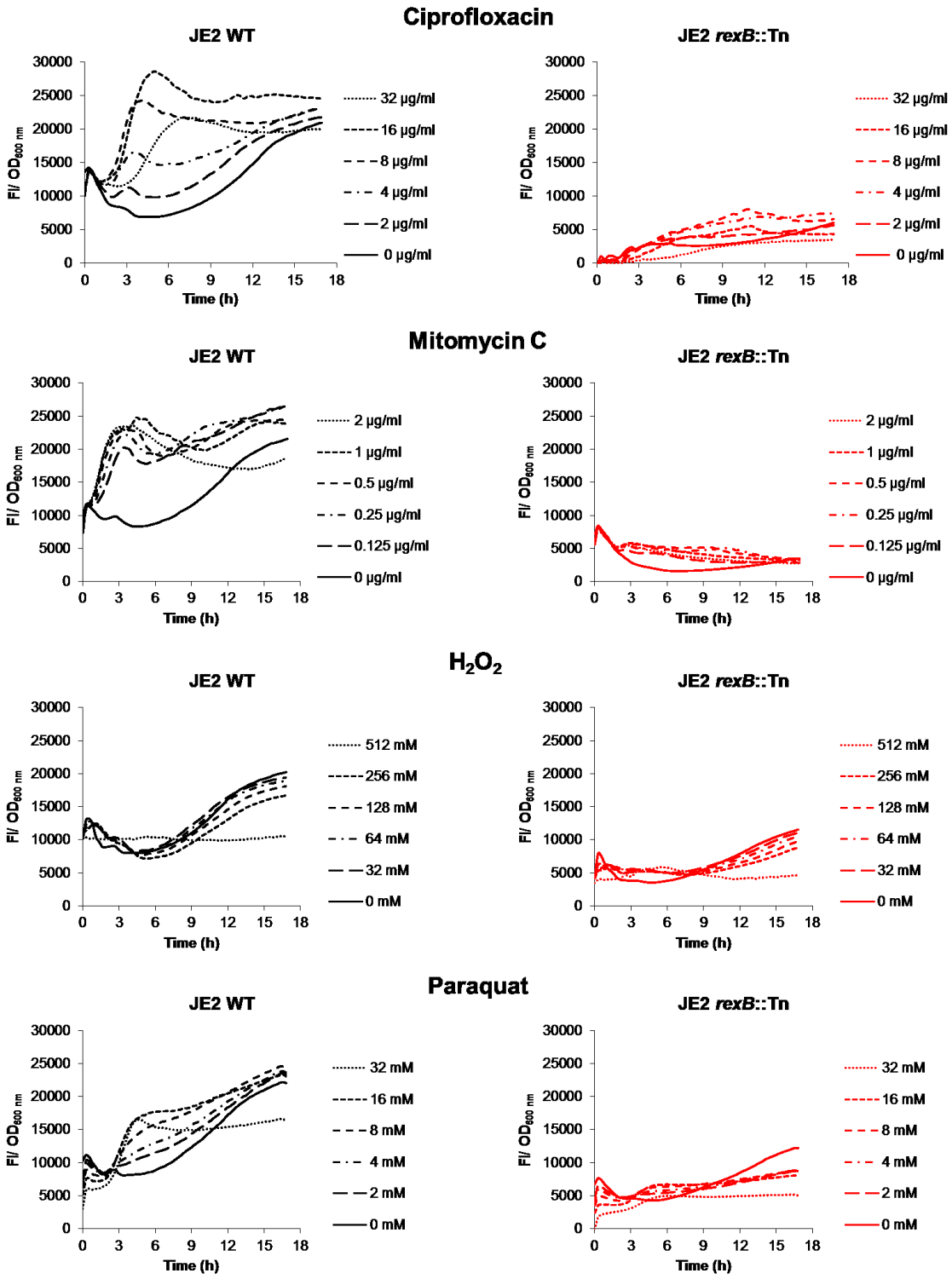

Figure 5.20. RexAB is required for induction of the SOS response.

S. aureus JE2 wild type and *rexB*::Tn mutant containing the pCN34 *PrecA-gfp* reporter plasmid were exposed to a range of concentrations of ciprofloxacin, mitomycin C, H_2O_2 and paraquat, and *recA* expression was measured over 17 h. Expression is shown relative to cell density ($Fl/OD_{600\ nm}$) over time. Graphs represent the mean of three biological replicates with error bars omitted for clarification.

5.8 Expressing *S. aureus* RexAB in an *E. coli recB* mutant

RecBCD and AddAB are multisubunit enzymes that process DSB ends to initiate recombinational repair. These complexes use different combinations of helicase and nuclease activities to process dsDNA ends, but both enzymes result in the production of a 3′ ssDNA overhang coated in RecA protein[429]. Previous studies have shown that *B. subtilis* AddAB is able to restore helicase and nuclease activities in an *E. coli recBCD* deletion mutant[579]. Therefore, to establish whether *S. aureus* RexAB could compensate for loss of RecBCD function in *E. coli*, the pET28b$^+$ *rexA, rexB* and *rexAB* expression plasmids from section 5.3.1 were transformed into an *E. coli recB* deletion mutant, and the ciprofloxacin MIC was determined for each strain. Although helicase activity in RecBCD is performed by both RecB and RecD subunits, only RecB has nuclease and ATPase activities[429,580]. Therefore, mutations in *recB* result in recombination deficiency and sensitivity to DNA-damaging agents due to loss of RecBCD function[580–583]. The *recB* mutant was obtained from the Keio Knockout Collection in the BW25113 background, which is an *E. coli* K-12 derivative. As this strain did not encode for the T7 RNA polymerase required for expression from pET plasmids, the mutant was lysogenised with λDE3. This enabled the cloned genes to be expressed from the T7 promoter of the pET28b$^+$ vector, via induction by IPTG. Successful transformation of pET28b$^+$ *rexA, rexB* and *rexAB* into *E. coli ΔrecB* was confirmed by PCR.

As expected, the *E. coli recB* mutant was significantly more sensitive to ciprofloxacin than the wild type, with a 53-fold reduction in the MIC value (Figure 5.21A), confirming that RecBCD is required for DNA DSB repair. The MIC remained the same after integration of the λDE3 prophage, which showed that the λDE3 prophage had no effect on ciprofloxacin-mediated DNA damage. However, when *ΔrecB* strains containing pET28b$^+$ *rexA, rexB* and *rexAB* were exposed to ciprofloxacin, they behaved similarly to the *recB* mutant (Figure 5.21A). This suggested that helicase and nuclease activities in *ΔrecB* were not restored. Since this could be a result of RexAB not being expressed in *E. coli*, rather than *S. aureus* RexAB not compensating for RecBCD function, SDS-PAGE and Western blot

analyses were performed to detect the expression of RexA, RexB, and RexAB. Samples were prepared from cultures induced with 1 mM IPTG and grown overnight at 37 °C. Neither RexA nor RexB were detected in whole cell lysates prepared from induced *ΔrecB* strains (Figure 5.21B, C), indicating that these proteins were not being expressed from the pET28b^{+} plasmids in BW25113 (DE3). Expression was also attempted using the optimised expression conditions described in section 5.3.2, but no difference was observed (data not shown). These results show that expression of *S. aureus* RexAB in *E. coli* is difficult, but do not rule out the possibility that *S. aureus* RexAB can compensate for RecBCD function. Nevertheless, loss of RecB strongly sensitises *E. coli* to ciprofloxacin-mediated DNA damage.

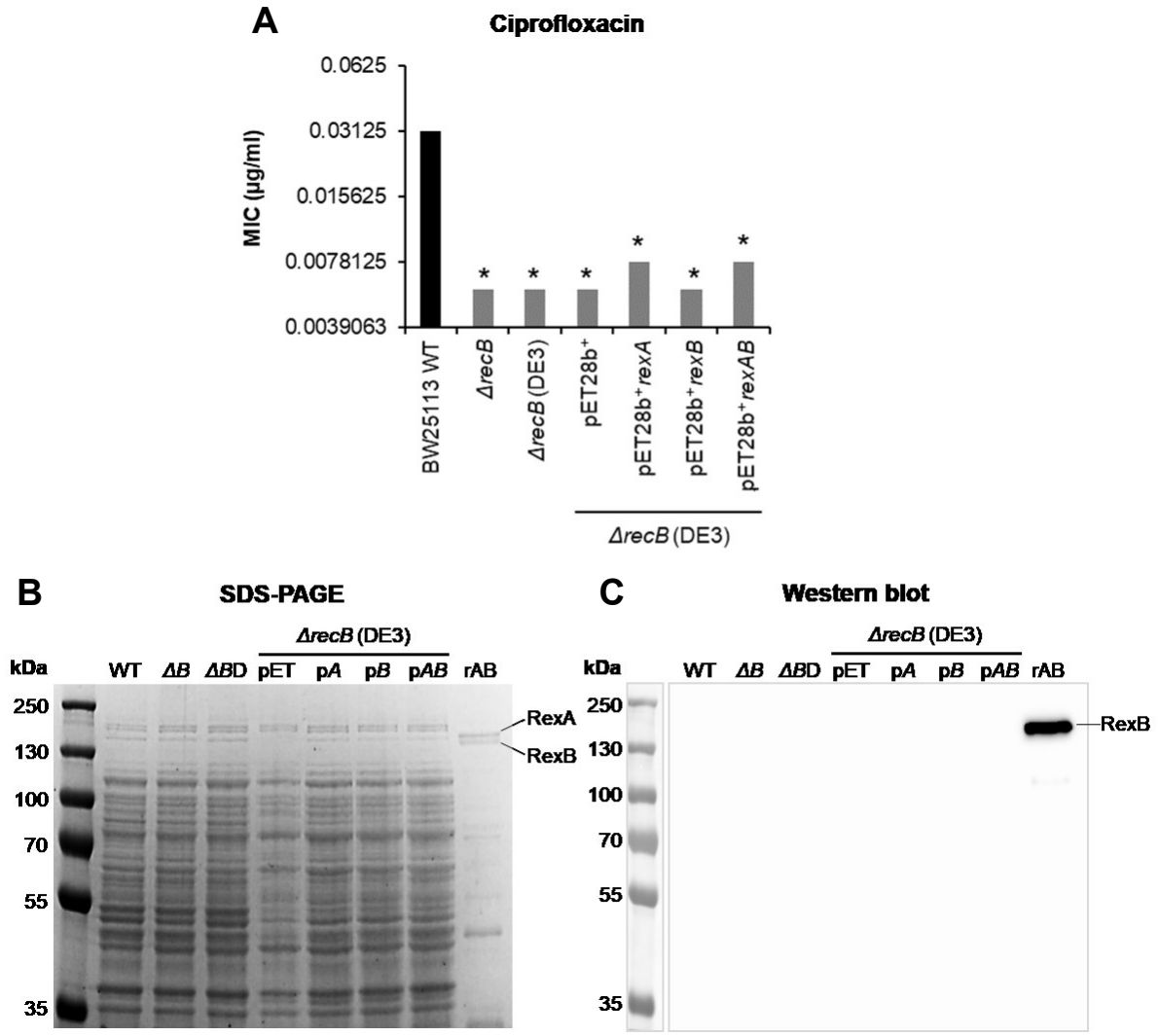

Figure 5.21. *S. aureus* RexAB could not be expressed in an *E. coli recB* mutant.

The MIC of ciprofloxacin was determined for *E. coli* BW25113 wild type, *ΔrecB*, *ΔrecB* (DE3) and complemented strains using the serial broth dilution method **(A)**. The MIC was defined as the lowest concentration at which no growth was observed after static incubation at 37 °C for 17 h. Graph represents the median of thee independent experiments. *E. coli* whole cell lysates were analysed by SDS-PAGE **(B)** and anti-His Western blot **(C)**. Expression from pET28b$^+$ *rexA* and *rexB* would produce His-RexA (145 kDa) or His-RexB (138 kDa), respectively. Expression from pET28b$^+$ *rexAB* would produce StrepII-RexA (145 kDa) and His-RexB (138 kDa). Recombinant RexA and RexB are indicated. Molecular weight of marker bands are indicated in kDa. WT = wild type, *ΔB* = *recB* mutant, *ΔB*D = *recB* mutant containing DE3, pET = *recB* (DE3) pET28b$^+$, p*A* = *recB* (DE3) pET28b$^+$ *rexA*, p*B* = *recB* (DE3) pET28b$^+$ *rexB*, p*AB* = *recB* (DE3) pET28b$^+$ *rexAB*, rAB = recombinant RexAB. Strains containing pET28b$^+$ plasmids were induced by the addition of 1 mM IPTG. *, $P < 0.05$ (one-way ANOVA with Dunnett's test, compared to the corresponding wild type).

5.9 Discussion

In bacteria, processing of DSBs for DNA repair is carried out by the RecBCD/AddAB family of helicase-nuclease enzymes. *S. aureus* RexAB was proposed to be an AddAB family member based on sequence alignments in other studies[426,427], but this had not yet been confirmed by experimental evidence. Results from this chapter confirm the presence of AddAB enzyme motifs in *S. aureus* RexAB and its sequential and structural homology to *B. subtilis* AddAB, as well as providing experimental evidence supporting this complex as an AddAB family member.

Direct homologues of *B. subtilis* AddAB, which is the most well-studied AddAB family member, have been identified in at least 12 different bacterial species, including *Lactococcus lactis, Clostridium acetobutylicum*, *Clostridium difficile, E. faecalis, S. aureus* and several streptococcal species[426,427,491]. Sequence alignments were performed with *S. aureus* RexAB, *B. subtilis* AddAB and a selection of AddAB proteins from other species to confirm *S. aureus* RexAB sequence similarity to AddAB family members. Results showed that functional AddAB enzyme motifs were conserved across the species analysed. In addition, structural modelling of the *S. aureus* RexAB subunits and superimposition with *B. subtilis* AddA and AddB crystal structures showed good structural alignment between the two proteins. This confirmed previous reports that *S. aureus* RexAB is likely an AddAB family member based on sequence homology[426,427].

Although functional AddAB motifs were conserved, it was found that AddA and AddB subunits displayed low sequence homology across the full-length of the proteins (~20-50% sequence identity). This was also reported by Chedin *et al.* (2002), in which AddB subunits shared only 25-40% sequence identity[491]. In contrast, other conserved proteins such as RecA show higher sequence homology, with up to 98% sequence similarity at the amino acid level for RecA (from 62 bacterial species)[584]. Furthermore, despite *addA* and *addB* closely co-occuring in most genomes, the *addB* gene of *B. subtilis* shows low similarity to those in proteobacteria (less than 25% identity on a global alignment)[426]. This indicates that unlike

other conserved proteins that may share sequence homology for the full-length of the protein, only the functional domains are conserved in AddAB enzymes[463,491,573].

S. aureus RexAB was expressed to satisfactory levels in *E. coli*, but there was difficulty in purification of the complex, which led to some degradation of the intact protein. Since the protein complex is 276 kDa in size, a centrifugal filter was used to remove fragments that were ≤100 kDa from the samples, but this was not entirely successful. Nevertheless, the objective of protein expression and purification was to enable characterisation of the RexAB complex via direct testing of enzyme activity. Therefore, it was required that enough of the intact (and presumed functioning) protein was purified to enable testing of enzyme activity, which was achieved. The issue of degradation could be addressed in future purifications with size-exclusion chomatography or the inclusion of protease inhibitors. There is ample reason to believe that RexAB is a helicase-nuclease (see section 5.1), but to provide additional confirmation that the bands were not contaminating proteins from the *E. coli* host, a control experiment with the same strain transformed with an empty vector should reveal any *E. coli* proteins that bind to the column. Eluted fractions could also be tested for enzyme activity, which should be present in samples purified from pET28b$^+$ *rexAB*-containing cells, but not from cells containing the empty vector[585].

In this chapter, *S. aureus* RexAB was shown to display enzyme activities that correspond to function as an AddAB protein. Experiments were performed using well-established assays for measuring AddAB nuclease, helicase or ATPase activities[560,577], adapted to enable testing of the enzyme without requiring radioactive labelling of DNA. Nuclease, helicase and ATPase activities were all present in *S. aureus* RexAB, providing strong evidence that this complex is a member of the AddAB family. Interestingly, ATPase activity was detected at low levels in *S. aureus* RexAB even in the absence of DNA substrate, differing from the DNA-dependent ATP hydrolysis reported in *B. subtilis* AddAB[585,586]. Nevertheless, RexAB enzyme activity was shown to occur very quickly after the start of the reaction (< 1 min), which is consistent with the report that end-processing activity occurred within the first 30 s in *B. subtilis* AddAB[560].

In *S. aureus* RexAB, the seven-nucleotide motif 5'-GAAGCGG-3' was shown previously to confer Chi activity of the complex in a cell-based screening assay[455]. To confirm the *S. aureus* Chi motif by direct enzyme testing, nuclease assays were performed using a 1 kb DNA substrate containing the motif in the middle of the sequence, which would be expected to produce a 500-bp ssDNA fragment after Chi recognition. However, Chi activity of RexAB was not detected, possibly due to low concentrations of ssDNA-SSB product in the agarose gel. To improve sensitivity in these assays, a fluorescent dsDNA-binding dye (Quantifluor) was used to detect dsDNA instead of SYBR Safe, but it was found that RexAB interfered with fluorescence and a reliable reading could not be obtained. Nevertheless, a fluorescent dsDNA-binding dye (Hoechst 33258) has been used previously to detect helicase activity in *B. subtilis* AddAB[577]. Future experiments could optimise detection of Chi activity by using Hoechst 33258 DNA dye, or by using DNA polyacrylamide gel electrophoresis, which provides better separation of smaller (< 1000 bp) DNA fragments[587].

RecBCD/AddAB family members process the ends of DNA DSBs for repair via the RecA protein[429]. Since activation of RecA is required for triggering the SOS response[588], RecBCD/AddAB enzymes are necessary for DSB-mediated SOS induction[589–592], which was confirmed in this chapter for *S. aureus* RexAB. The SOS response was induced in wild-type *S. aureus* by the DNA-damaging agents ciprofloxacin, mitomycin C and paraquat, which is in keeping with previous reports[318,588]. It was noted that low levels of *recA* expression were detected in all strains at the beginning of the assays. Since this small initial peak was not dose-dependent and was also observed in the *rexAB* mutant, it most likely corresponded to basal *recA* expression.

Although the ability of *S. aureus* RexAB to restore *E. coli* RecBCD activity could not be determined due to difficulties with expressing the complex in the *E. coli* BW25113 strain, *addAB* genes from *B. subtilis* have been shown to be fully functional in *E. coli*[579]. Kooistra *et al.* (1993) found that the *B. subtilis addAB* genes restored ATP-dependent nuclease and helicase activities in an *E. coli recBCD* mutant, in addition to cell viability, recombination ability and the ability to repair UV-damaged DNA[579]. Resistance to UV damage has also been shown

in *E. coli recBCD* mutants complemented with the *rexAB* genes from *Lactococcus lactis*[573]. However, individual subunits from *B. subtilis* AddAB are not able to form functional hybrids with those from *E. coli* RecBCD[579], which highlights the large structural differences between these complexes despite similarities in function. It is possible that the difficulties with protein expression in the *E. coli recB* mutant were due to use of a high-copy number plasmid, which may have led to small deletions in the insert and resulted in loss of expression and/or nuclease activity, as observed by Kooistra *et al.* (1993). In addition, *E. coli* BW25113 is not optimised for the expression of staphylococcal proteins, which may use codons that are rarely present in *E. coli*. Future experiments could improve expression by transforming the pRARE plasmid into BW25113 (DE3) to provide several tRNAs that are rare in *E. coli*[593], and/or cloning the *S. aureus rexAB* genes into a low-copy number plasmid such as pGV1[579].

To summarise, *S. aureus* RexAB is a functional member of the AddAB enzyme family. This was confirmed though directly testing the nuclease, helicase and ATPase activities of purified *S. aureus* RexAB. In addition, it was shown that *S. aureus* RexAB is required for SOS induction in response to antibiotic- and ROS-mediated DNA damage. The highly-conserved nature of AddAB enzymes and their importance in bacterial survival of host defences make them a good candidate target for novel therapeutics, and the next chapter will examine potential small-molecule inhibitors of *S. aureus* RexAB.

6 Assessment of putative small-molecule inhibitors of RexAB

6.1 Introduction

With the rise in incidence and prevalence of antibiotic-resistant strains, *S. aureus* infections have become a significant clinical and financial burden worldwide[59]. HA-MRSA strains account for over 40% of hospital-acquired infections due to antibiotic-resistant bacteria per year[65] and contribute to increased mortality, morbidity and greater healthcare costs[594]. In addition, CA-MRSA strains are capable of infecting healthy individuals and have become prevalent in community settings in North America[68,69]. Therefore, new approaches are required for the prevention and treatment of these infections.

One approach is to increase the sensitivity of *S. aureus* to host defences. Previous chapters have shown that DNA repair via RexAB plays an essential role in protecting *S. aureus* from the neutrophil oxidative burst, as well as being critical for survival in the presence of the quinolone antibiotic ciprofloxacin. This makes the complex a promising target for new therapeutics. Inhibition of RexAB would promote immune clearance of *S. aureus* in the host and enhance the action of DNA-damaging antibiotics. This could help prolong the clinical lifespan of these antibiotics, by resensitising resistant strains and possibly preventing emergence of resistance in susceptible strains via antibiotic potentiation. If used alone, RexAB inhibitors would be expected to act only on pathogenic bacteria targeted by the immune response, meaning that the commensal gut microbiota would not be disturbed, unlike with conventional antibiotic therapy[595]. This would reduce susceptibility to opportunistic secondary infections caused by pathogens such as *C. difficile*[596].

Another advantage of targeting RexAB is that the mutagenic SOS response would be blocked. Induction of the SOS regulon leads to expression of the low-fidelity DNA polymerase UmuC (Pol V), which enables bypass of DNA lesions during DNA replication and results in an increased rate of mutagenesis[320,597]. By blocking this mutagenic pathway, host

adaptation and acquisition of resistance could be reduced[598]. In addition, *S. aureus* RexAB is a member of the conserved RecBCD/AddAB family of helicase-nucleases, which is present in over 90% of sequenced bacteria[537]. This means that inhibition of RexAB has potential as a broad-spectrum therapeutic approach. RexAB homologues are also not present in eukaryotes, which reduces the likelihood of host toxicity.

RecBCD/AddAB inhibitors have been previously reported in the literature. RecBCD inhibitors include dozelesin, ecteinascidin 743, hedamycin, cisplatin and psoralen, all of which inhibit enzyme function via DNA alkylation[599,600]. However, this mechanism of action makes them unselective and highly cytotoxic[601]. RecBCD activity is also inhibited by the Gam protein of bacteriophage lambda[602]. This inhibition is achieved though direct competition for the DNA-binding site and leads to enhanced fluoroquinolone sensitivity in *E. coli* and *Klebsiella pneumoniae*. However, Wilkinson *et al.* (2016) also found that Gam inhibition of RecBCD was only temporary and that the Gam protein displayed poor *in vivo* stability and oral bioavailability[602].

More promisingly, Amundsen *et al.* (2012) identified a number of potent inhibitors of *E. coli* RecBCD and *H. pylori* AddAB in a screen of 326,100 small molecules from the National Institutes of Health (NIH) molecular libraries sample collection[603]. Their screen employed a cell-based assay using phage infection as a marker for inhibition of RecBCD/AddAB activity, based on the observation that the *gene 2* protein of T4 phage protects viral DNA from RecBCD/AddAB-mediated degradation[604]. Inhibition of RecBCD or AddAB by an active compound promoted growth of the T4 *gene 2* mutant, leading to killing of bacteria. After testing twelve hits for inhibition of purified *E. coli* RecBCD and *H. pylori* AddAB enzyme activities, similar tests were performed on a further 40 compounds structurally related to the two most active molecules, which identified six more potent inhibitors[603]. Sixty compounds from the “iminobenzothiazoles” class, previously reported in a large-scale screen of DNA helicase inhibitors[605], were also tested for inhibition of RecBCD nuclease activity, which identified thee more active compounds. In total, 21 potent inhibitors were identified, from

which CID 1517823 was most active against *E. coli* RecBCD, and CID 697851 was most active against *H. pylori* AddAB[603].

In this chapter, a selection of the Amundsen *et al.* (2012) compounds was tested to determine whether these compounds inhibited the activity of *S. aureus* RexAB. Compounds were assessed on their effect on *S. aureus* growth using chequerboard MIC assays in combination with various DNA-damaging agents. In addition, analogues of the lead compound synthesised in collaboration with Professor Edward Tate (Department of Chemistry, Imperial College London) were assessed, and the lead compound and its derivatives were characterised to determine their effect on *S. aureus* survival when co-treated with ciprofloxacin or in whole human blood. Finally, compounds were tested for inhibition of purified *S. aureus* RexAB enzyme activity and induction of the SOS response.

Aim: To identify and characterise small-molecule inhibitors of *S. aureus* RexAB, by screening a panel of compounds for their ability to potentiate ciprofloxacin activity and then testing for inhibition of RexAB function.

6.2 CID 1517823 (C1) enhances the sensitivity of *S. aureus* to ciprofloxacin

In a previous study, Amundsen *et al.* (2012) screened over 300,000 small molecules for inhibitors of *E. coli* RecBCD and *H. pylori* AddAB[603]. To determine whether these compounds had a similar effect in *S. aureus*, 14 of the most effective inhibitors from the screen were tested on wild-type *S. aureus* SH1000 and JE2. Structures of these compounds are shown in Figure 6.1, grouped based on their scaffold type: pyrimidopyridones, cyanothiophenes, nitrofurans, nitrothiazole (one member) and iminobenzothiazoles[603].

Chequerboard MIC assays were performed to assess whether the compounds potentiated the activity of the DNA-damaging agents ciprofloxacin, mitomycin C or H_2O_2. Two-fold serial dilutions of both the compound and DNA-damaging agent were performed in 96-well plates, which enabled different concentrations of the compound to be assessed. The highest concentration of compound tested was 100 μM. The plates were incubated at 37 °C for 17 h under static conditions, and the MIC was defined as the lowest concentration at which no growth was observed. The fold change in MIC for each DNA-damaging agent was determined after addition of compound at a subinhibitory concentration (0.5x MIC).

In the absence of DNA-damaging agents, more than half of the 14 compounds were able to inhibit growth in either wild-type SH1000 or JE2 (Table 6.1). The majority of these compounds belonged to the pyrimidopyridone or nitrothiazole structural classes, with one exception each from the cyanothiophenes (CID 2295461) and nitrofurans (CID 774021). However, compound MIC could not be determined for 6 out of 14 compounds in SH1000 and for half of the compounds in JE2, because even the highest concentration tested did not affect bacterial growth (100 μM; Table 6.1).

Pyrimidopyridone compounds caused the largest increases in sensitivity of the *S. aureus* strains to ciprofloxacin, with up to an 8-fold reduction in the ciprofloxacin MIC for SH1000, when in the presence of CID 1517823 (Table 6.1). The structural class that caused the second largest increase in the sensitivity of *S. aureus* to ciprofloxacin was the nitrothiazole,

CID 2743870, which reduced the ciprofloxacin MIC by 4-fold in JE2 (Table 6.1). In the presence of mitomycin C, the same two structural classes of compounds caused the largest increases in antibiotic sensitivity. CID 1517823 caused a 4-fold reduction in the MIC of mitomycin C for SH1000 and JE2 (Table 6.1), and CID 2743870 reduced the MIC of mitomycin C by 4-fold in SH1000 and by 2-fold in JE2 (Table 6.1). By contrast, the most potent compound in the presence of H_2O_2 was the nitrofuran CID 774021, which reduced the MIC by 2.7-fold in SH1000 and by 4-fold in JE2 (Table 6.1). In the cases where compound MIC could not be determined, the MICs of the DNA-damaging agents remained the same and no synergy was observed.

Most intriguingly, chequerboard MIC assays identified one compound, CID 1517823 (hereafter referred to as Compound 1 or C1), that reduced the MIC of ciprofloxacin in SH1000 by 8-fold when the compound was added at half of its MIC (Figure 6.2A). In JE2, this decrease was 4-fold (Figure 6.2D), demonstrating that this compound sensitises an antibiotic-resistant *S. aureus* strain to ciprofloxacin. This was also observed with mitomycin C, with 4-fold reductions in the MIC for both SH1000 and JE2 in the presence of the compound (Figure 6.2B and E). This demonstrated that C1 potentiates the action of DNA-damaging antibiotics. Therefore, this compound was taken forward for further testing and characterisation.

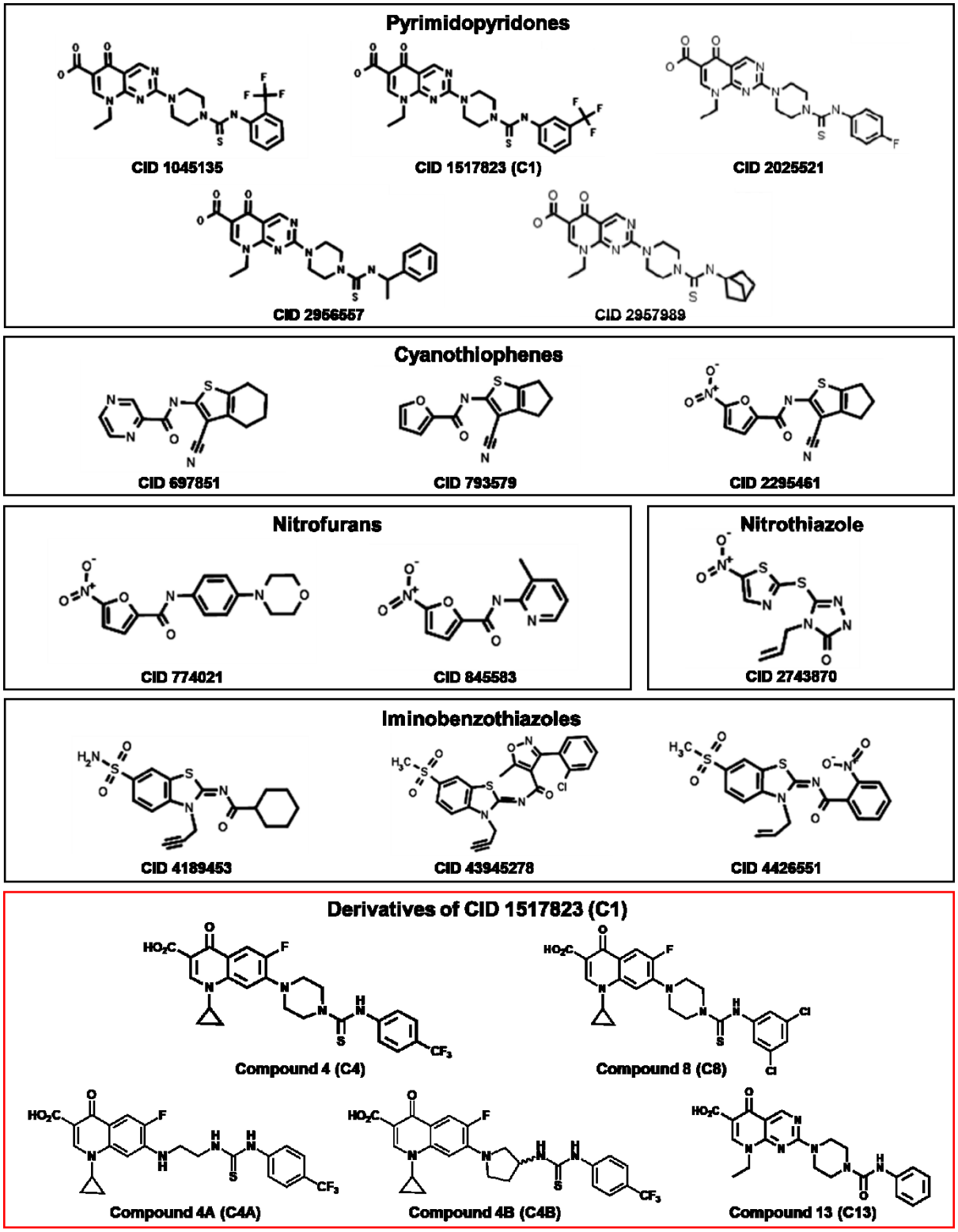

Figure 6.1. Structures of compounds.

Compounds are grouped by structural class (black boxes), with the exception of derivatives of CID 1517823 (hereafter referred to as Compound 1 or C1), which are boxed in red. Structure diagrams of C1 derivatives were provided by Carine Lim (Imperial College London). All other structures are based on those described by Amundsen *et al.* (2012)[603].

Table 6.1. Summary of MIC data for a panel of 14 compounds tested on *S. aureus* SH1000 and JE2.

Chequerboard MIC assays were performed for each compound with ciprofloxacin, mitomycin C or H_2O_2. The MIC was defined as the lowest concentration at which no growth was observed. Cells are coloured in grey where the MIC could not be determined. Highest compound concentration tested was 100 μM. Data shown represent the median of four biological replicates. [a]Compounds are grouped by structural class: pyrimidopyridone [A], cyanothiophene [B], nitrofuran [C], nitrothiazole [D] and iminobenzothiazole [E]. CID, compound identification number.

***S. aureus* SH1000**

CID, [structural class][a]	MIC of compound (μM)	MIC of ciprofloxacin (μg/ml)			MIC of mitomycin C (μg/ml)			MIC of H_2O_2 (mM)		
		Without compound	Compound added at 0.5x MIC	Fold change	Without compound	Compound added at 0.5x MIC	Fold change	Without compound	Compound added at 0.5x MIC	Fold change
1045135 [A]	6.25	0.5	0.25	-2.0	2	0.5	-4.0	0.25	0.25	-1.0
1517823 [A]	25	0.5	0.0625	-8.0	2	0.5	-4.0	0.25	0.25	-1.0
2025521 [A]	12.5	0.5	0.25	-2.0	0.5	0.25	-2.0	0.1875	0.1875	-1.0
2956557 [A]	12.5	0.5	0.125	-4.0	2	1	-2.0	0.25	0.25	-1.0
2957989 [A]	6.25	0.5	0.25	-2.0	0.5	0.125	-4.0	0.1875	0.1875	-1.0
697851 [B]	>100	0.5			0.5			0.25		
793579 [B]	>100	0.5			0.5			0.25		
2295461 [B]	6.25	0.5	0.5	-1.0	2	0.5	-4.0	0.25	0.16	-1.6
774021 [C]	12.5	0.5	0.25	-2.0	0.5	0.25	-2.0	0.25	0.09375	-2.7
845583 [C]	>100	0.5			0.5			0.25		
2743870 [D]	9.375	0.5	0.1875	-2.7	1	0.25	-4.0	0.25	0.25	-1.0
4189453 [E]	>100	0.5			0.5			0.25		
4426551 [E]	>100	0.5			0.5			0.25		
43945278 [E]	>100	0.5			0.5			0.25		

Table 6.1 – continued from previous page.

***S. aureus* JE2**

CID, [structural class][a]	MIC of compound (μM)	MIC of ciprofloxacin (μg/ml)			MIC of mitomycin C (μg/ml)			MIC of H_2O_2 (mM)		
		Without compound	Compound added at 0.5x MIC	Fold change	Without compound	Compound added at 0.5x MIC	Fold change	Without compound	Compound added at 0.5x MIC	Fold change
1045135 [A]	>100	16			0.5			0.09375		
1517823 [A]	25	16	4	-4.0	1	0.25	-4.0	0.0625	0.0625	-1.0
2025521 [A]	25	16	4	-4.0	0.5	0.1875	-2.7	0.09375	0.1025	-0.9
2956557 [A]	50	16	4	-4.0	0.5	0.125	-4.0	0.09375	0.09375	-1.0
2957989 [A]	9.375	16	6	-2.7	0.5	0.3125	-1.6	0.0625	0.0625	-1.0
697851 [B]	>100	16			0.75			0.0625		
793579 [B]	>100	16			1			0.09375		
2295461 [B]	12.5	16	8	-2.0	0.5	0.5	-1.0	0.0625	0.046875	-1.3
774021 [C]	12.5	16	8	-2.0	0.75	0.25	-3.0	0.125	0.03125	-4.0
845583 [C]	>100	16			0.75			0.0625		
2743870 [D]	12.5	16	4	-4.0	0.5	0.25	-2.0	0.25	0.125	-2.0
4189453 [E]	>100	16			0.5			0.09375		
4426551 [E]	>100	16			0.75			0.0625		
43945278 [E]	>100	16			0.5			0.0625		

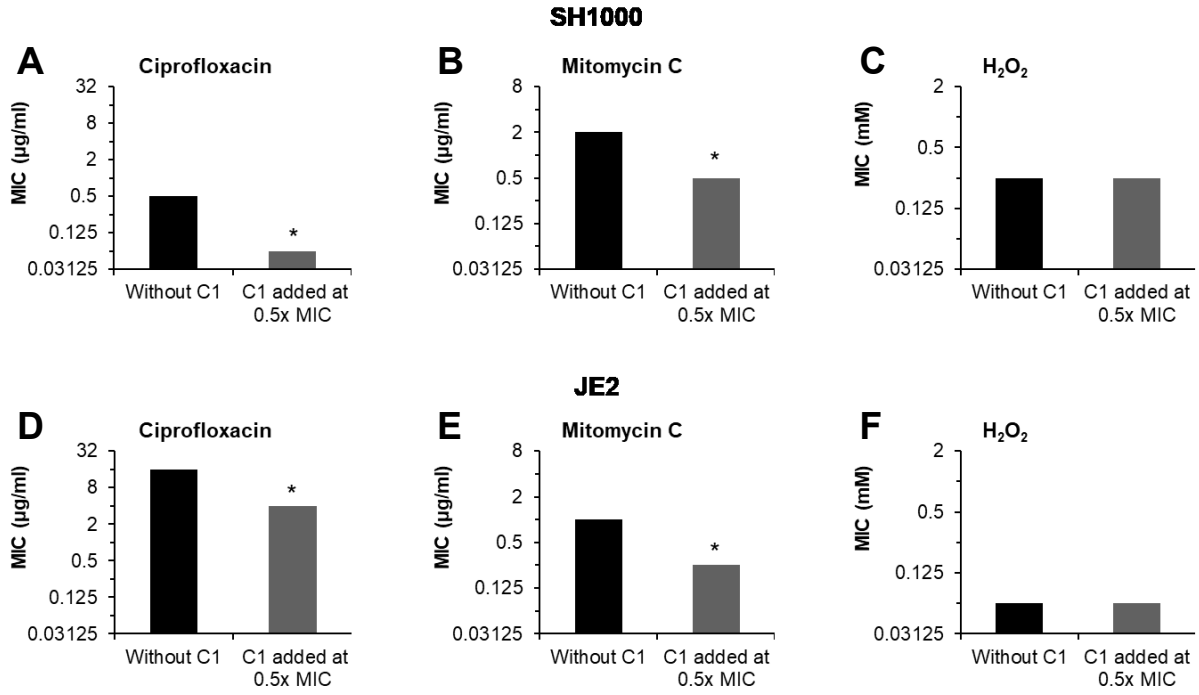

Figure 6.2. C1 enhances the sensitivity of *S. aureus* to ciprofloxacin and mitomycin C. Chequerboard MIC data for C1, presented in graphical form. Assays were performed using the serial broth dilution method in 96-well plates for ciprofloxacin, mitomycin C and H_2O_2 in *S. aureus* SH1000 **(A-C)** and JE2 **(D-F)**. The MIC of C1 is 25 µM for both SH1000 and JE2. The MIC was defined as the lowest concentration at which no growth was observed after static incubation at 37 °C for 17 h. Graphs represent the median of at least four biological replicates. *, $P < 0.05$ (paired t test, compared to the corresponding wild type).

6.3 C1 derivative shows enhanced potency

To find more potent compounds, synthetic analogues of C1 were produced in collaboration with Professor Edward Tate (Imperial College London). These C1 derivatives, listed in Table 6.2, were tested using a similar method to that described above, with the difference that two-fold serial dilutions of the compound were performed in the presence of a fixed concentration of ciprofloxacin. This enabled synergistic effects between the compound and ciprofloxacin to be detected even when the compound MIC could not be determined. Assays were carried out with *S. aureus* JE2, with ciprofloxacin added at 4 µg/ml (0.5x MIC). C13 was synthesised and included as an inactive control compound, as it was previously shown by Amundsen *et al.* (2012) to lack RecBCD/AddAB inhibitory activity[603]. Compound synthesis and MIC assays (for data shown in Table 6.2) were performed by Carine Lim (Imperial College London).

MIC data showed that the majority of C1 derivatives displayed greater synergy with ciprofloxacin than the original hit (Table 6.2). This contrasted with the control compound, C13, which had no effect on bacterial growth with the fluoroquinolone. The greatest activity was exhibited by Compound 4, with just 0.05 µM enough to enhance ciprofloxacin activity against *S. aureus* JE2 (Table 6.2). This was followed by Compound 8 and indicated that substituting the core structure of C1 with an alternative scaffold was highly effective, as well as changing the position of the CF_3 substituent group.

Table 6.2. MIC data for a panel of derivatives of C1.

MIC assays were performed in *S. aureus* JE2 for each compound, either alone or with ciprofloxacin added at 4 µg/ml (0.5x MIC of ciprofloxacin). Compound 13 (C13) was included as an inactive control. The MIC was defined as the lowest concentration at which no growth was observed. C8 and C13 were not tested above 12.5 µM, due to compound precipitation at higher concentrations. Data shown represents the median of at least thee biological replicates. Compound identity describes the core structure and substituent groups. PA, pipemidic acid; Cip, ciprofloxacin. Assays were performed by Carine Lim (Imperial College London).

***S. aureus* JE2**

Compound number	Compound identity	MIC of compound (µM)		
		Without ciprofloxacin	Ciprofloxacin added at 4 µg/ml	Fold change
1	PA + 3-CF_3	12.5	3	-4.2
2	PA + 4-CF_3	12.5	1.6	-7.8
3	Cip + 3-CF_3	12.5	0.8	-15.6
4	Cip + 4-CF_3	12.5	0.05	-250.0
5	PA + 3,5-CF_3	3	3	-1.0
6	Cip + 3,5-CF_3	6.25	1.6	-3.9
7	PA + 3,5-Cl	3	0.4	-7.5
8	Cip + 3,5-Cl	>12.5	0.1	(>) -125
9	PA + 3-F	50	1.6	-31.3
10	Cip + 3-F	12.5	0.8	-15.6
11	PA + 3-Cl	12.5	0.8	-15.6
12	Cip + 3-Cl	6.25	0.2	-31.3
13 (control)	PA + phenylisocyanate	>12.5	>12.5	

To determine whether the compounds could be optimised further, derivatives of C4 were produced in which the central aromatic ring of C4 was either removed or substituted (C4A and C4B, respectively; Figure 6.1). These new compounds, in addition to Compounds 1, 4 and 8 from above, were then tested using chequerboard MIC assays with ciprofloxacin in *S. aureus* SH1000 and JE2. Structures of these compounds are shown in Figure 6.1. All compounds were synthesised by Carine Lim. Chequerboard MIC assays were performed by Kam Pou Ha.

Chequerboard MIC data showed that C4 inhibited the growth of SH1000 and JE2 at lower concentrations than its parent compound, C1 (Figure 6.3A-D). In addition, C1 and C4 both increased the sensitivity of *S. aureus* to ciprofloxacin, resulting in a ciprofloxacin-resistant strain (JE2) being re-sensitised to the antibiotic. However, greater synergy with ciprofloxacin was observed with C4, in that the MIC of ciprofloxacin in JE2 was reduced by 4-fold when C4 was added at half of its MIC, when compared to only 2-fold for C1 (Figure 6.3B and D). This indicated that C4 was the more potent compound.

C8 displayed similar levels of synergy with ciprofloxacin when compared to C4 (4-fold reduction in ciprofloxacin MIC for both SH1000 and JE2; Figure 6.3E and F), but compound MIC was higher at 3.125 μM for SH1000 and >100 μM for JE2. As for the C4 derivatives, C4A was required at a concentration of at least 50 μM to observe synergy with ciprofloxacin (8-fold decrease in ciprofloxacin MIC at 100 μM for SH1000, 4-fold decrease at 50 μM for JE2; Figure 6.3G and H), whereas C4B was required at 100 μM (4-fold decrease in ciprofloxacin MIC; Figure 6.3J). Therefore, Compound 4 is more potent than Compounds 8, 4A and 4B.

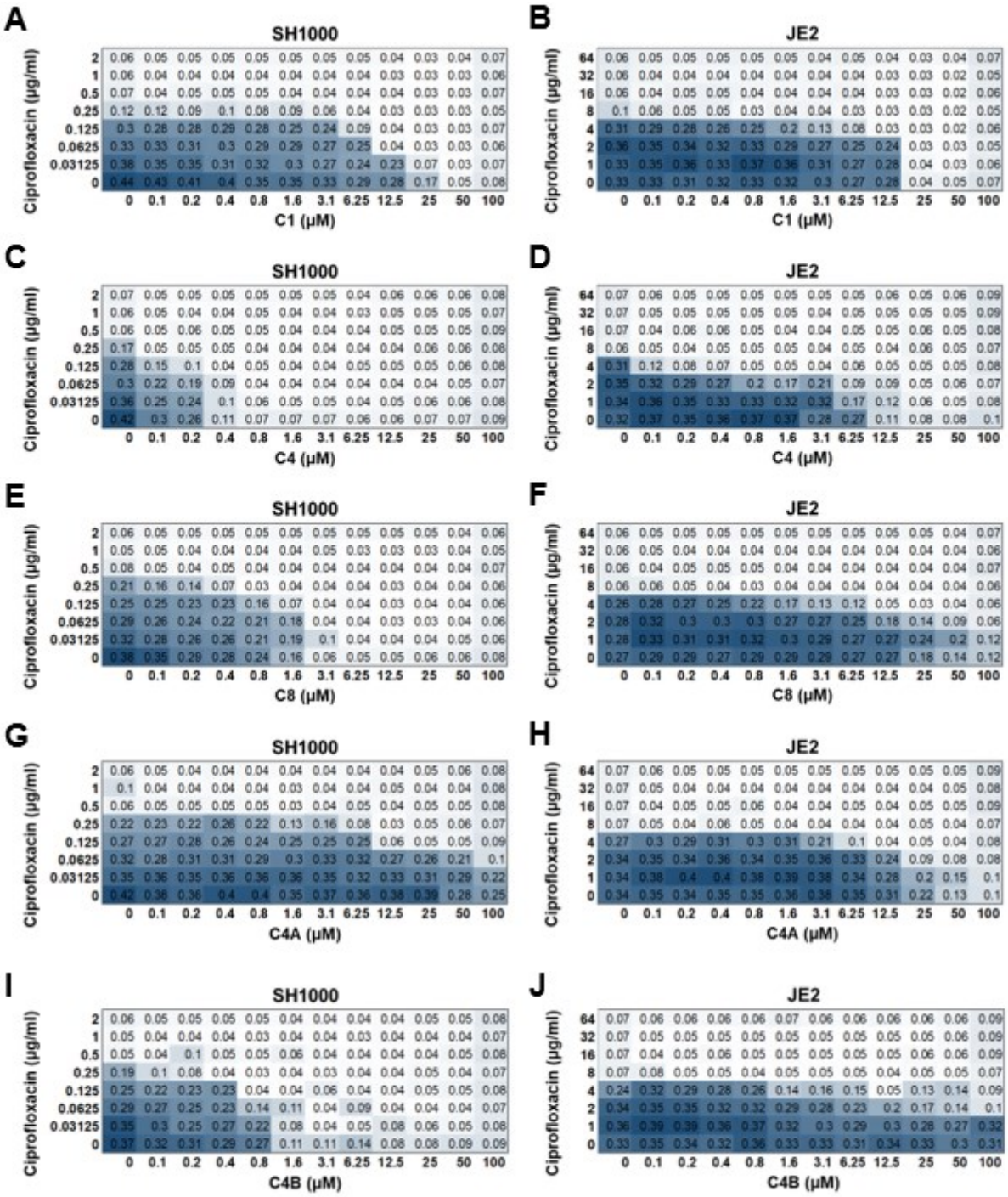

Figure 6.3. C4 is a more potent derivative of C1.

Heat maps of chequerboard MIC assays for C1 **(A, B)**, its derivatives C4 **(C, D)** and C8 **(E, F)**, and C4 derivatives C4A **(G, H)** and C4B **(I, J)** on *S. aureus* SH1000 and JE2. Assays were performed with ciprofloxacin using the serial broth dilution method in 96-well plates. The MIC was defined as the lowest concentration at which no growth was observed. Values refer to the culture optical density ($OD_{600\,nm}$). Greater intensity of colour indicates greater bacterial growth. Data shown represents the median of at least four biological replicates.

6.4 C1 is a bacteriostatic agent in *S. aureus*

Since C1 and C4 were able to inhibit bacterial growth in the absence of ciprofloxacin, it was decided to test whether these compounds were bacteriostatic and/or bactericidal. To do this, the OD_{600} of *S. aureus* cultures were measured over time, in the presence or absence of these compounds. Results showed that the compounds caused dose-dependent growth inhibition of both *S. aureus* strains (Figure 6.4). C4 inhibited growth of *S. aureus* more effectively than C1, supporting the MIC data. SH1000 was also more sensitive to inhibition by C4, when compared to JE2 (Figure 6.4C and D).

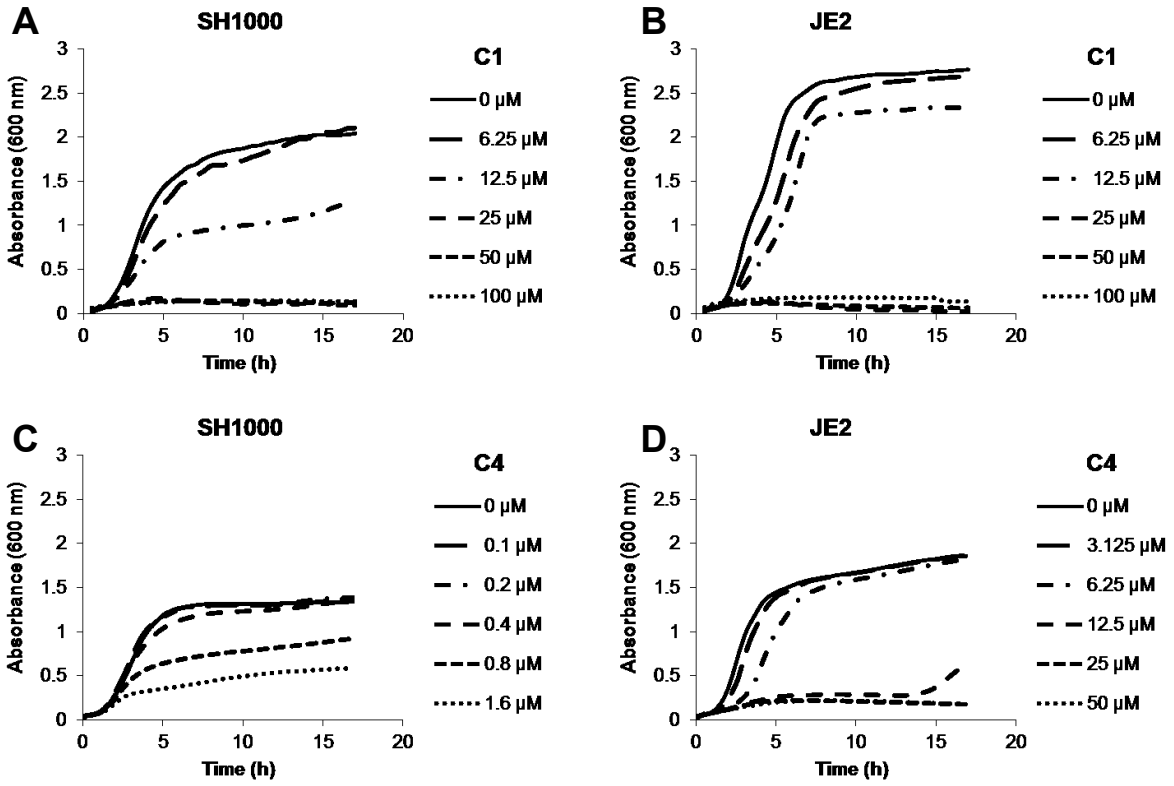

Figure 6.4. C1 and C4 inhibit growth of *S. aureus* SH1000 and JE2 in a dose-dependent manner.

S. aureus strains SH1000 and JE2 were grown in the presence of C1 **(A, B)** or C4 **(C, D)**. Growth was measured by taking $OD_{600\ nm}$ readings every 30 min for 17 h. Graphs represent the mean of three experiments in duplicate. Error bars were omitted for clarity.

Next, minimum bactericidal concentrations (MBCs) of C1 and C4 were determined by enumerating CFU from the wells of MIC assays that inhibited bacterial growth. The MBC was defined as the lowest concentration required for a 1000-fold reduction in CFU counts compared to the inoculum[459]. C1 reduced survival of SH1000 and JE2 at 25 μM, but CFU counts did not reduce further as the dose was increased to 100 μM (Figure 6.5A and B), demonstrating that C1 is bacteriostatic in these strains. Meanwhile, C4 caused a 10,000-fold reduction in CFU counts of SH1000 at 2 μM, but only reduced survival in JE2 at concentrations up to 50 μM (Figure 6.5C and D), demonstrating that C4 is bactericidal in SH1000, but bacteriostatic in JE2. The MBC of C4 in SH1000 was 2 μM, which is 5x MIC (0.4 μM) (Figure 6.5C). Therefore, whilst C1 is not bactericidal in *S. aureus,* it is able to enhance the bactericidal effect of ciprofloxacin.

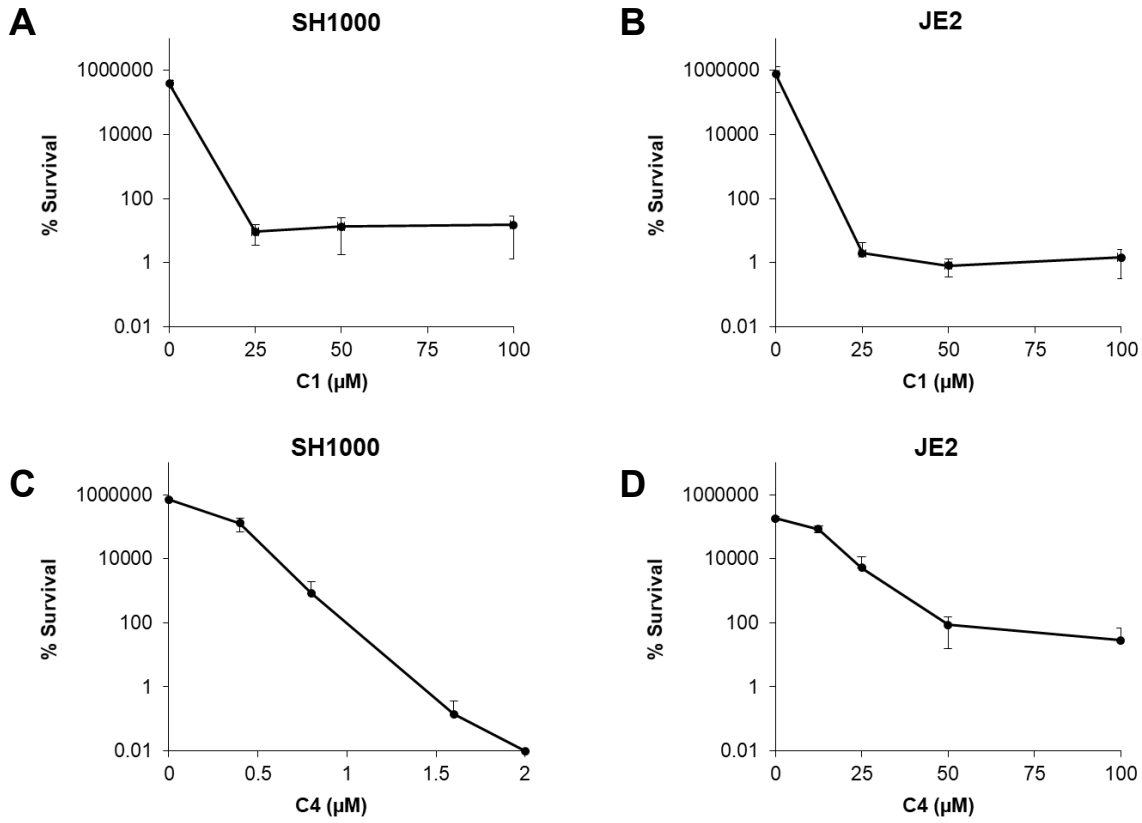

Figure 6.5. C1 is bacteriostatic in *S. aureus* SH1000 and JE2.
MBC assays were performed for C1 **(A, B)** and C4 **(C, D)**, for *S. aureus* SH1000 and JE2. The MBC was defined as the lowest concentration of antibiotic required for a 1000-fold reduction in CFU compared to the inoculum after 17 h (the duration of an MIC assay). Graphs represent the mean of four independent experiments. Error bars indicate the standard deviation.

6.5 C4 enhances ciprofloxacin-mediated killing of *S. aureus*

As described above, C4 enhances the sensitivity of *S. aureus* to ciprofloxacin, leading to greater inhibition of bacterial growth compared to the original compound, C1. To determine whether C4 enhanced susceptibility of *S. aureus* to killing by ciprofloxacin, antibiotic survival assays were performed with SH1000 and JE2 when exposed to C4 (at 1x MIC) and/or ciprofloxacin (at 10x MIC), and bacterial survival was measured over 24 h.

Survival of SH1000 was greatly reduced when exposed to ciprofloxacin alone, whereas survival of JE2 was unchanged due to its resistance to the quinolone (Figure 6.6). However, when ciprofloxacin and C4 were added together, survival of SH1000 and JE2 was slightly decreased at every time point after 0 h when compared to ciprofloxacin alone (Figure 6.6), though this was not statistically significant. Nevertheless, survival after 24 h was reduced by 2.4-fold in SH1000 (Figure 6.6A), and by 8-fold in JE2 (Figure 6.6B). Both strains also grew when exposed to C4 alone, demonstrating that the compound (at 1x MIC) influenced *S. aureus* survival only when added in combination with ciprofloxacin (Figure 6.6). Together, these data indicate that C4 is able to potentiate ciprofloxacin-mediated killing of *S. aureus* to some extent.

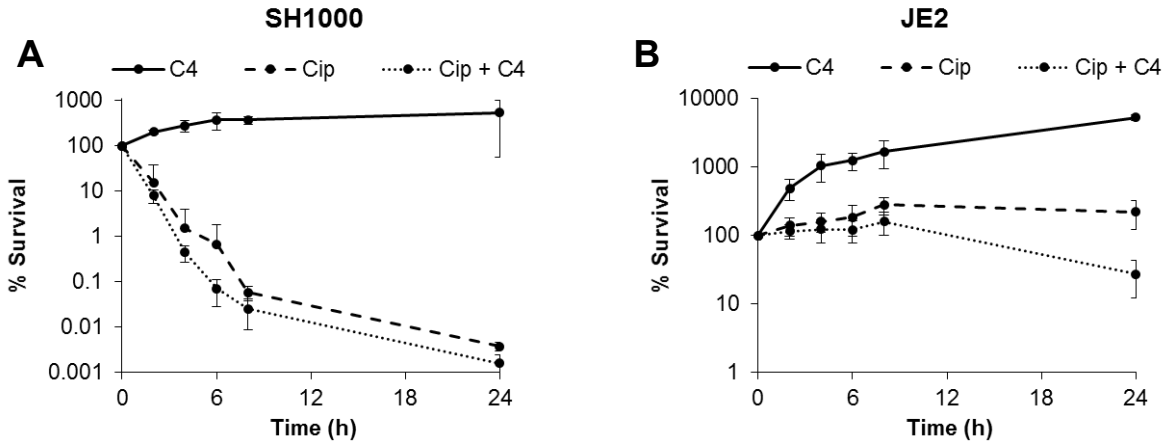

Figure 6.6. C4 increases susceptibility of *S. aureus* to killing by ciprofloxacin.
Percentage survival after 24 h in the presence of C4, ciprofloxacin or both is shown for *S. aureus* SH1000 **(A)** and JE2 **(B)**. C4 was added at 1x MIC, which is 0.4 µM for SH1000 and 12.5 µM for JE2. Ciprofloxacin was added at 10x MIC, which is 5 µg/ml for SH1000 and 160 µg/ml for JE2. Graphs represent the mean of four independent experiments. Error bars indicate the standard deviation. Cip, ciprofloxacin.

6.6 C4 enhances the sensitivity of *S. gordonii, E. faecalis* and *E. coli* to ciprofloxacin

To determine whether C4 potentiated the activity of ciprofloxacin in other bacterial species, chequerboard MIC assays were performed as described in section 6.2, on *S. gordonii, E. faecalis* and *E. coli*. In the presence of C4 alone, *S. gordonii* displayed the highest compound MIC at 12.5 μM, followed by *E. faecalis* at 3.125 μM and *E. coli* at 1.5625 μM (Figure 6.7). When the compound was added at half of its MIC (subinhibitory concentration), the MIC of ciprofloxacin was reduced by 4-fold in all thee species (Figure 6.7), indicating that C4 enhances ciprofloxacin activity in *S. gordonii, E. faecalis* and *E. coli.*

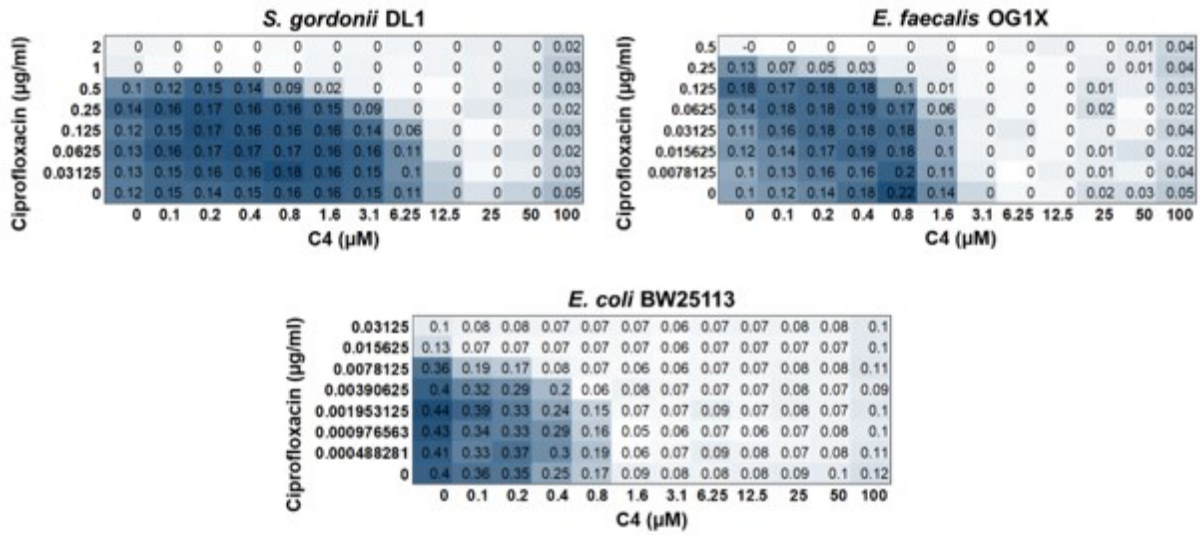

Figure 6.7. C4 increases the sensitivity of *S. gordonii, E. faecalis* and *E. coli* to ciprofloxacin.

Heat maps of chequerboard MIC assays for C4 and ciprofloxacin with *S. gordonii* DL1, *E. faecalis* OG1X and *E. coli* BW25113. Assays were performed with ciprofloxacin using the serial broth dilution method in 96-well plates. The MIC was defined as the lowest concentration at which no growth was observed. Values refer to the culture density ($OD_{600\ nm}$). Greater intensity of colour indicates greater bacterial growth. Data shown represents the median of at least four biological replicates.

6.7 C1 and C4 have no effect on killing of *S. aureus* in whole human blood

It was shown in Chapter 3 that neutrophil-generated ROS damage staphylococcal DNA and that repair of this DNA damage is required for *S. aureus* survival in whole human blood (sections 3.3, 3.8 and 3.9). To determine whether C1 or C4 influenced killing of *S. aureus* by the neutrophil oxidative burst, the *ex vivo* whole human blood model was employed. Wild-type SH1000 or JE2 was incubated in freshly-donated whole human blood in the presence of different concentrations of each compound, and survival was determined after 6 h by plating onto CBA. As a control for the direct antibacterial effects of the compounds, some samples of whole human blood were pre-treated for 15 min with the inhibitor DPI to block ROS production[475].

As expected, pre-treatment of blood with DPI led to an increase in bacterial survival when compared to DMSO-treated blood (Figure 6.8), confirming that ROS production via the neutrophil oxidative burst is required for killing of *S. aureus*. However, the addition of C1 or C4 had no effect on *S. aureus* survival in the absence or presence of DPI, even up to the maximum workable concentration tested (100 μM; Figure 6.8). This indicates that these compounds do not influence killing of *S. aureus* by the neutrophil oxidative burst.

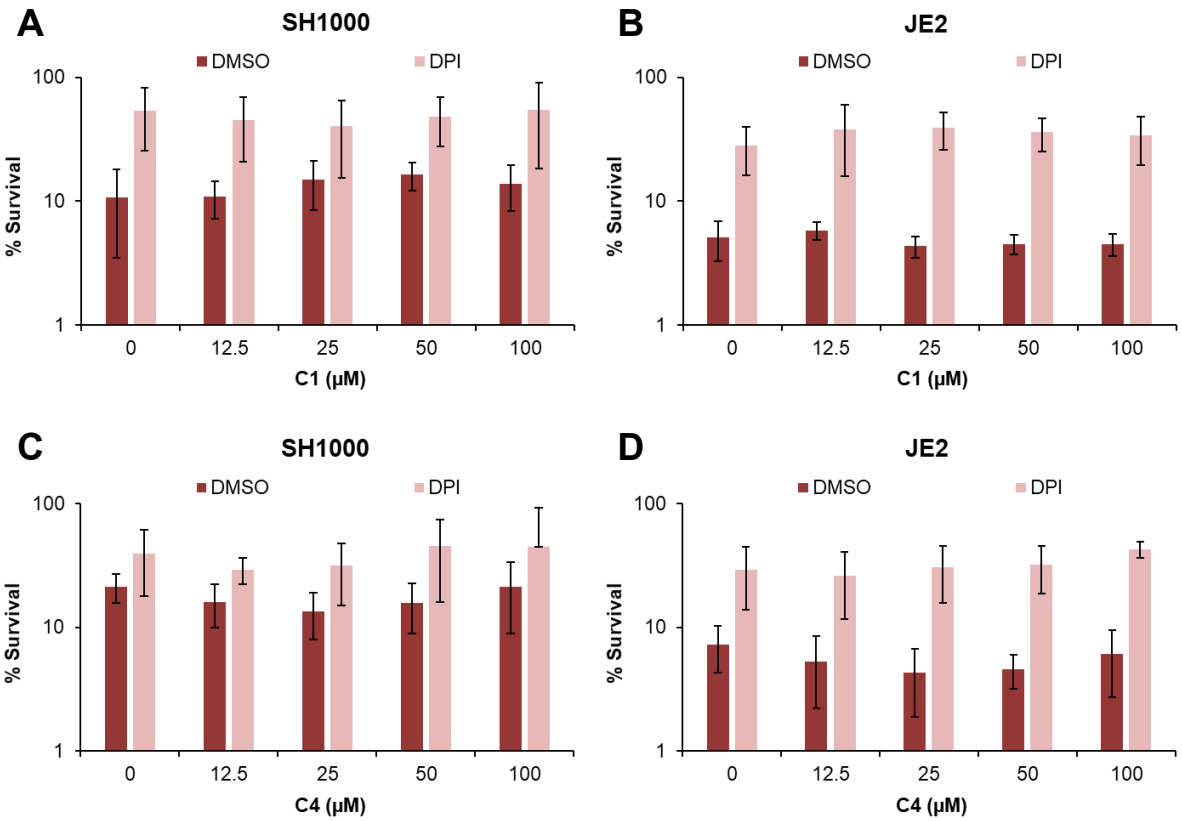

Figure 6.8. C1 and C4 have no influence on susceptibility of *S. aureus* to killing in whole human blood.

Percentage survival over 6 h incubation in whole human blood in the presence of C1 **(A, B)** or C4 **(C, D)** is shown for *S. aureus* SH1000 and JE2. Whole human blood was incubated for 15 min with the NADPH-oxidase inhibitor DPI, or DMSO as a control, before the addition of bacteria. Graphs represent the mean of three independent experiments. Error bars indicate the standard deviation.

6.8 C1 and C4 enhance the sensitivity of *rexAB* mutants to ciprofloxacin

C1 has been shown to inhibit both AddAB and RecBCD DNA repair complexes in *H. pylori* and *E. coli* respectively. However, whilst C1 and C4 both enhanced the susceptibility of *S. aureus* to ciprofloxacin, they had no effect on staphylococcal survival during exposure to the neutrophil oxidative burst, which conflicts with data from studies with *rexAB*-deficient mutants (section 3.9). Therefore, it was decided to determine whether these compounds targeted *S. aureus* RexAB. To do this, C1 and C4 were tested on *rexAB* mutants, as well as on the purified *S. aureus* RexAB enzyme (section 5.3).

To determine whether C1 and C4 enhanced the activity of ciprofloxacin on SH1000 and JE2 *rexAB* mutants, chequerboard MIC assays were performed using two-fold serial dilutions as described previously. Due to the greater sensitivity of the mutants to DNA-damaging antibiotics, ciprofloxacin was added at lower concentrations than for the wild type. Firstly, the MIC of the compounds alone for the *rexB*::Tn mutants was determined. As shown in Figure 6.9A-D, the MIC of C1 was reduced by 4-fold in the SH1000 *rexAB* mutant when compared to the wild type (6.25 μM vs. 25 μM), whereas no difference was observed in JE2 (both 25 μM). Meanwhile, the C4 MIC was reduced in both SH1000 and JE2 *rexAB* mutants when compared to their corresponding wild types (at least 4-fold reduction in SH1000, 2-fold in JE2; Figure 6.9E-H). Therefore, *S. aureus rexAB* mutants are more sensitive to C1 and C4 than the corresponding wild type strains.

Next, the effect of the compounds on the ciprofloxacin MIC was determined. SH1000 and JE2 *rexAB* mutants both displayed a reduction in the ciprofloxacin MIC when C1 or C4 was added at half of its MIC. In the JE2 *rexAB* mutant, this decrease was comparable to the wild type (2-fold reduction in ciprofloxacin MIC with C1, 4-fold with C4; Figure 6.9C, D and G, H). Therefore, both C1 and C4 potentiate the activity of ciprofloxacin in *S. aureus rexB*::Tn mutants, indicating that these compounds exhibit off-target effects and potentiate ciprofloxacin activity independently of RexAB inhibition. However, these assays did not

confirm whether C1 and C4 also inhibit *S. aureus* RexAB activity, which will be examined in the next section.

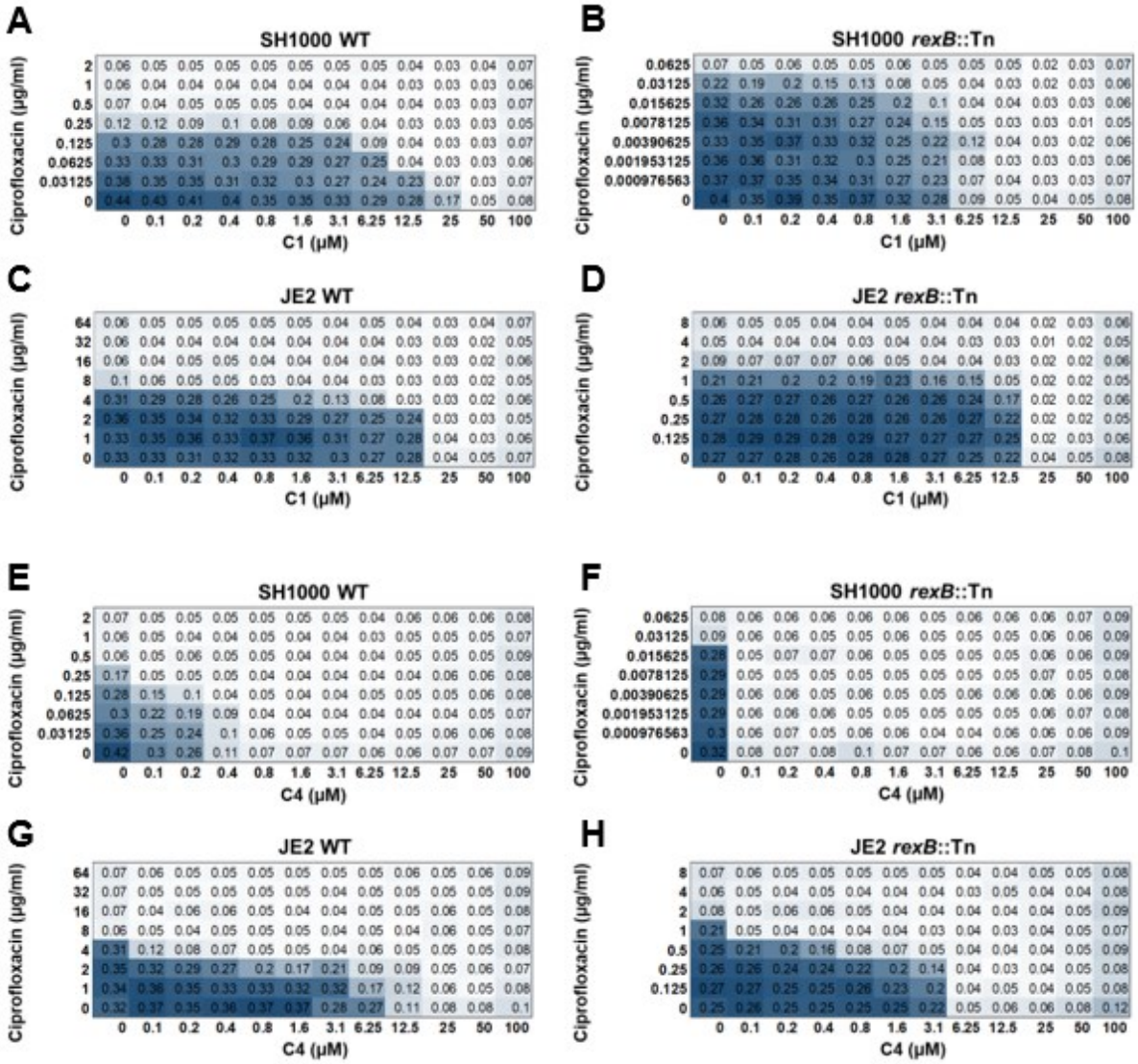

Figure 6.9. C1 and C4 increase the sensitivity of *S. aureus rexAB* mutants to ciprofloxacin.

Heat maps of chequerboard MIC assays for C1 **(A-D)** or C4 **(E-H)**, tested with ciprofloxacin on *S. aureus* SH1000 or JE2 wild type and *rexB*::Tn mutant strains. Assays were performed using the serial broth dilution method in 96-well plates. The MIC was defined as the lowest concentration at which no growth was observed. Values refer to the culture density ($OD_{600\ nm}$). Greater intensity of colour indicates greater bacterial growth. Data shown represents the median of at least four biological replicates.

To determine whether C4 potentiated ciprofloxacin activity in *rexAB* mutants from other bacterial species, the same chequerboard assays were performed on *S. gordonii* and *E. faecalis*. Results showed that, as for *S. aureus*, *S. gordonii* and *E. faecalis rexAB* mutants were more sensitive to C4 when compared to their corresponding wild types (Figure 6.10). In addition, the ciprofloxacin MIC was reduced by 4-fold in *S. gordonii ΔrexAB* when C4 was added at half of its MIC (Figure 6.10B), which is comparable to that of its wild type (also 4-fold reduction; Figure 6.10A). This indicates that C4 enhances the activity of ciprofloxacin in the *S. gordonii rexAB* mutant. Therefore, chequerboard MIC data from *S. aureus, S. gordonii* and *E. faecalis rexAB* mutants suggest that C1 and C4 exhibit off-target activity that is at least partially responsible for potentiating ciprofloxacin activity and do not solely inhibit RexAB.

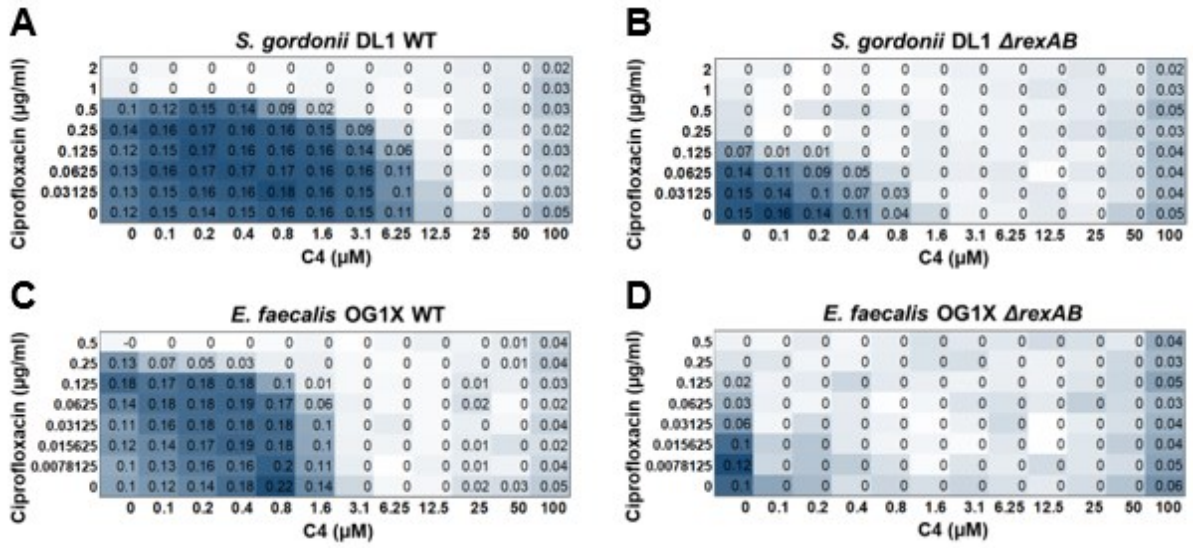

Figure 6.10. C4 increases the sensitivity of *S. gordonii* and *E. faecalis rexAB* mutants to ciprofloxacin.

Heat maps of chequerboard MIC assays with C4 and ciprofloxacin, on *S. gordonii* DL1 **(A, B)** or *E. faecalis* OG1X **(C, D)** wild type and *rexAB* mutant. Assays were performed with ciprofloxacin using the serial broth dilution method. The MIC was defined as the lowest concentration at which no growth was observed. Values refer to the culture density ($OD_{600\ nm}$). Greater intensity of colour indicates greater bacterial growth. Data shown represents the median of at least four biological replicates.

6.9 C1 and C4 have no effect on *S. aureus* RexAB enzyme activity

To determine whether C1 and C4 directly inhibited *S. aureus* RexAB function, RexAB nuclease, helicase and ATPase activities were measured in the presence of these compounds. Enzyme assays were performed as described in the previous chapter, with the addition of C1, C4 or C13 at 12.5 μM in the nuclease and helicase assays, and at 12.5 μM or 25 μM in the ATPase assays. DMSO was used as a solvent control. C13 (structure shown in Figure 6.1) was included as an inactive compound control, because it was previously shown by Amundsen *et al.* (2012) to lack RecBCD/AddAB inhibitory activity[603]. In nuclease and helicase activity assays, samples were taken at 30, 60 and 120 min and analysed by agarose gel electrophoresis to quantify DNA degradation, dsDNA unwinding and/or ssDNA formation.

No difference in DNA degradation was observed with C1, C4 or C13 when compared to the DMSO control, indicating that these compounds have no effect on RexAB nuclease activity when added at 12.5 μM (Figure 6.11). This was also observed for helicase activity, in which dsDNA unwinding and ssDNA formation in the presence of C1, C4 or C13 were comparable to DMSO at all time points (Figure 6.12). Further assays were performed to determine whether compounds influenced enzyme activity at time points earlier than what was tested (< 30 min), but nuclease and helicase activities were still comparable to the DMSO control, indicating that the absence of inhibitory activity was not time dependent (data not shown). Finally, the compounds were shown to have no effect on production of P_i (Figure 6.13), indicating that C1 and C4 do not inhibit RexAB ATPase activity when added at 12.5 μM or 25 μM. Taken together, these results suggest that C1 and C4 do not inhibit *S. aureus* RexAB enzyme activity.

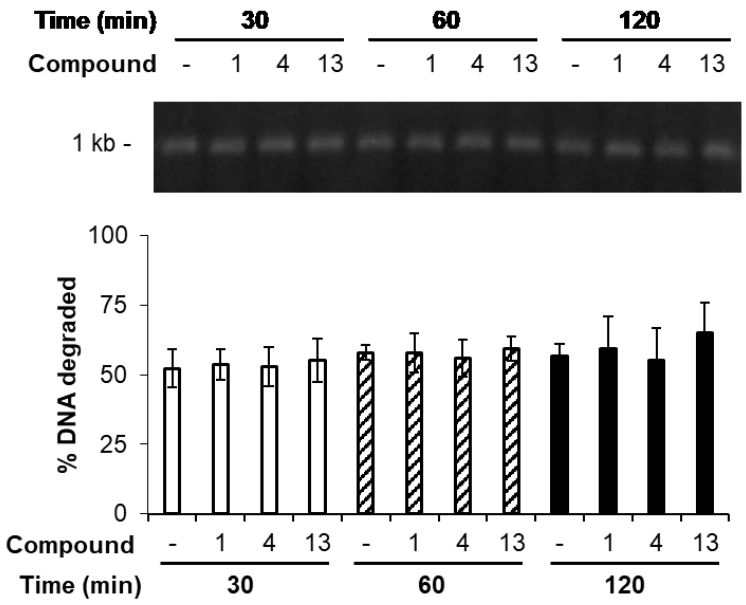

Figure 6.11. RexAB nuclease activity is unaffected by C1 or C4.

RexAB nuclease activity was measured in the presence of C1, C4 or C13 added at 12.5 μM, or in DMSO as a control ("-"). Nuclease activity was determined by incubating RexAB protein, DNA substrate and ATP at 37 °C, with or without compound. Samples were taken over 2 h and analysed by agarose gel electrophoresis. Gels were stained using SYBR Safe to detect dsDNA. Band intensity of the DNA substrate was quantified. Graph represents the mean of four independent experiments. Error bars indicate the standard deviation.

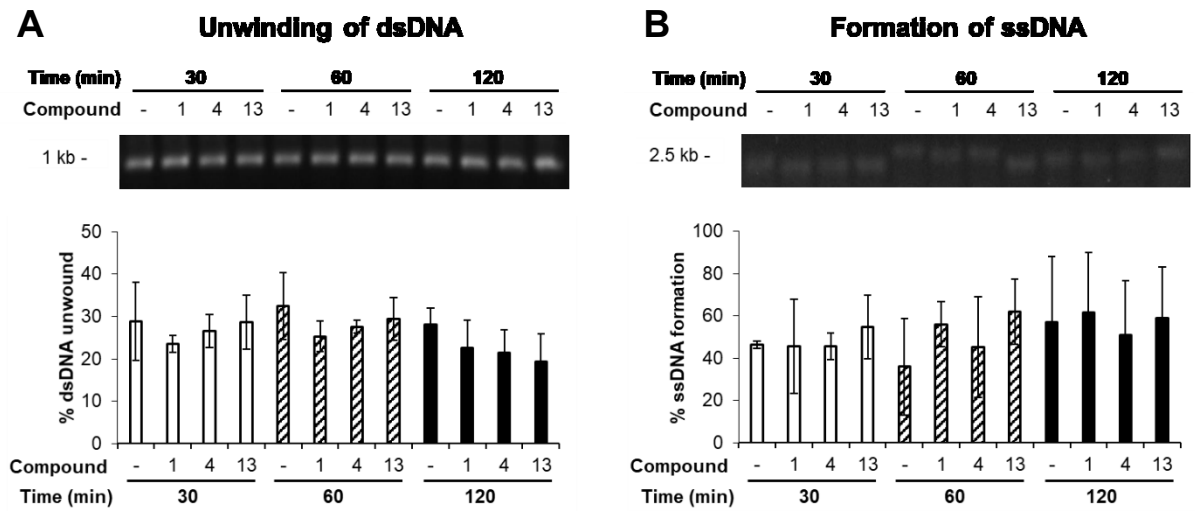

Figure 6.12. RexAB helicase activity is unaffected by C1 or C4.

RexAB helicase activity was assessed in the presence of C1, C4 or C13 added at 12.5 µM, or in DMSO as a control ("-"), by measuring unwinding of dsDNA **(A)** and formation of ssDNA **(B).** *E. coli* SSB was added to prevent reannealing of DNA. Samples were taken over 2 h and analysed by agarose gel electrophoresis with SYBR Green II staining. Band intensities of dsDNA substrate and ssDNA-SSB product were quantified. Graphs represent the mean of four independent experiments. Error bars indicate the standard deviation.

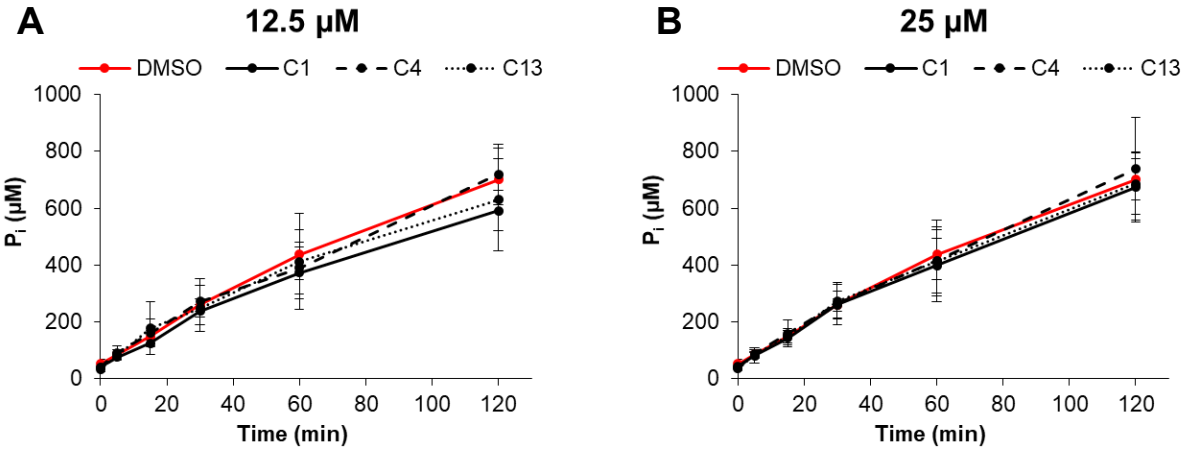

Figure 6.13. RexAB ATPase activity is unaffected by C1 or C4.

RexAB ATPase activity was measured in the presence of C1, C4 or C13 added at 12.5 µM **(A)** or 25 µM **(B)**, or in DMSO as a control. ATPase activity was determined by incubating RexAB protein, DNA substrate and ATP at 37 °C, with or without compound. The concentration of inorganic phosphate (P_i) was quantified over 2 h using the Expedeon PiColorLock Gold Phosphate Detection System assay kit and use of a standard curve. Graphs represent the mean of three independent experiments. Error bars indicate the standard deviation.

6.10 C1 and C4 display dose-dependent inhibition of *E. coli* DNA gyrase activity

Since C1 and C4 did not inhibit *S. aureus* RexAB enzyme activity, this indicated that they enhanced bacterial sensitivity to ciprofloxacin though another mechanism. To investigate how ciprofloxacin activity was potentiated, the chemical structures of C1 and C4 (Figure 6.1) were examined further. C1 has a pipemidic acid group as its core structure, whereas C4 has a ciprofloxacin group. Both of these core structures are members of the quinolone family of antibiotics, which inhibit topoisomerase IV and DNA gyrase. Therefore, it was hypothesised that C1 and C4 may act via a similar mechanism to quinolones. To test this, topoisomerase IV relaxation and DNA gyrase supercoiling activities were measured in the presence of C1, C4, C13, or ciprofloxacin as a positive control, using the Inspiralis *E. coli* topoisomerase IV or DNA gyrase assay kits. Reactions were performed without compound as a negative control. DNA substrate was incubated with the appropriate enzyme, ATP and each compound for 45 min, then analysed by agarose gel electrophoresis to quantify band intensities of supercoiled DNA, which were normalised to the no-compound control.

As shown in Figure 6.14, the addition of ciprofloxacin at 50 μM inhibited topoisomerase IV relaxation activity, but this was not observed for C1, C4 or C13, even when added at 50 μM. Therefore, C1 and C4 do not potentiate ciprofloxacin activity by inhibiting topoisomerase IV function. However, all compounds displayed dose-dependent inhibition of DNA gyrase supercoiling activity, albeit at concentrations far higher than seen with ciprofloxacin, which almost completely inhibited gyrase activity at 5 μM (Figure 6.15). C1 displayed no inhibitory activity at 12.5 μM, but the percentage of supercoiled DNA was reduced to 82% and 41% when added at 25 μM and 50 μM, respectively. C4 inhibited gyrase activity by 68% at 12.5 μM (32% supercoiled DNA; Figure 6.15), indicating that C4 is more potent than C1. Interestingly, C13 promoted gyrase activity when added at 12.5 μM and 25 μM (159% and 116% supercoiled DNA, respectively), but inhibited activity from 50 μM onwards (Figure 6.15), indicating a biphasic dose response. These data show that C1, C4 and C13 have no

effect on *E. coli* topoisomerase IV activity, but exhibit dose-dependent inhibition of *E. coli* DNA gyrase activity. However, they are significantly less active against DNA gyrase than ciprofloxacin.

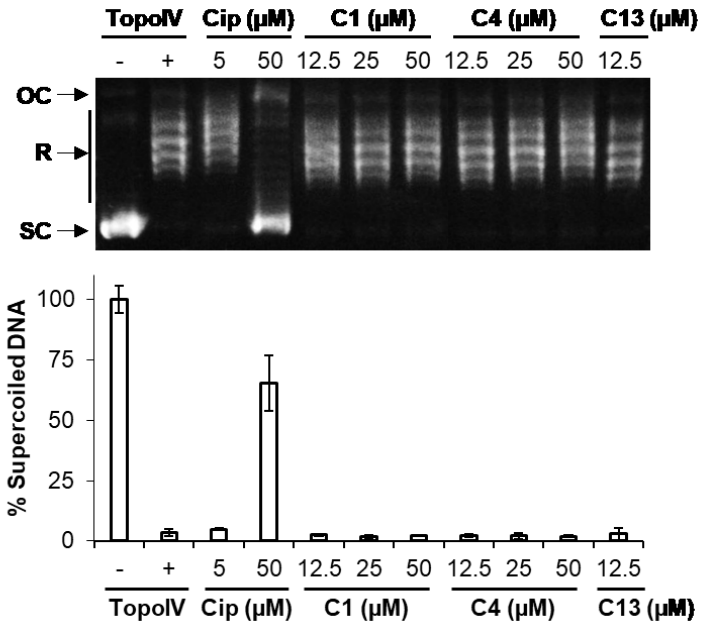

Figure 6.14. C1 and C4 have no effect on *E. coli* DNA topoisomerase IV activity.
Topoisomerase IV relaxation activity was measured in the presence of C1, C4, C13 or ciprofloxacin as a positive control. Assays were performed using the Inspiralis *E. coli* Topoisomerase IV relaxation assay kit. *E. coli* topoisomerase IV was incubated with supercoiled DNA substrate and ATP at 37 °C for 45 min, with or without compound. Samples were analysed by agarose gel electrophoresis and gels were stained using SYBR Safe to detect dsDNA. Band intensity of supercoiled DNA was quantified. Graph represents the mean of three independent experiments. Error bars indicate the standard deviation. TopoIV, topoisomerase IV; Cip, ciprofloxacin; OC, open-circular DNA; R, relaxed DNA; SC, supercoiled DNA.

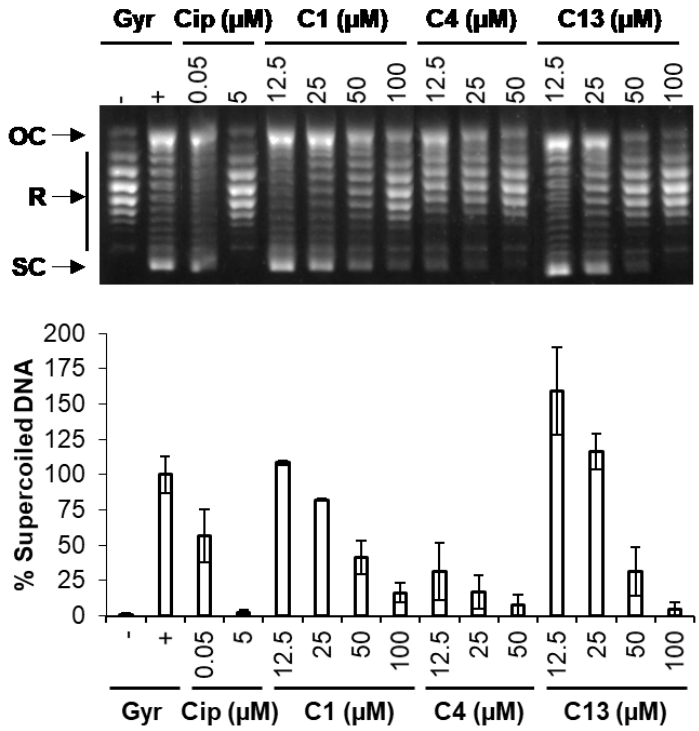

Figure 6.15. C1, C4 and C13 exhibit dose-dependent inhibition of *E. coli* DNA gyrase activity.

Gyrase supercoiling activity was measured in the presence of C1, C4, C13 or ciprofloxacin as a positive control. Assays were performed using the Inspiralis *E. coli* gyrase supercoiling assay kit. *E. coli* gyrase was incubated with relaxed DNA substrate and ATP at 37 °C for 1 h, with or without compound. Samples were analysed by agarose gel electrophoresis and gels were stained using SYBR Safe to detect dsDNA. Band intensity of supercoiled DNA was quantified. Graph represents the mean of three independent experiments. Error bars indicate the standard deviation. Gyr, gyrase; Cip, ciprofloxacin; OC, open-circular DNA; R, relaxed DNA; SC, supercoiled DNA.

6.11 C1 and C4 influence ciprofloxacin-mediated SOS induction in *S. aureus*

Previously, it was shown that C1 and C4 enhance the sensitivity of *S. aureus* to ciprofloxacin. Since ciprofloxacin is known to trigger the SOS response[318], the effect of these compounds on ciprofloxacin-mediated SOS induction was tested. *S. aureus* SH1000 and JE2 wild-type strains containing the *PrecA-gfp* reporter construct (section 3.2) were exposed to a range of ciprofloxacin concentrations, in the presence or absence of C1, C4, C13 or DMSO as a solvent control. Compounds were added at 0.4 µM in SH1000 or 12.5 µM in JE2, which are concentrations that do not affect bacterial growth. Expression of *recA* (indicating SOS induction) was measured over 17 h via GFP fluorescence.

In SH1000, *recA* expression levels in the presence of C1 or C13 were comparable to the DMSO control, indicating that these compounds have no effect on ciprofloxacin-mediated SOS induction (Figure 6.16). However, C4 exhibited various effects depending on the concentration of ciprofloxacin. At ciprofloxacin concentrations below 0.5 µg/ml, C4 enhanced SOS induction when compared to the DMSO control, but at ciprofloxacin concentrations above 0.5 µg/ml, SOS induction was inhibited instead (Figure 6.16). This effect was also observed in JE2, with both C1 and C4 (Figure 6.17). Ciprofloxacin-mediated SOS induction was potentiated by both compounds when the antibiotic was added at 8 µg/ml or below, but induction was inhibited at ciprofloxacin concentrations above 8 µg/ml (Figure 6.17). In the presence of C13, SOS induction was comparable to the DMSO control (Figure 6.17), indicating that this compound functions as an inactive compound control in both strains. Therefore, these results show that C1 and C4 influence ciprofloxacin-mediated SOS induction, depending on the antibiotic concentration.

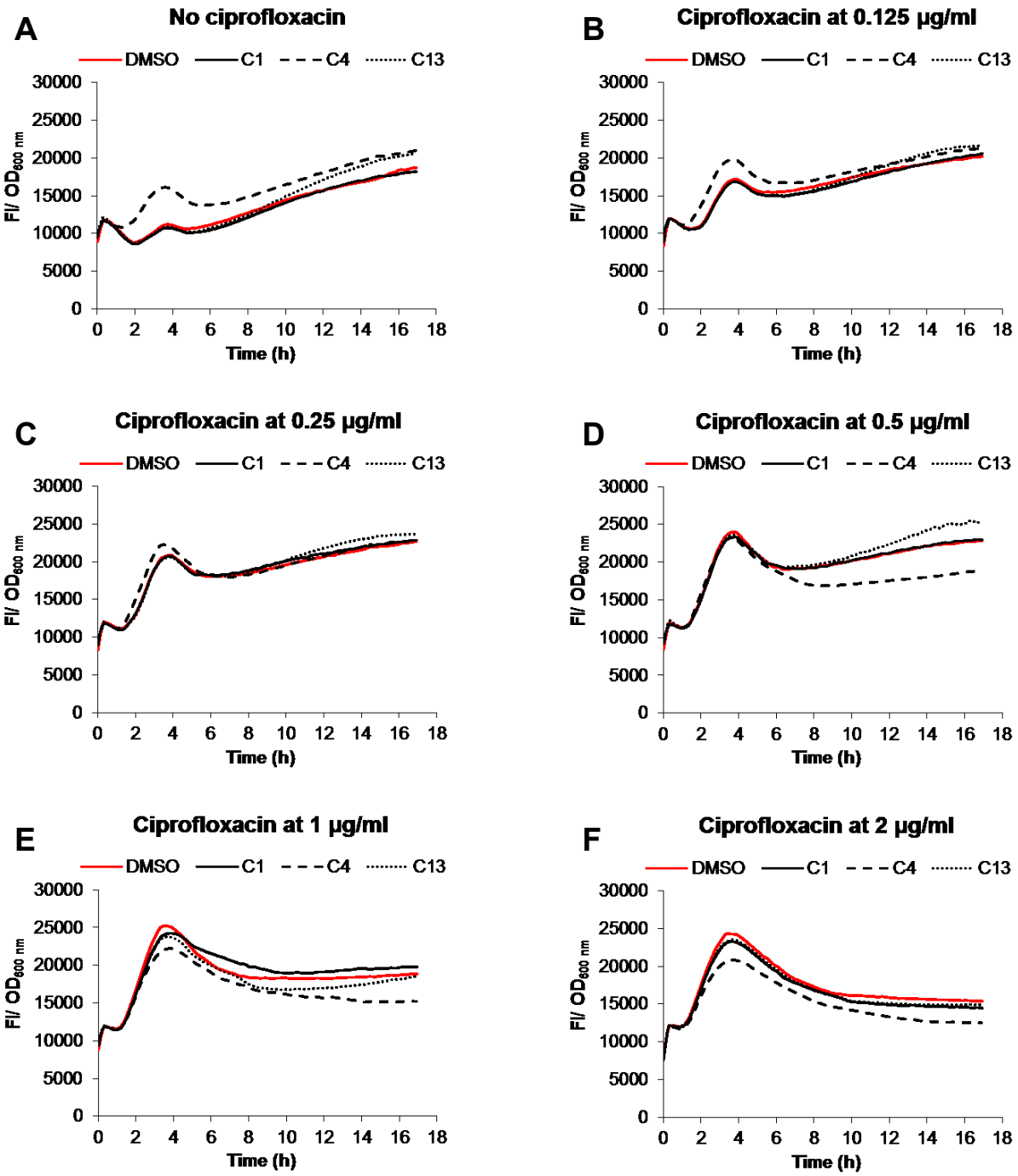

Figure 6.16. Ciprofloxacin-mediated SOS induction in the presence of compounds in *S. aureus* SH1000.

Wild-type *S. aureus* SH1000 containing the pCN34 *PrecA-gfp* reporter plasmid was exposed to a range of ciprofloxacin concentrations **(A-F)** in the presence of C1, C4, C13 or DMSO (control), and *recA* expression measured over 17 h. Compounds were added at 0.4 µM, which has no effect on SH1000 growth. Expression is shown relative to cell density ($FI/OD_{600\ nm}$) over time. Graphs represent the mean of three biological replicates with error bars omitted for clarification.

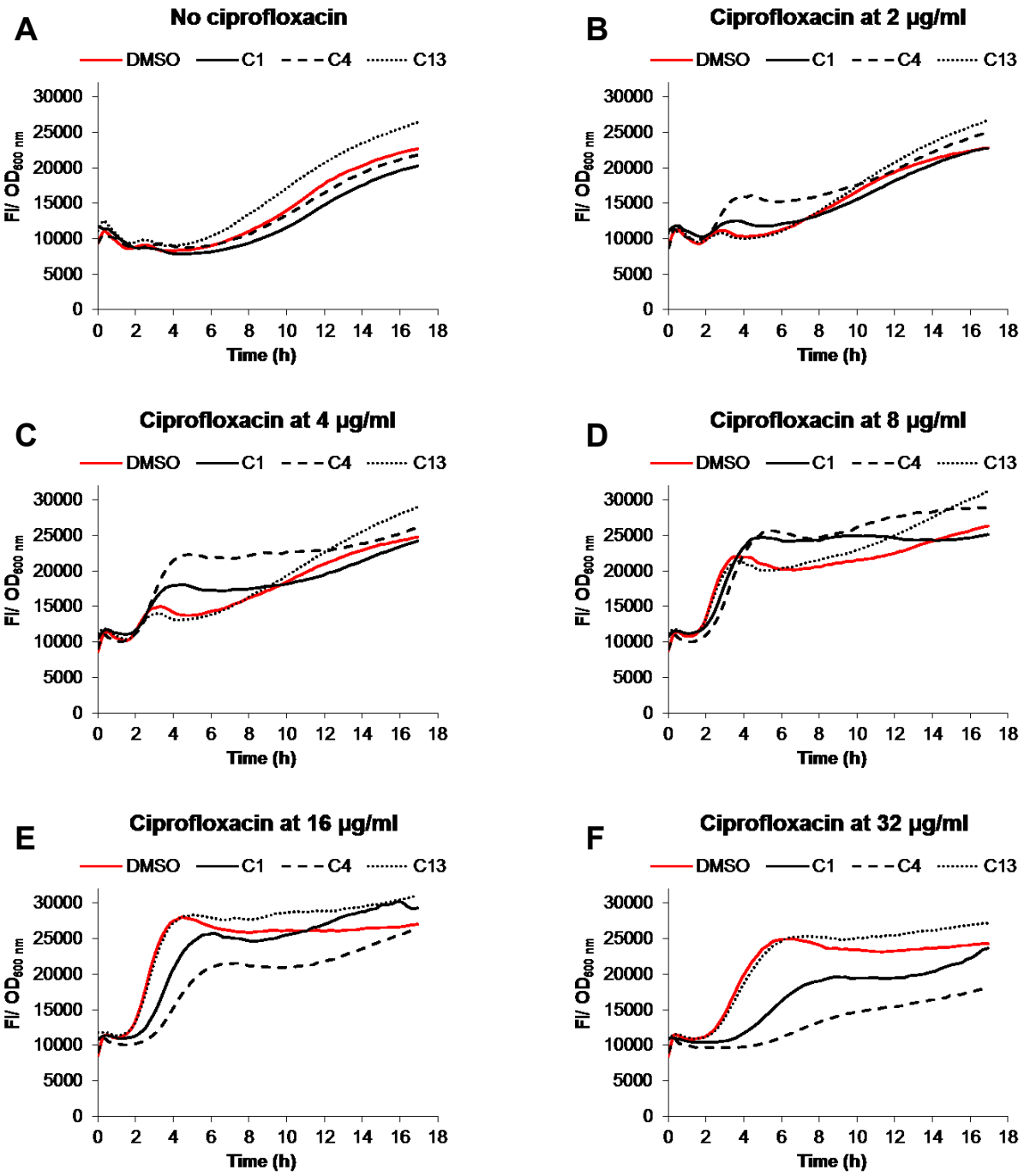

Figure 6.17. Ciprofloxacin-mediated SOS induction in the presence of compounds in *S. aureus* JE2.

Wild-type *S. aureus* JE2 containing the pCN34 *PrecA-gfp* reporter plasmid was exposed to a range of ciprofloxacin concentrations **(A-F)** in the presence of C1, C4, C13 or DMSO (control), and *recA* expression measured over 17 h. Compounds were added at 12.5 µM, which has no effect on JE2 growth. Expression is shown relative to cell density ($Fl/OD_{600\ nm}$) over time. Graphs represent the mean of three biological replicates with error bars omitted for clarification.

It was found that C4 triggered the SOS response in SH1000 in the absence of ciprofloxacin, but this was not observed with C1, and neither C1 nor C4 induced SOS activation in JE2 (Figure 6.16 and Figure 6.17). However, only one concentration of compound had been tested. Therefore, to determine whether C4 induced the SOS response in *S. aureus*, *recA* expression was measured in the presence of a range of C4 concentrations in SH1000 and JE2. Results showed that C4 triggered SOS in SH1000, but the peak occurred at much lower levels than with ciprofloxacin, with a maximum FI/$OD_{600\ nm}$ of ~17,000 (Figure 6.18A), compared to ~25,000 with ciprofloxacin (Figure 6.16E). In contrast, no peak corresponding to SOS induction was observed in JE2 (Figure 6.18B). Therefore, although C4 on its own affects SOS induction differently in SH1000 and JE2, similar effects are observed in both strains when the compound is added in combination with ciprofloxacin.

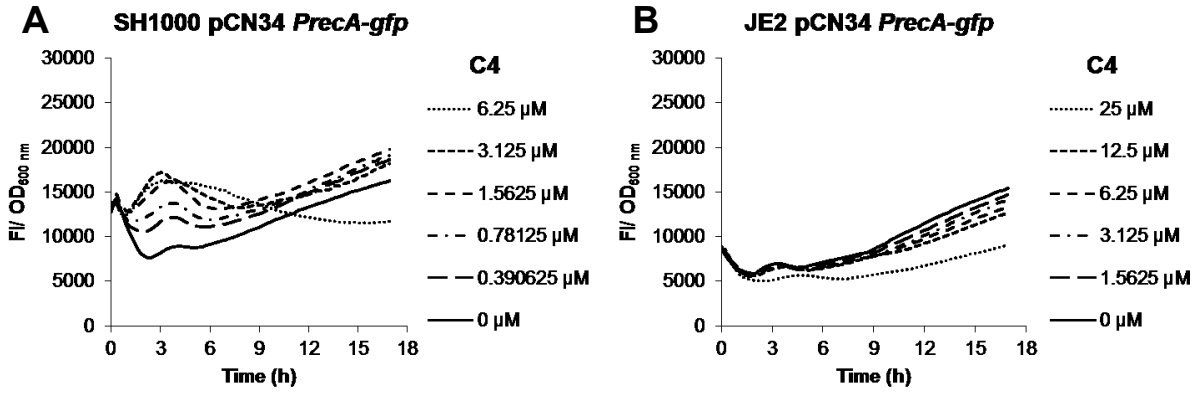

Figure 6.18. C4 induces the SOS response in *S. aureus* SH1000, but not in JE2.
S. aureus SH1000 and JE2 wild-type strains containing the pCN34 *PrecA-gfp* reporter plasmid were exposed to a range of concentrations of C4, and *recA* expression was measured over 17 h. Expression is shown relative to cell density (FI/$OD_{600\ nm}$) over time. Graphs represent the mean of three biological replicates with error bars omitted for clarification.

6.12 Discussion

Based on results from previous chapters, it was hypothesised that *S. aureus* RexAB would make a good target for novel therapeutics by promoting immune clearance and enhancing the activity of DNA-damaging antibiotics. Previously-reported AddAB inhibitors and their analogues were tested for potentiation of antibiotic activity using chequerboard MIC assays. In the initial panel of 14 compounds, results showed that 8 of these compounds potentiated the activity of ciprofloxacin or mitomycin C in *S. aureus*, with C1 displaying the greatest fold reduction in the MIC of the quinolone. However, except for CID 774021, these molecules had little to no effect on the MIC of H_2O_2. Since exposure of DNA to H_2O_2 can result in both DSBs and oxidised DNA bases, which are repaired by different repair pathways[606], it is possible that the compounds target specific DNA repair mechanisms within the cell.

The finding that these compounds potentiated the activity of antibiotics suggest that they may be clinically useful, especially as growth inhibition shown by the MIC data indicate direct entry of these compounds into the cell. When synthetic analogues of the lead compound (C1) were produced and tested using the chequerboard MIC method described above, this identified a more potent C1 derivative (C4). In the presence of this derivative, the MIC of ciprofloxacin for wild-type JE2 was reduced from 8 µg/ml to around 1-2 µg/ml. This is below the clinical breakpoint of this antibiotic, which is currently set at 2 µg/ml for a resistant *S. aureus* strain[607]. Clinical breakpoints for each antibiotic are set yearly by the European Committee on Antimicrobial Susceptibility Testing (EUCAST) to identify resistant strains and advise on patient therapy[607]. Therefore, this result showed that C4 was able to resensitise an MRSA strain (JE2) to ciprofloxacin, suggesting that combination therapy could prolong the clinical lifespan of this antibiotic.

However, enzyme activity assays with recombinant RexAB protein showed that neither C1 nor C4 target this complex. This finding differs from the report by Amundsen *et al.* (2012), who showed that C1 inhibited nuclease activities of both RecBCD and AddAB[603]. This may be due to differences in the bacterial species studied, as Amundsen *et al.* (2012) tested

C1 on the Gram-negative bacteria *E. coli* and *H. pylori*[603], whereas this study examined the effects of C1 on *S. aureus*, which is a Gram-positive bacterium.

Both C1 and C4 contain core structures from the quinolone family of antibiotics, which prevent DNA unwinding and replication by inhibiting type II topoisomerases, gyrase and topoisomerase IV activity[608]. Results showed that C1 and C4 did not affect topoisomerase IV function, but both compounds inhibited gyrase activity in a dose-dependent manner, indicating quinolone activity. However, C1 and C4 were far less active against gyrase than ciprofloxacin, meaning that the gyrase activity of C1 or C4 may not be relevant at the concentrations where an effect is seen in whole cells. In addition, the inactive control compound C13 also displayed inhibition of gyrase activity at high concentrations. Therefore, quinolone activity may only partly contribute towards C1 and C4 activity. Since *rexAB* mutants are more sensitive to these compounds, it is likely that C1 and C4 also cause DNA damage, though in the case of C1, this damage is not lethal. This was supported in part by the SOS reporter data, which showed that C4 triggered induction of the SOS response in the *S. aureus* SH1000 strain, indicating DNA damage.

Results also showed that the effect of C1 and C4 on ciprofloxacin-mediated SOS induction was dependent on the antibiotic concentration. C1 and C4 enabled the SOS response to be induced at lower concentrations of ciprofloxacin, supporting previous results that ciprofloxacin activity is potentiated. However, at higher concentrations of ciprofloxacin, these compounds inhibited SOS induction, suggesting that combination therapy could reduce the emergence of resistance by blocking SOS-induced mutagenic DNA repair[318]. In addition, the finding that SOS induction occurred in the presence of these compounds supported the data from recombinant RexAB enzyme activity assays that this complex is not the target of C1 or C4. Since RexAB is not the only protein required for SOS induction, it is possible that another SOS-related protein may be affected by these compounds, such as *recA* or *lexA*[609].

C4 has several desirable properties, including direct antibacterial activity, potentiation of ciprofloxacin activity and possibly causing DNA damage without triggering SOS in JE2, which make this compound a promising therapeutic. Future work could identify the

target(s) of C4, by performing pull-down assays to isolate proteins bound to the molecule using a modified form of the compound that enables it to be conjugated to sepharose beads. Another method would be to select for *S. aureus* strains resistant to this compound and comparing the genomic sequence of resistant mutants to the parent strain, to identify mutations in specific genes. This could be done by selecting for spontaneously-arising mutants resistant to C4.

Although *S. aureus* RexAB activity was not inhibited by the compounds tested, this enzyme complex is still a viable drug target. RecBCD/AddAB inhibitors reported so far do not appear to be highly selective or stable, and in the case of C1, which was identified by Amundsen *et al.* (2012)[603], may not be effective in all bacterial species. Future work could adapt the SOS reporter system for high-thoughput testing to more efficiently screen for *S. aureus* RexAB inhibitors, followed by testing in combination with ciprofloxacin and assessing their effect on RexAB enzyme activity. Since RexAB is not present in eukaryotes, compounds could also be tested on mammalian cell lines to determine host toxicity.

To summarise, a panel of small molecules was investigated in this chapter for the ability to inhibit *S. aureus* RexAB. C1 was identified to enhance the sensitivity and susceptibility of *S. aureus* to ciprofloxacin. In collaboration with chemists, derivatives of C1 were developed and C4 was shown to be more potent than the original hit, but it was found that potentiation of ciprofloxacin activity by these compounds was not due to *S. aureus* RexAB inhibition. However, C4 displays multiple desirable qualities with regards to antibacterial activity and SOS induction, which makes it useful for continued development towards a novel therapeutic.

7 Discussion

The rise in incidence and prevalence of antibiotic-resistant strains has meant that *S. aureus* infections have become a significant clinical and financial burden worldwide. This necessitates the development of new approaches for the prevention and treatment of infections[59]. One approach is to potentiate host defences, which can be achieved either by enhancing immunity or by blocking bacterial mechanisms of immune evasion. However, overstimulation of the immune system is potentially dangerous, because it can cause damage to host tissues[610]. Therefore, this project investigated how the immune system targets *S. aureus* so that strategies might be developed to enhance bacterial susceptibility to these host defences. Results showed that staphyloccocal DNA is a target of the host immune response. This led to the identification of a specific DNA repair component, RexAB as a potential drug target, which if inhibited would sensitise Gram-positive bacteria to immune killing by neutrophils.

7.1 DNA is a target of the neutrophil oxidative burst

Despite being the most important immune defence against *S. aureus*[140], the target of the oxidative burst of neutrophils is not well understood and there are likely to be multiple biological targets[154–156]. However, the lethal consequences of even a single DNA lesion has meant that the most significant impact of the oxidative burst is believed to be upon DNA[147,151,157–160]. The work performed in this thesis provide clear evidence that DNA is damaged by the neutrophil oxidative burst and that this damage must be repaired for *S. aureus* to survive. This was demonstrated in two physiologically-relevant contexts, *in vivo* using a murine model of systemic infection and *ex vivo* using both a whole human blood model and with purified human neutrophils. Previously, DNA damage caused by the oxidative burst had only been shown for *E. coli* and *Coxiella burnetii* when phagocytosed by macrophages[466,469]. Schlosser-Silverman *et al.* (2000) found that the rate of mutagenesis was higher in macrophage-phagocytosed *E. coli*[466], which is also likely to occur in neutrophil-phagocytosed *S. aureus* via activation of the SOS response after phagocytosis. SOS induction increases the

rate of mutagenesis by triggering expression of the DNA polymerase UmuC, which is responsible for error-prone DNA repair in *S. aureus*[318].

7.2 DNA repair is required for *S. aureus* survival during infection

In many bacteria, DSBs are repaired by homologous recombination, the first step of which involves the processing of DNA ends by either the RecBCD or AddAB (also called RexAB) helicase-nuclease complex[319,429,432]. Data from this study highlighted the importance of this complex for *S. aureus* virulence, with strains deficient in RexAB significantly attenuated for survival in mice when compared to the wild type. Previous reports have shown that loss of AddAB impairs the ability of *H. pylori* and *Campylobacter jejuni* to colonise mouse stomachs and chicken intestines respectively[463,505], and that loss of RecBC renders *Salmonella enterica* unable to establish an infection in mice[506]. These data demonstrate the importance of RecBCD and AddAB/RexAB for bacterial pathogenicity. The key role of RexAB in DNA repair also identifies DSBs as a potentially lethal type of DNA damage induced by the host immune response. This correlates with the report that DSBs are among the DNA lesions found in *E. coli* cells phagocytosed by macrophages[466].

In addition to RexAB, the screen of *S. aureus* DNA repair mutants identified RecF and RecA as important for survival in whole human blood. Whilst RecA has well-defined roles in SOS induction and recombinational repair[319,323,430], the role of RecF in *S. aureus* is less clear. In *B. subtilis,* loading of RecA onto the AddAB-processed ssDNA overhang is performed by the RecFOR complex, which is believed to be conserved in *S. aureus*[437,438]. In addition, the RecF pathway is able to compensate for loss of RecBCD activity in *E. coli recBC sbcBC* mutants[507–509]. However, this may not be the case with AddAB. Marsin *et al.* (2010) found that in contrast to the *E. coli* model, the RecF pathway cannot compensate for loss of AddAB activity in *H. pylori*[510]. Future experiments could determine the relative importance of RecF and RexAB in *S. aureus* by examining the susceptibility of *recF rexAB* triple mutants to neutrophil killing, in comparison to *recF* or *rexAB* mutants.

7.3 RexAB as a potential drug target

The importance of RexAB for *S. aureus* survival during infection makes the complex a potential target for new therapeutics. Inhibition of DNA repair via RexAB would promote immune clearance of *S. aureus* in the host and potentiate the action of DNA-damaging antibiotics. Inhibition of RexAB would also block the mutagenic SOS response, potentially slowing the rate of host adaptation and the acquisition of antibiotic resistance[598]. Furthermore, homologues of RexAB are not present in eukaryotes, reducing the likelihood of host toxicity. In eukaryotes, processing of DSB ends is mediated by separate helicase and nuclease enzymes, rather than a single helicase-nuclease complex[611]. In humans, DNA unwinding is performed by one of two helicases (Bloom or Werner), and DNA degradation carried out by the DNA2 nuclease[611].

Several studies have examined various aspects of bacterial DNA repair as targets for the discovery and development of new antibiotics[612–618]. However, the redundancy of these diverse DNA repair pathways has made it difficult to identify suitable targets. Special attention has been given to inhibition of the SOS response, which is responsible for induction of excision repair, recombinational repair and DNA mutagenesis. Most of these studies use *E. coli* as a model, targeting LexA or RecA[615,617,618]. Phthalocyanine tetrasulphonic acid (PcT)-based RecA inhibitors block SOS induction in *E. coli* and inhibited acquisition of ciprofloxacin resistance in a neutrapenic murine thigh infection model, demonstrating the potential effectiveness of targeting the SOS response[615]. However, RecA homologues are present in humans (Rad51 and Dmc1)[619], meaning that inhibitors of RecA may exhibit host toxicity.

Regarding SOS suppression in *S. aureus,* a report by Peng *et al.* (2011) found that baicalein, the main component of the Chinese herb *Scutellaria baicalensis*, inhibited expression of several SOS genes (*recA, lexA, umuC*)[464]. This effect correlated with a reduction in intracellular ATP production, suggesting that baicalein may act on ATP synthase. Another study identified an additional effect of novobiocin in suppressing the ciprofloxacin-induced SOS response in *S. aureus* by inhibiting *recA* expression[620]. Since novobiocin is an

aminocoumarin, a class of antibiotics that inhibit DNA gyrase without inducing DSBs, this finding suggests that clinical re-evaluation of existing antibiotics may help to combat the development of antibiotic resistance[620]. More recently, Carvalho *et al.* (2019) found that betulinic acid, a plant-derived triterpenoid, reduced ciprofloxacin-induced activation of the SOS response and potentiated ciprofloxacin activity in *S. aureus*[621].

Inhibitors of RecBCD and/or AddAB have also been reported. RecBCD inhibitors include dozelesin, ecteinascidin 743, hedamycin, cisplatin, psoralen and the Gam protein of bacteriophage lambda[599–602]. However, issues with these inhibitors include limited *in vivo* stability, poor oral bioavailability and a sub-optimal mechanism of action such as DNA alkylation, making them unselective and highly cytotoxic[599–602]. A screen of 326,100 small molecules by Amundsen *et al.* (2012) identified 21 potent inhibitors of *E. coli* RecBCD and *H. pylori* AddAB[603], of which a selection were tested in this thesis to investigate their effects on *S. aureus* RexAB. This identified one compound, C1, that potentiates ciprofloxacin activity and modulates ciprofloxacin-mediated SOS induction in *S. aureus*. However, C1 had no effect on *S. aureus* RexAB enzyme activity, indicating an alternative mechanism of action.

For treating *S. aureus* infections, RexAB inhibitors could be used as monotherapy for superficial infections in otherwise healthy patients, or in combination with ciprofloxacin or other antibiotics for invasive infections. RexAB inhibition may also reverse resistance to ciprofloxacin, providing an additional therapeutic against MRSA strains, many of which are resistant to fluoroquinolone antibiotics[63]. Furthermore, since RexAB is not essential for bacterial growth, inhibitors of this complex would be expected to affect only pathogenic bacteria that are targeted by the immune response, reducing undesired damage to the commensal gut microbiota and the risk of opportunistic secondary infections, unlike conventional antibiotic therapy[595].

7.3.1 Is targeting DNA repair via RexAB a broad-spectrum approach?

The emergence of antibiotic-resistant strains has made it increasingly difficult to find effective treatments for patients, such that multidrug-resistant bacteria are responsible for up to 16% of

all hospital-acquired infections in the world[622]. In particular, the ESKAPE pathogens (*Enterococcus faecium*, *S. aureus*, *Klebsiella pneumoniae*, *Acinetobacter baumannii*, *Pseudomonas aeruginosa* and *Enterobacter* spp.) are responsible for the majority of hospital infections and are associated with the highest risk of mortality[622].

The work in this thesis has shown that DNA repair via RexAB is essential for *S. aureus* survival during infection and has potential as a drug target in this pathogen. *S. aureus* RexAB is a member of the RecBCD/AddAB family of helicase-nucleases, which is present in over 90% of sequenced bacteria[537]. Therefore, inhibition of the RecBCD/AddAB complex has potential as a therapeutic approach for infections caused by Gram-positive and Gram-negative pathogens, especially as four out of the six ESKAPE pathogens are Gram negative, and new antibiotics that target these bacteria are greatly needed[622,623]. Although results from this study showed that RexAB is required for survival of the Gram-positive pathogens *S. gordonii* and *E. faecalis* in whole human blood, the role of RecBCD during infection still needs to be investigated. Future experiments could determine whether RecBCD is needed for bacterial survival of the oxidative burst, such that RecBCD and AddAB enzymes form a conserved defence against immune killing.

7.4 Summary

In summary, staphylococcal DNA is a target of the oxidative burst of neutrophils. Repair of DNA damage via the RexAB helicase-nuclease complex is essential for infection and therefore represents a novel drug target, with a number of potentially druggable activities. Additional work identified a novel compound that potentiated ciprofloxacin activity in Gram-positive and Gram-negative pathogens, such that a resistant *S. aureus* strain was resensitised to the antibiotic. Future work will focus on developing inhibitors of RexAB towards clinical applications.

7.5 Future work

The discovery that DNA repair via RexAB is essential for *S. aureus* survival during infection and the identification of a novel compound that resensitises MRSA to ciprofloxacin raises several key questions and potential areas for future research. In particular:

1. Does DNA repair protect Gram-negative bacteria against immune killing?
2. Does DNA repair protect against different classes of antibiotics?
3. Further investigation of RexAB expression and function
4. What is the target of C4?
5. Development of RexAB inhibitors

7.5.1 Does DNA repair protect Gram-negative bacteria against immune killing?

The results described in Chapters 3 and 4 show that DNA repair protects the Gram-positive pathogens *S. aureus, S. gordonii* and *E. faecalis* against killing by neutrophils. However, it is unclear whether DNA repair is similarly important for the survival of Gram-negative bacteria during interactions with host immunity.

To test this, the assays described in Chapters 3 and 4 could be performed on a selection of DNA repair mutants from two Gram-negative species, *E. coli* and *P. aeruginosa*, chosen due to their clinical importance and slightly different mechanisms of DSB repair. Whilst both species have recombinational repair, *P. aeruginosa* also has the NHEJ pathway[421–424]. DNA repair mutants (*recA, lexA, recBCD* and *recFOR*) would be obtained from the *E. coli* Keio Knockout Collection and the *P. aeruginosa* PA14 Transposon Insertion Library[450,624]. As the RecF pathway is able to compensate for loss of RecBCD activity in *E. coli recBC sbcBC* mutants[507–509], both *recBCD/recB* and *recFOR/recF* mutants should be examined.

To determine the role of DNA repair in immune killing, wild-type and mutant strains would be subjected to the *ex vivo* whole human blood model (with or without DPI to block the oxidative burst) and bacterial survival measured as described previously. Strains would also be exposed to H_2O_2 to directly assess susceptibility to ROS-mediated DNA damage, and to purified neutrophils (with or without DPI and/or cytochalasin D to inhibit phagocytosis,

described previously) to assess the importance of neutrophil-mediated killing in the bloodstream.

7.5.2 Does DNA repair protect *S. aureus* against different classes of antibiotics?

In the host, pathogens are subjected to the twin theat of the immune system and antibiotic treatment. The results described in this thesis show that DNA repair protects *S. aureus* against killing by the immune system and by DNA-damaging antibiotics such as ciprofloxacin. In 2007, Kohanski *et al.* proposed that several different classes of bactericidal antibiotics trigger endogenous ROS production, which contributes to bacterial killing independent of their drug-target interactions[493]. Whilst controversial, this work has since been supported and extended by multiple independent lines of evidence[494–501]. Therefore, it is hypothesised that DNA repair protects against multiple classes of antibiotics.

To test this hypothesis, future work could determine whether different classes of antibiotics damage DNA and whether inhibition of RexAB sensitises *S. aureus* to both antibiotic and immune killing. Firstly, to determine whether loss of RexAB affects *S. aureus* growth in the presence of antibiotics, MIC assays would be performed on wild-type and *rexAB* mutant strains using a selection of different antibiotics. These should include clinically-relevant antibiotics such as cloxacillin and vancomycin, as well as representatives from different antibiotic classes, including cephalosporins (ceftazidime, ceftaroline), sulphonamides (co-trimoxazole), aminoglycosides (gentamicin) and the lipopeptide daptomycin. Next, *S. aureus* wild-type and *rexAB* mutant strains would be exposed to these antibiotics at 10x MIC and bacterial survival measured over time. This would determine whether loss of RexAB makes *S. aureus* more susceptible to antibiotic killing. If this is the case, then this would provide evidence that the antibiotic causes DNA damage, such that DNA repair is required for survival. To determine whether antibiotic-induced DNA damage is caused by ROS, experiments could be repeated under anaerobic conditions. Experiments would be performed on *S. aureus* SH1000 and JE2 to account for differences in antibiotic susceptibility between strains.

7.5.3 Further investigation into RexAB expression and function

The results in Chapter 5 demonstrate that *S. aureus* RexAB is a functional member of the RecBCD/AddAB family of helicase-nuclease complexes. Although the end-processing function of these complexes is well known[319,429,432], some aspects of RexAB expression and function are less well understood. The regulatory profile of RexAB in response to DNA-damaging stress is uncharacterised and it is unclear how DSBs are recognised by *S. aureus* RexAB. Therefore, future work will aim to address these gaps in our knowledge.

In *E. coli,* expression of the RecBCD enzyme is extremely low, at about 10 molecules of the enzyme per cell, and the natural promoters of the *recBCD* genes are apparently constitutive[625]. In contrast, Mertens *et al.* (2008) showed that expression of *addAB* in *Coxiella burnetii* is induced by oxidative stress[469]. However, unlike most AddAB-containing bacteria, *C. burnetii* lacks key components of the SOS response (*lexA*, *umuCD, polB, dinB*)[469]. Therefore, to determine whether RexAB expression is inducible in *S. aureus*, mRNA and protein expression levels could be measured in the presence and absence of ciprofloxacin, H_2O_2 or purified neutrophils. This would be achieved using quantitative reverse-transcription PCR (qRT-PCR) to measure mRNA levels, and/or by generating *S. aureus* strains expressing RexAB-GFP fusions to measure protein expression levels (since the results from Chapter 3 showed that native RexAB protein levels could not be accurately detected by Western blot).

In *B. subtilis,* DSBs are recognised by RecN, which binds to the break and recruits AddAB for end processing[430,431]. However, DSB recognition is poorly characterised in other bacteria[430]. It is unclear whether RecN is also required by *S. aureus* to recognise DSBs or whether DSBs are recognised directly by RexAB within the cell. Initially, a *recN*-deficient mutant would be examined to determine if it is more susceptible to the oxidative burst and ciprofloxacin. If that indicated a role for RecN in DSB repair, an interaction with RexAB would be investigated by generating *S. aureus* strains expressing RecN-YFP and RexAB-GFP and comparing the localisation of these proteins at 0.5, 1, 2 and 3 h after exposure to ciprofloxacin using fluorescence microscopy, similar to that described for *B. subtilis*[431,592]. If RecN is required for DSB recognition, RecN-YFP foci will be expected to form within 30 min of exposure to the

antibiotic. If RecN is required for RexAB recruitment, then these two proteins will be expected to co-localise within the cell.

7.5.4 What is the target of C4?

The results in Chapter 6 describe the identification of a novel compound (named C4) that exhibited direct antibacterial activity and potentiated ciprofloxacin activity, such that antibiotic resistance was reversed in an MRSA strain. Characterisation of C4 using direct enzyme assays indicated quinolone activity. However, C4 was far less active than for ciprofloxacin, suggesting that this activity may not be relevant at the concentrations used in whole cells for growth inhibition. Therefore, the main target of C4 is still unknown.

Future work would seek to identify this target by using a modified form of C4 that enables conjugation to sepharose beads and performing pull-down assays on whole-cell mixtures to isolate proteins bound to the compound. This would be followed by proteomic analysis, such as liquid chomatography–mass spectrometry (LC-MS), to identify extracted proteins[626]. Another method to identify target proteins is the use of photoaffinity probes, where a photoreactive group attached to C4 will covalently bind the target in response to UV light, providing a more stable interaction for proteomic analysis[627]. Finally, spontaneously-arising mutants that are resistant to C4 could be selected for and sequenced to identify mutations in specific genes. If the mutation is in the active site of the target protein, then further testing will be carried out to confirm this interaction, including chequerboard assays with ciprofloxacin and C4, and complementation of the gene to restore the wild-type phenotype.

7.5.5 Development of RexAB inhibitors

Results from this thesis identify RexAB as a potential drug target. Therefore, future work will aim to develop inhibitors of RexAB using the assays developed during this project as tools for whole-cell screening and *in vitro* enzyme activity confirmation.

High-thoughput screening of small-molecule libraries would be carried out using ciprofloxacin and the *S. aureus* wild-type *PrecA-gfp* reporter strain, after optimisation of the assay for a high-thoughput application. By measuring absorbance at 600 nm and expression

of *recA* via GFP fluorescence, this screen would identify compounds that inhibit the ciprofloxacin-induced SOS response, which would be expected to be due to inhibition of RexAB or RecA. Next, a secondary screen would be performed to confirm these hits using the recombinant RexAB enzyme assays, which would then be followed by chequerboard MIC assays (ciprofloxacin and the hit) in the wild type and *rexAB* mutant. Whilst synergy between compound and ciprofloxacin would be expected for the wild type, no such synergy should be observed in the *rexB* mutant.

Hits from these screens will prioritised based on activity and chemical tractability, after which structure-activity relationship (SAR) analysis would be performed on the prioritised molecules. In this process, the nature and positions of substituents are modified using the Topliss decision tree, which was developed to guide the choice of substituents to identify the most potent compounds[628]. The effects on inhibitor potency would then be assessed using the assays described above. Iterative rounds of chemical modification and biological assays would result in the generation of the most effective compound. Activity of the optimised compounds would be tested against clinical isolates and other bacterial species (*S. gordonii, E. faecalis, E. coli, P. aeruginosa*) using chequerboard MIC assays, after which the toxicity of these compounds will be assessed on mammalian cell lines, liver microsomes and animals.

If compounds are generated that are active against bacteria and non-toxic to mammalian cells, they would be assessed in *ex vivo* systems such as whole human blood and purified neutrophils to determine whether they sensitise *S. aureus* and other bacteria to neutrophil-mediated killing. Subsequently, animal infection models would be used to understand compound efficacy *in vivo*.

In summary, there is sufficient evidence to suggest that small-molecule inhibitors of RexAB may have therapeutic value by sensitising *S. aureus* and other pathogens to neutrophils. Such inhibitors would constitute a novel class of antibacterial therapeutic and help address the growing theat of antibiotic resistance.

References

1. Schleifer K-H, Bell JA. Family VIII. Staphylococcaceae fam. nov. In: *Bergey's Manual of Systematic Bacteriology*. Springer; 2009:392.
2. Ogston A. Micrococcus Poisoning. *J Anat Physiol*. 1882;17(Pt 1):24-58.
3. Orenstein A. The discovery and naming of *Staphylococcus aureus*. Antimicrobe. http://www.antimicrobe.org/h04c.files/history/S-aureus.pdf. Published 2011. Accessed July 16, 2019.
4. Liu GY, Essex A, Buchanan JT, et al. *Staphylococcus aureus* golden pigment impairs neutrophil killing and promotes virulence through its antioxidant activity. *J Exp Med*. 2005;202(2):209-215. doi:10.1084/jem.20050846
5. Kuroda M, Ohta T, Uchiyama I, et al. Whole genome sequencing of meticillin-resistant *Staphylococcus aureus*. *Lancet*. 2001;357(9264):1225-1240. doi:10.1016/S0140-6736(00)04403-2
6. Fitzgerald JR, Holden MTG. Genomics of natural populations of *Staphylococcus aureus*. *Annu Rev Microbiol*. 2016;70(1):459-478. doi:10.1146/annurev-micro-102215-095547
7. Lindsay JA. *Staphylococcus aureus* genomics and the impact of horizontal gene transfer. *Int J Med Microbiol*. 2014;304(2):103-109. doi:10.1016/J.IJMM.2013.11.010
8. Lowy FD. *Staphylococcus aureus* infections. *N Engl J Med*. 1998;339(8):520-532. doi:10.1056/NEJM199808203390806
9. Chapman GH. The significance of sodium chloride in studies of staphylococci. *J Bacteriol*. 1945;50(2):201-203.
10. Wertheim HFL, Melles DC, Vos MC, et al. The role of nasal carriage in *Staphylococcus aureus* infections. *Lancet Infect Dis*. 2005;5(12):751-762. doi:10.1016/S1473-3099(05)70295-4
11. Edwards AM, Massey RC, Clarke SR. Molecular mechanisms of *Staphylococcus aureus* nasopharyngeal colonization. *Mol Oral Microbiol*. 2012;27(1):1-10. doi:10.1111/j.2041-1014.2011.00628.x
12. van Belkum A, Verkaik NJ, de Vogel CP, et al. Reclassification of *Staphylococcus aureus* nasal carriage types. *J Infect Dis*. 2009;199(12):1820-1826. doi:10.1086/599119
13. Verhoeven PO, Gagnaire J, Botelho-Nevers E, et al. Detection and clinical relevance of *Staphylococcus aureus* nasal carriage: an update. *Expert Rev Anti Infect Ther*. 2014;12(1):75-89. doi:10.1586/14787210.2014.859985
14. Lebon A, Labout JAM, Verbrugh HA, et al. Dynamics and determinants of *Staphylococcus aureus* carriage in infancy: the Generation R Study. *J Clin Microbiol*. 2008;46(10):3517-3521. doi:10.1128/JCM.00641-08
15. Peacock SJ, Justice A, Griffiths D, et al. Determinants of acquisition and carriage of *Staphylococcus aureus* in infancy. *J Clin Microbiol*. 2003;41(12):5718-5725. doi:10.1128/jcm.41.12.5718-5725.2003
16. Wertheim HFL, Kleef M van, Vos MC, Ott A, Verbrugh HA, Fokkens W. Nose picking and nasal carriage of *Staphylococcus aureus*. *Infect Control Hosp Epidemiol*. 2006;27(08):863-867. doi:10.1086/506401
17. Tong SYC, Davis JS, Eichenberger E, Holland TL, Fowler VG. *Staphylococcus aureus* infections: epidemiology, pathophysiology, clinical manifestations, and management. *Clin Microbiol Rev*. 2015;28(3):603-661. doi:10.1128/CMR.00134-14
18. Corrigan RM, Miajlovic H, Foster TJ. Surface proteins that promote adherence of *Staphylococcus aureus* to human desquamated nasal epithelial cells. *BMC Microbiol*. 2009;9(1):22. doi:10.1186/1471-2180-9-22
19. Quinn GA, Cole AM. Suppression of innate immunity by a nasal carriage strain of *Staphylococcus aureus* increases its colonization on nasal epithelium. *Immunology*.

2007;122(1):80-89. doi:10.1111/J.1365-2567.2007.02615.X

20. Mulcahy ME, Geoghegan JA, Monk IR, et al. Nasal colonisation by *Staphylococcus aureus* depends upon clumping factor B binding to the squamous epithelial cell envelope protein loricrin. Peschel A, ed. *PLoS Pathog*. 2012;8(12):e1003092. doi:10.1371/journal.ppat.1003092

21. Wertheim HFL, Walsh E, Choudhurry R, et al. Key role for clumping factor B in *Staphylococcus aureus* nasal colonization of humans. Chambers H, ed. *PLoS Med*. 2008;5(1):e17. doi:10.1371/journal.pmed.0050017

22. von Eiff C, Becker K, Machka K, Stammer H, Peters G. Nasal carriage as a source of *Staphylococcus aureus* bacteremia. *N Engl J Med*. 2001;344(1):11-16. doi:10.1056/NEJM200101043440102

23. Ki V, Rotstein C. Bacterial skin and soft tissue infections in adults: A review of their epidemiology, pathogenesis, diagnosis, treatment and site of care. *Can J Infect Dis Med Microbiol*. 2008;19(2):173-184. doi:10.1155/2008/846453

24. Kobayashi SD, Malachowa N, DeLeo FR. Pathogenesis of *Staphylococcus aureus* abscesses. *Am J Pathol*. 2015;185(6):1518-1527. doi:10.1016/j.ajpath.2014.11.030

25. Stryjewski ME, Chambers HF. Skin and soft-tissue infections caused by community-acquired methicillin-resistant *Staphylococcus aureus*. *Clin Infect Dis*. 2008;46(S5):S368-S377. doi:10.1086/533593

26. Dryden MS. Complicated skin and soft tissue infection. *J Antimicrob Chemother*. 2010;65(Supplement 3):iii35-iii44. doi:10.1093/jac/dkq302

27. Foster TJ, Geoghegan JA, Ganesh VK, Höök M. Adhesion, invasion and evasion: the many functions of the surface proteins of *Staphylococcus aureus*. *Nat Rev Microbiol*. 2014;12(1):49-62. doi:10.1038/nrmicro3161

28. Paharik AE, Horswill AR. The staphylococcal biofilm: adhesins, regulation, and host response. In: *Virulence Mechanisms of Bacterial Pathogens, Fifth Edition*. Vol 4. American Society of Microbiology; 2016:529-566. doi:10.1128/microbiolspec.VMBF-0022-2015

29. Thwaites GE, Edgeworth JD, Gkrania-Klotsas E, et al. Clinical management of *Staphylococcus aureus* bacteraemia. *Lancet Infect Dis*. 2011;11(3):208-222. doi:10.1016/S1473-3099(10)70285-1

30. Diekema DJ, Hsueh P-R, Mendes RE, et al. The microbiology of bloodstream infection: 20-Year trends from the SENTRY antimicrobial surveillance program. *Antimicrob Agents Chemother*. 2019;63(7):e00355-19. doi:10.1128/AAC.00355-19

31. Wyllie DH, Crook DW, Peto TEA. Mortality after *Staphylococcus aureus* bacteraemia in two hospitals in Oxfordshire, 1997-2003: cohort study. *BMJ*. 2006;333(7562):281. doi:10.1136/bmj.38834.421713.2F

32. Thomer L, Schneewind O, Missiakas D. Pathogenesis of *Staphylococcus aureus* Bloodstream Infections. *Annu Rev Pathol Mech Dis*. 2016;11(1):343-364. doi:10.1146/annurev-pathol-012615-044351

33. van Hal SJ, Jensen SO, Vaska VL, Espedido BA, Paterson DL, Gosbell IB. Predictors of mortality in *Staphylococcus aureus* bacteremia. *Clin Microbiol Rev*. 2012;25(2):362-386. doi:10.1128/CMR.05022-11

34. Wertheim HF, Vos MC, Ott A, et al. Risk and outcome of nosocomial *Staphylococcus aureus* bacteraemia in nasal carriers versus non-carriers. *Lancet*. 2004;364(9435):703-705. doi:10.1016/S0140-6736(04)16897-9

35. Fowler VG, Olsen MK, Corey GR, et al. Clinical identifiers of complicated *Staphylococcus aureus* bacteremia. *Arch Intern Med*. 2003;163(17):2066. doi:10.1001/archinte.163.17.2066

36. Kaasch AJ, Barlow G, Edgeworth JD, et al. *Staphylococcus aureus* bloodstream infection: A pooled analysis of five prospective, observational studies. *J Infect*. 2014;68(3):242-251. doi:10.1016/J.JINF.2013.10.015

37. Lodise TP, McKinnon PS, Swiderski L, Rybak MJ. Outcomes analysis of delayed antibiotic treatment for hospital-acquired *Staphylococcus aureus* bacteremia. *Clin Infect Dis*.

2003;36(11):1418-1423. doi:10.1086/375057

38. Paul M, Kariv G, Goldberg E, et al. Importance of appropriate empirical antibiotic therapy for methicillin-resistant *Staphylococcus aureus* bacteraemia. *J Antimicrob Chemother*. 2010;65(12):2658-2665. doi:10.1093/jac/dkq373

39. Marchaim D, Kaye KS, Fowler VG, et al. Case–control study to identify factors associated with mortality among patients with methicillin-resistant *Staphylococcus aureus* bacteraemia. *Clin Microbiol Infect*. 2010;16(6):747-752. doi:10.1111/J.1469-0691.2009.02934.X

40. Joint Formulary Committee. British National Formulary. BMJ Group and Pharmaceutical Press. http://www.medicinescomplete.com. Published 2018. Accessed July 24, 2019.

41. Rayner C, Munckhof WJ. Antibiotics currently used in the treatment of infections caused by *Staphylococcus aureus*. *Intern Med J*. 2005;35(s2):S3-S16. doi:10.1111/j.1444-0903.2005.00976.x

42. Kaplan SL, Mason EO, Feigin RD. Clindamycin versus nafcillin or methicillin in the treatment of *Staphylococcus aureus* osteomyelitis in children. *South Med J*. 1982;75(2):138-142. doi:10.1097/00007611-198202000-00005

43. Ardati KO, Thirumoorthi MC, Dajani AS. Intravenous trimethoprim-sulfamethoxazole in the treatment of serious infections in children. *J Pediatr*. 1979;95(5):801-806. doi:10.1016/S0022-3476(79)80740-4

44. Levine DP, Fromm BS, Reddy BR. Slow response to vancomycin or vancomycin plus rifampin in methicillin-resistant *Staphylococcus aureus* endocarditis. *Ann Intern Med*. 1991;115(9):674. doi:10.7326/0003-4819-115-9-674

45. Liu C, Bayer A, Cosgrove SE, et al. Clinical practice guidelines by the Infectious Diseases Society of America for the treatment of methicillin-resistant *Staphylococcus aureus* infections in adults and children. *Clin Infect Dis*. 2011;52(3):e18-e55. doi:10.1093/cid/ciq146

46. Corey GR. *Staphylococcus aureus* bloodstream infections: definitions and treatment. *Clin Infect Dis*. 2009;48(s4):S254-S259. doi:10.1086/598186

47. Fowler VG, Boucher HW, Corey GR, et al. Daptomycin versus standard therapy for bacteremia and endocarditis caused by *Staphylococcus aureus*. *N Engl J Med*. 2006;355(7):653-665. doi:10.1056/NEJMoa053783

48. Diggins FW. The true history of the discovery of penicillin, with refutation of the misinformation in the literature. *Br J Biomed Sci*. 1999;56(2):83-93.

49. Tipper DJ, Strominger JL. Mechanism of action of penicillins: a proposal based on their structural similarity to acyl-D-alanyl-D-alanine. *Proc Natl Acad Sci U S A*. 1965;54(4):1133-1141. doi:10.1073/pnas.54.4.1133

50. Yocum RR, Amanuma H, O'Brien TA, Waxman DJ, Strominger JL. Penicillin is an active-site inhibitor for four genera of bacteria. *J Bacteriol*. 1982;149(3):1150-1153.

51. Stapleton PD, Taylor PW. Methicillin resistance in *Staphylococcus aureus*: mechanisms and modulation. *Sci Prog*. 2002;85(1):57-72. doi:10.3184/003685002783238870

52. Peacock SJ, Paterson GK. Mechanisms of Methicillin Resistance in *Staphylococcus aureus*. *Annu Rev Biochem*. 2015;84(1):577-601. doi:10.1146/annurev-biochem-060614-034516

53. Skinner D, Keefer CS. Significance of bacteraemia caused by *Staphylococcus aureus*. *Arch Intern Med*. 1941;68(5):851. doi:10.1001/archinte.1941.00200110003001

54. Rammelkamp CH, Maxon T. Resistance of *Staphylococcus aureus* to the action of penicillin. *Exp Biol Med*. 1942;51(3):386-389. doi:10.3181/00379727-51-13986

55. Kirby WM. Extraction of a highly potent inactivator from penicillin resistant Staphylococci. *Science (80-)*. 1944;99(2579):452-453. doi:10.1126/science.99.2579.452

56. Lowy FD. Antimicrobial resistance: the example of *Staphylococcus aureus*. *J Clin Invest*. 2003;111(9):1265-1273. doi:10.1172/JCI18535

57. Bondi A, Dietz CC. Penicillin Resistant Staphylococci. *Exp Biol Med*. 1945;60(1):55-58. doi:10.3181/00379727-60-15089

58. Barber M. Methicillin-resistant staphylococci. *J Clin Pathol*. 1961;14(4):385-393. doi:10.1136/jcp.14.4.385

59. Grundmann H, Aires-de-Sousa M, Boyce J, Tiemersma E. Emergence and resurgence of meticillin-resistant *Staphylococcus aureus* as a public-health threat. *Lancet*. 2006;368(9538):874-885. doi:10.1016/S0140-6736(06)68853-3

60. Katayama Y, Ito T, Hiramatsu K. A new class of genetic element, staphylococcus cassette chromosome mec, encodes methicillin resistance in *Staphylococcus aureus*. *Antimicrob Agents Chemother*. 2000;44(6):1549-1555. doi:10.1128/aac.44.6.1549-1555.2000

61. Hartman BJ, Tomasz A. Low-affinity penicillin-binding protein associated with beta-lactam resistance in *Staphylococcus aureus*. *J Bacteriol*. 1984;158(2):513-516.

62. International Working Group on the Classification of Staphylococcal Cassette Chromosome Elements (IWG-SCC) IWG on the C of SCCE. Classification of staphylococcal cassette chromosome mec (SCCmec): guidelines for reporting novel SCCmec elements. *Antimicrob Agents Chemother*. 2009;53(12):4961-4967. doi:10.1128/AAC.00579-09

63. Uhlemann A-C, Otto M, Lowy FD, DeLeo FR. Evolution of community- and healthcare-associated methicillin-resistant *Staphylococcus aureus*. *Infect Genet Evol*. 2014;21:563-574. doi:10.1016/J.MEEGID.2013.04.030

64. Boye K, Bartels MD, Andersen IS, Møller JA, Westh H. A new multiplex PCR for easy screening of methicillin-resistant *Staphylococcus aureus* SCCmec types I–V. *Clin Microbiol Infect*. 2007;13(7):725-727. doi:10.1111/J.1469-0691.2007.01720.X

65. European Centre for Disease Prevention and Control (ECDC)/ European Medicines Agency (EMA). *The Bacterial Challenge: Time to React*. doi:10.2900/2518

66. Wyllie D, Paul J, Crook D. Waves of trouble: MRSA strain dynamics and assessment of the impact of infection control. *J Antimicrob Chemother*. 2011;66(12):2685-2688. doi:10.1093/jac/dkr392

67. Turner NA, Sharma-Kuinkel BK, Maskarinec SA, et al. Methicillin-resistant *Staphylococcus aureus*: an overview of basic and clinical research. *Nat Rev Microbiol*. 2019;17(4):203-218. doi:10.1038/s41579-018-0147-4

68. Stefani S, Chung DR, Lindsay JA, et al. Meticillin-resistant *Staphylococcus aureus* (MRSA): global epidemiology and harmonisation of typing methods. *Int J Antimicrob Agents*. 2012;39(4):273-282. doi:10.1016/J.IJANTIMICAG.2011.09.030

69. Voyich JM, Braughton KR, Sturdevant DE, et al. Insights into mechanisms used by *Staphylococcus aureus* to avoid destruction by human neutrophils. *J Immunol*. 2005;175(6):3907-3919. doi:10.4049/JIMMUNOL.175.6.3907

70. Uhlemann A-C, Knox J, Miller M, et al. The environment as an unrecognized reservoir for community-associated methicillin resistant *Staphylococcus aureus* USA300: A case-control study. Otto M, ed. *PLoS One*. 2011;6(7):e22407. doi:10.1371/journal.pone.0022407

71. David MZ, Daum RS. Community-associated methicillin-resistant *Staphylococcus aureus*: epidemiology and clinical consequences of an emerging epidemic. *Clin Microbiol Rev*. 2010;23(3):616-687. doi:10.1128/CMR.00081-09

72. Otto M. Community-associated MRSA: What makes them special? *Int J Med Microbiol*. 2013;303(6-7):324-330. doi:10.1016/J.IJMM.2013.02.007

73. Collins J, Rudkin J, Recker M, Pozzi C, O'Gara JP, Massey RC. Offsetting virulence and antibiotic resistance costs by MRSA. *ISME J*. 2010;4(4):577-584. doi:10.1038/ismej.2009.151

74. Thurlow LR, Joshi GS, Richardson AR. Virulence strategies of the dominant USA300 lineage of community-associated methicillin-resistant *Staphylococcus aureus* (CA-MRSA). *FEMS Immunol Med Microbiol*. 2012;65(1):5-22. doi:10.1111/J.1574-695X.2012.00937.X

75. Chambers HF, DeLeo FR. Waves of resistance: *Staphylococcus aureus* in the antibiotic era. *Nat Rev Microbiol*. 2009;7(9):629-641. doi:10.1038/nrmicro2200

76. García-Álvarez L, Holden MTG, Lindsay H, et al. Meticillin-resistant *Staphylococcus aureus* with a novel *mecA* homologue in human and bovine populations in the UK and Denmark: a

descriptive study. *Lancet Infect Dis*. 2011;11(8):595-603. doi:10.1016/S1473-3099(11)70126-8

77. Smith TC, Pearson N. The emergence of *Staphylococcus aureus* ST398. *Vector-Borne Zoonotic Dis*. 2011;11(4):327-339. doi:10.1089/vbz.2010.0072

78. Price LB, Stegger M, Hasman H, et al. *Staphylococcus aureus* CC398: host adaptation and emergence of methicillin resistance in livestock. *MBio*. 2012;3(1):e00305-11. doi:10.1128/mBio.00305-11

79. Smith EM, Green LE, Medley GF, et al. Multilocus sequence typing of intercontinental bovine *Staphylococcus aureus* isolates. *J Clin Microbiol*. 2005;43(9):4737-4743. doi:10.1128/JCM.43.9.4737-4743.2005

80. Hiramatsu K, Aritaka N, Hanaki H, et al. Dissemination in Japanese hospitals of strains of *Staphylococcus aureus* heterogeneously resistant to vancomycin. *Lancet*. 1997;350(9092):1670-1673. doi:10.1016/S0140-6736(97)07324-8

81. Howden BP, Davies JK, Johnson PDR, Stinear TP, Grayson ML. Reduced vancomycin susceptibility in *Staphylococcus aureus*, including vancomycin-intermediate and heterogeneous vancomycin-intermediate strains: resistance mechanisms, laboratory detection, and clinical implications. *Clin Microbiol Rev*. 2010;23(1):99-139. doi:10.1128/CMR.00042-09

82. Watanakunakorn C. Mode of action and in-vitro activity of vancomycin. *J Antimicrob Chemother*. 1984;14(suppl D):7-18. doi:10.1093/jac/14.suppl_D.7

83. Weigel LM, Clewell DB, Gill SR, et al. Genetic analysis of a high-level vancomycin-resistant isolate of Staphylococcus aureus. *Science (80-)*. 2003;302(5650):1569-1571. doi:10.1126/science.1090956

84. Hiramatsu K, Hanaki H, Ino T, Yabuta K, Oguri T, Tenover FC. Methicillin-resistant *Staphylococcus aureus* clinical strain with reduced vancomycin susceptibility. *J Antimicrob Chemother*. 1997;40(1):135-136. doi:10.1093/jac/40.1.135

85. Hiramatsu K, Kayayama Y, Matsuo M, et al. Vancomycin-intermediate resistance in *Staphylococcus aureus*. *J Glob Antimicrob Resist*. 2014;2(4):213-224. doi:10.1016/J.JGAR.2014.04.006

86. Hanaki H, Kuwahara-Arai K, Boyle-Vavra S, Daum RS, Labischinski H, Hiramatsu K. Activated cell-wall synthesis is associated with vancomycin resistance in methicillin-resistant *Staphylococcus aureus* clinical strains Mu3 and Mu50. *J Antimicrob Chemother*. 1998;42(2):199-209. doi:10.1093/jac/42.2.199

87. Tenover FC, Moellering RC. The rationale for revising the clinical and laboratory standards institute vancomycin minimal inhibitory concentration interpretive criteria for *Staphylococcus aureus*. *Clin Infect Dis*. 2007;44(9):1208-1215. doi:10.1086/513203

88. Viedma E, Sanz F, Orellana MA, et al. Relationship between *agr* dysfunction and reduced vancomycin susceptibility in methicillin-susceptible *Staphylococcus aureus* causing bacteraemia. *J Antimicrob Chemother*. 2014;69(1):51-58. doi:10.1093/jac/dkt337

89. Tsuji BT, Rybak MJ, Lau KL, Sakoulas G. Evaluation of accessory gene regulator (*agr*) group and function in the proclivity towards vancomycin intermediate resistance in *Staphylococcus aureus*. *Antimicrob Agents Chemother*. 2007;51(3):1089-1091. doi:10.1128/AAC.00671-06

90. Harigaya Y, Ngo D, Lesse AJ, Huang V, Tsuji BT. Characterization of heterogeneous vancomycin-intermediate resistance, MIC and accessory gene regulator (*agr*) dysfunction among clinical bloodstream isolates of *Staphylococcus aureus*. *BMC Infect Dis*. 2011;11(1):287. doi:10.1186/1471-2334-11-287

91. Boyle-Vavra S, Yin S, Jo DS, Montgomery CP, Daum RS. VraT/YvqF is required for methicillin resistance and activation of the VraSR regulon in *Staphylococcus aureus*. *Antimicrob Agents Chemother*. 2013;57(1):83-95. doi:10.1128/AAC.01651-12

92. Berscheid A, Francois P, Strittmatter A, et al. Generation of a vancomycin-intermediate *Staphylococcus aureus*(VISA) strain by two amino acid exchanges in VraS. *J Antimicrob Chemother*. 2014;69(12):3190-3198. doi:10.1093/jac/dku297

93. Cui L, Isii T, Fukuda M, et al. An RpoB mutation confers dual heteroresistance to daptomycin

and vancomycin in *Staphylococcus aureus*. *Antimicrob Agents Chemother*. 2010;54(12):5222-5233. doi:10.1128/AAC.00437-10

94. Matsuo M, Hishinuma T, Katayama Y, Hiramatsu K. A mutation of RNA polymerase β' subunit (RpoC) converts heterogeneously vancomycin-intermediate *Staphylococcus aureus* (hVISA) into "slow" VISA. *Antimicrob Agents Chemother*. 2015;59(7):4215-4225. doi:10.1128/AAC.00135-15

95. Chang S, Sievert DM, Hageman JC, et al. Infection with vancomycin-resistant *Staphylococcus aureus* containing the *vanA* resistance gene. *N Engl J Med*. 2003;348(14):1342-1347. doi:10.1056/NEJMoa025025

96. Bugg TDH, Wright GD, Dutka-Malen S, Arthur M, Courvalin P, Walsh CT. Molecular basis for vancomycin resistance in *Enterococcus faecium* BM4147: biosynthesis of a depsipeptide peptidoglycan precursor by vancomycin resistance proteins VanH and VanA. *Biochemistry*. 1991;30(43):10408-10415. doi:10.1021/bi00107a007

97. Seaton RA, Gonzalez-Ruiz A, Cleveland KO, Couch KA, Pathan R, Hamed K. Real-world daptomycin use across wide geographical regions: results from a pooled analysis of CORE and EU-CORE. *Ann Clin Microbiol Antimicrob*. 2016;15(1):18. doi:10.1186/s12941-016-0130-8

98. Taylor SD, Palmer M. The action mechanism of daptomycin. *Bioorg Med Chem*. 2016;24(24):6253-6268. doi:10.1016/J.BMC.2016.05.052

99. Silverman JA, Perlmutter NG, Shapiro HM. Correlation of daptomycin bactericidal activity and membrane depolarization in *Staphylococcus aureus*. *Antimicrob Agents Chemother*. 2003;47(8):2538-2544. doi:10.1128/aac.47.8.2538-2544.2003

100. Muthaiyan A, Silverman JA, Jayaswal RK, Wilkinson BJ. Transcriptional profiling reveals that daptomycin induces the *Staphylococcus aureus* cell wall stress stimulon and genes responsive to membrane depolarization. *Antimicrob Agents Chemother*. 2008;52(3):980-990. doi:10.1128/AAC.01121-07

101. Miller WR, Bayer AS, Arias CA. Mechanism of Action and Resistance to Daptomycin in *Staphylococcus aureus* and Enterococci. *Cold Spring Harb Perspect Med*. 2016;6(11):a026997. doi:10.1101/cshperspect.a026997

102. Mishra NN, Bayer AS. Correlation of cell membrane lipid profiles with daptomycin resistance in methicillin-resistant *Staphylococcus aureus*. *Antimicrob Agents Chemother*. 2013;57(2):1082-1085. doi:10.1128/AAC.02182-12

103. Pader V, Hakim S, Painter KL, Wigneshweraraj S, Clarke TB, Edwards AM. *Staphylococcus aureus* inactivates daptomycin by releasing membrane phospholipids. *Nat Microbiol*. 2016;2(1):16194. doi:10.1038/nmicrobiol.2016.194

104. Janeway CA, Travers P, Walport M, Schlomchik MJ. *Immunobiology*. 5th ed. New York: Garland Science; 2001.

105. Rigby KM, DeLeo FR. Neutrophils in innate host defense against *Staphylococcus aureus* infections. *Semin Immunopathol*. 2012;34(2):237-259. doi:10.1007/s00281-011-0295-3

106. Mogensen TH. Pathogen recognition and inflammatory signaling in innate immune defenses. *Clin Microbiol Rev*. 2009;22(2):240-273, Table of Contents. doi:10.1128/CMR.00046-08

107. Kobayashi SD, Voyich JM, Burlak C, DeLeo FR. Neutrophils in the innate immune response. *Arch Immunol Ther Exp (Warsz)*. 2005;53(6):505-517.

108. Bekeredjian-Ding I, Stein C, Uebele J. The innate immune response against *Staphylococcus aureus*. In: Springer, Cham; 2015:385-418. doi:10.1007/82_2015_5004

109. Takeuchi O, Hoshino K, Akira S, Tuomanen E, Dziarski R, Golenbock D. Cutting edge: TLR2-deficient and MyD88-deficient mice are highly susceptible to Staphylococcus aureus infection. *J Immunol*. 2000;165(10):5392-5396. doi:10.4049/jimmunol.165.10.5392

110. Fournier B, Philpott DJ. Recognition of *Staphylococcus aureus* by the innate immune system. *Clin Microbiol Rev*. 2005;18(3):521-540. doi:10.1128/CMR.18.3.521-540.2005

111. Kawai T, Akira S. The role of pattern-recognition receptors in innate immunity: update on Toll-like receptors. *Nat Immunol*. 2010;11(5):373-384. doi:10.1038/ni.1863

112. Bubeck Wardenburg J, Williams WA, Missiakas D. Host defenses against *Staphylococcus aureus* infection require recognition of bacterial lipoproteins. *Proc Natl Acad Sci U S A*. 2006;103(37):13831-13836. doi:10.1073/pnas.0603072103

113. Inden K, Kaneko J, Miyazato A, et al. Toll-like receptor 4-dependent activation of myeloid dendritic cells by leukocidin of *Staphylococcus aureus*. *Microbes Infect*. 2009;11(2):245-253. doi:10.1016/J.MICINF.2008.11.013

114. Kanneganti T-D, Lamkanfi M, Núñez G. Intracellular NOD-like receptors in host defense and disease. *Immunity*. 2007;27(4):549-559. doi:10.1016/j.immuni.2007.10.002

115. Chamaillard M, Hashimoto M, Horie Y, et al. An essential role for NOD1 in host recognition of bacterial peptidoglycan containing diaminopimelic acid. *Nat Immunol*. 2003;4(7):702-707. doi:10.1038/ni945

116. Girardin SE, Boneca IG, Carneiro LAM, et al. Nod1 detects a unique muropeptide from Gram-negative bacterial peptidoglycan. *Science (80-)*. 2003;300(5625):1584-1587. doi:10.1126/science.1084677

117. Girardin SE, Boneca IG, Viala J, et al. Nod2 is a general sensor of peptidoglycan through muramyl dipeptide (MDP) detection. *J Biol Chem*. 2003;278(11):8869-8872. doi:10.1074/jbc.C200651200

118. Inohara N, Ogura Y, Fontalba A, et al. Host recognition of bacterial muramyl dipeptide mediated through NOD2. Implications for Crohn's disease. *J Biol Chem*. 2003;278(8):5509-5512. doi:10.1074/jbc.C200673200

119. Karauzum H, Datta SK. Adaptive Immunity Against *Staphylococcus aureus*. In: Springer, Cham; 2016:419-439. doi:10.1007/82_2016_1

120. Zorman JK, Esser M, Raedler M, et al. Naturally occurring IgG antibody levels to the *Staphylococcus aureus* protein IsdB in humans. *Hum Vaccin Immunother*. 2013;9(9):1857-1864. doi:10.4161/hv.25253

121. Ragle BE, Bubeck Wardenburg J. Anti-alpha-hemolysin monoclonal antibodies mediate protection against *Staphylococcus aureus* pneumonia. *Infect Immun*. 2009;77(7):2712-2718. doi:10.1128/IAI.00115-09

122. Spaan AN, Surewaard BGJ, Nijland R, van Strijp JAG. Neutrophils Versus *Staphylococcus aureus*: A Biological Tug of War. *Annu Rev Microbiol*. 2013;67(1):629-650. doi:10.1146/annurev-micro-092412-155746

123. Foster TJ. Immune evasion by staphylococci. *Nat Rev Microbiol*. 2005;3(12):948-958. doi:10.1038/nrmicro1289

124. Bainton DF, Ullyot JL, Farquhar MG. The development of neutrophilic polymorphonuclear leukocytes in human bone marrow. *J Exp Med*. 1971;134(4):907-934. doi:10.1084/jem.134.4.907

125. Weissman IL, Anderson DJ, Gage F. Stem and progenitor cells: origins, phenotypes, lineage commitments, and transdifferentiations. *Annu Rev Cell Dev Biol*. 2001;17(1):387-403. doi:10.1146/annurev.cellbio.17.1.387

126. Li Y, Karlin A, Loike JD, Silverstein SC. A critical concentration of neutrophils is required for effective bacterial killing in suspension. *Proc Natl Acad Sci U S A*. 2002;99(12):8289-8294. doi:10.1073/pnas.122244799

127. McGuinness W, Kobayashi S, DeLeo F. Evasion of neutrophil killing by *Staphylococcus aureus*. *Pathogens*. 2016;5(1):32. doi:10.3390/pathogens5010032

128. Manz MG, Boettcher S. Emergency granulopoiesis. *Nat Rev Immunol*. 2014;14(5):302-314. doi:10.1038/nri3660

129. Dinauer MC. Disorders of Neutrophil Function. In: Humana Press; 2007:489-504. doi:10.1007/978-1-59745-467-4_30

130. Repine JE, Clawson CC. Quantitative measurement of the bactericidal capability of neutrophils from patients and carriers of chronic granulomatous disease. *J Lab Clin Med*. 1977;90(3):522-528.

131. Root RK, Rosenthal AS, Balestra DJ. Abnormal bactericidal, metabolic, and lysosomal functions of Chediak-Higashi Syndrome leukocytes. *J Clin Invest*. 1972;51(3):649-665. doi:10.1172/JCI106854

132. Greenlee-Wacker M, DeLeo FR, Nauseef WM. How methicillin-resistant *Staphylococcus aureus* evade neutrophil killing. *Curr Opin Hematol*. 2015;22(1):30-35. doi:10.1097/MOH.0000000000000096

133. Phillipson M, Kubes P. The neutrophil in vascular inflammation. *Nat Med*. 2011;17(11):1381-1390. doi:10.1038/nm.2514

134. von Aulock S, Morath S, Hareng L, et al. Lipoteichoic acid from *Staphylococcus aureus* is a potent stimulus for neutrophil recruitment. *Immunobiology*. 2003;208(4):413-422. doi:10.1078/0171-2985-00285

135. Schiffmann E, Corcoran BA, Wahl SM. N-formylmethionyl peptides as chemoattractants for leucocytes. *Proc Natl Acad Sci U S A*. 1975;72(3):1059-1062. doi:10.1073/pnas.72.3.1059

136. Kennedy AD, DeLeo FR. Neutrophil apoptosis and the resolution of infection. *Immunol Res*. 2009;43(1-3):25-61. doi:10.1007/s12026-008-8049-6

137. Amulic B, Cazalet C, Hayes GL, Metzler KD, Zychlinsky A. Neutrophil Function: From Mechanisms to Disease. *Annu Rev Immunol*. 2012;30(1):459-489. doi:10.1146/annurev-immunol-020711-074942

138. Paoliello-Paschoalato AB, Marchi LF, Andrade MF de, Kabeya LM, Donadi EA, Lucisano-Valim YM. Fcγ and complement receptors and complement proteins in neutrophil activation in rheumatoid arthritis: contribution to pathogenesis and progression and modulation by natural products. *Evidence-Based Complement Altern Med*. 2015;2015:1-22. doi:10.1155/2015/429878

139. Wright HL, Moots RJ, Bucknall RC, Edwards SW. Neutrophil function in inflammation and inflammatory diseases. *Rheumatology*. 2010;49(9):1618-1631. doi:10.1093/rheumatology/keq045

140. Sbarra A, Karnovsky M. The biochemical basis of phagocytosis. I. Metabolic changes during the ingestion of particles by polymorphonuclear leukocytes. *J Biol Chem*. 1959;234(6):1355-1362.

141. Ben-Ari J, Wolach O, Gavrieli R, Wolach B. Infections associated with chronic granulomatous disease: linking genetics to phenotypic expression. *Expert Rev Anti Infect Ther*. 2012;10(8):881-894. doi:10.1586/eri.12.77

142. Pollock JD, Williams DA, Gifford MAC, et al. Mouse model of X–linked chronic granulomatous disease, an inherited defect in phagocyte superoxide production. *Nat Genet*. 1995;9(2):202-209. doi:10.1038/ng0295-202

143. Hampton MB, Kettle AJ, Winterbourn CC. Involvement of superoxide and myeloperoxidase in oxygen-dependent killing of *Staphylococcus aureus* by neutrophils. *Infect Immun*. 1996;64(9):3512-3517.

144. Yang H-C, Cheng M-L, Ho H-Y, Tsun-Yee Chiu D. The microbicidal and cytoregulatory roles of NADPH oxidases. *Microbes Infect*. 2011;13(2):109-120. doi:10.1016/j.micinf.2010.10.008

145. Paiva CN, Bozza MT. Are Reactive Oxygen Species Always Detrimental to Pathogens? *Antioxid Redox Signal*. 2014;20(6):1000-1037. doi:10.1089/ars.2013.5447

146. Halliwell B. Phagocyte-derived reactive species: salvation or suicide? *Trends Biochem Sci*. 2006;31(9):509-515. doi:10.1016/J.TIBS.2006.07.005

147. Imlay JA, Chin SM, Linn S. Toxic DNA damage by hydrogen peroxide through the Fenton reaction *in vivo* and *in vitro*. *Science (80-)*. 1988;240(4852):640-642. doi:10.1126/science.2834821

148. Buvelot H, Posfay-Barbe KM, Linder P, Schrenzel J, Krause K-H. *Staphylococcus aureus* , phagocyte NADPH oxidase and chronic granulomatous disease. Shen A, ed. *FEMS Microbiol Rev*. 2016;41(2):fuw042. doi:10.1093/femsre/fuw042

149. Buettner GR. The pecking order of free radicals and antioxidants: Lipid peroxidation, α-tocopherol, and ascorbate. *Arch Biochem Biophys*. 1993;300(2):535-543. doi:10.1006/ABBI.1993.1074

150. Augusto O, Miyamoto S. *Oxygen Radicals and Related Species*. Vol 1.; 2011.

151. Imlay JA. Pathways of Oxidative Damage. *Annu Rev Microbiol*. 2003;57(1):395-418. doi:10.1146/annurev.micro.57.030502.090938

152. Maisch T, Eichner A, Späth A, et al. Fast and effective photodynamic inactivation of multiresistant bacteria by cationic riboflavin derivatives. van Veen HW, ed. *PLoS One*. 2014;9(12):e111792. doi:10.1371/journal.pone.0111792

153. Hampton MB, Kettle AJ, Winterbourn CC. Inside the neutrophil phagosome: oxidants, myeloperoxidase, and bacterial killing. *Blood*. 1998;92(9):3007 LP - 3017.

154. Berlett BS, Stadtman ER. Protein oxidation in aging, disease, and oxidative stress. *J Biol Chem*. 1997;272(33):20313-20316. doi:10.1074/jbc.272.33.20313

155. Slauch JM. How does the oxidative burst of macrophages kill bacteria? Still an open question. *Mol Microbiol*. 2011;80(3):580-583. doi:10.1111/j.1365-2958.2011.07612.x

156. Ayala A, Muñoz MF, Argüelles S. Lipid peroxidation: production, metabolism, and signaling mechanisms of malondialdehyde and 4-hydroxy-2-nonenal. *Oxid Med Cell Longev*. 2014;2014:360438. doi:10.1155/2014/360438

157. Imlay JA. Cellular defenses against superoxide and hydrogen peroxide. *Annu Rev Biochem*. 2008;77(1):755-776. doi:10.1146/annurev.biochem.77.061606.161055

158. Lloyd DR, Carmichael PL, Phillips DH. Comparison of the formation of 8-hydroxy-2‘-deoxyguanosine and single- and double-strand breaks in DNA mediated by Fenton reactions. 1998. doi:10.1021/TX970156L

159. Galhardo RS, Almeida CEB, Leitão AC, Cabral-Neto JB. Repair of DNA lesions induced by hydrogen peroxide in the presence of iron chelators in *Escherichia coli*: participation of endonuclease IV and Fpg. *J Bacteriol*. 2000;182(7):1964-1968. doi:10.1128/JB.182.7.1964-1968.2000

160. Imlay JA, Linn S. Bimodal pattern of killing of DNA-repair-defective or anoxically grown *Escherichia coli* by hydrogen peroxide. *J Bacteriol*. 1986;166(2):519-527. doi:10.1128/jb.166.2.519-527.1986

161. Cadet J, Wagner JR. DNA base damage by reactive oxygen species, oxidizing agents, and UV radiation. *Cold Spring Harb Perspect Biol*. 2013;5(2):a012559. doi:10.1101/cshperspect.a012559

162. Cheng KC, Cahill DS, Kasai H, Nishimura S, Loeb LA. 8-Hydroxyguanine, an abundant form of oxidative DNA damage, causes G----T and A----C substitutions. *J Biol Chem*. 1992;267(1):166-172.

163. Reeves EP, Lu H, Jacobs HL, et al. Killing activity of neutrophils is mediated through activation of proteases by K+ flux. *Nature*. 2002;416(6878):291-297. doi:10.1038/416291a

164. Rothfork JM, Timmins GS, Harris MN, et al. Inactivation of a bacterial virulence pheromone by phagocyte-derived oxidants: new role for the NADPH oxidase in host defense. *Proc Natl Acad Sci U S A*. 2004;101(38):13867-13872. doi:10.1073/pnas.0402996101

165. Fang FC. Antimicrobial reactive oxygen and nitrogen species: concepts and controversies. *Nat Rev Microbiol*. 2004;2(10):820-832. doi:10.1038/nrmicro1004

166. Patel RP, McAndrew J, Sellak H, et al. Biological aspects of reactive nitrogen species. *Biochim Biophys Acta - Bioenerg*. 1999;1411(2-3):385-400. doi:10.1016/S0005-2728(99)00028-6

167. Sasaki S, Miura T, Nishikawa S, Yamada K, Hirasue M, Nakane A. Protective role of nitric oxide in *Staphylococcus aureus* infection in mice. *Infect Immun*. 1998;66(3):1017-1022.

168. Richardson AR, Dunman PM, Fang FC. The nitrosative stress response of *Staphylococcus aureus* is required for resistance to innate immunity. *Mol Microbiol*. 2006;61(4):927-939. doi:10.1111/j.1365-2958.2006.05290.x

169. Chang Y-C, Li P-C, Chen B-C, et al. Lipoteichoic acid-induced nitric oxide synthase expression in RAW 264.7 macrophages is mediated by cyclooxygenase-2, prostaglandin E2, protein kinase A, p38 MAPK, and nuclear factor-κB pathways. *Cell Signal*. 2006;18(8):1235-1243.

doi:10.1016/J.CELLSIG.2005.10.005

170. Malawista SE, Montgomery RR, van Blaricom G. Evidence for reactive nitrogen intermediates in killing of staphylococci by human neutrophil cytoplasts. A new microbicidal pathway for polymorphonuclear leukocytes. *J Clin Invest*. 1992;90(2):631-636. doi:10.1172/JCI115903

171. Hirsch J, Cohn Z. Degranulation of polymorphonuclear leucocytes following phagocytosis of microorganisms. *J Exp Med*. 1960;112(6):1005-1014. doi:10.1084/jem.112.6.1005

172. DeLeo FR, Diep BA, Otto M. Host defense and pathogenesis in *Staphylococcus aureus* infections. *Infect Dis Clin North Am*. 2009;23(1):17-34. doi:10.1016/J.IDC.2008.10.003

173. Jesaitis AJ, Buescher ES, Harrison D, et al. Ultrastructural localization of cytochrome b in the membranes of resting and phagocytosing human granulocytes. *J Clin Invest*. 1990;85(3):821-835. doi:10.1172/JCI114509

174. Faurschou M, Borregaard N. Neutrophil granules and secretory vesicles in inflammation. *Microbes Infect*. 2003;5(14):1317-1327. doi:10.1016/J.MICINF.2003.09.008

175. Oram JD, Reiter B. Inhibition of bacteria by lactoferrin and other iron-chelating agents. *Biochim Biophys Acta - Gen Subj*. 1968;170(2):351-365. doi:10.1016/0304-4165(68)90015-9

176. Corbin BD, Seeley EH, Raab A, et al. Metal chelation and inhibition of bacterial growth in tissue abscesses. *Science (80-)*. 2008;319(5865):962-965. doi:10.1126/science.1152449

177. Thorne KJI, Oliver RC, Barrett AJ. *Lysis and Killing of Bacteria by Lysosomal Proteinases*.; 1976.

178. Odeberg H, Olsson I. Antibacterial activity of cationic proteins from human granulocytes. *J Clin Invest*. 1975;56(5):1118-1124. doi:10.1172/JCI108186

179. Cardot-Martin E, Casalegno JS, Badiou C, et al. *α* -Defensins partially protect human neutrophils against Panton-Valentine leukocidin produced by *Staphylococcus aureus*. *Lett Appl Microbiol*. 2015;61(2):158-164. doi:10.1111/lam.12438

180. Belaaouaj A, McCarthy R, Baumann M, et al. Mice lacking neutrophil elastase reveal impaired host defense against gram negative bacterial sepsis. *Nat Med*. 1998;4(5):615-618. doi:10.1038/nm0598-615

181. Standish AJ, Weiser JN. Human neutrophils kill *Streptococcus pneumoniae* via serine proteases. *J Immunol*. 2009;183(4):2602-2609. doi:10.4049/jimmunol.0900688

182. Brinkmann V, Reichard U, Goosmann C, et al. Neutrophil extracellular traps kill bacteria. *Science (80-)*. 2004;303(5663):1532-1535. doi:10.1126/SCIENCE.1092385

183. McDonald B, Urrutia R, Yipp BG, Jenne CN, Kubes P. Intravascular neutrophil extracellular traps capture bacteria from the bloodstream during sepsis. *Cell Host Microbe*. 2012;12(3):324-333. doi:10.1016/J.CHOM.2012.06.011

184. Pilsczek FH, Salina D, Poon KKH, et al. A novel mechanism of rapid nuclear neutrophil extracellular trap formation in response to Staphylococcus aureus. *J Immunol*. 2010;185(12):7413-7425. doi:10.4049/jimmunol.1000675

185. Clark SR, Ma AC, Tavener SA, et al. Platelet TLR4 activates neutrophil extracellular traps to ensnare bacteria in septic blood. *Nat Med*. 2007;13(4):463-469. doi:10.1038/nm1565

186. Malachowa N, Kobayashi SD, Freedman B, Dorward DW, DeLeo FR. *Staphylococcus aureus* leukotoxin GH promotes formation of neutrophil extracellular traps. *J Immunol*. 2013;191(12):6022-6029. doi:10.4049/jimmunol.1301821

187. Fuchs TA, Abed U, Goosmann C, et al. Novel cell death program leads to neutrophil extracellular traps. *J Cell Biol*. 2007;176(2):231-241. doi:10.1083/jcb.200606027

188. Jorch SK, Kubes P. An emerging role for neutrophil extracellular traps in noninfectious disease. *Nat Med*. 2017;23(3):279-287. doi:10.1038/nm.4294

189. Yipp BG, Kubes P. NETosis: how vital is it? *Blood*. 2013;122(16):2784-2794. doi:10.1182/blood-2013-04-457671

190. Yipp BG, Petri B, Salina D, et al. Infection-induced NETosis is a dynamic process involving neutrophil multitasking *in vivo*. *Nat Med*. 2012;18(9):1386-1393. doi:10.1038/nm.2847

191. Hammer ND, Skaar EP. The impact of metal sequestration on *Staphylococcus aureus* metabolism. *Curr Opin Microbiol*. 2012;15(1):10-14. doi:10.1016/J.MIB.2011.11.004

192. Waldron KJ, Robinson NJ. How do bacterial cells ensure that metalloproteins get the correct metal? *Nat Rev Microbiol*. 2009;7(1):25-35. doi:10.1038/nrmicro2057

193. Andreini C, Bertini I, Rosato A. A hint to search for metalloproteins in gene banks. *Bioinformatics*. 2004;20(9):1373-1380. doi:10.1093/bioinformatics/bth095

194. Weinberg ED. Iron availability and infection. *Biochim Biophys Acta - Gen Subj*. 2009;1790(7):600-605. doi:10.1016/J.BBAGEN.2008.07.002

195. Pishchany G, McCoy AL, Torres VJ, et al. Specificity for human hemoglobin enhances *Staphylococcus aureus* infection. *Cell Host Microbe*. 2010;8(6):544-550. doi:10.1016/j.chom.2010.11.002

196. Haley KP, Skaar EP. A battle for iron: host sequestration and *Staphylococcus aureus* acquisition. *Microbes Infect*. 2012;14(3):217-227. doi:10.1016/J.MICINF.2011.11.001

197. Hammer ND, Skaar EP. Molecular mechanisms of Staphylococcus aureus iron acquisition. *Annu Rev Microbiol*. 2011;65(1):129-147. doi:10.1146/annurev-micro-090110-102851

198. Hamzeh-Cognasse H, Damien P, Chabert A, Pozzetto B, Cognasse F, Garraud O. Platelets and infections - complex interactions with bacteria. *Front Immunol*. 2015;6:82. doi:10.3389/fimmu.2015.00082

199. Fitzgerald JR, Foster TJ, Cox D. The interaction of bacterial pathogens with platelets. *Nat Rev Microbiol*. 2006;4(6):445-457. doi:10.1038/nrmicro1425

200. Cognasse F, Nguyen KA, Damien P, et al. The Inflammatory Role of Platelets via Their TLRs and Siglec Receptors. *Front Immunol*. 2015;6:83. doi:10.3389/fimmu.2015.00083

201. Hally KE, La Flamme AC, Larsen PD, Harding SA. Platelet Toll-like receptor (TLR) expression and TLR-mediated platelet activation in acute myocardial infarction. *Thromb Res*. 2017;158:8-15. doi:10.1016/J.THROMRES.2017.07.031

202. Parimon T, Li Z, Bolz DD, et al. *Staphylococcus aureus* α-hemolysin promotes platelet-neutrophil aggregate formation. *J Infect Dis*. 2013;208(5):761-770. doi:10.1093/infdis/jit235

203. Brown GT, McIntyre TM. Lipopolysaccharide signaling without a nucleus: kinase cascades stimulate platelet shedding of proinflammatory IL-1β-rich microparticles. *J Immunol*. 2011;186(9):5489-5496. doi:10.4049/jimmunol.1001623

204. Bayer AS, Cheng D, Yeaman MR, et al. *In vitro* resistance to thrombin-induced platelet microbicidal protein among clinical bacteremic isolates of *Staphylococcus aureus* correlates with an endovascular infectious source. *Antimicrob Agents Chemother*. 1998;42(12):3169-3172. doi:10.1128/AAC.42.12.3169

205. Wu T, Yeaman MR, Bayer AS. *In vitro* resistance to platelet microbicidal protein correlates with endocarditis source among bacteremic staphylococcal and streptococcal isolates. *Antimicrob Agents Chemother*. 1994;38(4):729-732. doi:10.1128/aac.38.4.729

206. Fowler, Jr. VG, Sakoulas G, McIntyre LM, et al. Persistent bacteremia due to methicillin-resistant *Staphylococcus aureus* infection is associated with *agr* dysfunction and low-level *in vitro* resistance to thrombin-induced platelet microbicidal protein. *J Infect Dis*. 2004;190(6):1140-1149. doi:10.1086/423145

207. Yeaman MR, Bayer AS, Koo SP, Foss W, Sullam PM. Platelet microbicidal proteins and neutrophil defensin disrupt the *Staphylococcus aureus* cytoplasmic membrane by distinct mechanisms of action. *J Clin Invest*. 1998;101(1):178-187. doi:10.1172/JCI562

208. Bayer AS, Ramos MD, Menzies BE, Yeaman MR, Shen AJ, Cheung AL. Hyperproduction of alpha-toxin by *Staphylococcus aureus* results in paradoxically reduced virulence in experimental endocarditis: a host defense role for platelet microbicidal proteins. *Infect Immun*. 1997;65(11):4652-4660.

209. Walenkamp AME, Boer IGJ, Bestebroer J, et al. Staphylococcal superantigen-like 10 inhibits CXCL12-induced human tumor cell migration. *Neoplasia*. 2009;11(4):333-344. doi:10.1593/neo.81508

210. Bestebroer J, van Kessel KPM, Azouagh H, et al. Staphylococcal SSL5 inhibits leukocyte activation by chemokines and anaphylatoxins. *Blood*. 2009;113(2):328-337. doi:10.1182/blood-2008-04-153882

211. Haas P-J, de Haas CJC, Kleibeuker W, et al. N-terminal residues of the chemotaxis inhibitory protein of Staphylococcus aureus are essential for blocking formylated peptide receptor but not C5a receptor. *J Immunol*. 2004;173(9):5704-5711. doi:10.4049/jimmunol.173.9.5704

212. Guerra FE, Borgogna TR, Patel DM, Sward EW, Voyich JM. Epic Immune Battles of History: Neutrophils vs. *Staphylococcus aureus*. *Front Cell Infect Microbiol*. 2017;7:286. doi:10.3389/fcimb.2017.00286

213. Stemerding AM, Köhl J, Pandey MK, et al. Staphylococcus aureus formyl peptide receptor-like 1 inhibitor (FLIPr) and its homologue FLIPr-like are potent FcγR antagonists that inhibit IgG-mediated effector functions. *J Immunol*. 2013;191(1):353-362. doi:10.4049/jimmunol.1203243

214. Laarman AJ, Mijnheer G, Mootz JM, et al. *Staphylococcus aureus* Staphopain A inhibits CXCR2-dependent neutrophil activation and chemotaxis. *EMBO J*. 2012;31(17):3607-3619. doi:10.1038/emboj.2012.212

215. Rooijakkers SHM, Ruyken M, Roos A, et al. Immune evasion by a staphylococcal complement inhibitor that acts on C3 convertases. *Nat Immunol*. 2005;6(9):920-927. doi:10.1038/ni1235

216. Lee LYL, Höök M, Haviland D, et al. Inhibition of complement activation by a secreted *Staphylococcus aureus* protein. *J Infect Dis*. 2004;190(3):571-579. doi:10.1086/422259

217. Ko Y-P, Kuipers A, Freitag CM, et al. Phagocytosis escape by a *Staphylococcus aureus* protein that connects complement and coagulation proteins at the bacterial surface. Skaar EP, ed. *PLoS Pathog*. 2013;9(12):e1003816. doi:10.1371/journal.ppat.1003816

218. Jongerius I, Garcia BL, Geisbrecht B V, van Strijp JAG, Rooijakkers SHM. Convertase inhibitory properties of Staphylococcal extracellular complement-binding protein. *J Biol Chem*. 2010;285(20):14973-14979. doi:10.1074/jbc.M109.091975

219. Laarman AJ, Ruyken M, Malone CL, van Strijp JAG, Horswill AR, Rooijakkers SHM. *Staphylococcus aureus* metalloprotease aureolysin cleaves complement C3 to mediate immune evasion. *J Immunol*. 2011;186(11):6445-6453. doi:10.4049/jimmunol.1002948

220. Forsgren A, Nordström K. Protein A from *Staphylococcus aureus*: the biological significance of its reaction with IgG. *Ann N Y Acad Sci*. 1974;236(1 Recent Advanc):252-266. doi:10.1111/j.1749-6632.1974.tb41496.x

221. Zhang L, Jacobsson K, Vasi J, Lindberg M, Frykberg L. A second IgG-binding protein in Staphylococcus aureus. *Microbiology*. 1998;144(4):985-991. doi:10.1099/00221287-144-4-985

222. Smith EJ, Visai L, Kerrigan SW, Speziale P, Foster TJ. The Sbi protein is a multifunctional immune evasion factor of *Staphylococcus aureus*. *Infect Immun*. 2011;79(9):3801-3809. doi:10.1128/IAI.05075-11

223. Burman JD, Leung E, Atkins KL, et al. Interaction of human complement with Sbi, a staphylococcal immunoglobulin-binding protein: indications of a novel mechanism of complement evasion by *Staphylococcus aureus*. *J Biol Chem*. 2008;283(25):17579-17593. doi:10.1074/jbc.M800265200

224. Upadhyay A, Burman JD, Clark EA, et al. Structure-function analysis of the C3 binding region of *Staphylococcus aureus* immune subversion protein Sbi. *J Biol Chem*. 2008;283(32):22113-22120. doi:10.1074/jbc.M802636200

225. Rooijakkers SHM, van Wamel WJB, Ruyken M, van Kessel KPM, van Strijp JAG. Anti-opsonic properties of staphylokinase. *Microbes Infect*. 2005;7(3):476-484. doi:10.1016/J.MICINF.2004.12.014

226. O'Riordan K, Lee JC. *Staphylococcus aureus* capsular polysaccharides. *Clin Microbiol Rev*. 2004;17(1):218-234. doi:10.1128/cmr.17.1.218-234.2004

227. Guggenberger C, Wolz C, Morrissey JA, Heesemann J. Two distinct coagulase-dependent barriers protect *Staphylococcus aureus* from neutrophils in a three dimensional *in vitro* infection model. Sullam PM, ed. *PLoS Pathog*. 2012;8(1):e1002434. doi:10.1371/journal.ppat.1002434

228. Malachowa N, Whitney AR, Kobayashi SD, et al. Global changes in *Staphylococcus aureus* gene expression in human blood. Chakravortty D, ed. *PLoS One*. 2011;6(4):e18617. doi:10.1371/journal.pone.0018617

229. Palazzolo-Ballance AM, Reniere ML, Braughton KR, et al. Neutrophil microbicides induce a pathogen survival response in community-associated methicillin-resistant *Staphylococcus aureus*. *J Immunol*. 2008;180(1):500-509. doi:10.4049/jimmunol.180.1.500

230. Schwartz J, Leidal KG, Femling JK, Weiss JP, Nauseef WM. Neutrophil bleaching of GFP-expressing staphylococci: probing the intraphagosomal fate of individual bacteria. *J Immunol*. 2009;183(4):2632-2641. doi:10.4049/jimmunol.0804110

231. Liu C-I, Liu GY, Song Y, et al. A cholesterol biosynthesis inhibitor blocks *Staphylococcus aureus* virulence. *Science (80-)*. 2008;319(5868):1391-1394. doi:10.1126/science.1153018

232. Malachowa N, Kohler PL, Schlievert PM, et al. Characterization of a *Staphylococcus aureus* surface virulence factor that promotes resistance to oxidative killing and infectious endocarditis. *Infect Immun*. 2011;79(1):342-352. doi:10.1128/IAI.00736-10

233. Karavolos MH, Horsburgh MJ, Ingham E, Foster SJ. Role and regulation of the superoxide dismutases of *Staphylococcus aureus*. *Microbiology*. 2003;149(10):2749-2758. doi:10.1099/mic.0.26353-0

234. Cosgrove K, Coutts G, Jonsson I-M, et al. Catalase (KatA) and alkyl hydroperoxide reductase (AhpC) have compensatory roles in peroxide stress resistance and are required for survival, persistence, and nasal colonization in Staphylococcus aureus. *J Bacteriol*. 2007;189(3):1025-1035. doi:10.1128/JB.01524-06

235. Richardson AR, Libby SJ, Fang FC. A nitric oxide-inducible lactate dehydrogenase enables *Staphylococcus aureus* to resist innate immunity. *Science (80-)*. 2008;319(5870):1672-1676. doi:10.1126/science.1155207

236. Morikawa K, Ohniwa RL, Kim J, Maruyama A, Ohta T, Takeyasu K. Bacterial nucleoid dynamics: oxidative stress response in *Staphylococcus aureus*. *Genes to Cells*. 2006;11(4):409-423. doi:10.1111/j.1365-2443.2006.00949.x

237. Singh VK, Moskovitz J. Multiple methionine sulfoxide reductase genes in *Staphylococcus aureus*: expression of activity and roles in tolerance of oxidative stress. *Microbiology*. 2003;149(10):2739-2747. doi:10.1099/mic.0.26442-0

238. Singh VK, Vaish M, Johansson TR, et al. Significance of Four Methionine Sulfoxide Reductases in *Staphylococcus aureus*. Freitag NE, ed. *PLoS One*. 2015;10(2):e0117594. doi:10.1371/journal.pone.0117594

239. Pang YY, Schwartz J, Bloomberg S, Boyd JM, Horswill AR, Nauseef WM. Methionine sulfoxide reductases protect against oxidative stress in *Staphylococcus aureus* encountering exogenous oxidants and human neutrophils. *J Innate Immun*. 2014;6(3):353-364. doi:10.1159/000355915

240. Sun F, Ji Q, Jones MB, et al. AirSR, a [2Fe-2S] Cluster-Containing Two-Component System, Mediates Global Oxygen Sensing and Redox Signaling in *Staphylococcus aureus*. *J Am Chem Soc*. 2012;134(1):305-314. doi:10.1021/ja2071835

241. Brunskill EW, de Jonge BLM, Bayles KW. The *Staphylococcus aureus scdA* gene: a novel locus that affects cell division and morphogenesis. *Microbiology*. 1997;143(9):2877-2882. doi:10.1099/00221287-143-9-2877

242. Chang W, Small DA, Toghrol F, Bentley WE. Global transcriptome analysis of *Staphylococcus aureus* response to hydrogen peroxide. *J Bacteriol*. 2006;188(4):1648-1659. doi:10.1128/JB.188.4.1648-1659.2006

243. Uziel O, Borovok I, Schreiber R, Cohen G, Aharonowitz Y. Transcriptional regulation of the *Staphylococcus aureus* thioredoxin and thioredoxin reductase genes in response to oxygen and disulfide stress. *J Bacteriol*. 2004;186(2):326-334. doi:10.1128/jb.186.2.326-334.2004

244. Lee J-W, Helmann JD. The PerR transcription factor senses H_2O_2 by metal-catalysed histidine oxidation. *Nature*. 2006;440(7082):363-367. doi:10.1038/nature04537

245. Horsburgh MJ, Clements MO, Crossley H, Ingham E, Foster SJ. PerR controls oxidative stress

resistance and iron storage proteins and is required for virulence in *Staphylococcus aureus*. *Infect Immun*. 2001;69(6):3744-3754. doi:10.1128/IAI.69.6.3744-3754.2001

246. Chen PR, Bae T, Williams WA, et al. An oxidation-sensing mechanism is used by the global regulator MgrA in *Staphylococcus aureus*. *Nat Chem Biol*. 2006;2(11):591-595. doi:10.1038/nchembio820

247. Luong TT, Dunman PM, Murphy E, Projan SJ, Lee CY. Transcription Profiling of the mgrA Regulon in *Staphylococcus aureus*. *J Bacteriol*. 2006;188(5):1899-1910. doi:10.1128/JB.188.5.1899-1910.2006

248. Gaupp R, Ledala N, Somerville GA. Staphylococcal response to oxidative stress. *Front Cell Infect Microbiol*. 2012;2:33. doi:10.3389/fcimb.2012.00033

249. Chen PR, Nishida S, Poor CB, et al. A new oxidative sensing and regulation pathway mediated by the MgrA homologue SarZ in *Staphylococcus aureus*. *Mol Microbiol*. 2009;71(1):198-211. doi:10.1111/j.1365-2958.2008.06518.x

250. Fuangthong M, Atichartpongkul S, Mongkolsuk S, Helmann JD. OhrR is a repressor of ohrA, a key organic hydroperoxide resistance determinant in *Bacillus subtilis*. *J Bacteriol*. 2001;183(14):4134-4141. doi:10.1128/JB.183.14.4134-4141.2001

251. Ballal A, Manna AC. Regulation of superoxide dismutase (*sod*) genes by SarA in *Staphylococcus aureus*. *J Bacteriol*. 2009;191(10):3301-3310. doi:10.1128/JB.01496-08

252. Ballal A, Manna AC. Control of thioredoxin reductase gene (*trxB*) transcription by SarA in *Staphylococcus aureus*. *J Bacteriol*. 2010;192(1):336-345. doi:10.1128/JB.01202-09

253. Bera A, Herbert S, Jakob A, Vollmer W, Götz F. Why are pathogenic staphylococci so lysozyme resistant? The peptidoglycan O-acetyltransferase OatA is the major determinant for lysozyme resistance of *Staphylococcus aureus*. *Mol Microbiol*. 2004;55(3):778-787. doi:10.1111/j.1365-2958.2004.04446.x

254. Stapels DAC, Ramyar KX, Bischoff M, et al. *Staphylococcus aureus* secretes a unique class of neutrophil serine protease inhibitors. *Proc Natl Acad Sci U S A*. 2014;111(36):13187-13192. doi:10.1073/pnas.1407616111

255. Peschel A, Otto M, Jack RW, Kalbacher H, Jung G, Götz F. Inactivation of the *dlt* operon in *Staphylococcus aureus* confers sensitivity to defensins, protegrins, and other antimicrobial peptides. *J Biol Chem*. 1999;274(13):8405-8410. doi:10.1074/jbc.274.13.8405

256. Peschel A, Jack RW, Otto M, et al. *Staphylococcus aureus* resistance to human defensins and evasion of neutrophil killing via the novel virulence factor MprF is based on modification of membrane lipids with l-lysine. *J Exp Med*. 2001;193(9):1067-1076. doi:10.1084/jem.193.9.1067

257. Falord M, Karimova G, Hiron A, Msadek T. GraXSR proteins interact with the VraFG ABC transporter to form a five-component system required for cationic antimicrobial peptide sensing and resistance in *Staphylococcus aureus*. *Antimicrob Agents Chemother*. 2012;56(2):1047-1058. doi:10.1128/AAC.05054-11

258. Collins LV, Kristian SA, Weidenmaier C, et al. *Staphylococcus aureus* strains lacking D-alanine modifications of teichoic acids are highly susceptible to human neutrophil killing and are virulence attenuated in mice. *J Infect Dis*. 2002;186(2):214-219. doi:10.1086/341454

259. Jin T, Bokarewa M, Foster T, Mitchell J, Higgins J, Tarkowski A. Staphylococcus aureus resists human defensins by production of staphylokinase, a novel bacterial evasion mechanism. *J Immunol*. 2004;172(2):1169-1176. doi:10.4049/jimmunol.172.2.1169

260. Sieprawska-Lupa M, Mydel P, Krawczyk K, et al. Degradation of human antimicrobial peptide LL-37 by *Staphylococcus aureus*-derived proteinases. *Antimicrob Agents Chemother*. 2004;48(12):4673-4679. doi:10.1128/AAC.48.12.4673-4679.2004

261. Berends ETM, Horswill AR, Haste NM, Monestier M, Nizet V, von Köckritz-Blickwede M. Nuclease expression by *Staphylococcus aureus* facilitates escape from neutrophil extracellular traps. *J Innate Immun*. 2010;2(6):576-586. doi:10.1159/000319909

262. Thammavongsa V, Missiakas DM, Schneewind O. *Staphylococcus aureus* degrades neutrophil extracellular traps to promote immune cell death. *Science (80-)*. 2013;342(6160):863-866.

doi:10.1126/science.1242255

263. Thammavongsa V, Kern JW, Missiakas DM, Schneewind O. *Staphylococcus aureus* synthesizes adenosine to escape host immune responses. *J Exp Med*. 2009;206(11):2417-2427. doi:10.1084/jem.20090097

264. Novick RP, Geisinger E. Quorum sensing in staphylococci. *Annu Rev Genet*. 2008;42(1):541-564. doi:10.1146/annurev.genet.42.110807.091640

265. Painter KL, Hall A, Ha KP, Edwards AM. The electron transport chain sensitizes *Staphylococcus aureus* and *Enterococcus faecalis* to the oxidative burst. *Infect Immun*. 2017;85(12):e00659-17. doi:10.1128/IAI.00659-17

266. James EH, Edwards AM, Wigneshweraraj S. Transcriptional downregulation of *agr* expression in *Staphylococcus aureus* during growth in human serum can be overcome by constitutively active mutant forms of the sensor kinase AgrC. *FEMS Microbiol Lett*. 2013;349(2):153-162. doi:10.1111/1574-6968.12309

267. Carnes EC, Lopez DM, Donegan NP, et al. Confinement-induced quorum sensing of individual *Staphylococcus aureus* bacteria. *Nat Chem Biol*. 2010;6(1):41-45. doi:10.1038/nchembio.264

268. Pang YY, Schwartz J, Thoendel M, Ackermann LW, Horswill AR, Nauseef WM. *agr*-dependent interactions of *Staphylococcus aureus* USA300 with human polymorphonuclear neutrophils. *J Innate Immun*. 2010;2(6):546-559. doi:10.1159/000319855

269. Cheung GYC, Wang R, Khan BA, Sturdevant DE, Otto M. Role of the accessory gene regulator *agr* in community-associated methicillin-resistant *Staphylococcus aureus* pathogenesis. *Infect Immun*. 2011;79(5):1927-1935. doi:10.1128/IAI.00046-11

270. Bubeck Wardenburg J, Bae T, Otto M, DeLeo FR, Schneewind O. Poring over pores: α-hemolysin and Panton-Valentine leukocidin in *Staphylococcus aureus* pneumonia. *Nat Med*. 2007;13(12):1405-1406. doi:10.1038/nm1207-1405

271. Wang R, Braughton KR, Kretschmer D, et al. Identification of novel cytolytic peptides as key virulence determinants for community-associated MRSA. *Nat Med*. 2007;13(12):1510-1514. doi:10.1038/nm1656

272. Jayasinghe L, Bayley H. The leukocidin pore: Evidence for an octamer with four LukF subunits and four LukS subunits alternating around a central axis. *Protein Sci*. 2005;14(10):2550-2561. doi:10.1110/ps.051648505

273. Thammavongsa V, Kim HK, Missiakas D, Schneewind O. Staphylococcal manipulation of host immune responses. *Nat Rev Microbiol*. 2015;13(9):529-543. doi:10.1038/nrmicro3521

274. Koop G, Vrieling M, Storisteanu DML, et al. Identification of LukPQ, a novel, equid-adapted leukocidin of Staphylococcus aureus. *Sci Rep*. 2017;7. doi:10.1038/srep40660

275. Löffler B, Hussain M, Grundmeier M, et al. *Staphylococcus aureus* Panton-Valentine leukocidin is a very potent cytotoxic factor for human neutrophils. Cheung A, ed. *PLoS Pathog*. 2010;6(1):e1000715. doi:10.1371/journal.ppat.1000715

276. Prévost G, Cribier B, Couppié P, et al. Panton-Valentine leucocidin and gamma-hemolysin from *Staphylococcus aureus* ATCC 49775 are encoded by distinct genetic loci and have different biological activities. *Infect Immun*. 1995;63(10):4121-4129.

277. DuMont AL, Nygaard TK, Watkins RL, et al. Characterization of a new cytotoxin that contributes to *Staphylococcus aureus* pathogenesis. *Mol Microbiol*. 2011;79(3):814-825. doi:10.1111/j.1365-2958.2010.07490.x

278. Reyes-Robles T, Alonzo F, Kozhaya L, Lacy DB, Unutmaz D, Torres VJ. *Staphylococcus aureus* leukotoxin ED targets the chemokine receptors CXCR1 and CXCR2 to kill leukocytes and promote infection. *Cell Host Microbe*. 2013;14(4):453-459. doi:10.1016/j.chom.2013.09.005

279. Vrieling M, Koymans KJ, Heesterbeek DAC, et al. Bovine *Staphylococcus aureus* secretes the leukocidin LukMF′ to kill migrating neutrophils through CCR1. *MBio*. 2015;6(3):e00335-15. doi:10.1128/MBIO.00335-15

280. Valeva A, Walev I, Pinkernell M, et al. Transmembrane β-barrel of staphylococcal α-toxin forms in sensitive but not in resistant cells. *Proc Natl Acad Sci*. 1997;94(21):11607-11611.

doi:10.1073/PNAS.94.21.11607

281. Kobayashi SD, Braughton KR, Whitney AR, et al. Bacterial pathogens modulate an apoptosis differentiation program in human neutrophils. *Proc Natl Acad Sci U S A*. 2003;100(19):10948-10953. doi:10.1073/pnas.1833375100

282. Martin CJ, Peters KN, Behar SM. Macrophages clean up: efferocytosis and microbial control. *Curr Opin Microbiol*. 2014;17:17-23. doi:10.1016/J.MIB.2013.10.007

283. Greenlee-Wacker MC, Rigby KM, Kobayashi SD, Porter AR, DeLeo FR, Nauseef WM. Phagocytosis of *Staphylococcus aureus* by human neutrophils prevents macrophage efferocytosis and induces programmed necrosis. *J Immunol*. 2014;192(10):4709-4717. doi:10.4049/jimmunol.1302692

284. Zurek OW, Pallister KB, Voyich JM. *Staphylococcus aureus* Inhibits Neutrophil-derived IL-8 to Promote Cell Death. *J Infect Dis*. 2015;212(6):934-938. doi:10.1093/infdis/jiv124

285. Xiong A, Singh VK, Cabrera G, Jayaswal RK. Molecular characterization of the ferric-uptake regulator, Fur, from Staphylococcus aureus. *Microbiology*. 2000;146(3):659-668. doi:10.1099/00221287-146-3-659

286. Horsburgh MJ, Ingham E, Foster SJ. In *Staphylococcus aureus*, Fur is an interactive regulator with PerR, contributes to virulence, and is necessary for oxidative stress resistance through positive regulation of catalase and iron homeostasis. *J Bacteriol*. 2001;183(2):468-475. doi:10.1128/JB.183.2.468-475.2001

287. Skaar EP. The battle for iron between bacterial pathogens and their vertebrate hosts. Madhani HD, ed. *PLoS Pathog*. 2010;6(8):e1000949. doi:10.1371/journal.ppat.1000949

288. Skaar EP, Humayun M, Bae T, DeBord KL, Schneewind O. Iron-source preference of *Staphylococcus aureus* infections. *Science (80-)*. 2004;305(5690):1626-1628. doi:10.1126/science.1099930

289. Muryoi N, Tiedemann MT, Pluym M, Cheung J, Heinrichs DE, Stillman MJ. Demonstration of the iron-regulated surface determinant (Isd) heme transfer pathway in *Staphylococcus aureus*. *J Biol Chem*. 2008;283(42):28125-28136. doi:10.1074/jbc.M802171200

290. Courcol RJ, Trivier D, Bissinger MC, Martin GR, Brown MR. Siderophore production by *Staphylococcus aureus* and identification of iron-regulated proteins. *Infect Immun*. 1997;65(5):1944-1948.

291. Beasley FC, Marolda CL, Cheung J, Buac S, Heinrichs DE. *Staphylococcus aureus* transporters Hts, Sir, and Sst capture iron liberated from human transferrin by Staphyloferrin A, Staphyloferrin B, and catecholamine stress hormones, respectively, and contribute to virulence. *Infect Immun*. 2011;79(6):2345-2355. doi:10.1128/IAI.00117-11

292. Hawiger J, Steckley S, Hammond D, et al. Staphylococci-induced human platelet injury mediated by protein A and immunoglobulin G Fc fragment receptor. *J Clin Invest*. 1979;64(4):931-937. doi:10.1172/JCI109559

293. Shannon O, Flock J-I. Extracellular fibrinogen binding protein, Efb, from *Staphylococcus aureus* binds to platelets and inhibits platelet aggregation. *Thromb Haemost*. 2004;91(04):779-789. doi:10.1160/TH03-05-0287

294. Mantegazza AR, Magalhaes JG, Amigorena S, Marks MS. Presentation of phagocytosed antigens by MHC Class I and II. *Traffic*. 2013;14(2):135-152. doi:10.1111/tra.12026

295. Goldmann O, Medina E. *Staphylococcus aureus* strategies to evade the host acquired immune response. *Int J Med Microbiol*. 2018;308(6):625-630. doi:10.1016/J.IJMM.2017.09.013

296. Choi Y, Lafferty JA, Clements JR, et al. Selective expansion of T cells expressing V beta 2 in toxic shock syndrome. *J Exp Med*. 1990;172(3):981-984. doi:10.1084/jem.172.3.981

297. Fraser JD, Proft T. The bacterial superantigen and superantigen-like proteins. *Immunol Rev*. 2008;225(1):226-243. doi:10.1111/j.1600-065X.2008.00681.x

298. Stach CS, Herrera A, Schlievert PM. Staphylococcal superantigens interact with multiple host receptors to cause serious diseases. *Immunol Res*. 2014;59(1-3):177-181. doi:10.1007/s12026-014-8539-7

299. Argudín MÁ, Mendoza MC, Rodicio MR. Food poisoning and *Staphylococcus aureus* enterotoxins. *Toxins (Basel)*. 2010;2(7):1751-1773. doi:10.3390/toxins2071751

300. Chesney PJ, Bergdoll MS, Davis JP, Vergeront JM. The disease spectrum, epidemiology, and etiology of toxic-shock syndrome. *Annu Rev Microbiol*. 1984;38(1):315-338. doi:10.1146/annurev.mi.38.100184.001531

301. Löffler B, Tuchscherr L, Niemann S, Peters G. *Staphylococcus aureus* persistence in non-professional phagocytes. *Int J Med Microbiol*. 2014;304(2):170-176. doi:10.1016/J.IJMM.2013.11.011

302. Sinha B, Francois P, Que YA, et al. Heterologously expressed *Staphylococcus aureus* fibronectin-binding proteins are sufficient for invasion of host cells. *Infect Immun*. 2000;68(12):6871-6878. doi:10.1128/iai.68.12.6871-6878.2000

303. Jarry TM, Memmi G, Cheung AL. The expression of alpha-haemolysin is required for *Staphylococcus aureus* phagosomal escape after internalization in CFT-1 cells. *Cell Microbiol*. 2008;10(9):1801-1814. doi:10.1111/j.1462-5822.2008.01166.x

304. Qazi SN, Counil E, Morrissey J, et al. *agr* expression precedes escape of internalized *Staphylococcus aureus* from the host endosome. *Infect Immun*. 2001;69(11):7074-7082. doi:10.1128/IAI.69.11.7074-7082.2001

305. Edwards AM, Massey RC. How does *Staphylococcus aureus* escape the bloodstream? *Trends Microbiol*. 2011;19(4):184-190. doi:10.1016/J.TIM.2010.12.005

306. Painter KL, Strange E, Parkhill J, Bamford KB, Armstrong-James D, Edwards AM. *Staphylococcus aureus* adapts to oxidative stress by producing H_2O_2-resistant small-colony variants via the SOS Response. *Infect Immun*. 2015;83(5):1830-1844. doi:10.1128/IAI.03016-14

307. Vesga O, Groeschel MC, Otten MF, Brar DW, Vann JM, Proctor RA. *Staphylococcus aureus* small colony variants are induced by the endothelial cell intracellular milieu. *J Infect Dis*. 1996;173(3):739-742. doi:10.1093/infdis/173.3.739

308. Garzoni C, Kelley WL. Return of the Trojan horse: intracellular phenotype switching and immune evasion by *Staphylococcus aureus*. *EMBO Mol Med*. 2011;3(3):115-117. doi:10.1002/emmm.201100123

309. Schröder A, Kland R, Peschel A, von Eiff C, Aepfelbacher M. Live cell imaging of phagosome maturation in *Staphylococcus aureus* infected human endothelial cells: small colony variants are able to survive in lysosomes. *Med Microbiol Immunol*. 2006;195(4):185-194. doi:10.1007/s00430-006-0015-0

310. Proctor RA, Kriegeskorte A, Kahl BC, Becker K, Löffler B, Peters G. *Staphylococcus aureus* small colony variants (SCVs): a road map for the metabolic pathways involved in persistent infections. *Front Cell Infect Microbiol*. 2014;4:99. doi:10.3389/fcimb.2014.00099

311. von Eiff C, Vaudaux P, Kahl BC, et al. Bloodstream infections caused by small-colony variants of coagulase-negative Staphylococci following pacemaker implantation. *Clin Infect Dis*. 1999;29(4):932-934. doi:10.1086/520462

312. Seifert H, Wisplinghoff H, Schnabel P, von Eiff C. Small colony variants of *Staphylococcus aureus* and pacemaker-related infection. *Emerg Infect Dis*. 2003;9(10):1316-1318. doi:10.3201/eid0910.0302000

313. Friedberg EC, Wood RD, Walker GC, Schultz RA, Siede W, Ellenberger T. *DNA Repair and Mutagenesis*. American Society for Microbiology Press; 2006.

314. Karschau J, de Almeida C, Richard MC, et al. A matter of life or death: modeling DNA damage and repair in bacteria. *Biophys J*. 2011;100(4):814-821. doi:10.1016/j.bpj.2010.12.3713

315. Kelley WL. Lex marks the spot: the virulent side of SOS and a closer look at the LexA regulon. *Mol Microbiol*. 2006;62(5):1228-1238. doi:10.1111/j.1365-2958.2006.05444.x

316. Wolf C, Hochgräfe F, Kusch H, Albrecht D, Hecker M, Engelmann S. Proteomic analysis of antioxidant strategies of *Staphylococcus aureus*: Diverse responses to different oxidants. *Proteomics*. 2008;8(15):3139-3153. doi:10.1002/pmic.200701062

317. Anderson KL, Roberts C, Disz T, et al. Characterization of the *Staphylococcus aureus* heat shock, cold shock, stringent, and SOS responses and their effects on log-phase mRNA turnover. *J Bacteriol*. 2006;188(19):6739-6756. doi:10.1128/JB.00609-06

318. Cirz RT, Jones MB, Gingles NA, et al. Complete and SOS-mediated response of *Staphylococcus aureus* to the antibiotic ciprofloxacin. *J Bacteriol*. 2007;189(2):531-539. doi:10.1128/JB.01464-06

319. Lenhart JS, Schroeder JW, Walsh BW, Simmons LA. DNA repair and genome maintenance in *Bacillus subtilis*. *Microbiol Mol Biol Rev*. 2012;76(3):530 LP - 564. doi:10.1128/MMBR.05020-11

320. Reuven NB, Arad G, Maor-Shoshani A, Livneh Z. The mutagenesis protein UmuC is a DNA polymerase activated by UmuD', RecA, and SSB and is specialized for translesion replication. *J Biol Chem*. 1999;274(45):31763-31766. doi:10.1074/jbc.274.45.31763

321. McKenzie GJ, Harris RS, Lee PL, Rosenberg SM. The SOS response regulates adaptive mutation. *Proc Natl Acad Sci U S A*. 2000;97(12):6646-6651. doi:10.1073/pnas.120161797

322. Sale JE, Lehmann AR, Woodgate R. Y-family DNA polymerases and their role in tolerance of cellular DNA damage. *Nat Rev Mol Cell Biol*. 2012;13(3):141-152. doi:10.1038/nrm3289

323. Bisognano C, Kelley WL, Estoppey T, et al. A RecA-LexA-dependent pathway mediates ciprofloxacin-induced fibronectin binding in *Staphylococcus aureus*. *J Biol Chem*. 2004;279(10):9064-9071. doi:10.1074/jbc.M309836200

324. Janion C. Inducible SOS response system of DNA repair and mutagenesis in *Escherichia coli*. *Int J Biol Sci*. 2008;4(6):338-344. doi:10.7150/ijbs.4.338

325. Sung H-M, Yeamans G, Ross CA, Yasbin RE. Roles of YqjH and YqjW, homologs of the *Escherichia coli* UmuC/DinB or Y superfamily of DNA polymerases, in stationary-phase mutagenesis and UV-induced mutagenesis of *Bacillus subtilis*. *J Bacteriol*. 2003;185(7):2153-2160. doi:10.1128/jb.185.7.2153-2160.2003

326. Au N, Kuester-Schoeck E, Mandava V, et al. Genetic composition of the *Bacillus subtilis* SOS system. *J Bacteriol*. 2005;187(22):7655-7666. doi:10.1128/JB.187.22.7655-7666.2005

327. Le Chatelier E, Bécherel OJ, D'Alençon E, et al. Involvement of DnaE, the second replicative DNA polymerase from *Bacillus subtilis*, in DNA mutagenesis. *J Biol Chem*. 2004;279(3):1757-1767. doi:10.1074/jbc.M310719200

328. Úbeda C, Maiques E, Knecht E, Lasa Í, Novick RP, Penadés JR. Antibiotic-induced SOS response promotes horizontal dissemination of pathogenicity island-encoded virulence factors in staphylococci. *Mol Microbiol*. 2005;56(3):836-844. doi:10.1111/j.1365-2958.2005.04584.x

329. Úbeda C, Maiques E, Tormo M, et al. SaPI operon I is required for SaPI packaging and is controlled by LexA. *Mol Microbiol*. 2007;65(1):41-50. doi:10.1111/j.1365-2958.2007.05758.x

330. Goerke C, Köller J, Wolz C. Ciprofloxacin and trimethoprim cause phage induction and virulence modulation in *Staphylococcus aureus*. *Antimicrob Agents Chemother*. 2006;50(1):171-177. doi:10.1128/AAC.50.1.171-177.2006

331. Maiques E, Ubeda C, Campoy S, et al. Beta-lactam antibiotics induce the SOS response and horizontal transfer of virulence factors in *Staphylococcus aureus*. *J Bacteriol*. 2006;188(7):2726-2729. doi:10.1128/JB.188.7.2726-2729.2006

332. Yi C, He C. DNA repair by reversal of DNA damage. *Cold Spring Harb Perspect Biol*. 2013;5(1):a012575. doi:10.1101/cshperspect.a012575

333. Sancar A. Structure and function of DNA photolyase and cryptochrome blue-light photoreceptors. *Chem Rev*. 2003;103(6):2203-2238. doi:10.1021/cr0204348

334. Li YF, Kim ST, Sancar A. Evidence for lack of DNA photoreactivating enzyme in humans. *Proc Natl Acad Sci U S A*. 1993;90(10):4389-4393. doi:10.1073/pnas.90.10.4389

335. Hsu DS, Zhao X, Zhao S, et al. Putative human blue-light photoreceptors hCRY1 and hCRY2 are flavoproteins. 1996. doi:10.1021/BI962209O

336. Morita R, Nakane S, Shimada A, et al. Molecular mechanisms of the whole DNA repair system: a comparison of bacterial and eukaryotic systems. *J Nucleic Acids*. 2010;2010:179594.

doi:10.4061/2010/179594

337. Essen LO, Klar T. Light-driven DNA repair by photolyases. *Cell Mol Life Sci*. 2006;63(11):1266-1277. doi:10.1007/s00018-005-5447-y

338. Park HW, Kim ST, Sancar A, Deisenhofer J. Crystal structure of DNA photolyase from *Escherichia coli*. *Science*. 1995;268(5219):1866-1872. doi:10.1126/science.7604260

339. Komori H, Masui R, Kuramitsu S, et al. Crystal structure of thermostable DNA photolyase: pyrimidine-dimer recognition mechanism. *Proc Natl Acad Sci U S A*. 2001;98(24):13560-13565. doi:10.1073/pnas.241371398

340. Nicholson WL. Photoreactivation in the genus *Bacillus*. *Curr Microbiol*. 1995;31(6):361-364. doi:10.1007/BF00294700

341. Riordan JT, Dupre JM, Cantore-Matyi SA, et al. Alterations in the transcriptome and antibiotic susceptibility of *Staphylococcus aureus* grown in the presence of diclofenac. *Ann Clin Microbiol Antimicrob*. 2011;10(1):30. doi:10.1186/1476-0711-10-30

342. Sung JM-L, Lloyd DH, Lindsay JA. *Staphylococcus aureus* host specificity: comparative genomics of human versus animal isolates by multi-strain microarray. *Microbiology*. 2008;154(7):1949-1959. doi:10.1099/mic.0.2007/015289-0

343. Sedgwick B, Lindahl T. Recent progress on the Ada response for inducible repair of DNA alkylation damage. *Oncogene*. 2002;21(58):8886-8894. doi:10.1038/sj.onc.1205998

344. Kreuzer KN. DNA damage responses in prokaryotes: regulating gene expression, modulating growth patterns, and manipulating replication forks. *Cold Spring Harb Perspect Biol*. 2013;5(11):a012674. doi:10.1101/cshperspect.a012674

345. Mishina Y, Duguid EM, He C. Direct reversal of DNA alkylation damage. *Chem Rev*. 2006;106(2):215-232. doi:10.1021/cr0404702

346. Krokan HE, Bjørås M. Base excision repair. *Cold Spring Harb Perspect Biol*. 2013;5(4):a012583. doi:10.1101/cshperspect.a012583

347. Kleibl K. Molecular mechanisms of adaptive response to alkylating agents in *Escherichia coli* and some remarks on O^6-methylguanine DNA-methyltransferase in other organisms. *Mutat Res Mutat Res*. 2002;512(1):67-84. doi:10.1016/S1383-5742(02)00025-X

348. Trewick SC, Henshaw TF, Hausinger RP, Lindahl T, Sedgwick B. Oxidative demethylation by *Escherichia coli* AlkB directly reverts DNA base damage. *Nature*. 2002;419(6903):174-178. doi:10.1038/nature00908

349. Falnes PØ, Johansen RF, Seeberg E. AlkB-mediated oxidative demethylation reverses DNA damage in *Escherichia coli*. *Nature*. 2002;419(6903):178-182. doi:10.1038/nature01048

350. Rippa V, Duilio A, di Pasquale P, Amoresano A, Landini P, Volkert MR. Preferential DNA damage prevention by the *E. coli* AidB gene: A new mechanism for the protection of specific genes. *DNA Repair (Amst)*. 2011;10(9):934-941. doi:10.1016/J.DNAREP.2011.06.001

351. Rohankhedkar MS, Mulrooney SB, Wedemeyer WJ, Hausinger RP. The AidB component of the *Escherichia coli* adaptive response to alkylating agents is a flavin-containing, DNA-binding protein. *J Bacteriol*. 2006;188(1):223-230. doi:10.1128/JB.188.1.223-230.2006

352. Bowles T, Metz AH, O'Quin J, Wawrzak Z, Eichman BF. Structure and DNA binding of alkylation response protein AidB. *Proc Natl Acad Sci U S A*. 2008;105(40):15299-15304. doi:10.1073/pnas.0806521105

353. Morohoshi F, Hayashi K, Munakata N. Molecular analysis of *Bacillus subtilis ada* mutants deficient in the adaptive response to simple alkylating agents. *J Bacteriol*. 1991;173(24):7834-7840. doi:10.1128/JB.173.24.7834-7840.1991

354. Aamodt RM, Falnes PØ, Johansen RF, Seeberg E, Bjørås M. The *Bacillus subtilis* counterpart of the mammalian 3-methyladenine DNA glycosylase has hypoxanthine and 1,N6-ethenoadenine as preferred substrates. *J Biol Chem*. 2004;279(14):13601-13606. doi:10.1074/jbc.M314277200

355. Jurelevicius D, Alvarez VM, Peixoto R, Rosado AS, Seldin L. The use of a combination of *alkB*

primers to better characterize the distribution of alkane-degrading bacteria. Mormile MR, ed. *PLoS One*. 2013;8(6):e66565. doi:10.1371/journal.pone.0066565

356. Li S-W, Liu M-Y, Yang R-Q. Comparative genome characterization of a petroleum-degrading *Bacillus subtilis* strain DM2. *Int J Genomics*. 2019;2019:1-16. doi:10.1155/2019/7410823

357. Shi R, Mullins EA, Shen X, et al. Selective base excision repair of DNA damage by the non-base-flipping DNA glycosylase AlkC. *EMBO J*. 2018;37(1):63-74. doi:10.15252/embj.201797833

358. Yang M, Aamodt RM, Dalhus B, et al. The *ada* operon of *Mycobacterium tuberculosis* encodes two DNA methyltransferases for inducible repair of DNA alkylation damage. *DNA Repair (Amst)*. 2011;10(6):595-602. doi:10.1016/J.DNAREP.2011.03.007

359. Ambur OH, Davidsen T, Frye SA, et al. Genome dynamics in major bacterial pathogens. *FEMS Microbiol Rev*. 2009;33(3):453-470. doi:10.1111/j.1574-6976.2009.00173.x

360. Zhang X, Xu X, Yuan W, et al. Complete genome sequence of Staphylococcus aureus XN108, an ST239-MRSA-SCCmec III Strain with intermediate vancomycin resistance isolated in mainland China. *Genome Announc*. 2014;2(4):e00449-14. doi:10.1128/genomeA.00449-14

361. Krwawicz J, Arczewska KD, Speina E, Maciejewska A, Grzesiuk E. Bacterial DNA repair genes and their eukaryotic homologues: 1. Mutations in genes involved in base excision repair (BER) and DNA-end processors and their implication in mutagenesis and human disease. *Acta Biochim Pol*. 2007;54(3):413-434.

362. Dalhus B, Laerdahl JK, Backe PH, Bjørås M. DNA base repair – recognition and initiation of catalysis. *FEMS Microbiol Rev*. 2009;33(6):1044-1078. doi:10.1111/j.1574-6976.2009.00188.x

363. Baños B, Lázaro JM, Villar L, Salas M, de Vega M. Characterization of a *Bacillus subtilis* 64-kDa DNA polymerase X potentially involved in DNA repair. *J Mol Biol*. 2008;384(5):1019-1028. doi:10.1016/J.JMB.2008.09.081

364. Kunst F, Ogasawara N, Moszer I, et al. The complete genome sequence of the Gram-positive bacterium *Bacillus subtilis*. *Nature*. 1997;390(6657):249-256. doi:10.1038/36786

365. Salas-Pacheco JM, Urtiz-Estrada N, Martínez-Cadena G, Yasbin RE, Pedraza-Reyes M. YqfS from *Bacillus subtilis* is a spore protein and a new functional member of the type IV apurinic/apyrimidinic-endonuclease family. *J Bacteriol*. 2003;185(18):5380-5390. doi:10.1128/jb.185.18.5380-5390.2003

366. Shida T, Kaneda K, Ogawa T, Sekiguchi J. Abasic site recognition mechanism by the *Escherichia coli* exonuclease III. *Nucleic Acids Symp Ser*. 1999;42(1):195-196. doi:10.1093/nass/42.1.195

367. Baños B, Villar L, Salas M, de Vega M. Intrinsic apurinic/apyrimidinic (AP) endonuclease activity enables *Bacillus subtilis* DNA polymerase X to recognize, incise, and further repair abasic sites. *Proc Natl Acad Sci U S A*. 2010;107(45):19219-19224. doi:10.1073/pnas.1013603107

368. Fey PD, Endres JL, Yajjala VK, et al. A genetic resource for rapid and comprehensive phenotype screening of nonessential *Staphylococcus aureus* genes. *MBio*. 2013;4(1):e00537-12. doi:10.1128/MBIO.00537-12

369. O'Leary NA, Wright MW, Brister JR, et al. Reference sequence (RefSeq) database at NCBI: current status, taxonomic expansion, and functional annotation. *Nucleic Acids Res*. 2016;44(D1):D733-D745. doi:10.1093/nar/gkv1189

370. Shibutani S, Takeshita M, Grollman AP. Insertion of specific bases during DNA synthesis past the oxidation-damaged base 8-oxodG. *Nature*. 1991;349(6308):431-434. doi:10.1038/349431a0

371. Hsu GW, Ober M, Carell T, Beese LS. Error-prone replication of oxidatively damaged DNA by a high-fidelity DNA polymerase. *Nature*. 2004;431(7005):217-221. doi:10.1038/nature02908

372. Michaels ML, Miller JH. The GO system protects organisms from the mutagenic effect of the spontaneous lesion 8-hydroxyguanine (7,8-dihydro-8-oxoguanine). *J Bacteriol*. 1992;174(20):6321-6325. doi:10.1128/jb.174.20.6321-6325.1992

373. Michaels ML, Pham L, Cruz C, Miller JH. MutM, a protein that prevents G C→T A transversions,

is formamidopyrimidine-DNA glycosylase. *Nucleic Acids Res*. 1991;19(13):3629-3632. doi:10.1093/nar/19.13.3629

374. Michaels ML, Cruz C, Grollman AP, Miller JH. Evidence that MutY and MutM combine to prevent mutations by an oxidatively damaged form of guanine in DNA. *Proc Natl Acad Sci U S A*. 1992;89(15):7022-7025. doi:10.1073/pnas.89.15.7022

375. Maki H, Sekiguchi M. MutT protein specifically hydrolyses a potent mutagenic substrate for DNA synthesis. *Nature*. 1992;355(6357):273-275. doi:10.1038/355273a0

376. Sasaki M, Kurusu Y. Analysis of spontaneous base substitutions generated in mutator strains of *Bacillus subtilis*. *FEMS Microbiol Lett*. 2004;234(1):37-42. doi:10.1111/j.1574-6968.2004.tb09510.x

377. Canfield GS, Schwingel JM, Foley MH, et al. Evolution in fast forward: a potential role for mutators in accelerating *Staphylococcus aureus* pathoadaptation. *J Bacteriol*. 2013;195(3):615-628. doi:10.1128/JB.00733-12

378. Wallace SS. DNA glycosylases search for and remove oxidized DNA bases. *Environ Mol Mutagen*. 2013;54(9):691-704. doi:10.1002/em.21820

379. Strniste GF, Wallace SS. Endonucleolytic incision of X-irradiated deoxyribonucleic acid by extracts of *Escherichia coli*. *Proc Natl Acad Sci U S A*. 1975;72(6):1997-2001.

380. Melamede RJ, Hatahet Z, Kow YW, Ide H, Wallace SS. Isolation and characterization of endonuclease VIII from *Escherichia coli*. *Biochemistry*. 1994;33(5):1255-1264. doi:10.1021/bi00171a028

381. Jiang D, Hatahet Z, Melamede RJ, Kow YW, Wallace SS. Characterization of *Escherichia coli endonuclease* VIII. *J Biol Chem*. 1997;272(51):32230-32239. doi:10.1074/jbc.272.51.32230

382. Collier C, Machón C, Briggs GS, Smits WK, Soultanas P. Untwisting of the DNA helix stimulates the endonuclease activity of *Bacillus subtilis* Nth at AP sites. *Nucleic Acids Res*. 2012;40(2):739-750. doi:10.1093/nar/gkr785

383. Barajas-Ornelas R del C, Ramírez-Guadiana FH, Juárez-Godínez R, et al. Error-prone processing of apurinic/apyrimidinic (AP) sites by PolX underlies a novel mechanism that promotes adaptive mutagenesis in *Bacillus subtilis*. *J Bacteriol*. 2014;196(16):3012-3022. doi:10.1128/JB.01681-14

384. Roberts CA, Al-Tameemi HM, Mashruwala AA, et al. The Suf iron-sulfur cluster biosynthetic system Is essential in *Staphylococcus aureus*, and decreased Suf function results in global metabolic defects and reduced survival in human neutrophils. *Infect Immun*. 2017;85(6):e00100-17. doi:10.1128/IAI.00100-17

385. Pearl LH. Structure and function in the uracil-DNA glycosylase superfamily. *Mutat Res Repair*. 2000;460(3-4):165-181. doi:10.1016/S0921-8777(00)00025-2

386. Lindahl T. An N-glycosidase from *Escherichia coli* that releases free uracil from DNA containing deaminated cytosine residues. *Proc Natl Acad Sci U S A*. 1974;71(9):3649-3653. doi:10.1073/pnas.71.9.3649

387. Cone R, Duncan J, Hamilton L, Friedberg EC. Partial purification and characterization of a uracil DNA N-glycosidase from *Bacillus subtilis*. *Biochemistry*. 1977;16(14):3194-3201. doi:10.1021/bi00633a024

388. Wang H-C, Hsu K-C, Yang J-M, et al. *Staphylococcus aureus* protein SAUGI acts as a uracil-DNA glycosylase inhibitor. *Nucleic Acids Res*. 2014;42(2):1354-1364. doi:10.1093/nar/gkt964

389. Van Houten B. Nucleotide excision repair in *Escherichia coli*. *Microbiol Rev*. 1990;54(1):18-51.

390. Sancar A. DNA excision repair. *Annu Rev Biochem*. 1996;65(1):43-81. doi:10.1146/annurev.bi.65.070196.000355

391. Lin JJ, Sancar A. Reconstitution of nucleotide excision nuclease with UvrA and UvrB proteins from *Escherichia coli* and UvrC protein from *Bacillus subtilis*. *J Biol Chem*. 1990;265(34):21337-21341.

392. Ayora S, Rojo F, Ogasawara N, Nakai S, Alonso JC. The Mfd Protein of *Bacillus subtilis* 168 is

involved in both transcription-coupled DNA repair and DNA recombination. *J Mol Biol*. 1996;256(2):301-318. doi:10.1006/JMBI.1996.0087

393. Martin HA, Porter KE, Vallin C, et al. Mfd protects against oxidative stress in *Bacillus subtilis* independently of its canonical function in DNA repair. *BMC Microbiol*. 2019;19(1):26. doi:10.1186/s12866-019-1394-x

394. Grosser MR, Paluscio E, Thurlow LR, et al. Genetic requirements for *Staphylococcus aureus* nitric oxide resistance and virulence. Peschel A, ed. *PLOS Pathog*. 2018;14(3):e1006907. doi:10.1371/journal.ppat.1006907

395. Nakano T, Katafuchi A, Shimizu R, et al. Repair activity of base and nucleotide excision repair enzymes for guanine lesions induced by nitrosative stress. *Nucleic Acids Res*. 2005;33(7):2181-2191. doi:10.1093/nar/gki513

396. Kunkel TA, Erie DA. DNA mismatch repair. *Annu Rev Biochem*. 2005;74(1):681-710. doi:10.1146/annurev.biochem.74.082803.133243

397. Schofield MJ, Hsieh P. DNA mismatch repair: Molecular mechanisms and biological function. *Annu Rev Microbiol*. 2003;57(1):579-608. doi:10.1146/annurev.micro.57.030502.090847

398. McHenry CS. Breaking the rules: bacteria that use several DNA polymerase IIIs. *EMBO Rep*. 2011;12(5):408-414. doi:10.1038/embor.2011.51

399. Bruck I, Georgescu RE, O'Donnell M. Conserved interactions in the *Staphylococcus aureus* DNA PolC chromosome replication machine. *J Biol Chem*. 2005;280(18):18152-18162. doi:10.1074/jbc.M413595200

400. Sanders GM, Dallmann HG, McHenry CS. Reconstitution of the *B. subtilis* replisome with 13 proteins including two distinct replicases. *Mol Cell*. 2010;37(2):273-281. doi:10.1016/j.molcel.2009.12.025

401. Paschalis V, Le Chatelier E, Green M, Képès F, Soultanas P, Janniere L. Interactions of the *Bacillus subtilis* DnaE polymerase with replisomal proteins modulate its activity and fidelity. *Open Biol*. 2017;7(9):170146. doi:10.1098/rsob.170146

402. Scheuermann RH, Echols H. A separate editing exonuclease for DNA replication: the epsilon subunit of *Escherichia coli* DNA polymerase III holoenzyme. *Proc Natl Acad Sci U S A*. 1984;81(24):7747-7751. doi:10.1073/pnas.81.24.7747

403. Klocko AD, Schroeder JW, Walsh BW, Lenhart JS, Evans ML, Simmons LA. Mismatch repair causes the dynamic release of an essential DNA polymerase from the replication fork. *Mol Microbiol*. 2011;82(3):648-663. doi:10.1111/j.1365-2958.2011.07841.x

404. Smith BT, Grossman AD, Walker GC. Visualization of mismatch repair in bacterial cells. *Mol Cell*. 2001;8(6):1197-1206. doi:10.1016/s1097-2765(01)00402-6

405. Schaaper RM. Base selection, proofreading, and mismatch repair during DNA replication in *Escherichia coli*. *J Biol Chem*. 1993;268(32):23762-23765.

406. Ginetti F, Perego M, Albertini AM, Galizzi A. *Bacillus subtilis mutS mutL* operon: identification, nucleotide sequence and mutagenesis. *Microbiology*. 1996;142(8):2021-2029. doi:10.1099/13500872-142-8-2021

407. Prunier A-L, Leclercq R. Role of *mutS* and *mutL* genes in hypermutability and recombination in *Staphylococcus aureus*. *J Bacteriol*. 2005;187(10):3455-3464. doi:10.1128/JB.187.10.3455-3464.2005

408. O'Neill AJ, Chopra I. Insertional inactivation of *mutS* in *Staphylococcus aureus* reveals potential for elevated mutation frequencies, although the prevalence of mutators in clinical isolates is low. *J Antimicrob Chemother*. 2002;50(2):161-169. doi:10.1093/jac/dkf118

409. Chopra I, O'Neill AJ, Miller K. The role of mutators in the emergence of antibiotic-resistant bacteria. *Drug Resist Updat*. 2003;6(3):137-145. doi:10.1016/S1368-7646(03)00041-4

410. Pillon MC, Lorenowicz JJ, Uckelmann M, et al. Structure of the endonuclease domain of MutL: unlicensed to cut. *Mol Cell*. 2010;39(1):145-151. doi:10.1016/j.molcel.2010.06.027

411. Kadyrov FA, Dzantiev L, Constantin N, Modrich P. Endonucleolytic function of MutLα in human

mismatch repair. *Cell*. 2006;126(2):297-308. doi:10.1016/J.CELL.2006.05.039

412. Fukui K, Nishida M, Nakagawa N, Masui R, Kuramitsu S. Bound nucleotide controls the endonuclease activity of mismatch repair enzyme MutL. *J Biol Chem*. 2008;283(18):12136-12145. doi:10.1074/jbc.M800110200

413. Mauris J, Evans TC. Adenosine triphosphate stimulates *Aquifex aeolicus* MutL endonuclease activity. Marinus MG, ed. *PLoS One*. 2009;4(9):e7175. doi:10.1371/journal.pone.0007175

414. Liu L, Ortiz Castro MC, Rodríguez González J, Pillon MC, Guarné A. The endonuclease domain of *Bacillus subtilis* MutL is functionally asymmetric. *DNA Repair (Amst)*. 2019;73:1-6. doi:10.1016/J.DNAREP.2018.10.003

415. Duppatla V, Bodda C, Urbanke C, Friedhoff P, Rao DN. The C-terminal domain is sufficient for endonuclease activity of *Neisseria gonorrhoeae* MutL. *Biochem J*. 2009;423(2):265-277. doi:10.1042/BJ20090626

416. Fukui K, Shimada A, Iino H, Masui R, Kuramitsu S. Biochemical properties of MutL, a DNA mismatch repair endonuclease. In: *DNA Repair - On the Pathways to Fixing DNA Damage and Errors*. InTech; 2011. doi:10.5772/23758

417. Dreiseikelmann B, Wackernagel W. Absence in *Bacillus subtilis* and *Staphylococcus aureus* of the sequence-specific deoxyribonucleic acid methylation that is conferred in *Escherichia coli* K-12 by the Dam and Dcm enzymes. *J Bacteriol*. 1981;147(1):259-261.

418. Cromie GA, Connelly JC, Leach DRF. Recombination at double-Strand breaks and DNA ends: Conserved mechanisms from phage to humans. *Mol Cell*. 2001;8(6):1163-1174. doi:10.1016/S1097-2765(01)00419-1

419. Chapman JR, Taylor MRG, Boulton SJ. Playing the end game: DNA double-strand break repair pathway choice. *Mol Cell*. 2012;47(4):497-510. doi:10.1016/J.MOLCEL.2012.07.029

420. Shuman S, Glickman MS. Bacterial DNA repair by non-homologous end joining. *Nat Rev Microbiol*. 2007;5(11):852-861. doi:10.1038/nrmicro1768

421. Weller GR, Kysela B, Roy R, et al. Identification of a DNA nonhomologous end-joining complex in bacteria. *Science (80-)*. 2002;297(5587):1686-1689. doi:10.1126/science.1074584

422. Doherty AJ, Jackson SP, Weller GR. Identification of bacterial homologues of the Ku DNA repair proteins. *FEBS Lett*. 2001;500(3):186-188. doi:10.1016/S0014-5793(01)02589-3

423. Aravind L, Koonin E V. Prokaryotic homologs of the eukaryotic DNA-end-binding protein Ku, novel domains in the Ku protein and prediction of a prokaryotic double-strand break repair system. *Genome Res*. 2001;11(8):1365-1374. doi:10.1101/gr.181001

424. Wilson TE, Topper LM, Palmbos PL. Non-homologous end-joining: bacteria join the chromosome breakdance. *Trends Biochem Sci*. 2003;28(2):62-66. doi:https://doi.org/10.1016/S0968-0004(03)00005-7

425. Chayot R, Montagne B, Mazel D, Ricchetti M. An end-joining repair mechanism in *Escherichia coli*. *Proc Natl Acad Sci U S A*. 2010;107(5):2141-2146. doi:10.1073/pnas.0906355107

426. Rocha EPC, Cornet E, Michel B. Comparative and Evolutionary Analysis of the Bacterial Homologous Recombination Systems. *PLoS Genet*. 2005;1(2):e15. doi:10.1371/journal.pgen.0010015

427. Zuñiga-Castillo J, Romero D, Martínez-Salazar JM. The recombination genes *addAB* are not restricted to Gram-positive bacteria: genetic analysis of the recombination initiation enzymes RecF and AddAB in *Rhizobium etli*. *J Bacteriol*. 2004;186(23):7905-7913. doi:10.1128/JB.186.23.7905-7913.2004

428. Podos SD, Thanassi JA, Pucci MJ. Mechanistic assessment of DNA ligase as an antibacterial target in *Staphylococcus aureus*. *Antimicrob Agents Chemother*. 2012;56(8):4095-4102. doi:10.1128/AAC.00215-12

429. Wigley DB. Bacterial DNA repair: recent insights into the mechanism of RecBCD, AddAB and AdnAB. *Nat Rev Microbiol*. 2013;11(1):9-13. doi:10.1038/nrmicro2917

430. Ayora S, Carrasco B, Cárdenas PP, et al. Double-strand break repair in bacteria: a view from

Bacillus subtilis. *FEMS Microbiol Rev*. 2011;35(6):1055-1081. doi:10.1111/j.1574-6976.2011.00272.x

431. Sanchez H, Kidane D, Castillo Cozar M, Graumann PL, Alonso JC. Recruitment of *Bacillus subtilis* RecN to DNA double-strand breaks in the absence of DNA end processing. *J Bacteriol*. 2006;188(2):353-360. doi:10.1128/JB.188.2.353-360.2006

432. Yeeles JTP, Dillingham MS. The processing of double-stranded DNA breaks for recombinational repair by helicase–nuclease complexes. *DNA Repair (Amst)*. 2010;9(3):276-285. doi:10.1016/J.DNAREP.2009.12.016

433. Kuzminov A. Recombinational repair of DNA damage in Escherichia coli and bacteriophage lambda. *Microbiol Mol Biol Rev*. 1999;63(4):751-813.

434. Umezu K, Nakayama K, Nakayama H. *Escherichia coli* RecQ protein is a DNA helicase. *Proc Natl Acad Sci U S A*. 1990;87(14):5363-5367. doi:10.1073/PNAS.87.14.5363

435. Lovett ST, Kolodner RD. Identification and purification of a single-stranded-DNA-specific exonuclease encoded by the *recJ* gene of *Escherichia coli*. *Proc Natl Acad Sci U S A*. 1989;86(8):2627-2631. doi:10.1073/PNAS.86.8.2627

436. Morimatsu K, Kowalczykowski SC. RecFOR proteins load RecA protein onto gapped DNA to accelerate DNA strand exchange. *Mol Cell*. 2003;11(5):1337-1347. doi:10.1016/S1097-2765(03)00188-6

437. Lenhart JS, Brandes ER, Schroeder JW, Sorenson RJ, Showalter HD, Simmons LA. RecO and RecR are necessary for RecA loading in response to DNA damage and replication fork stress. *J Bacteriol*. 2014;196(15):2851-2860. doi:10.1128/JB.01494-14

438. Alonso JC, Fisher LM. Nucleotide sequence of the *recF* gene cluster from *Staphylococcus aureus* and complementation analysis in *Bacillus subtilis recF* mutants. *MGG Mol Gen Genet*. 1995;246(6):680-686. doi:10.1007/BF00290713

439. West SC. Processing of recombination intermediates by the RuvABC proteins. *Annu Rev Genet*. 1997;31(1):213-244. doi:10.1146/annurev.genet.31.1.213

440. Niga T, Yoshida H, Hattori H, Nakamura S, Ito H. Cloning and sequencing of a novel gene (*recG*) that affects the quinolone susceptibility of *Staphylococcus aureus*. *Antimicrob Agents Chemother*. 1997;41(8):1770-1774. doi:10.1128/AAC.41.8.1770

441. McGregor N, Ayora S, Sedelnikova S, et al. The structure of *Bacillus subtilis* RecU Holliday junction resolvase and its role in substrate selection and sequence-specific cleavage. *Structure*. 2005;13(9):1341-1351. doi:10.1016/j.str.2005.05.011

442. Pereira AR, Reed P, Veiga H, Pinho MG. The Holliday junction resolvase RecU is required for chromosome segregation and DNA damage repair in *Staphylococcus aureus*. *BMC Microbiol*. 2013;13(1):18. doi:10.1186/1471-2180-13-18

443. Carlsson J, Carpenter VS. The *recA* gene product is more important than catalase and superoxide dismutase in protecting *Escherichia coli* against hydrogen peroxide toxicity. *J Bacteriol*. 1980;142(1):319-321.

444. Goerlich O, Quillardet P, Hofnung M. Induction of the SOS response by hydrogen peroxide in various *Escherichia coli* mutants with altered protection against oxidative DNA damage. *J Bacteriol*. 1989;171(11):6141-6147. doi:10.1128/JB.171.11.6141-6147.1989

445. Konola JT, Sargent KE, Gow J-B. Efficient repair of hydrogen peroxide-induced DNA damage by *Escherichia coli* requires SOS induction of RecA and RuvA proteins. *Mutat Res Repair*. 2000;459(3):187-194. doi:10.1016/S0921-8777(99)00073-7

446. Stohl EA, Seifert HS. *Neisseria gonorrhoeae* DNA recombination and repair enzymes protect against oxidative damage caused by hydrogen peroxide. *J Bacteriol*. 2006;188(21):7645-7651. doi:10.1128/JB.00801-06

447. Imlay JA, Linn S. Mutagenesis and stress responses induced in *Escherichia coli* by hydrogen peroxide. *J Bacteriol*. 1987;169(7):2967-2976. doi:10.1128/JB.169.7.2967-2976.1987

448. Horsburgh MJ, Aish JL, White IJ, Shaw L, Lithgow JK, Foster SJ. SigmaB modulates virulence determinant expression and stress resistance: characterization of a functional *rsbU* strain

derived from *Staphylococcus aureus* 8325-4. *J Bacteriol*. 2002;184(19):5457-5467. doi:10.1128/JB.184.19.5457-5467.2002

449. Monk IR, Shah IM, Xu M, Tan M-W, Foster TJ. Transforming the untransformable: application of direct transformation to manipulate genetically *Staphylococcus aureus* and *Staphylococcus epidermidis*. *MBio*. 2012;3(2):e00277-11. doi:10.1128/mBio.00277-11

450. Baba T, Ara T, Hasegawa M, et al. Construction of *Escherichia coli* K-12 in-frame, single-gene knockout mutants: the Keio collection. *Mol Syst Biol*. 2006;2(1):2006.0008. doi:10.1038/MSB4100050

451. Cisar JO, Kolenbrander PE, McIntire FC. Specificity of coaggregation reactions between human oral streptococci and strains of *Actinomyces viscosus* or *Actinomyces naeslundii*. *Infect Immun*. 1979;24(3):742-752.

452. Ike Y, Craig RA, White BA, Yagi Y, Clewell DB. Modification of *Streptococcus faecalis* sex pheromones after acquisition of plasmid DNA. *Proc Natl Acad Sci U S A*. 1983;80(17):5369-5373. doi:10.1073/PNAS.80.17.5369

453. Gründling A, Schneewind O. Genes required for glycolipid synthesis and lipoteichoic acid anchoring in *Staphylococcus aureus*. *J Bacteriol*. 2007;189(6):2521-2530. doi:10.1128/JB.01683-06

454. Charpentier E, Anton AI, Barry P, Alfonso B, Fang Y, Novick RP. Novel cassette-based shuttle vector system for Gram-positive bacteria. *Appl Environ Microbiol*. 2004;70(10):6076-6085. doi:10.1128/AEM.70.10.6076-6085.2004

455. Halpern D, Chiapello H, Schbath S, et al. Identification of DNA motifs implicated in maintenance of bacterial core genomes by predictive modeling. *PLoS Genet*. 2007;3(9):e153. doi:10.1371/journal.pgen.0030153

456. Schneider CA, Rasband WS, Eliceiri KW. NIH Image to ImageJ: 25 years of image analysis. *Nat Methods*. 2012;9(7):671-675. doi:10.1038/nmeth.2089

457. Pader V, James EH, Painter KL, Wigneshweraraj S, Edwards AM. The Agr quorum- sensing system regulates fibronectin binding but not hemolysis in the absence of a functional electron transport chain. *Infect Immun*. 2014;82(10):4337-4347. doi:10.1128/IAI.02254-14

458. Wiegand I, Hilpert K, Hancock REW. Agar and broth dilution methods to determine the minimal inhibitory concentration (MIC) of antimicrobial substances. *Nat Protoc*. 2008;3(2):163-175. doi:10.1038/nprot.2007.521

459. Sader HS, Fritsche TR, Jones RN. Daptomycin bactericidal activity and correlation between disk and broth microdilution method results in testing of *Staphylococcus aureus* strains with decreased susceptibility to vancomycin. *Antimicrob Agents Chemother*. 2006;50(7):2330-2336. doi:10.1128/AAC.01491-05

460. Faul F, Erdfelder E, Lang A-G, Buchner A. G*Power 3: A flexible statistical power analysis program for the social, behavioral, and biomedical sciences. *Behav Res Methods*. 2007;39(2):175-191. doi:10.3758/BF03193146

461. Kelley LA, Mezulis S, Yates CM, Wass MN, Sternberg MJE. The Phyre2 web portal for protein modeling, prediction and analysis. *Nat Protoc*. 2015;10(6):845-858. doi:10.1038/nprot.2015.053

462. Roy A, Kucukural A, Zhang Y. I-TASSER: a unified platform for automated protein structure and function prediction. *Nat Protoc*. 2010;5(4):725-738. doi:10.1038/nprot.2010.5

463. Amundsen SK, Fero J, Hansen LM, et al. *Helicobacter pylori* AddAB helicase-nuclease and RecA promote recombination-related DNA repair and survival during stomach colonization. *Mol Microbiol*. 2008;69(4):994-1007. doi:10.1111/j.1365-2958.2008.06336.x

464. Peng Q, Zhou S, Yao F, et al. Baicalein suppresses the SOS response system of *Staphylococcus aureus* induced by ciprofloxacin. *Cell Physiol Biochem*. 2011;28(5):1045-1050. doi:10.1159/000335791

465. Michel B. After 30 years of study, the bacterial SOS response still surprises us. *PLoS Biol*. 2005;3(7):e255. doi:10.1371/journal.pbio.0030255

466. Schlosser-Silverman E, Elgrably-Weiss M, Rosenshine I, Kohen R, Altuvia S. Characterization

of *Escherichia coli* DNA lesions enerated within J774 macrophages. *J Bacteriol*. 2000;182(18):5225-5230. doi:10.1128/JB.182.18.5225-5230.2000

467. Mesak LR, Miao V, Davies J. Effects of subinhibitory concentrations of antibiotics on SOS and DNA repair gene expression in *Staphylococcus aureus*. *Antimicrob Agents Chemother*. 2008;52(9):3394-3397. doi:10.1128/AAC.01599-07

468. Miller C, Thomsen LE, Gaggero C, Mosseri R, Ingmer H, Cohen SN. SOS response induction by beta-lactams and bacterial defense against antibiotic lethality. *Science (80-)*. 2004;305(5690):1629-1631. doi:10.1126/science.1101630

469. Mertens K, Lantsheer L, Ennis DG, Samuel JE. Constitutive SOS expression and damage-inducible AddAB-mediated recombinational repair systems for *Coxiella burnetii* as potential adaptations for survival within macrophages. *Mol Microbiol*. 2008;69(6):1411-1426. doi:10.1111/j.1365-2958.2008.06373.x

470. McCool JD, Long E, Petrosino JF, Sandler HA, Rosenberg SM, Sandler SJ. Measurement of SOS expression in individual *Escherichia coli* K-12 cells using fluorescence microscopy. *Mol Microbiol*. 2004;53(5):1343-1357. doi:10.1111/j.1365-2958.2004.04225.x

471. Diep BA, Gill SR, Chang RF, et al. Complete genome sequence of USA300, an epidemic clone of community-acquired meticillin-resistant Staphylococcus aureus. *Lancet*. 2006;367(9512):731-739. doi:10.1016/S0140-6736(06)68231-7

472. Jenkins TC, McCollister BD, Sharma R, et al. Epidemiology of healthcare-associated bloodstream infection caused by USA300 strains of methicillin-resistant *Staphylococcus aureus* in 3 affiliated hospitals. *Infect Control Hosp Epidemiol*. 2009;30(03):233-241. doi:10.1086/595963

473. Lee CY, Buranen SL, Zhi-Hai Y. Construction of single-copy integration vectors for *Staphylococcus aureus*. *Gene*. 1991;103(1):101-105. doi:10.1016/0378-1119(91)90399-V

474. Nakamura MM, Liew S-Y, Cummings CA, Brinig MM, Dieterich C, Relman DA. Growth phase- and nutrient limitation-associated transcript abundance regulation in *Bordetella pertussis*. *Infect Immun*. 2006;74(10):5537-5548. doi:10.1128/IAI.00781-06

475. Li Y, Trush MA. Diphenyleneiodonium, an NAD(P)H oxidase inhibitor, also potently inhibits mitochondrial reactive oxygen species production. *Biochem Biophys Res Commun*. 1998;253(2):295-299. doi:10.1006/BBRC.1998.9729

476. Kennedy AD, Porcella SF, Martens C, et al. Complete nucleotide sequence analysis of plasmids in strains of *Staphylococcus aureus* clone USA300 reveals a high level of identity among isolates with closely related core genome sequences. *J Clin Microbiol*. 2010;48(12):4504-4511. doi:10.1128/JCM.01050-10

477. White MJ, Boyd JM, Horswill AR, Nauseef WM. Phosphatidylinositol-specific phospholipase C contributes to survival of *Staphylococcus aureus* USA300 in human blood and neutrophils. *Infect Immun*. 2014;82(4):1559-1571. doi:10.1128/IAI.01168-13

478. Drlica K. Mechanism of fluoroquinolone action. *Curr Opin Microbiol*. 1999;2(5):504-508. doi:10.1016/S1369-5274(99)00008-9

479. Lee Y-J, Park S-J, Ciccone SLM, Kim C-R, Lee S-H. An *in vivo* analysis of MMC-induced DNA damage and its repair. *Carcinogenesis*. 2006;27(3):446-453. doi:10.1093/carcin/bgi254

480. Kapoor G, Saigal S, Elongavan A. Action and resistance mechanisms of antibiotics: A guide for clinicians. *J Anaesthesiol Clin Pharmacol*. 2017;33(3):300-305. doi:10.4103/joacp.JOACP_349_15

481. Winterbourn CC, Hampton MB, Livesey JH, Kettle AJ. Modeling the reactions of superoxide and myeloperoxidase in the neutrophil phagosome: implications for microbial killing. *J Biol Chem*. 2006;281(52):39860-39869. doi:10.1074/jbc.M605898200

482. Gresham HD, Ray CJ, O'Sullivan FX, Wilson BS, Cheung AL, Lindberg FP. Defective neutrophil function in the autoimmune mouse strain MRL/lpr. Potential role of transforming growth factor-beta. *J Immunol*. 1991;146(11):3911-3921. doi:10.4049/jimmunol.164.7.3713

483. Ali RA, Wuescher LM, Dona KR, Worth RG. Platelets mediate host defense against

Staphylococcus aureus through direct bactericidal activity and by enhancing macrophage activities. *J Immunol*. 2017;198(1):344-351. doi:10.4049/jimmunol.1601178

484. Payne CM, Glasser L, Tischler ME, et al. Programmed cell death of the normal human neutrophil: An *in vitro* model of senescence. *Microsc Res Tech*. 1994;28(4):327-344. doi:10.1002/jemt.1070280408

485. Oh H, Siano B, Diamond S. Neutrophil isolation protocol. *J Vis Exp*. 2008;(17):e745. doi:10.3791/745

486. Kobayashi SD, Braughton KR, Palazzolo-Ballance AM, et al. Rapid neutrophil destruction following phagocytosis of *Staphylococcus aureus*. *J Innate Immun*. 2010;2(6):560-575. doi:10.1159/000317134

487. Imlay JA, Linn S. DNA damage and oxygen radical toxicity. *Science (80-)*. 1988;240(4857):1302-1309. doi:10.1126/SCIENCE.3287616

488. Keyer K, Imlay JA. Superoxide accelerates DNA damage by elevating free-iron levels. *Proc Natl Acad Sci U S A*. 1996;93(24):13635-13640. doi:10.1073/PNAS.93.24.13635

489. Jann NJ, Schmaler M, Kristian SA, et al. Neutrophil antimicrobial defense against *Staphylococcus aureus* is mediated by phagolysosomal but not extracellular trap-associated cathelicidin. *J Leukoc Biol*. 2009;86(5):1159-1169. doi:10.1189/jlb.0209053

490. Segal AW. How neutrophils kill microbes. *Annu Rev Immunol*. 2005;23(1):197-223. doi:10.1146/annurev.immunol.23.021704.115653

491. Chedin F, Kowalczykowski SC. A novel family of regulated helicases/nucleases from Gram-positive bacteria: insights into the initiation of DNA recombination. *Mol Microbiol*. 2002;43(4):823-834. doi:10.1046/j.1365-2958.2002.02785.x

492. Halpern D, Gruss A, Claverys J-P, Karoui M El. *rexAB* mutants in *Streptococcus pneumoniae*. *Microbiology*. 2004;150(7):2409-2414. doi:10.1099/mic.0.27106-0

493. Kohanski MA, Dwyer DJ, Hayete B, Lawrence CA, Collins JJ. A common mechanism of cellular death induced by bactericidal antibiotics. *Cell*. 2007;130(5):797-810. doi:10.1016/j.cell.2007.06.049

494. Dwyer DJ, Belenky PA, Yang JH, et al. Antibiotics induce redox-related physiological alterations as part of their lethality. *Proc Natl Acad Sci U S A*. 2014;111(20). doi:10.1073/pnas.1401876111

495. Wang X, Zhao X. Contribution of oxidative damage to antimicrobial lethality. *Antimicrob Agents Chemother*. 2009;53(4):1395-1402. doi:10.1128/AAC.01087-08

496. Yeom J, Imlay JA, Park W. Iron homeostasis affects antibiotic-mediated cell death in *Pseudomonas* species. *J Biol Chem*. 2010;285(29):22689-22695. doi:10.1074/jbc.M110.127456

497. Shatalin K, Shatalina E, Mironov A, Nudler E. H_2S: A universal defense against antibiotics in bacteria. *Science (80-)*. 2011;334(6058):986-990. doi:10.1126/science.1209855

498. Calhoun LN, Kwon YM. The ferritin-like protein Dps protects *Salmonella enterica* serotype Enteritidis from the Fenton-mediated killing mechanism of bactericidal antibiotics. *Int J Antimicrob Agents*. 2011;37(3):261-265. doi:10.1016/j.ijantimicag.2010.11.034

499. Foti JJ, Devadoss B, Winkler JA, Collins JJ, Walker GC. Oxidation of the guanine nucleotide pool underlies cell death by bactericidal antibiotics. *Science (80-)*. 2012;336(6079):315-319. doi:10.1126/science.1219192

500. Liu Y, Liu X, Qu Y, Wang X, Li L, Zhao X. Inhibitors of reactive oxygen species accumulation delay and/or reduce the lethality of several antistaphylococcal agents. *Antimicrob Agents Chemother*. 2012;56(11):6048-6050. doi:10.1128/AAC.00754-12

501. Sampson TR, Liu X, Schroeder MR, Kraft CS, Burd EM, Weiss DS. Rapid killing of *Acinetobacter baumannii* by polymyxins is mediated by a hydroxyl radical death pathway. *Antimicrob Agents Chemother*. 2012;56(11):5642-5649. doi:10.1128/AAC.00756-12

502. Buchmeier NA, Lipps CJ, So MYH, Heffron F. Recombination-deficient mutants of *Salmonella typhimurium* are avirulent and sensitive to the oxidative burst of macrophages. *Mol Microbiol*.

1993;7(6):933-936. doi:10.1111/j.1365-2958.1993.tb01184.x

503. Buchmeier NA, Libby SJ, Xu Y, et al. DNA repair is more important than catalase for *Salmonella* virulence in mice. *J Clin Invest*. 1995;95(3):1047. doi:10.1172/JCI117750

504. Tatum FM, Morfitt DC, Halling SM. Construction of a *Brucella abortus* RecA mutant and its survival in mice. *Microb Pathog*. 1993;14(3):177-185. doi:10.1006/MPAT.1993.1018

505. Gourley CR, Negretti NM, Konkel ME. The food-borne pathogen *Campylobacter jejuni* depends on the AddAB DNA repair system to defend against bile in the intestinal environment. *Sci Rep*. 2017;7(1). doi:10.1038/s41598-017-14646-9

506. Cano DA, Pucciarelli MG, García-Del Portillo F, Casadesús J. Role of the RecBCD recombination pathway in *Salmonella* virulence. *J Bacteriol*. 2002;184(2):592-595. doi:10.1128/JB.184.2.592-595.2002

507. Amundsen SK, Smith GR. Interchangeable parts of the *Escherichia coli* recombination machinery. *Cell*. 2003;112(6):741-744. doi:10.1016/S0092-8674(03)00197-1

508. Ivančić-Baće I, Peharec P, Moslavac S, Škrobot N, Salaj-Šmic† E, Brčić-Kostić K. RecFOR Function is required for DNA repair and recombination in a RecA loading-deficient *recB* mutant of *Escherichia coli*. *Genetics*. 2003;163(2):485 LP - 494.

509. Horii Z-I, Clark AJ. Genetic analysis of the *recF* pathway to genetic recombination in *Escherichia coli* k12: Isolation and characterization of mutants. *J Mol Biol*. 1973;80(2):327-344. doi:10.1016/0022-2836(73)90176-9

510. Marsin S, Lopes A, Mathieu A, et al. Genetic dissection of *Helicobacter pylori* AddAB role in homologous recombination. *FEMS Microbiol Lett*. 2010;311(1):44-50. doi:10.1111/j.1574-6968.2010.02077.x

511. Cannan WJ, Pederson DS. Mechanisms and consequences of double-strand DNA break formation in chromatin. *J Cell Physiol*. 2016;231(1):3-14. doi:10.1002/jcp.25048

512. Thoms B, Wackernagel W. Interaction of RecBCD enzyme with DNA at double-strand breaks produced in UV-irradiated *Escherichia coli*: requirement for DNA end processing. *J Bacteriol*. 1998;180(21):5639-5645.

513. Kooistra J, Vosman B, Venema G. Cloning and characterization of a *Bacillus subtilis* transcription unit involved in ATP-dependent DNase synthesis. *J Bacteriol*. 1988;170(10):4791-4797. doi:10.1128/JB.170.10.4791-4797.1988

514. Capaldo FN, Ramsey G, Barbour SD. Analysis of the growth of recombination-deficient strains of *Escherichia coli* K-12. *J Bacteriol*. 1974;118(1):242-249.

515. Kooistra J, Small GD, Setlow JK, Shapanka R. Genetics and complementation of *Haemophilus influenzae* mutants deficient in adenosine 5'-triphosphate-dependent nuclease. *J Bacteriol*. 1976;126(1):31-37.

516. Murdoch DR, Corey GR, Hoen B, et al. Clinical presentation, etiology, and outcome of infective endocarditis in the 21st century. *Arch Intern Med*. 2009;169(5):463. doi:10.1001/archinternmed.2008.603

517. Selton-Suty C, Célard M, Le Moing V, et al. Preeminence of *Staphylococcus aureus* in infective endocarditis: A 1-year population-based survey. *Clin Infect Dis*. 2012;54(9):1230-1239. doi:10.1093/cid/cis199

518. Yew H Sen, Murdoch DR. Global trends in infective endocarditis epidemiology. *Curr Infect Dis Rep*. 2012;14(4):367-372. doi:10.1007/s11908-012-0265-5

519. Cahill TJ, Prendergast BD. Infective endocarditis. *Lancet*. 2016;387(10021):882-893. doi:10.1016/S0140-6736(15)00067-7

520. Durack DT, Beeson PB, Petersdorf RG. Experimental bacterial endocarditis: Production and progress of the disease in rabbits. *Br J Exp Pathol*. 1973;54(2):142-151.

521. Holland TL, Baddour LM, Bayer AS, Hoen B, Miro JM, Fowler VG. Infective endocarditis. *Nat Rev Dis Prim*. 2016;2:16059. doi:10.1038/nrdp.2016.59

522. Scheld WM, Strunk RW, Balian G, Calderone RA. Microbial adhesion to fibronectin *in vitro*

correlates with production of endocarditis in rabbits. *Proc Soc Exp Biol Med*. 1985;180(3):474-482.

523. Lowrance JH, Baddour LM, Simpson WA. The role of fibronectin binding in the rat model of experimental endocarditis caused by *Streptococcus sanguis*. *J Clin Invest*. 1990;86(1):7-13. doi:10.1172/JCI114717

524. Hamill RJ, Vann JM, Proctor RA. Phagocytosis of *Staphylococcus aureus* by cultured bovine aortic endothelial cells: model for postadherence events in endovascular infections. *Infect Immun*. 1986;54(3):833-836.

525. Moreillon P, Entenza JM, Francioli P, et al. Role of *Staphylococcus aureus* coagulase and clumping factor in pathogenesis of experimental endocarditis. *Infect Immun*. 1995;63(12):4738-4743.

526. Clawson CC, Rao GH, White JG. Platelet interaction with bacteria. IV. Stimulation of the release reaction. *Am J Pathol*. 1975;81(2):411-420.

527. Herzberg MC, MacFarlane GD, Gong K, et al. The platelet interactivity phenotype of *Streptococcus sanguis* influences the course of experimental endocarditis. *Infect Immun*. 1992;60(11):4809-4818.

528. Duval X, Iung B, Klein I, et al. Effect of early cerebral magnetic resonance imaging on clinical decisions in infective endocarditis. *Ann Intern Med*. 2010;152(8):497. doi:10.7326/0003-4819-152-8-201004200-00006

529. Bleich HL, Boro ES, Weinstein L, Schlesinger JJ. Pathoanatomic, pathophysiologic and clinical correlations in endocarditis. *N Engl J Med*. 1974;291(21):1122-1126. doi:10.1056/NEJM197411212912110

530. Christaki E, Giamarellos-Bourboulis EJ. The complex pathogenesis of bacteremia. *Virulence*. 2014;5(1):57-65. doi:10.4161/viru.26514

531. Gould FK, Denning DW, Elliott TSJ, et al. Guidelines for the diagnosis and antibiotic treatment of endocarditis in adults: A report of the Working Party of the British Society for Antimicrobial Chemotherapy. *J Antimicrob Chemother*. 2012;67(2):269-289. doi:10.1093/jac/dkr450

532. Baddour LM, Wilson WR, Bayer AS, et al. Infective endocarditis in adults: diagnosis, antimicrobial therapy, and management of complications. *Circulation*. 2015;132(15):1435-1486. doi:10.1161/CIR.0000000000000296

533. Pericàs JM, Nathavitharana R, Garcia-de-la-Mària C, et al. Endocarditis caused by highly penicillin-resistant viridans group streptococci: Still room for vancomycin-based regimens. *Antimicrob Agents Chemother*. 2019;63(8). doi:10.1128/aac.00516-19

534. Hullahalli K, Rodrigues M, Palmer KL. Exploiting CRISPR-Cas to manipulate *Enterococcus faecalis populations*. *Elife*. 2017;6. doi:10.7554/eLife.26664

535. Sinel C, Cacaci M, Meignen P, et al. Subinhibitory concentrations of ciprofloxacin enhance antimicrobial resistance and pathogenicity of *Enterococcus faecium*. *Antimicrob Agents Chemother*. 2017;61(5):e02763-16. doi:10.1128/AAC.02763-16

536. Gasc AM, Sicard N, Claverys JP, Sicard AM. Lack of SOS repair in *Streptococcus pneumoniae*. *Mutat Res Mol Mech Mutagen*. 1980;70(2):157-165. doi:10.1016/0027-5107(80)90155-4

537. Cromie GA. Phylogenetic ubiquity and shuffling of the bacterial RecBCD and AddAB recombination complexes. *J Bacteriol*. 2009;191(16):5076-5084. doi:10.1128/JB.00254-09

538. Young Lee S, Cisar JO, Bryant JL, Eckhaus MA, Sandberg AL. Resistance of *Streptococcus gordonii* to polymorphonuclear leukocyte killing is a potential virulence determinant of infective endocarditis. *Infect Immun*. 2006;74(6):3148-3155. doi:10.1128/IAI.00087-06

539. Dunny GM, Brown BL, Clewell DB. Induced cell aggregation and mating in *Streptococcus faecalis*: evidence for a bacterial sex pheromone. *Proc Natl Acad Sci U S A*. 1978;75(7):3479-3483. doi:10.1073/PNAS.75.7.3479

540. Gold OG, Jordan HV, van Houte J. The prevalence of enterococci in the human mouth and their pathogenicity in animal models. *Arch Oral Biol*. 1975;20(7):473-IN15. doi:10.1016/0003-9969(75)90236-8

541. Wheeler MA, Smith SD, García-Cardeña G, Nathan CF, Weiss RM, Sessa WC. Bacterial infection induces nitric oxide synthase in human neutrophils. *J Clin Invest*. 1997;99(1):110-116. doi:10.1172/JCI119121

542. Ting-Beall HP, Lee AS, Hochmuth RM. Effect of cytochalasin D on the mechanical properties and morphology of passive human neutrophils. *Ann Biomed Eng*. 1995;23(5):666-671. doi:10.1007/BF02584463

543. Darrigo C, Guillemet E, Dervyn R, Ramarao N. The bacterial Mfd protein prevents DNA damage induced by the host nitrogen immune response in a NER-independent but RecBC-dependent pathway. Neyrolles O, ed. *PLoS One*. 2016;11(10):e0163321. doi:10.1371/journal.pone.0163321

544. Schapiro JM, Libby SJ, Fang FC. Inhibition of bacterial DNA replication by zinc mobilization during nitrosative stress. *Proc Natl Acad Sci U S A*. 2003;100(14):8496-8501. doi:10.1073/pnas.1033133100

545. Harvey BS, Baker CJ, Edwards MS. Contributions of complement and immunoglobulin to neutrophil-mediated killing of enterococci. *Infect Immun*. 1992;60(9):3635-3640.

546. Arduino RC, Murray BE, Rakita RM. Roles of antibodies and complement in phagocytic killing of enterococci. *Infect Immun*. 1994;62(3):987-993.

547. Mitchell T, Lo A, Logan MR, Lacy P, Eitzen G. Primary granule exocytosis in human neutrophils is regulated by Rac-dependent actin remodeling. *Am J Physiol Physiol*. 2008;295(5):C1354-C1365. doi:10.1152/ajpcell.00239.2008

548. Yu Y, Kwon K, Tsitrin T, et al. Characterization of early-phase neutrophil extracellular traps in urinary tract infections. Weiss D, ed. *PLOS Pathog*. 2017;13(1):e1006151. doi:10.1371/journal.ppat.1006151

549. Gonzalez AS, Bardoel BW, Harbort CJ, Zychlinsky A. Induction and quantification of neutrophil extracellular traps. *Methods Mol Biol*. 2014;1124:307-318. doi:10.1007/978-1-62703-845-4_20

550. Shafer WM, Pohl J, Onunka VC, Bangalore N, Travis J. Human lysosomal cathepsin G and granzyme B share a functionally conserved broad spectrum antibacterial peptide. *J Biol Chem*. 1991;266(1):112-116.

551. Cole AM, Shi J, Ceccarelli A, Kim YH, Park A, Ganz T. Inhibition of neutrophil elastase prevents cathelicidin activation and impairs clearance of bacteria from wounds. *Blood*. 2001;97(1):297-304. doi:10.1182/BLOOD.V97.1.297

552. Zarember KA, Sugui JA, Chang YC, Kwon-Chung KJ, Gallin JI. Human polymorphonuclear leukocytes inhibit *Aspergillus fumigatus* conidial growth by lactoferrin-mediated iron depletion. *J Immunol*. 2014;178(10):6367-6373. doi:10.4049/jimmunol.178.10.6367

553. Sinha KM, Unciuleac M-C, Glickman MS, Shuman S. AdnAB: a new DSB-resecting motor-nuclease from mycobacteria. *Genes Dev*. 2009;23(12):1423-1437. doi:10.1101/gad.1805709

554. Saikrishnan K, Yeeles JT, Gilhooly NS, Krajewski WW, Dillingham MS, Wigley DB. Insights into Chi recognition from the structure of an AddAB-type helicase-nuclease complex. *EMBO J*. 2012;31(6):1568-1578. doi:10.1038/emboj.2012.9

555. Singleton MR, Dillingham MS, Wigley DB. Structure and mechanism of helicases and nucleic acid translocases. *Annu Rev Biochem*. 2007;76(1):23-50. doi:10.1146/annurev.biochem.76.052305.115300

556. Smith GR, Kunes SM, Schultz DW, Taylor A, Triman KL. Structure of chi hotspots of generalized recombination. *Cell*. 1981;24(2):429-436. doi:10.1016/0092-8674(81)90333-0

557. Bianco PR, Kowalczykowski SC. The recombination hotspot Chi is recognized by the translocating RecBCD enzyme as the single strand of DNA containing the sequence 5'-GCTGGTGG-3'. *Proc Natl Acad Sci U S A*. 1997;94(13):6706-6711. doi:10.1073/pnas.94.13.6706

558. Chédin F, Noirot P, Biaudet V, Ehrlich SD. A five-nucleotide sequence protects DNA from exonucleolytic degradation by AddAB, the RecBCD analogue of *Bacillus subtilis*. *Mol Microbiol*. 1998;29(6):1369-1377. doi:10.1046/j.1365-2958.1998.01018.x

559. Dixon DA, Kowalczykowski SC. The recombination hotspot χ is a regulatory sequence that acts by attenuating the nuclease activity of the *E. coli* RecBCD enzyme. *Cell*. 1993;73(1):87-96. doi:10.1016/0092-8674(93)90162-J

560. Yeeles JTP, Dillingham MS. A Dual-nuclease mechanism for DNA break processing by AddAB-type helicase-nucleases. *J Mol Biol*. 2007;371(1):66-78. doi:10.1016/J.JMB.2007.05.053

561. Spies M, Kowalczykowski SC. The RecA binding locus of RecBCD is a general domain for recruitment of DNA strand exchange proteins. *Mol Cell*. 2006;21(4):573-580. doi:10.1016/j.molcel.2006.01.007

562. Anderson DG, Kowalczykowski SC. The translocating RecBCD enzyme stimulates recombination by directing RecA protein onto ssDNA in a Chi-regulated manner. *Cell*. 1997;90(1):77-86. doi:10.1016/S0092-8674(00)80315-3

563. Badrinarayanan A, Le TBK, Spille J-H, Cisse II, Laub MT. Global analysis of double-strand break processing reveals *in vivo* properties of the helicase-nuclease complex AddAB. Lichten M, ed. *PLOS Genet*. 2017;13(5):e1006783. doi:10.1371/journal.pgen.1006783

564. Niu H, Raynard S, Sung P. Multiplicity of DNA end resection machineries in chromosome break repair. *Genes Dev*. 2009;23(13):1481-1486. doi:10.1101/gad.1824209

565. Singleton MR, Dillingham MS, Gaudier M, Kowalczykowski SC, Wigley DB. Crystal structure of RecBCD enzyme reveals a machine for processing DNA breaks. *Nature*. 2004;432(7014):187-193. doi:10.1038/nature02988

566. Handa N, Yang L, Dillingham MS, Kobayashi I, Wigley DB, Kowalczykowski SC. Molecular determinants responsible for recognition of the single-stranded DNA regulatory sequence, χ, by RecBCD enzyme. *Proc Natl Acad Sci*. 2012;109(23):8901-8906. doi:10.1073/PNAS.1206076109

567. Yang L, Handa N, Liu B, Dillingham MS, Wigley DB, Kowalczykowski SC. Alteration of χ recognition by RecBCD reveals a regulated molecular latch and suggests a channel-bypass mechanism for biological control. *Proc Natl Acad Sci*. 2012;109(23):8907-8912. doi:10.1073/PNAS.1206081109

568. Chédin F, Ehrlich SD, Kowalczykowski SC. The *Bacillus subtilis* AddAB helicase/nuclease is regulated by its cognate Chi sequence *in vitro*. *J Mol Biol*. 2000;298(1):7-20. doi:10.1006/JMBI.2000.3556

569. Unciuleac M-C, Shuman S. Double strand break unwinding and resection by the mycobacterial helicase-nuclease AdnAB in the presence of single strand DNA-binding protein (SSB). *J Biol Chem*. 2010;285(45):34319-34329. doi:10.1074/jbc.M110.162925

570. Singh A. Guardians of the mycobacterial genome: A review on DNA repair systems in *Mycobacterium tuberculosis*. *Microbiology*. 2017;163(12):1740-1758. doi:10.1099/mic.0.000578

571. Kooistra J, Venema G. Cloning, sequencing, and expression of *Bacillus subtilis* genes involved in ATP-dependent nuclease synthesis. *J Bacteriol*. 1991;173(12):3644-3655. doi:10.1128/JB.173.12.3644-3655.1991

572. Kooistra J, Haijema BJ, Hesseling-Meinders A, Venema G. A conserved helicase motif of the AddA subunit of the *Bacillus subtilis* ATP-dependent nuclease (AddAB) is essential for DNA repair and recombination. *Mol Microbiol*. 1997;23(1):137-149. doi:10.1046/j.1365-2958.1997.1991570.x

573. Quiberoni A, Biswas I, Karoui M El, Rezaïki L, Tailliez P, Gruss A. *In Vivo* evidence for two active nuclease motifs in the double-strand break repair enzyme RexAB of *Lactococcus lactis*. *J Bacteriol*. 2001;183(13):4071-4078. doi:10.1128/JB.183.13.4071-4078.2001

574. Levoin N, Calmels T, Krief S, et al. Homology model versus X-ray structure in receptor-based drug design: A retrospective analysis with the dopamine D3 receptor. *ACS Med Chem Lett*. 2011;2(4):293-297. doi:10.1021/ml100288q

575. Berman HM, Westbrook J, Feng Z, et al. The Protein Data Bank. *Nucleic Acids Res*. 2000;28(1):235-242. doi:10.1093/nar/28.1.235

576. Chédin F, Handa N, Dillingham MS, Kowalczykowski SC. The AddAB Helicase/Nuclease Forms

a Stable Complex with Its Cognate χ Sequence During Translocation. *J Biol Chem*. 2006;281(27):18610-18617. doi:10.1074/JBC.M600882200

577. Yeeles JTP, Cammack R, Dillingham MS. An iron-sulfur cluster is essential for the binding of broken DNA by AddAB-type helicase-nucleases. *J Biol Chem*. 2009;284(12):7746-7755. doi:10.1074/jbc.M808526200

578. Tartoff KD, Hobbs CA. Improved media for growing plasmid and cosmid clones. *Bethesda Res Lab Focus*. 1987;9:12.

579. Kooistra J, Haijema BJ, Venema G. The *Bacillus subtilis addAB* genes are fully functional in *Escherichia coli*. *Mol Microbiol*. 1993;7(6):915-923. doi:10.1111/j.1365-2958.1993.tb01182.x

580. Masterson C, Boehmer PE, McDonald F, Chaudhuri S, Hickson ID, Emmerson PT. Reconstitution of the activities of the RecBCD holoenzyme of *Escherichia coli* from the purified subunits. *J Biol Chem*. 1992;267(19):13564-13572.

581. Willetts NS, Mount DW. Genetic analysis of recombination-deficient mutants of *Escherichia coli* K-12 carrying *rec* mutations cotransducible with *thyA*. *J Bacteriol*. 1969;100(2):923-934.

582. Willetts NS, Clark AJ, Low B. Genetic location of certain mutations conferring recombination deficiency in *Escherichia coli*. *J Bacteriol*. 1969;97(1):244-249.

583. Smith GR. How RecBCD enzyme and Chi promote DNA break repair and recombination: a molecular biologist's view. *Microbiol Mol Biol Rev*. 2012;76(2):217 LP - 228. doi:10.1128/MMBR.05026-11

584. Karlin S, Weinstock GM, Brendel V. Bacterial classifications derived from RecA protein sequence comparisons. *J Bacteriol*. 1995;177(23):6881-6893. doi:10.1128/jb.177.23.6881-6893.1995

585. Chen HW, Ruan B, Yu M, Wang J d, Julin DA. The RecD subunit of the RecBCD enzyme from *Escherichia coli* is a single-stranded DNA-dependent ATPase. *J Biol Chem*. 1997;272(15):10072-10079. doi:10.1074/jbc.272.15.10072

586. Haijema BJ, Meima R, Kooistra J, Venema G. Effects of lysine-to-glycine mutations in the ATP-binding consensus sequences in the AddA and AddB subunits on the *Bacillus subtilis* AddAB enzyme activities. *J Bacteriol*. 1996;178(17):5130-5137. doi:10.1128/jb.178.17.5130-5137.1996

587. Stellwagen NC. Electrophoresis of DNA in agarose gels, polyacrylamide gels and in free solution. *Electrophoresis*. 2009;30(S1):S188-S195. doi:10.1002/elps.200900052

588. Brawn MK, Fridovich I. Increased superoxide radical production evokes inducible DNA repair in *Escherichia coli*. *J Biol Chem*. 1985;260(2):922-925.

589. Anderson DG, Kowalczykowski SC. Reconstitution of an SOS response pathway: derepression of transcription in response to DNA breaks. *Cell*. 1998;95(7):975-979. doi:10.1016/S0092-8674(00)81721-3

590. Chaudhury AM, Smith GR. Role of *Escherichia coli* RecBC enzyme in SOS induction. *Mol Gen Genet*. 1985;201(3):525-528. doi:10.1007/BF00331350

591. McPartland A, Green L, Echols H. Control of *recA* gene RNA in *E. coli*: Regulatory and signal genes. *Cell*. 1980;20(3):731-737. doi:10.1016/0092-8674(80)90319-0

592. Kidane D, Sanchez H, Alonso JC, Graumann PL. Visualization of DNA double-strand break repair in live bacteria reveals dynamic recruitment of *Bacillus subtilis* RecF, RecO and RecN proteins to distinct sites on the nucleoids. *Mol Microbiol*. 2004;52(6):1627-1639. doi:10.1111/j.1365-2958.2004.04102.x

593. Umlauf BJ, McGuire MJ, Brown KC. Introduction of plasmid encoding for rare tRNAs reduces amplification bias in phage display biopanning. *Biotechniques*. 2015;58(2). doi:10.2144/000114256

594. Cosgrove SE. The relationship between antimicrobial resistance and patient outcomes: mortality, length of hospital stay, and health care costs. *Clin Infect Dis*. 2006;42(Supplement_2):S82-S89. doi:10.1086/499406

595. Jernberg C, Lofmark S, Edlund C, Jansson JK. Long-term impacts of antibiotic exposure on the

human intestinal microbiota. *Microbiology*. 2010;156(11):3216-3223. doi:10.1099/mic.0.040618-0

596. Falcone M, Russo A, Iraci F, et al. Risk factors and outcomes for bloodstream infections secondary to *Clostridium difficile* infection. *Antimicrob Agents Chemother*. 2016;60(1):252-257. doi:10.1128/AAC.01927-15

597. Cirz RT, Chin JK, Andes DR, de Crécy-Lagard V, Craig WA, Romesberg FE. Inhibition of mutation and combating the evolution of antibiotic resistance. Waldor M, ed. *PLoS Biol*. 2005;3(6):e176. doi:10.1371/journal.pbio.0030176

598. Recacha E, Machuca J, Díaz-Díaz S, et al. Suppression of the SOS response modifies spatiotemporal evolution, post-antibiotic effect, bacterial fitness and biofilm formation in quinolone-resistant *Escherichia coli*. *J Antimicrob Chemother*. 2018;74(1):66-73. doi:10.1093/jac/dky407

599. Dziegielewska B, Beerman TA, Bianco PR. Inhibition of RecBCD Enzyme by Antineoplastic DNA Alkylating Agents. *J Mol Biol*. 2006;361(5):898-919. doi:10.1016/J.JMB.2006.06.068

600. Karu AE, Linn S. Uncoupling of the *recBC* ATPase from DNase by DNA crosslinked with psoralen. *Proc Natl Acad Sci U S A*. 1972;69(10):2855-2859. doi:10.1073/pnas.69.10.2855

601. Sun D, Hurley LH. Structure-activity relationships of (+)-CC-1065 analogs in the inhibition of helicase-catalyzed unwinding of duplex DNA. *J Med Chem*. 1992;35(10):1773-1782. doi:10.1021/jm00088a012

602. Wilkinson M, Troman L, Wan Nur Ismah WA, et al. Structural basis for the inhibition of RecBCD by Gam and its synergistic antibacterial effect with quinolones. *Elife*. 2016;5. doi:10.7554/eLife.22963

603. Amundsen SK, Spicer T, Karabulut AC, et al. Small-Molecule Inhibitors of Bacterial AddAB and RecBCD Helicase-Nuclease DNA Repair Enzymes. *ACS Chem Biol*. 2012;7(5):879-891. doi:10.1021/cb300018x

604. Oliver DB, Goldberg EB. Protection of parental T4 DNA from a restriction exonuclease by the product of gene 2. *J Mol Biol*. 1977;116(4):877-881. doi:10.1016/0022-2836(77)90276-5

605. Aiello D, Barnes MH, Biswas EE, et al. Discovery, characterization and comparison of inhibitors of *Bacillus anthracis* and *Staphylococcus aureus* replicative DNA helicases. *Bioorg Med Chem*. 2009;17(13):4466-4476. doi:10.1016/J.BMC.2009.05.014

606. Collins AR, Ai-guo M, Duthie SJ. The kinetics of repair of oxidative DNA damage (strand breaks and oxidised pyrimidines) in human cells. *Mutat Res Repair*. 1995;336(1):69-77. doi:10.1016/0921-8777(94)00043-6

607. The European Committee on Antimicrobial Susceptibility Testing. *Breakpoint Tables for Interpretation of MICs and Zone Diameters, Version 9.0*.; 2019.

608. Aldred KJ, Kerns RJ, Osheroff N. Mechanism of quinolone action and resistance. *Biochemistry*. 2014;53(10):1565-1574. doi:10.1021/bi5000564

609. Erill I, Campoy S, Barbé J. Aeons of distress: an evolutionary perspective on the bacterial SOS response. *FEMS Microbiol Rev*. 2007;31(6):637-656. doi:10.1111/j.1574-6976.2007.00082.x

610. Blach-Olszewska Z, Leszek J. Mechanisms of over-activated innate immune system regulation in autoimmune and neurodegenerative disorders. *Neuropsychiatr Dis Treat*. 2007;3(3):365-372.

611. Cejka P. DNA end resection: Nucleases team up with the right partners to initiate homologous recombination. *J Biol Chem*. 2015;290(38):22931-22938. doi:10.1074/jbc.R115.675942

612. Amarh V, Arthur PK. DNA double-strand break formation and repair as targets for novel antibiotic combination chemotherapy. *Futur Sci OA*. 2019;5(8):FSO411. doi:10.2144/fsoa-2019-0034

613. Reiche MA, Warner DF, Mizrahi V. Targeting DNA replication and repair for the development of novel therapeutics against tuberculosis. *Front Mol Biosci*. 2017;4(NOV). doi:10.3389/fmolb.2017.00075

614. Su LY, Willner DL, Segall AM. An antimicrobial peptide that targets DNA repair intermediates in vitro inhibits *Salmonella* growth within murine macrophages. *Antimicrob Agents Chemother*.

2010;54(5):1888-1899. doi:10.1128/AAC.01610-09

615. Alam MK, Alhhazmi A, Decoteau JF, Luo Y, Geyer CR. RecA inhibitors potentiate antibiotic activity and block evolution of antibiotic resistance. *Cell Chem Biol*. 2016;23(3):381-391. doi:10.1016/j.chembiol.2016.02.010

616. da Silva LCN, Diniz RC, Lima IM de SF, et al. SOS response and *Staphylococcus aureus*: Implications for drug development. In: *The Rise of Virulence and Antibiotic Resistance in Staphylococcus Aureus*. InTech; 2017. doi:10.5772/65960

617. Sexton JZ, Wigle TJ, He Q, et al. Novel inhibitors of *E. coli* RecA ATPase activity. *Curr Chem Genomics*. 2010;4:34-42. doi:10.2174/1875397301004010034

618. Peterson EJR, Janzen WP, Kireev D, Singleton SF. High-throughput screening for RecA inhibitors using a transcreener adenosine 5′-O-diphosphate assay. *Assay Drug Dev Technol*. 2012;10(3):260-268. doi:10.1089/adt.2011.0409

619. Noirot P, Gupta RC, Radding CM, Kolodner RD. Hallmarks of homology recognition by RecA-like recombinases are exhibited by the unrelated *Escherichia coli* RecT protein. *EMBO J*. 2003;22(2):324-334. doi:10.1093/emboj/cdg027

620. Schröder W, Goerke C, Wolz C. Opposing effects of aminocoumarins and fluoroquinolones on the SOS response and adaptability in *Staphylococcus aureus*. *J Antimicrob Chemother*. 2013;68(3):529-538. doi:10.1093/jac/dks456

621. Carvalho AR, Martins ALDB, Cutrim BDS, et al. Betulinic acid prevents the acquisition of ciprofloxacin-mediated mutagenesis in *Staphylococcus aureus*. *Molecules*. 2019;24(9). doi:10.3390/molecules24091757

622. Mulani MS, Kamble EE, Kumkar SN, Tawre MS, Pardesi KR. Emerging strategies to combat ESKAPE pathogens in the era of antimicrobial resistance: A review. *Front Microbiol*. 2019;10(APR). doi:10.3389/fmicb.2019.00539

623. Slama TG. Gram-negative antibiotic resistance: there is a price to pay. *Crit Care*. 2008;12(4):S4. doi:10.1186/cc6820

624. Liberati NT, Urbach JM, Miyata S, et al. An ordered, nonredundant library of *Pseudomonas aeruginosa* strain PA14 transposon insertion mutants. *Proc Natl Acad Sci U S A*. 2006;103(8):2833-2838. doi:10.1073/pnas.0511100103

625. Dermić D, Halupecki E, Zahradka D, Petranović M. RecBCD enzyme overproduction impairs DNA repair and homologous recombination in *Escherichia coli*. *Res Microbiol*. 2005;156(3):304-311. doi:10.1016/j.resmic.2004.10.005

626. Kool J, Jonker N, Irth H, Niessen WMA. Studying protein-protein affinity and immobilized ligand-protein affinity interactions using MS-based methods. *Anal Bioanal Chem*. 2011;401(4):1109-1125. doi:10.1007/s00216-011-5207-9

627. Smith E, Collins I. Photoaffinity labeling in target- and binding-site identification. *Future Med Chem*. 2015;7(2):159-183. doi:10.4155/fmc.14.152

628. Topliss JG. Utilization of operational schemes for analog synthesis in drug design. *J Med Chem*. 1972;15(10):1006-1011. doi:10.1021/jm00280a002